

University of Southampton Research Repository  
ePrints Soton

Copyright © and Moral Rights for this thesis are retained by the author and/or other copyright owners. A copy can be downloaded for personal non-commercial research or study, without prior permission or charge. This thesis cannot be reproduced or quoted extensively from without first obtaining permission in writing from the copyright holder/s. The content must not be changed in any way or sold commercially in any format or medium without the formal permission of the copyright holders.

When referring to this work, full bibliographic details including the author, title, awarding institution and date of the thesis must be given e.g.

AUTHOR (year of submission) "Full thesis title", University of Southampton, name of the University School or Department, PhD Thesis, pagination

University of Southampton  
FACULTY OF NATURAL AND ENVIRONMENTAL SCIENCES  
School of Ocean and Earth Science

# Environmental and physiological influences on otolith chemistry in a marine fish

by  
Anna M. Sturrock



Thesis towards the degree of Doctor of Philosophy  
May 2012



UNIVERSITY OF SOUTHAMPTON  
ABSTRACT

FACULTY OF NATURAL AND ENVIRONMENTAL SCIENCES  
Ocean and Earth Sciences  
Doctor of Philosophy

ENVIRONMENTAL AND PHYSIOLOGICAL INFLUENCES ON  
OTOLITH CHEMISTRY IN A MARINE FISH

by Anna Michelle Sturrock

The aim of this project was to determine whether otolith trace element chemistry can be used to track migrations in fully marine fish. This question was addressed through a semi-controlled experiment where Irish Sea and North Sea plaice (*Pleuronectes platessa*) were maintained in a monitored environment. The relationships between water, blood and otolith chemistry were assessed and with reference to environmental and physiological variables and through comparisons of otolith trace element chemistry in wild plaice tagged by data storage tags (DST). Specifically, the thesis is divided into five sections.

First, the current understanding of the underlying mechanisms governing element incorporation into the otolith is reviewed, using 'hard and soft acid and base' (HSAB) theory to explore the differences in chemical behaviours, distributions and affinities between elements. A number of case studies are examined that have used otolith microchemistry to infer distributions of marine fish and attempted to corroborate their results with alternative additional proxies.

Second, method development is described for a simple dilution method that allowed simultaneous determination of twelve elements (Li, Mg, K, Ca, Mn, Cu, Zn, Se, Rb, Sr, Ba, Pb) in the blood plasma of plaice by high resolution inductively coupled plasma mass spectrometry (HR-ICPMS).

Third, temporal trends in environmental and blood elemental concentrations in the experimental population of plaice are described, and the main influences explored via linear mixed-effects models. Significant physiological influences on blood elemental concentrations were observed for almost every element, but particularly the 'soft' metals (Cu, Zn, Se, Pb) and Ca and Sr. Blood protein concentrations appeared to drive many of the patterns observed and differences among the sexes.

Fourth, trends in otolith concentrations (Li, Mg, K, Mn, Cu, Zn, Ba), as determined by laser ablation HR-ICPMS and secondary ion mass spectrometry (SIMS), are presented for the experimental plaice. Physiological and environmental effects on otolith elemental concentrations were examined using linear mixed-effects models. Differences in the patterns exhibited by water, blood and otolith concentrations indicated significant elemental partitioning at all major interfaces. A novel method of calibrating time between annual increments in otoliths using SIMS oxygen isotope analysis is also presented.

Finally, concentrations of four elements (Li, Mn, Sr and Ba) are described in the otoliths of 11 wild plaice tagged with DSTs and possible physiological and environmental effects examined, again, using linear mixed-effects models. This is the first study (to our knowledge) to have coupled archival tag records (i.e. 'known' migrations) with otolith trace element concentrations in free-ranging marine fish. The results generally corroborated observations in the tank-maintained fish. A significant negative temperature effect on otolith Li/Ca ratios was observed, as well as significant differences in Ba/Ca ratios among subpopulations.

# Table of contents

Table of contents.....	iv
List of figures.....	ix
List of abbreviations.....	xiv
Declaration of authorship.....	xv
Acknowledgements.....	xvii
Chapter 1.....	1.1
1.1    Abstract.....	1.1
1.2    Introduction.....	1.2
1.3    How does otolith microchemistry serve as an environmental tag?.....	1.6
1.3.1    Chemistry of relevant elements and the mechanisms governing their incorporation into the otolith	1.6
1.3.2    Influences on otolith microchemistry .....	1.10
1.4    Application of otolith microchemistry to reconstruct fish migrations in the marine environment	
1.14	
1.4.1    The marine system .....	1.14
1.4.2    Marine species .....	1.15
1.4.3    Practical considerations.....	1.16
1.5    Case studies .....	1.17
1.5.1    Otolith chemistry vs. genetic tags.....	1.17
1.5.2    Otolith chemistry vs. otolith shape.....	1.19
1.5.3    Otolith chemistry vs. morphometrics .....	1.19
1.5.4    Otolith chemistry vs. applied tags .....	1.20
1.6    Discussion.....	1.21
1.7    Conclusions.....	1.22
1.8    Acknowledgements.....	1.23
Chapter 2.....	2.25
2.1    Introduction.....	2.25
2.1.1    Blood elemental chemistry in marine fish .....	2.27
2.2    Methods.....	2.32
2.2.1    Collection and maintenance of study animals.....	2.32
2.2.2    Selection criteria .....	2.34

2.2.3	Blood sampling.....	2.35
2.2.4	Analysis methods .....	2.36
2.2.4.1	Instrumentation .....	2.36
2.2.4.2	Reagents and solutions.....	2.36
2.2.4.3	Dilution method .....	2.36
2.2.4.4	Memory effects .....	2.38
2.2.4.5	Sample preparation, analysis and calculations.....	2.38
2.3	Results and Discussion.....	2.39
2.3.1	Dilution method.....	2.39
2.3.2	Calibrations and blanks.....	2.39
2.3.3	Precision and detection limits .....	2.41
2.3.4	Accuracy .....	2.42
2.3.5	Reference ranges.....	2.45
2.4	Conclusions.....	2.46
2.5	Acknowledgements.....	2.47
Chapter 3	.....	3.49
3.1	Introduction.....	3.49
3.2	Methods .....	3.51
3.2.1	Environmental variables.....	3.52
3.2.1.1	Water elemental analysis.....	3.52
3.2.1.2	Smoothing of environmental data .....	3.56
3.2.2	Physiological variables.....	3.57
3.2.2.1	Gonadosomatic index (GSI).....	3.57
3.2.2.2	Blood proteins.....	3.59
3.2.2.3	Blood element concentrations.....	3.59
3.2.3	Data analysis .....	3.59
3.2.3.1	Summary of the variables included in the current chapter .....	3.59
3.2.3.2	Distribution coefficients (D).....	3.59
3.2.3.3	Data exploration and Pearson correlations.....	3.60
3.2.3.4	Linear mixed-effects models.....	3.60
3.3	Results.....	3.62
3.3.1	Physiological conditions.....	3.62
3.3.1.1	Correlations among physiological variables.....	3.65
3.3.2	Environmental conditions.....	3.66

3.3.2.1	Salinity, temperature and seawater element concentrations over time .....	3.66
3.3.2.2	Correlations between water element concentrations and environmental variables....	3.68
3.3.2.3	Description of blood element concentrations over time .....	3.70
3.3.2.4	Correlations among blood elemental concentrations and distribution coefficients....	3.73
3.3.2.5	Blood:water distribution coefficients .....	3.74
3.3.3	What are the primary influences on blood element concentrations? .....	3.76
3.3.3.1	Relationship between blood and ambient concentrations .....	3.76
3.3.3.2	Modelling blood element concentrations using environmental and physiological variables	3.77
3.4	Discussion.....	3.93
3.4.1	'Hard' elements .....	3.95
3.4.2	Calcium and strontium .....	3.97
3.4.3	The 'soft' elements .....	3.98
Chapter 4	.....	4.103
4.1	Introduction.....	4.103
4.2	Methods.....	4.105
4.2.1	Otolith analyses .....	4.105
4.2.1.1	Cleaning and mounting procedures.....	4.105
4.2.1.2	$\delta^{18}\text{O}$ analysis by SIMS (Cameca 1270) .....	4.108
4.2.1.3	Elemental analysis by SIMS (Cameca 4f).....	4.109
4.2.1.4	Elemental analysis by HR-ICPMS .....	4.111
4.2.2	Otolith timelines, growth rates and opacity.....	4.113
4.2.3	Data analysis .....	4.116
4.2.3.1	Distribution coefficients (D).....	4.116
4.2.3.2	Linear mixed effects modelling .....	4.117
4.3	Results .....	4.118
4.3.1	Physiological conditions.....	4.118
4.3.2	Otolith growth rates and opacity .....	4.118
4.3.3	Patterns among otolith elements.....	4.122
4.3.4	Time matching using $\delta^{18}\text{O}$ values.....	4.122
4.3.5	Descriptions of otolith elemental concentrations over time .....	4.125
4.3.6	Element fractionation from blood to otolith and water to otolith .....	4.128
4.3.6.1	Patterns in distribution coefficients.....	4.128
4.3.6.2	Element fractionation: blood to otolith .....	4.130

4.3.6.3	Element fractionation: seawater to otolith .....	4.130
4.3.7	Modelling otolith elemental concentrations.....	4.134
4.3.7.1	Were otolith element concentrations correlated with ambient water and/or blood concentrations?.....	4.134
4.3.7.2	Which variables best explain variation in otolith elemental concentrations and otolith:blood distribution coefficients? .....	4.135
4.4	Discussion.....	4.148
4.4.1	$\text{Li}_\text{O}$ and $\text{K}_\text{O}$ .....	4.149
4.4.2	$\text{Mn}_\text{O}$ and $\text{Mg}_\text{O}$ .....	4.150
4.4.3	$\text{Sr}_\text{O}$ and $\text{Ba}_\text{O}$ .....	4.152
4.4.4	$\text{Cu}_\text{O}$ and $\text{Zn}_\text{O}$ .....	4.153
Chapter 5	.....	5.155
5.1	Introduction.....	5.155
5.2	Methods .....	5.161
5.2.1	Analytical methods.....	5.161
5.2.2	Description of study animals.....	5.162
5.2.3	Data analysis .....	5.166
5.3	Results.....	5.167
5.3.1	Environmental and physiological trends.....	5.167
5.3.2	Otolith elemental concentrations vs. environmental and physiological variables in wild plaice	5.170
5.3.2.1	Lithium .....	5.170
5.3.2.2	Manganese .....	5.174
5.3.2.3	Strontium.....	5.176
5.3.2.4	Barium .....	5.182
5.3.3	Temporal trends in otolith elemental concentrations within fish.....	5.186
5.3.4	Otolith oxygen stable isotopic composition.....	5.189
5.3.5	Evidence for repeat migrations?.....	5.189
5.4	Discussion.....	5.192
5.4.1	Lithium.....	5.192
5.4.2	Manganese.....	5.194
5.4.3	Strontium .....	5.195
5.4.4	Barium.....	5.196
5.4.5	Implications and applications .....	5.200

Chapter 6.....	6.203
Conclusions .....	6.203
6.1    Otolith element concentrations as natural tags .....	6.205
6.2    Limitations of the current study .....	6.206
6.3    Future directions.....	6.207
References.....	6.209
Appendix .....	A1

# List of figures

Figure 1.1 Yearly numbers of publications featuring otolith chemistry over the past two decades.....	1.5
Figure 1.2 Schematic summarising the chemical behaviour of key elements used in otolith research.....	1.8
Figure 2.1 Map of the UK showing locations of collection sites in the Irish Sea and English Channel, and the location of the CEFAS aquarium in Lowestoft .....	2.33
Figure 2.2 Internal standard counts (Be, Rh, and Re) in fish plasma and Seronorm diluted with Mix 1 and Mix 2.....	2.40
Figure 3.1 Concentrations of Li, Rb and Sr for the same seawater samples measured on the X-Series ICPMS and Element 2 HR-ICPMS.....	3.55
Figure 3.2 Method for measuring the area of the ovary shadow using Image J software .....	3.58
Figure 3.3 Relationship between ovary area and mass .....	3.58
Figure 3.4 Monthly average condition, somatic growth rate, blood protein and gonadosomatic index (GSI) of plaice sampled from 02/06/09 to 28/05/10.....	3.64
Figure 3.5 Distributions, scatterplots and Pearson pairwise correlations among physiological variables, temperature and salinity .....	3.65
Figure 3.6 Temperature and salinity of the CEFAS aquarium seawater over the experimental period.....	3.67
Figure 3.7 Element concentrations and element/Ca ratios in seawater samples during the experimental period.....	3.69
Figure 3.8 Monthly average blood elemental concentrations in plaice sampled from 02/06/09 to 28/05/10 .....	3.72
Figure 3.9 Monthly average distribution coefficients ( $D = [\text{element}]_{\text{blood}} / [\text{element}]_{\text{water}}$ ) in plaice sampled from 02/06/09 to 28/05/10 .....	3.75
Figure 3.10 Patterns in $\text{Li}_B$ .....	3.79
Figure 3.11 Patterns in $\text{K}_B$ .....	3.80
Figure 3.12 Patterns in $\text{Mg}_B$ .....	3.81
Figure 3.13 Patterns in $\text{Ca}_B$ .....	3.83
Figure 3.14 Patterns in $\text{Sr}_B$ .....	3.84
Figure 3.15 The relationship between $\text{Ca}_B$ and $\text{Sr}_B$ concentrations in females and males .....	3.84
Figure 3.16 Patterns in $\text{Ba}_B$ .....	3.85
Figure 3.17 Patterns in $\text{Mn}_B$ .....	3.87
Figure 3.18 Patterns in $\text{Cu}_B$ .....	3.88
Figure 3.19 Patterns in $\text{Zn}_B$ .....	3.90

Figure 3.20 Patterns in $Se_B$ .....	3.91
Figure 3.21 Patterns in $Pb_B$ .....	3.92
Figure 4.1 Plaice sagittae and otolith sections.....	4.107
Figure 4.2 Internal precision of SIMS $\delta^{18}O$ analyses over time. ....	4.108
Figure 4.3 Graph showing the calibration curve for Ba/Ca concentrations based on three standards (M93, Haxby and Oka).....	4.110
Figure 4.4 An example of the "wiggle matching" carried out in AnalySeries 2.0.....	4.114
Figure 4.5 Photograph of a frontal otolith section under reflected light showing pits left from the three types of analyses used in the current study .....	4.115
Figure 4.6 Somatic vs. otolith daily growth rates.....	4.119
Figure 4.7 Average otolith growth rate in plaice sampled from 02/06/09 to 28/05/10.....	4.120
Figure 4.8 Monthly proportion of otoliths exhibiting opaque growth in plaice sampled from 02/06/09 to 28/05/10.....	4.121
Figure 4.9 Plot showing measured vs. predicted $\delta^{18}O$ measurements from experimental plaice maintained under ambient, but monitored conditions for 12 months. ....	4.123
Figure 4.10 Example of an otolith ("DC062", mature IS female) for which growth was elevated in the first half of the experiment. ....	4.124
Figure 4.11 Monthly average otolith element concentrations for 19 experimental plaice sampled from 02/06/09 to 28/05/10.....	4.127
Figure 4.12 Monthly average blood El/Ca ratios for 19 plaice sampled from 02/06/09 to 28/05/10 .....	4.131
Figure 4.13 Monthly average distribution coefficients for otolith:blood element concentrations and element/Ca ratios ( $D_{El(o/b)}$ and $D_{El/Ca(o/b)}$ , respectively) for 19 experimental plaice sampled from 02/06/09 to 28/05/10.....	4.132
Figure 4.14 Monthly average distribution coefficients for otolith:seawater element concentrations and element/Ca ratios ( $D_{El(o/b)}$ and $D_{El/Ca(o/b)}$ , respectively) for 19 experimental plaice sampled from 02/06/09 to 28/05/10.....	4.133
Figure 4.15 Patterns in $Li_O$ .....	4.138
Figure 4.16 Patterns in $D_{K(O/B)}$ .....	4.138
Figure 4.17 Patterns in $Mg_O$ and $D_{Mg(O/B)}$ .....	4.140
Figure 4.18 Patterns in $Sr_O$ and $D_{Sr(O/B)}$ .....	4.141
Figure 4.19 Patterns in $Ba_O$ and $D_{Ba(O/B)}$ .....	4.143
Figure 4.20 Patterns in $Mn_O$ and $D_{Mn(O/B)}$ .....	4.144
Figure 4.21 Patterns in $Cu_O$ and $D_{Cu(O/B)}$ .....	4.146
Figure 4.22 Patterns in $Zn_O$ and $D_{Zn(O/B)}$ .....	4.147

Figure 5.1 Variation in Sr/Ca ratios in female plaice otoliths exhibiting four migration types.....	5.157
Figure 5.2 Plaice population sub-units.....	5.158
Figure 5.3 Migration pathways, details and temperature histories of four WNS (blue subunit) plaice.....	5.163
Figure 5.4 Migration pathways, details and temperature histories of four CNS (red subunit) plaice.....	5.164
Figure 5.5 Migration pathways, details and temperature histories of three ENS (green subunit) plaice ...	5.165
Figure 5.6 Average monthly DST recorded temperature for the eleven featured plaice. ....	5.168
Figure 5.7 (A) Average monthly GETM-estimated salinity for the eleven featured plaice and (B) longitudinal gradients in salinity.....	5.168
Figure 5.8 Boxplots showing the differences in end condition, otolith growth rate and age between the tagged males and females featured in the current study.....	5.169
Figure 5.9 Boxplots to show trends in $\text{Li}_\text{O}$ over time and among North Sea population subunits.....	5.171
Figure 5.10 Trends in $\text{Li}_\text{O}$ in wild plaice tagged by DST.....	5.172
Figure 5.11 $\text{Li}_\text{O}$ concentrations over time for the two pairs of male and female fish from the WNS and CNS during the tagged period .....	5.173
Figure 5.12 Boxplots to show trends in $\text{Mn}_\text{O}$ over time .....	5.174
Figure 5.13 Trends in $\text{Mn}_\text{O}$ in wild plaice tagged with DST.....	5.175
Figure 5.14 Boxplots to show trends in $\text{Sr}_\text{O}$ over time and among North Sea population subunits (separated by sex) in DST tagged plaice. ....	5.177
Figure 5.15 Trends in $\text{Sr}_\text{O}$ concentrations in wild plaice tagged with DST .....	5.178
Figure 5.16 SIMS-measured $\text{Sr}_\text{O}$ profiles for five fish released in October 2004; three from the central North Sea and two from the western subunit.....	5.179
Figure 5.17 Boxplot showing $\text{Sr}_\text{O}$ in females and males during spawning and non-spawning seasons. ....	5.181
Figure 5.18 Relationship between $\text{Sr}/\text{Ca}_\text{O}$ variance during time at liberty vs. migration area.....	5.181
Figure 5.19 Boxplots to show trends in $\text{Ba}_\text{O}$ over time and among North Sea subunits by season in DST tagged plaice.....	5.183
Figure 5.20 Trends in $\text{Ba}_\text{O}$ in wild plaice tagged by DST .....	5.184
Figure 5.21 Exploring differences in $\text{Ba}_\text{O}$ among population subunits.....	5.185
Figure 5.22 Trace element profiles for 4 DST tagged plaice .....	5.187
Figure 5.23 Trace element profiles for 4 DST tagged plaice. ....	5.188
Figure 5.24 Average otolith $\delta^{18}\text{O}$ for plaice from blue (WNS), red (CNS) and green (ENS) subunits....	5.190
Figure 5.25 (A) Otolith $\delta^{18}\text{O}$ and $\text{Ba}_\text{O}$ profiles for the final 4 years of A12522 (CNS male) and (B) $\delta^{18}\text{O}$ and $\text{Li}_\text{O}$ profiles for the final 2 years of A12454 (WNS female).....	5.191
Figure 5.26 Temporal variations in $\text{Li}_\text{O}$ and $\text{Ba}_\text{O}$ concentrations for WNS male A12382. ....	5.199

# List of tables

Table 1.1 Review of significant and non-significant (NS) effects of different influences (water chemistry, temperature, diet, vital and intrinsic effects) on otolith element concentrations and their partition coefficients,.....	1.12
Table 2.1 Concentrations of 14 elements in serum (S), plasma (P) or whole blood (B) collected from fish inhabiting freshwater (FW) or seawater (SW). .....	2.28
Table 2.2 Isotopes, resolutions and operating conditions for HR-ICPMS .....	2.37
Table 2.3 Concentration ranges for external calibration of fish plasma and Seronorm.....	2.37
Table 2.4 Contents of the dilution mixtures .....	2.37
Table 2.5 Average detection limits and precision for plaice plasma and Seronorm analyses.....	2.42
Table 2.6 Measured concentrations and reference ranges for 12 elements in male and female plaice plasma and Seronorm .....	2.43
Table 3.1 Collection details for the environmental variables measured during the aquarium study.....	3.52
Table 3.2 Isotopes and operating conditions for seawater analyses on the X-Series ICPMS and Element 2 HR-ICPMS.....	3.54
Table 3.3 Detection limits and average internal and external precision for seawater analyses carried out on the X-Series ICPMS and Element 2 HR-ICPMS .....	3.56
Table 3.4 Details of the physiological variables measured each month during the aquarium study.....	3.57
Table 3.5 Physiological and environmental variables measured as possible controls on plaice blood elemental concentrations. Element concentrations are divided among broad chemical groups .....	3.60
Table 3.6 Average total length, total weight, growth rate, Fulton's condition factor, gonadosomatic index and age of subject animals presented in the current chapter at the end of the experiment (28/05/10) .....	3.63
Table 3.7 Pearson product-moment correlation coefficients (PCCs) for pairwise comparisons between temperature, salinity and seawater element concentrations.....	3.68
Table 3.8 PCCs for pairwise comparisons of temperature, salinity and (A) blood element concentrations and (B) blood/seawater distribution coefficients,.....	3.73
Table 3.9 Average distribution coefficients ( $D_{EI(B/W)}$ ) for blood plasma vs. water element concentrations for all samples in the current study and whole blood vs. water element concentrations for two freshwater species (Melancon <i>et al.</i> , 2009).....	3.74
Table 3.10 Pearson's product Correlation Coefficients (PCC) for pairwise comparisons of blood and water elemental concentrations and the data transformations used in the remainder of the statistical analyses. ....	3.76

Table 3.11 Summary of linear mixed effects model outputs for blood element concentrations in 25 experimental plaice sampled c.monthly for one year.....	3.78
Table 4.1 Standard bulk concentrations for three calcite reference materials, Oka, Haxby and M93. External inter-day precision provided in parentheses .....	4.109
Table 4.2 Analysis and operating details used for LA-HR-ICPMS analyses of frontal otolith sections.....	4.112
Table 4.3 Detection limits and external precision for LA-HR-ICPMS analyses.....	4.112
Table 4.4 Elemental, physiological and environmental variables examined in the current study.....	4.116
Table 4.5 Average total length , total weight, somatic and otolith growth rate, Fulton's condition factor, gonadosomatic index (GSI) and age of subject animals presented in the current chapter at the end of the experiment (28/05/10).....	4.118
Table 4.6 Correlation coefficients for pairwise comparisons of somatic and otolith daily growth rates for all experimental plaice.....	4.119
Table 4.7 Correlation coefficients for pairwise comparisons of otolith element concentrations.....	4.122
Table 4.8 Average and range for distribution coefficients for element concentrations and element/Ca ratios between otoliths and blood (O/B), and otoliths and seawater (O/W). .....	4.128
Table 4.9 Table showing average distribution coefficients for element/Ca ratios between otolith and water ( $D_{El/Ca(O/W)}$ ) for the current study alongside values from the literature .....	4.129
Table 4.10 Pearson product-moment correlation coefficients for fitted otolith element concentrations and concomitant concentrations in the water and blood for the experimental plaice.....	4.134
Table 4.11 Linear mixed effects model outputs for otolith element concentrations otoliths of 19 experimental plaice.....	4.136
Table 4.12 Linear mixed effects model outputs for otolith:blood distribution coefficients ( $D_{El(o/b)}$ ) for 19 experimental plaice.....	4.137
Table 5.1 Details for the 11 fish presented in the current chapter, ordered by population subunit ( .....	5.162
Table 5.2 Results from mixed effects model analyses for the four selected elements in otoliths of the DST fish .....	5.180

# List of abbreviations

A/G	Albumin: globulin ratio
Ba	Barium
Bi	Bismuth
BSA	Bovine Serum Albumin
Ca	Calcium
CaCO <sub>3</sub>	Calcium carbonate
Cl	Chlorine
Cu	Copper
$\delta^{13}\text{C}$	Measure of the ratio of <sup>13</sup> C: <sup>12</sup> C
$\delta^{18}\text{O}$	Measure of the ratio of <sup>18</sup> O: <sup>16</sup> O
DST	Data Storage Tag
GnRH	Gondotropin releasing hormone
GSI	Gonadosomatic index
HCl	Hydrochloric acid
HNO <sub>3</sub>	Nitric acid
ICPMS	Inductively coupled plasma mass spectrometry
LA- ICPMS	Laser ablation inductively coupled plasma-mass spectrometry
Pb	Lead
Li	Lithium
Me/Ca	Metal/Calcium ratio
Mg	Magnesium
Mn	Manganese
MQ	Milli-Q water (18.2 $\Omega$ resistance)
Na	Sodium
NS	North Sea or non-significant
O	Oxygen
OTC	Oxytetracycline
POF	Post-ovulatory follicles
ppb	parts per billion
ppm	parts per million
ppt	parts per thousand
PIT	Passive Integrated Transponder
permil (‰)	permil (parts per thousand). Notation used for stable isotope ratios
K	Potassium
Rb	Rubidium
sGnRHa	Salmon gondotropin releasing hormone analogue
SIMS	Secondary Ion Mass Spectrometry
Sr/Ca	Strontium/calcium ratio
Sc	Scandium
Se	Selenium
SSB	Spawning stock biomass
Sr	Strontium
TL	Total length
TW	Total weight
Zn	Zinc

## **Declaration of authorship**

I, Anna Michelle Sturrock, declare that this thesis and the work presented in it are my own and has been generated by me as the result of my own original research.

### **Environmental and physiological influences on otolith chemistry in a marine fish**

I confirm that:

1. This work was done wholly or mainly while in candidature for a research degree at this University;
2. Where any part of this thesis has previously been submitted for a degree or any other qualification at this University or any other institution, this has been clearly stated;
3. Where I have consulted the published work of others, this is always clearly attributed;
4. Where I have quoted from the work of others, the source is always given. With the exception of such quotations, this thesis is entirely my own work;
5. I have acknowledged all main sources of help;
6. Where the thesis is based on work done by myself jointly with others, I have made clear exactly what was done by others and what I have contributed myself;
7. None of this work has been published before submission

Signed: .....

Date: .....



# Acknowledgements

I would firstly like to thank Clive Trueman & Ewan Hunter for being such wonderful supervisors. Your expertise, patience and friendship were so much appreciated - I feel privileged to have worked with you both. You both went well beyond the call of duty, for which I am extremely grateful.

I would also like to express my sincere gratitude to the FSBI for providing financial support in the form of a studentship and grants to attend the Otolith Symposium in 2009 and the 2011 FSBI meeting. I would like to thank Rob Britton and Ian McCarthy for their mentorship and Gordon Copp for all his work as treasurer.

At NOCS, I am deeply indebted to Andy Milton and Matt Cooper for their never ending support in the lab – patiently working through calculations and samples with me and staying late on countless occasions! Many thanks also to Antony Jensen and Martin Palmer for useful advice and support through many meetings, and Antony for helping me so much in the field. Also my heartfelt thanks go to Bob and John for all their help, humour and advice when preparing samples. I also greatly appreciate the statistical advice and various pieces of code provided by Peter Challenor (NOCS), Rich Inger and Xavier Harrison (University of Exeter).

At CEFAS, I have so many people to thank for keeping the experiment running smoothly. Firstly, thanks to Christie Stewart, Julian Metcalfe, Stuart Hetherington, Matt Eade, Sam Roslyn and Matt Smith, for their calm advice and hands on support keeping the experiment running smoothly. I would also like to thank Alexander Scott, Johan van der Molen, Glenn Saunders, Andy Smith, Stefan White, Lorraine Greenwood, Steve Milligan, Antonio Pliru, James Pettigrew, James Hammond, Michael Godard and Lucia Privitera for their advice and efforts before, during and after the experiment. Thanks also to Christie, Sophie and Ewan for having me to stay all those times when I was homeless in East Anglia! Now based in Montpelier, the hard work that Audrey Darnaude put into getting the DST fish-otolith project up and running when she was at CEFAS was hugely appreciated, as was all her advice and support throughout the current project.

At EIMF, the Herculean efforts of John Craven, Richard Hinton, Cees-Jan De Hoog and Mike Hall must be acknowledged, particularly John for spending such long hours getting through that Christmas backlog. Their help and support has been immense and truly appreciated.

At University of Portsmouth, I am so grateful to Colin Waring and Gary Fones for their help and generosity in the lab, and to everyone at the Institute of Marine Sciences for making me feel so welcome. The patience with which Colin let mess up his incredibly orderly lab and leave piles of washing up was quite remarkable!

Thanks also to Jim Kennedy (Moreforsking Marin) for his advice and help and to Cindy Van Damme (IMARES) and Gary Wordsworth (Othniel) for their advice and provision of samples

I would like to express my deepest gratitude to Audrey Geffen and Jon Copley for their patience and understanding with the quick turn around time on the viva! Their thoughtful and interesting comments and corrections were very helpful for improving the thesis and I genuinely enjoyed the lively viva discussion.

Finally, I would like to express my deepest gratitude to my wonderful husband for helping me through those “R moments”, and for sticking up with my odd fish obsession! I would also like to thank my family and friends, particularly Mike, Ed, Debs, Ally, Jess, Jessy, Clara, Michael, Si, Andy, Hamish, Nico, Libby and Adrian, for all their amazing love and support (...read chocolate and caffeine!), and most of all my wonderful mum for looking after me so well during the write up. I couldn’t have done it without you.

# Chapter 1

---

## *General Introduction*

*This chapter has been slightly adapted from a review article recently accepted for publication in Journal of Fish Biology: “A. Sturrock, C. Trueman, A. Darnaude & E. Hunter. **Can otolith microchemistry track individual movements of fully marine fish?**”. It was written by A. Sturrock, but included feedback from all co-authors, particularly from C. Trueman in Section 1.3.1.*

### 1.1 Abstract

Otolith microchemistry can provide valuable information about stock structure and mixing patterns of fully marine fish when the magnitude of environmental differences among areas is greater than the cumulative influence of any ‘vital effects’. Here, the current understanding of the underlying mechanisms governing element incorporation into the otolith is reviewed. ‘Hard and soft acid and base’ (HSAB) theory is employed to explore the differences in chemical behaviours, distributions and affinities between elements. Hard acid cations (e.g.  $\text{Sr}^{2+}$ ,  $\text{Li}^+$ ,  $\text{Ba}^{2+}$ ) tend to be less physiologically influenced and accepted more readily into the otolith crystal lattice but are relatively homogeneous in seawater. Soft acid cations (e.g.  $\text{Zn}^{2+}$ ,  $\text{Cu}^{2+}$ ) on the other hand, exhibit more varied distributions in seawater, but are more likely to be bound to blood proteins and less available for uptake into the otolith. The factors influencing the geographical distribution of elements in the sea, and their incorporation into the otoliths of fully marine fish are reviewed. Particular emphasis is placed on examining physiological processes, including gonad development, on the uptake of elements commonly used in population studies, notably Sr. Finally, a selection of case studies is presented that either directly or indirectly compare population structuring or movements inferred by otolith elemental

fingerprints with the patterns indicated by additional, alternative proxies. The main obstacle currently limiting the application of otolith elemental microchemistry to infer individual movements of marine fish appears to lie in the largely homogeneous distribution of those elements most reliably measured in the otolith. Evolving technologies will improve the discriminatory power of otolith chemistry by allowing measurement of spatially explicit, low level elements; however, for the time being, the combination of otolith minor and trace element fingerprints with alternative proxies and (or) stable isotopic ratios can greatly extend the scope of migration studies. Among the otolith elements that routinely occur above instrument detection limits, Ba, Mn and Li are the most likely to prove reliable geographic markers in fully marine species.

## 1.2 Introduction

An understanding of the spatial structure of fish stocks and the connectivity within and between them is increasingly considered an important pre-requisite for sustainable fisheries management (Pulliam, 1988; Botsford *et al.*, 2009). The concept of “open” marine fish populations with individuals evenly distributed about a homogeneous environment is now largely redundant. Rather, marine habitats and their inhabitants are known to exhibit patchy distributions as a result of spatial and temporal shifts in physical (e.g. hydrodynamics, temperature, salinity) and biological (e.g. productivity, predator abundance) characteristics (Hixon *et al.*, 2002). Identifying such ‘patches’ is particularly challenging in the open ocean, given its vast, three-dimensional structure and scarcity of geographically and temporally stable boundaries. However, advances in satellite telemetry and remote sensing have greatly increased the sophistication with which water masses and their inhabitants can be linked (Sims *et al.*, 2006) and improved our understanding of the migratory behaviour of individual fish (e.g. Righton *et al.*, 2010; Block *et al.*, 2011).

Historically, catch data and mark-recapture experiments have formed the foundation of our broad understanding of marine fish distributions. However, the resolution of such data tends to be relatively coarse, with patterns inextricably linked to the distribution of the fishing fleets (e.g. Bolle *et al.*, 2005; Righton *et al.*, 2010). The use of pop-up satellite archival tags (PSATs) and electronic data storage tags (DSTs) has increased dramatically over the past decade, with improved miniaturisation and recording capacity allowing sometimes multi-year recordings of the ambient experience of individual fish (Metcalfe and Arnold, 1997; Hunter *et al.*, 2003a; Metcalfe *et al.*, 2006; Block *et al.*, 2011). These new technologies have provided exciting new insights into the migratory behaviours and mechanisms that underpin population structuring. Their use, however, is often precluded by cost, battery life, low rates of return and size constraints, with observations largely restricted to the adult phase in top predators.

In order to obtain a full picture of ontogenetic fish movements, a “toolbox” approach is required, where a range of independent techniques providing information at specific spatial and (or) temporal scales can be used to understand connectivity across life-history stages (Begg and Waldman, 1999; Fromentin *et al.*, 2009; Kaplan *et al.*, 2010). A number of natural tags are employed for this purpose, including stable isotopes in soft tissues (Rodgers and Wing, 2008), amino acid signatures (Riveiro *et al.*, 2011), molecular genetics (Cook *et al.*, 2007), parasite loadings (Sequeira *et al.*, 2010), phenotypic markers such as morphometrics (Lawton *et al.*, 2010), colour (Arnegard *et al.*, 1999) and otolith shape (Ferguson *et al.*, 2011), as well as the chemical composition of calcified structures such as otoliths and scales (Campana, 1999). Each method has shown potential for determining population structure and (or) discriminating among resident and migrant fish, however, otolith chemistry has shown the greatest promise for reconstructing lifetime movements. The technique relies on the basic assumption that as the otolith grows, chemical markers from the ambient environment are incorporated into its microstructure, resulting in a ‘fingerprint’ that reflects, at least in part, the physicochemical properties of the environment in which it was formed (e.g. Bath *et al.*, 2000; Elsdon and Gillanders, 2003a).

Otoliths are paired crystalline structures located in the inner ear of all bony fish, used for sound reception, maintaining equilibrium and processing directional cues (Popper and Fay, 2011). They display a number of key properties that have resulted in their chemical composition being increasingly exploited in the field of fish spatial dynamics. First, they exhibit unrivalled time-keeping properties. Otoliths develop very early in the fish’s life, usually during the embryonic stages, and grow continuously through daily accretions of calcium carbonate ( $\text{CaCO}_3$ ) aragonitic crystals onto a fibroprotein organic matrix (Campana and Neilson, 1985; Tohse and Mugiya, 2002; Payan *et al.*, 2004a). Diurnal and seasonal rhythms result in growth bands that have been used in the field of sclerochronology for over a century and provide a baseline for carrying out time-resolved chemical analyses (Campana and Thorrold, 2001). Second, as otoliths are acellular and metabolically inert, they are not reworked or resorbed, even during times of starvation (Campana and Neilson, 1985). Chemical fingerprints are thus retained permanently within the microstructure. Third, while the precise relationships are not always clear, there is no question that otolith composition is affected by environmental conditions. This has been exploited by studies using otolith shape and whole otolith chemistry to infer stock structure, and chemical patterns across growth bands to provide information across life history stages (Elsdon *et al.*, 2008). Fourth, otoliths are common to all teleost species, which is particularly appealing for investigating habitat use in inaccessible fish (e.g. from deep or remote environments), where external tags cannot be applied or are unlikely to be recovered. Finally, while otolith

processing and chemical analyses are not inexpensive, sample acquisition is equivalent to all individuals being tagged and the technique is often significantly cheaper than an equivalent tagging study (Fairclough *et al.*, 2011).

While the last two properties are common to most natural tags, the capacity of otoliths to record (and retain) time-resolved lifetime environmental histories provides unique opportunity for ‘geolocating’ individual fish in time and space. Accordingly, otolith microchemistry represents a hugely valuable resource: a means to infer past conditions, stock structure, connectivity patterns and individual migrations. Indeed, otolith microchemistry has appeared in almost 700 peer-reviewed papers to date (Web of Science search on 26.09.11, Topic=otolith chemistry OR otolith microchemistry) and growth within the field shows no sign of slowing (Figure 1.1). However, the precise mechanisms governing elemental incorporation into the otolith are still not fully understood (reviewed in Campana, 1999) and inconsistent patterns of element incorporation among species and studies undermine the routine application of otolith microchemistry to movement reconstruction (reviewed in Elsdon *et al.*, 2008). Here, we examine the use of otolith microchemistry, specifically minor and trace element concentrations, as a tool for describing the movements of fully marine fish. We review the current understanding of the mechanisms underpinning otolith microchemistry and discuss its application specifically within the marine environment. Finally, we present case studies that have used otolith microchemistry to infer spatial distributions of marine fish and attempted to validate their interpretations using alternative proxies.

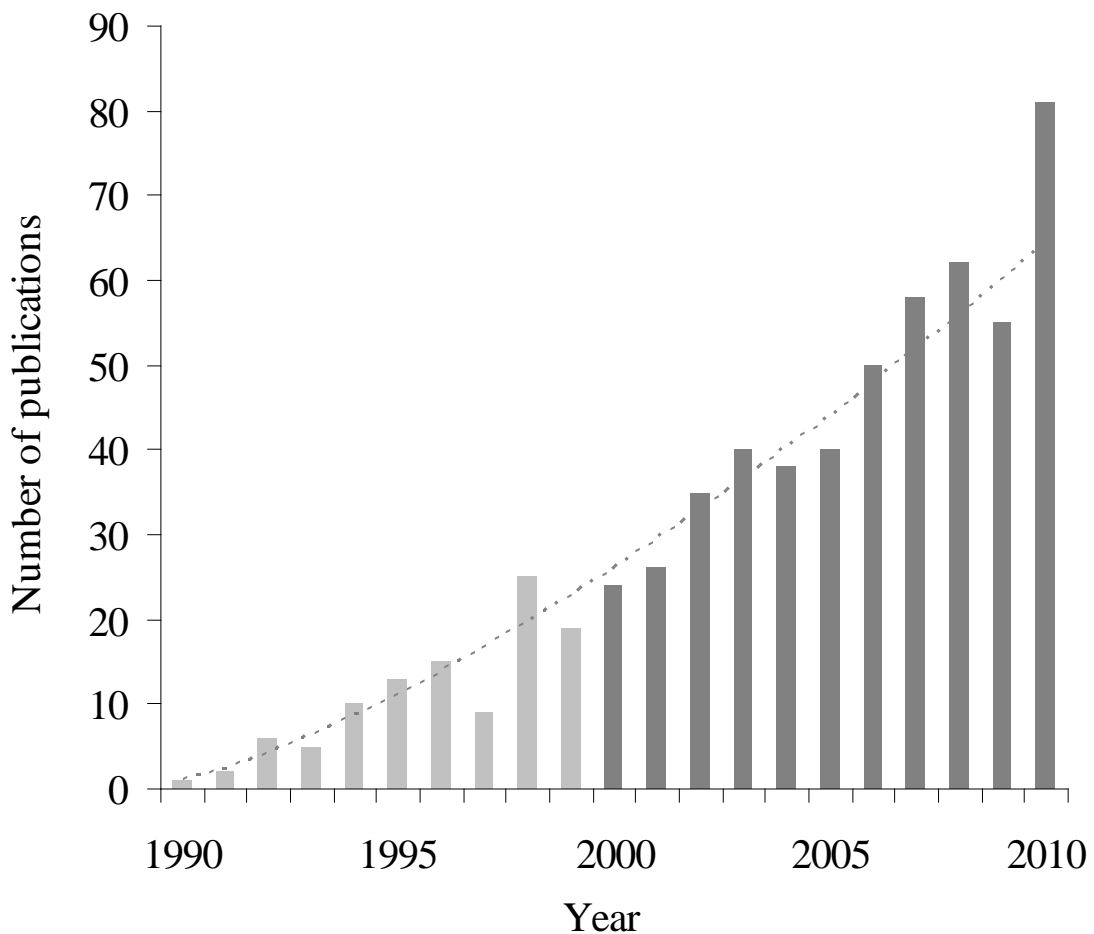


Figure 1.1 Yearly numbers of publications featuring otolith chemistry over the past two decades (Web of Science search on 26.09.11, Topic=otolith chemistry OR otolith microchemistry). Pale grey bars indicate years overlapping with Campana & Thorrold (2001). A power curve closely fits the data ( $y = 0.91x^{1.40}$ ,  $r^2 = 0.97$ ), although the sharp rise in 2010 can be explained, in part, by two special issues of Environmental Biology of Fishes dedicated to "Proceedings of the 4th International Otolith Symposium"

## 1.3 How does otolith microchemistry serve as an environmental tag?

### 1.3.1 Chemistry of relevant elements and the mechanisms governing their incorporation into the otolith

The mechanisms governing otolith formation are quite different to those controlling bone, shell and coral growth, as the otolith crystallises within the endolymph fluid and is not in direct contact with epithelial tissue or the surrounding water (Payan *et al.*, 2004a). Moreover, the mechanism of otolith crystal growth is biologically controlled, and thus likely to differ considerably to inorganic crystal precipitation from a saturated solution (Weiner, 2008). Element incorporation into otolith aragonite is a complex, multistage process, involving the movement of ions from the ambient water into the blood plasma via branchial or intestinal uptake, across inner ear membranes into the endolymph fluid, and finally into the growing surface of the otolith (Payan *et al.*, 2004a). As such, elemental discrimination can occur at any of four major interfaces: environment-blood, blood-blood binding proteins, blood-endolymph and endolymph-otolith (Campana, 1999). Changes in element concentrations across these four interfaces provide a tangible means to examine their relative control on elemental fractionation. Here, it is useful to consider the similarities and differences in chemical affinities and behaviours between elements. In the 1960s, chemists developed a concept known as “hard and soft acid and base” (HSAB) theory (Pearson, 1963). HSAB theory categorises reactants as acids or bases, depending on whether they donate or accept electrons within a reaction, and as hard, soft or intermediate, depending on their polarisability, oxidation state and electronegativity (Figure 1.2). Hard acids and bases are typically small ions or molecules with relatively high charge density that are weakly polarisable. Soft acids and bases tend to be large and strongly polarisable. The value of this concept is that acids and bases form strong bonds when binding with similar counterparts (i.e. hard acids form stronger bonds with hard bases and soft acids with soft bases). In a dynamic medium like seawater, and particularly blood plasma, where the number of available ligands outweighs the number of metal ions, strong bonds will tend to dominate the speciation of any elemental ion, and the behaviour of elements can be loosely predicted (Williams, 1971).

So far, 50 elements have been detected in otoliths, at major (Ca, C, O, N), minor (>100ppm: Cl, S, Mg, Na, P, Sr, and K) and trace levels (<100ppm: Ag, Al, As, B, Ba, Bi, Br, Cd, Ce, Co, Cr, Cs, Cu, Dy, Er, Fe, Gd, Hg, Ho, La, Li, Lu, Mn, Nd, Ni, Pb, Pr, Rb, Sc, Se, Si, Sm, Tb, Tm, U, V, Y, Yb, Zn) (Campana, 1999; Chen and Jones, 2006). However, only seven elements are routinely used to infer past location in fish (Li, Mg, Mn, Cu, Zn, Sr and Ba; Fig. 2), due to their environmental heterogeneity and otolith concentrations often above detection limits. In seawater, hard acid ions such as  $\text{Li}^+$ ,  $\text{Mg}^{2+}$ ,  $\text{Ca}^{2+}$ ,  $\text{Sr}^{2+}$  and  $\text{Ba}^{2+}$  form strong bonds with

$\cdot\text{OH}$  radicals and are mainly found as hydrated free ions (Figure 1.2). These ions typically have a residence time longer than the mixing time of the ocean and consequently their concentrations tend to vary with salinity. By contrast, soft and intermediate acid ions such as  $\text{Cu}^{2+}$ ,  $\text{Zn}^{2+}$  and (to a lesser extent)  $\text{Mn}^{2+}$ , bind to softer bases in seawater such as  $\text{Cl}^-$  and  $\text{CO}_3^{2-}$ . These bonds are relatively weak, making soft elements reactive and readily removed from seawater (Henderson, 1984).

Little is known about the relative bioavailability of different elements to being taken up in marine fish, but it is likely that they will be fractionated from one another during transport across the gut, gills and skin.

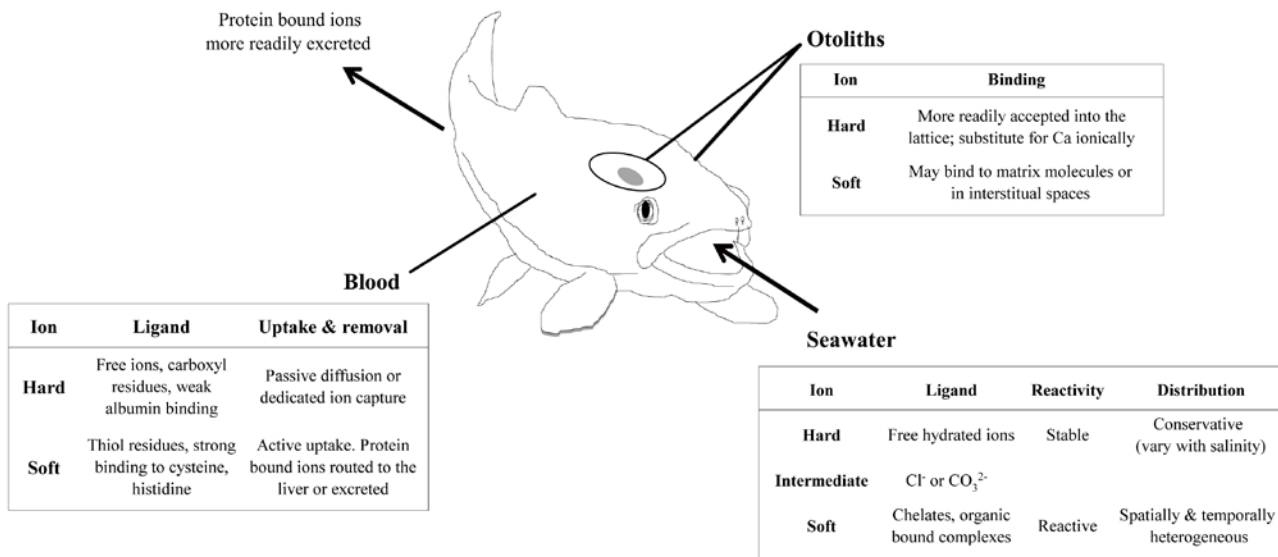
Osmoregulation is largely effected across gut membranes, particularly in marine species (Smith, 1930), and maintains relatively constant concentrations of blood Ca, Na, K, Mg and Cl in marine and freshwater fish despite considerable differences in ambient concentrations (Campana, 1999). Once within the circulatory system, the transport, availability and ultimate fate of elements will depend on their chemical characteristics and requirement in metabolic reactions, as well as the composition of the blood fluid. Elements that are constituent parts of functioning enzymes or structural tissues are likely to have relatively long mean residence times in the body due to the continued recycling of enzymes and tissues. By comparison, elements with no major structural or physiological role may be removed rapidly, resulting in low residence times. Exceptions include the quintessentially toxic metals (Cd, Pb, Hg), which have very long residence times due to comparatively ineffective excretion mechanisms (Williams, 1971). The relative timing of elemental changes across an otolith may therefore reflect differences in turnover times and the number of body pools for those particular elements. Elements with short turnover times (e.g. Mn, Ba) may be better suited to studying detailed temporal changes than elements with potentially longer turnover times (e.g. Sr, Pb).

In the blood plasma, soft acid cations such as  $\text{Cu}^{2+}$ ,  $\text{Zn}^{2+}$  and possibly  $\text{Mn}^{2+}$  are actively bound to the histidine, methionine and cysteine residues of plasma proteins and used in metabolic reactions or actively transported to the liver where they are excreted (Watanabe *et al.*, 1997). Less than 10% of total blood Cu (Williams, 1971) and less than 1% of Zn (Fletcher and Fletcher, 1980) are estimated to be present as free ions. Hard acid cations (e.g.  $\text{Li}^+$ ,  $\text{Mg}^{2+}$ ,  $\text{Ca}^{2+}$ ,  $\text{Sr}^{2+}$  and  $\text{Ba}^{2+}$ ) on the other hand, are largely transported as free ions or weakly bound to small molecular complexes, albumins or globulins (Williams, 1971). Calcium (and Ca homologues) may also be strongly bound to carboxyl residues in Ca-binding proteins, allowing plasma Ca to be divided into protein bound (30-40%) and ultrafiltrable fractions (60-70%). The ultrafiltrable fraction is dominated by ionised Ca, meaning that more than 50% of total Ca (and thus probably Sr) is estimated to be present in plasma as the free ion (Mugiy, 1966; Andreasen, 1985; Hanssen *et al.*, 1989). Therefore, hard and soft acid ions are very likely to be fractionated from one another within the blood plasma.

Figure 1.2 Schematic summarising the chemical behaviour of key elements used in otolith research. ‘Hard’ acid elements such as Mg, Sr, Ca and Ba are typically held as hydrated ion complexes in both seawater and blood and their relative concentrations will be passed to otoliths with less influence from blood protein chemistry. By contrast, ‘soft’ acid elements such as Cu and Pb are strongly bound to organic ligands and have a greater affinity for protein-binding in blood. The practical outcome is that while soft ions hold greater promise for geolocating in marine settings, they are also the ions most susceptible to physiological fractionation in the body. Figure is based on “hard and soft acid and base” (HSAB) theory and data in Williams (1971), Henderson (1984) and Kaim and Schwederski (1994).

Hard soft acid base (HSAB)	Element	Type of distribution <sup>†</sup>	Ocean residence time (yrs)	Ion radius	Charge	Electronegativity
<b>Hard</b>	Li	c	$10^8$	0.76	1+	0.98
	Mg	c	$10^8$	0.72	2+	1.31
	Ca	almost c	$10^8$	1	2+	1
	Sr	almost c	$10^8$	1.18	2+	0.95
	Ba	n	$10^4$	1.35	2+	0.89
<b>Intermediate</b>	Mn	s	$10^4$	0.67	2+	1.55
	Zn	n	$10^4$	0.74	2+	1.65
<b>Soft</b>	Cu	s + n	$10^4$	0.77	2+	1.9

<sup>†</sup> c = conservative, s = scavenged, n = nutrient-like (after Steele et al., 2009)



Mg may behave somewhat differently to other Group II elements due to an ionic radius that is very small unless hydrated, when it becomes extremely large (Kaim and Schwederski, 1994). Moreover, it has been implicated in stabilising amorphous mineral phases during otolith biomineralisation and, due to its participation in a number of biological processes, is tightly regulated in the body (Weiner, 2008).

Because the speciation of metal ions within blood plasma is dynamic, it is likely that blood chemistry, particularly the composition and relative abundances of blood proteins, will influence the proportion of free ions, and thus affect their ability to cross the plasma-endolymph membrane barrier (Kalish, 1991).

Physiological variation in the composition of blood plasma proteins is more likely to influence the soft acid ions, as they are more strongly associated with blood proteins. However, depletion of all major elements in the endolymph except K (Kalish, 1991) indicates active discrimination against most ion types by the saccular epithelium (Payan *et al.*, 2004a).

Finally, incorporation of an element into the otolith depends on its compatibility to bind directly into the crystal lattice, within interstitial spaces or to the organic matrix (Campana, 1999). Based on HSAB theory, the strong protein binding affinities of soft metals will likely favour their incorporation into the otolith bound to the organic matrix. This is corroborated by spatial heterogeneity in otolith Cu (Milton *et al.*, 2000; Milton and Chinery, 2001b) and an estimated 70-100% of otolith Cu and 40-60% of otolith Zn associated with the protein matrix (Miller *et al.*, 2006). Inclusion of elements within the otolith mineral phase occurs (i) via substitution for Ca, where partitioning will be controlled by ion charge, radius and crystal elasticity influences, (ii) within dislocation sites on the growing crystal surface, where partitioning may be controlled by kinetic influences such as precipitation rate (Reeder and Rakovan, 1999), or (iii) possibly through inclusion in amorphous precursor mineral phases (Weiner, 2008). Fractionation of elements during their incorporation into the otolith is further complicated by additional effects of temperature. It is debatable whether any such temperature effects are direct or indirect however, with many studies attributing them to physiological processes, such as growth rate, which are in turn controlled by ambient temperatures. Walther *et al.* (2010) discuss possible mechanisms underpinning 'growth rate effects' on otolith microchemistry, grouping them into 2 broad types: mineralogical kinetic and physiological. Kinetic hypotheses include greater entrapment of trace element impurities into the growing crystal at higher temperatures, due to faster growth and increased numbers of crystal defects (Gaetani and Cohen, 2006). Another 'kinetic hypothesis' relates faster accretion rates with greater supply of  $\text{Ca}^{2+}$  ions to the endolymph, effectively diluting the other elements within the precipitating fluid (Sinclair, 2005). While crystal growth rate has been shown to influence elemental partitioning during abiotic  $\text{CaCO}_3$  formation, biogenic  $\text{CaCO}_3$  forms via a transient

amorphous phase associated with the organic matrix (Weiner, 2008), thus extrapolating patterns directly from inorganic crystal theory is potentially misleading. Finally, the ‘physiological hypothesis’ is based on the coupling of somatic growth rates with protein synthesis, with significant changes in growth rate affecting the protein composition of biological fluids and the availability of ions for uptake into the otolith (Kalish, 1991).

### 1.3.2 Influences on otolith microchemistry

In the early days of otolith microchemistry, it was assumed that trace elements would be incorporated into the otolith in proportion to their availability in the surrounding water. For most elements, this is now known not to be the case (Table I). However, positive relationships have been observed between ambient and otolith concentrations for a number of elements, particularly the hard acid elements, Sr and Ba. It is estimated that marine fish derive 83% and 98% of their otolith Sr and Ba from the surrounding water, respectively (Walther and Thorrold, 2006). Occasionally, freshwater systems exhibit Sr concentrations higher than marine systems (e.g. Kraus and Secor, 2004; Elsdon and Gillanders, 2005a), but water Sr generally follows a quasiconservative distribution, allowing otolith Sr/Ca ratios to act as a powerful marker of movement across extreme salinity gradients. As such, otolith Sr/Ca ratios are fairly routinely applied to reconstructing migrations of diadromous species (e.g. Kalish, 1990; Babaluk *et al.*, 1997; Secor *et al.*, 2001; Thorrold *et al.*, 2001; Gillanders, 2005; Milton and Chenery, 2005; Walther and Thorrold, 2010; Panfili *et al.*, In press). Interpretation of the Sr/Ca signal still requires some caution, however, given considerable interspecific variation in Sr uptake rates (Swearer *et al.*, 2003; Rooker *et al.*, 2004), potential for vateritic inclusions to be misidentified as freshwater excursions (Tzeng *et al.*, 2007) and possibly confounding effects of temperature and physiology (e.g. Kalish, 1991; Elsdon and Gillanders, 2004; Brown and Severin, 2009; Miller, 2011).

Occasionally, elements other than Sr and Ba have exhibited positive correlations between otolith and ambient concentrations (e.g. Geffen *et al.*, 1998; Milton and Chenery, 2001b; Ranaldi and Gagnon, 2008), but more often than not, no relationship is found or there are contradictions among species and studies (Table I). Some of these contradictions are likely due to species-specific elemental processing, but some may be artefact of reporting method, with studies expressing water chemistry in terms of absolute water concentrations, water element/Ca ratios and (or) salinity. It is still not clear which of these three ‘measures’ has the greatest influence on otolith chemistry (Bath *et al.*, 2000; Milton and Chenery, 2001b; Elsdon and Gillanders, 2004; Hicks *et al.*, 2010), but is clearly an area requiring further research. Another important consideration is the true bioavailability of the element in question. Reported concentrations tend to represent total dissolved metals, which may be dominated by ligand-bound complexes that cannot cross

biological membranes (Campana, 1999). Also, alternative sources of metals, such as sediment and diet, are rarely discussed but may prove significant for certain elements, such as Cd (Ranaldi and Gagnon, 2009).

As shown by the sheer volume of studies (and contradictions) summarised in Table I, temperature, diet and 'vital effects' such as age, growth rate and gonad maturation, can all influence element incorporation into the otolith, often in multiplicative, complex ways (Kalish, 1991). Given the substantial variation in physiology, biochemistry and otolith morphology among fish species (Söllner *et al.*, 2003; Popper and Fay, 2011), it is perhaps not surprising that interspecific differences in otolith elemental incorporation have been observed. However, within-species differences in elemental processing may also be important, with recent experiments indicating different temperature effects on otolith Mg, Mn and Ba incorporation according to the population from which the fish were sourced (Clarke *et al.*, 2011). Such intrinsic effects on otolith microchemistry have not been previously demonstrated, but have important implications for understanding the underlying mechanisms and theoretically enhance its application for stock discrimination.

Temperature has frequently been cited as a major control on otolith chemistry. Reports of negative relationships between temperature and otolith Sr/Ca ratios, akin to responses of inorganic aragonite and corals, have generally arisen from studies working with larvae of marine, temperate species (Radtke, 1989; Townsend *et al.*, 1992; DiMaria *et al.*, 2010). Otherwise, where significant temperature effects have been observed, the majority of studies have reported positive relationships between temperature and otolith Sr (Bath *et al.*, 2000; Elsdon and Gillanders, 2002; Martin *et al.*, 2004) and Ba (Miller, 2009). While separating the effects of temperature and growth remains a challenge, a number of studies have reported negative relationships between growth rate and otolith Sr/Ca (e.g. Sadovy and Severin, 1994; Walther and Thorrold, 2010), and more recently, Ba/Ca (Miller, 2009; 2011). Experiments examining temperature or vital effects on otolith elements other than Sr and Ba are scarce, but a negative temperature effect was reported for otolith Mn/Ca ratios (Miller, 2009) and a positive growth rate effect reported for otolith Mg/Ca ratios (Martin and Thorrold, 2005). Recently, increasing numbers of studies have reported significant interactive effects of water concentrations and temperature on Mg, Sr and Ba incorporation (e.g. Elsdon and Gillanders, 2004; Miller, 2011). Such findings have serious implications, particularly for studies using otolith Sr/Ca ratios to reconstruct migrations among salinity regimes (Martin and Wuenschel, 2006).

Table 1.1 Review of significant and non-significant (NS) effects of different influences (water chemistry, temperature, diet, vital and intrinsic effects) on otolith element concentrations and their partition coefficients, focusing on fish that spend at least part of their lifetime in seawater; the few fully freshwater studies are indicated (FW). Elements have been loosely ordered into hard and soft acids, with Mn and Zn ions behaving as something of intermediaries

Element	vs.	Water chemistry (including Me/Ca, absolute concentrations & salinity)	Temperature	Other (including diet, vital and intrinsic effects)
	Sr	<p>POSITIVE - in the laboratory (Gallahar and Kingsford, 1996; Tzeng, 1996; Bath <i>et al.</i>, 2000; Milton and Chenery, 2001; Elsdon and Gillanders, 2003; Martin <i>et al.</i>, 2004; Elsdon and Gillanders, 2005a; Zimmerman, 2005; Walther and Thorrold, 2006; Hicks <i>et al.</i>, 2010; Macdonald and Crook, 2010; Miller, 2011)</p> <p>POSITIVE - in the field (oft-inferred rather than measured) (Thorrold <i>et al.</i>, 1997b; Babaluk <i>et al.</i>, 1997; Secor &amp; Rooker, 2000; Milton &amp; Chenery, 2005; Tzeng <i>et al.</i>, 2005)</p>	<p>POSITIVE (Kalish, 1989; Fowler <i>et al.</i>, 1995b; Hoff and Fuiman, 1995; Bath <i>et al.</i>, 2000; Elsdon and Gillanders, 2002; Elsdon and Gillanders, 2004; Martin <i>et al.</i>, 2004; Martin and Wuenschel, 2006)</p> <p>NEGATIVE (Radtke <i>et al.</i>, 1990; Townsend <i>et al.</i>, 1992; DiMaria <i>et al.</i> 2010)</p> <p>NS (Gallahar &amp; Kingsford, 1996)</p>	<p><b>Somatic growth rate:</b> NEGATIVE (Sadovy and Severin, 1992; 1994; de Pontual <i>et al.</i>, 2003)</p> <p><b>Otolith precipitation &amp; somatic growth rate:</b> NS or weakly negative (Bath <i>et al.</i>, 2000; Martin <i>et al.</i>, 2004; DiMaria <i>et al.</i>, 2010))</p> <p><b>Reproduction:</b> SIGNIFICANT (Kalish, 1989; Kalish, 1991; Fuiman and Hoff, 1995; Friedland <i>et al.</i>, 1998; Clarke and Friedland, 2004)</p> <p><b>Stress:</b> POSITIVE (Kalish, 1992; Townsend <i>et al.</i>, 1992). <i>In the latter it was proposed that stress caused by low temperature reduces ability to discriminate against Sr</i></p> <p><b>Age/size:</b> POSITIVE (Kalish, 1989; Fowler <i>et al.</i>, 1995b; Fuiman and Hoff, 1995; Proctor <i>et al.</i>, 1995; Fowler <i>et al.</i>, 2005; Steer <i>et al.</i>, 2009); NS (Elsdon and Gillanders, 2005a)</p> <p><b>Ontogeny:</b> SIGNIFICANT (Toole <i>et al.</i>, 1993; Fowler <i>et al.</i>, 1995a; Tzeng, 1996; de Pontual <i>et al.</i>, 2003); NS (Elsdon and Gillanders, 2005a)</p> <p><b>Intrinsic (among species):</b> (Kalish, 1989; Sweareen <i>et al.</i>, 2003; Rooker <i>et al.</i>, 2004; Martin and Wuenschel, 2006; Hamer and Jenkins, 2007)</p> <p><b>Diet :</b> POSITIVE (Limburg, 1995; Gallahar and Kingsford, 1996; Buckel <i>et al.</i>, 2004); NS (Hoff and Fuiman, 1995; Farrell and Campana, 1996; Sanchez-Jerez <i>et al.</i>, 2002; Walther and Thorrold, 2006)</p>
	See also Secor & Rooker review (2000)			
Ba		<p>POSITIVE vs. water Ba/Ca and (or) NEGATIVE vs. salinity (Bath <i>et al.</i>, 2000; Elsdon and Gillanders, 2002; Elsdon and Gillanders, 2003; 2004; de Vries <i>et al.</i>, 2005; Elsdon and Gillanders, 2005a; Elsdon and Gillanders, 2005b; Martin and Thorrold, 2005; Martin and Wuenschel, 2006; Walther and Thorrold, 2006; Miller, 2009)</p> <p>POSITIVE - in field studies (Thorrold <i>et al.</i>, 1997; Elsdon and Gillanders, 2005a; Elsdon and Gillanders, 2005b; Dorval <i>et al.</i>, 2007)</p> <p>INTERACTION WITH Sr (de Vries <i>et al.</i>, 2005)</p> <p>NS - in field (Forrester, 2005)</p>	<p>POSITIVE (Elsdon and Gillanders, 2002; Elsdon and Gillanders, 2004; Miller, 2009)</p> <p>NEGATIVE (DiMaria <i>et al.</i>, 2010)</p> <p>NS (Bath <i>et al.</i>, 2000; Martin and Thorrold, 2005; Martin and Wuenschel, 2006)</p> <p>INTERACTION WITH WATER CHEMISTRY (Elsdon and Gillanders, 2002; Elsdon and Gillanders, 2004; Miller, 2011)</p>	<p><b>Somatic growth rate:</b> NEGATIVE (Miller, 2011), NS (DiMaria <i>et al.</i>, 2010)</p> <p><b>Ontogeny:</b> NS (Elsdon and Gillanders, 2005a; Hamer <i>et al.</i>, 2006)</p> <p><b>Diet:</b> POSITIVE (Sanchez-Jerez <i>et al.</i>, 2002; Buckel <i>et al.</i>, 2004); NS (Walther &amp; Thorrold, 2006)</p> <p><b>Intrinsic (within species):</b> SIGNIFICANT (Clarke <i>et al.</i>, 2011)</p>

Table 1.1 continued

<b>Mg</b>	NS (Elsdon and Gillanders, 2002; Martin and Thorrold, 2005; Hamer <i>et al.</i> , 2006; Miller, 2011)	NS (DiMaria 2010)	<b>Somatic &amp; otolith growth rate:</b> NEGATIVE (Martin and Thorrold, 2005), NS (DiMaria 2010) <b>Diet:</b> NS (Hoff and Fuiman, 1995) <b>Intrinsic (within species):</b> SIGNIFICANT (Clarke <i>et al.</i> , 2011)
<b>Li</b>	NEGATIVE vs. water Li/Ca, but POSITIVE vs. salinity (Milton and Chenery, 2001) POSITIVE (Hicks <i>et al.</i> , 2010)		
<b>Rb</b>	NEGATIVE (Hicks <i>et al.</i> , 2010)		
<b>K &amp; Na</b>		NEGATIVE (Hoff and Fuiman, 1995)	<b>Reproduction:</b> SIGNIFICANT (Fuiman and Hoff, 1995) <b>Diet:</b> NS (Hoff and Fuiman, 1995)
<b>Mn</b>	NS/NEGATIVE, particularly in the core (Hanson & Zdanowicz, 1999; Brophy <i>et al.</i> , 2003; Elsdon & Gillanders, 2003b; Brophy <i>et al.</i> , 2004; Miller, 2009) POSITIVE – in field (Dorval <i>et al.</i> , 2007), POSITIVE but NS – in field (Hamer <i>et al.</i> , 2006) NS (cf. sediment concentrations) (Hanson & Zdanowicz, 1999)	NEGATIVE (Miller, 2009)	<b>Diet:</b> POSITIVE (Sanchez-Jerez <i>et al.</i> , 2002); NS (Buckel <i>et al.</i> , 2004) <b>Intrinsic (within species):</b> SIGNIFICANT (Clarke <i>et al.</i> , 2011)
<b>Zn</b>	POSITIVE (Arai <i>et al.</i> , 2007) POSITIVE (FW)? (Halden <i>et al.</i> , 2000) NS (Thorrold <i>et al.</i> , 1997b; Hanson & Zdanowicz, 1999; Ranaldi & Gagnon, 2008b)		<b>Reproduction?</b> POSITIVE (FW)? (Halden <i>et al.</i> , 2000) <b>Diet:</b> POSITIVE (Ranaldi & Gagnon, 2008b)
<b>Cu</b>	NS (cf. sediment concentrations) (Hanson & Zdanowicz, 1999) POSITIVE (Milton & Chenery, 2001b)		<b>Reproduction?</b> <b>Diet:</b> NS (Milton and Chenery, 2001)
<b>Pb</b>	POSITIVE (Ranaldi & Gagnon, 2008a; Milton & Chenery, 2001b); POSITIVE for 2 spp; NS for plaice (Geffen <i>et al.</i> , 1998)		<b>Diet:</b> NS (Milton and Chenery, 2001).
<b>Hg</b>	POSITIVE for 2 spp; NS for plaice (Geffen <i>et al.</i> , 1998)		
<b>Se</b>	POSITIVE (Lochet <i>et al.</i> , 2010); POSITIVE (FW) – in field (Limburg <i>et al.</i> , 2010)		<b>Reproduction?</b>
<b>Fe</b>	POSITIVE (Ranaldi and Gagnon, 2008)		<b>Age:</b> NEGATIVE (Papadopoulou <i>et al.</i> , 1980)
<b>Cd</b>	POSITIVE (Ranaldi and Gagnon, 2009)		<b>Diet:</b> POSITIVE (Ranaldi & Gagnon, 2009);
<b>Al</b>	POSITIVE – (Mugiyia <i>et al.</i> , 1991)		
<b>Others</b>	Cr, Ni: NS (cf. sediment concentrations) (Hanson & Zdanowicz, 1999)		<b>Age:</b> NEGATIVE for Cs, Co and Ag (Papadopoulou <i>et al.</i> , 1980)

<sup>†</sup> Crucial in vertebrate reproductive processes (Versieck and Cornelis, 1989; Bedwal and Bahuguna, 1994; Watanabe *et al.*, 1997); possible effects on otolith chemistry unknown

## 1.4 Application of otolith microchemistry to reconstruct fish migrations in the marine environment

### 1.4.1 The marine system

The marine system is a dynamic environment with elements constantly added, removed and recycled through biological, physical and chemical processes (Hunter and Boyd, 1999). Yet global averages for seawater element concentrations have remained remarkably conserved, particularly when compared with estuarine and freshwater systems (Turekian, 1968). As such, many marine fish, particularly open ocean pelagics, experience a relatively uniform physicochemical environment with limited potential for spatial discrimination using inorganic chemical proxies (Proctor *et al.*, 1995), although there are some exceptions (e.g. Ashford *et al.*, 2008). Coastal areas generally offer greater chemical heterogeneity due to upwelling, fluvial and anthropogenic inputs, but often the ‘pollutants’ that would contribute to such geographic variation (e.g. Ni, Zn) are soft acid metals that are physiologically discriminated against and typically present below detection levels in the otoliths (Hanson and Zdanowicz, 1999). Importantly, unlike estuarine systems (Elsdon and Gillanders, 2005b), Sr/Ca and Ba/Ca ratios are not inversely related in seawater (Ashford *et al.*, 2005), with Sr exhibiting a quasiconservative distribution (Steele *et al.*, 2009) and Ba readily removed from surface waters as barite adsorbed to settling particles (Bruland and Lohan, 2003). Primary productivity is correlated with barite accumulation, resulting in a nutrient-type distribution (Dehairs *et al.*, 1997). At mesopelagic depths, bacterial activity releases the barite, allowing it to accumulate and dissolve, enriching Ba with depth and producing a useful open ocean otolith marker (Ashford *et al.*, 2005). Manganese on the other hand, is a scavenged element and concentrations thus tend to decrease with depth and distance from coastlines and point sources such as hydrothermal vents (Bruland and Lohan, 2003).

While greater environmental heterogeneity in coastal areas generally increases the discriminatory power of associated otolith signatures, it is, unfortunately, usually at the expense of temporal stability. Indeed inter- and intra-annual differences in water chemistry (Elsdon *et al.*, 2008) and otolith chemical fingerprints (Gillanders, 2002; Swearer *et al.*, 2003; Chittaro *et al.*, 2004; Bergenius *et al.*, 2005; Elsdon and Gillanders, 2006; Walther and Thorrold, 2009) are more the norm than the exception. For this reason, reference collections of otolith elemental fingerprints for relevant year classes and locations are recommended to elucidate site-specific information from unknown otolith chemistries, particularly for more variable habitats, such as lagoons (Gillanders, 2002; Walther and Thorrold, 2009).

### 1.4.2 Marine species

Although the physiology of marine, euryhaline and freshwater fishes differs significantly, particularly with regards to osmoregulation (Evans, 1993), there is little to suggest inherent differences in otolith element incorporation mechanisms from laboratory studies (Farrell and Campana, 1996; Walther and Thorrold, 2006). When considering different life history stages, however, ontogenetic effects on otolith Sr/Ca ratios are often observed in species spending at least part of their lifecycle in saltwater (e.g. Fowler *et al.*, 1995; Walther *et al.*, 2010), particularly during significant metabolic events such as metamorphosis (Arai *et al.*, 2000; de Pontual *et al.*, 2003). Despite water Sr/Ca ratios varying little at salinities above  $\sim 8$  (Secor *et al.*, 1995; Babaluk *et al.*, 1997; Zimmerman, 2005), Sr/Ca ratios in otoliths of marine fish often exhibit considerable interspecific differences (Kalish, 1989; Hamer and Jenkins, 2007), general increases with age (Kalish, 1989; Walther *et al.*, 2010) and intra-annual fluctuations often larger than those exhibited by diadromous species (Brown and Severin, 2009). Explanations for these patterns have been sought, but to date, no single causal factor has been found, although temperature, age, somatic and otolith growth rate, stress and gonad maturation have all been implicated (Table I).

Unfortunately, no experimental work has systematically tested the relationship between ambient temperature and otolith Sr/Ca in adult marine fish across a full reproductive cycle. However, in adult blue grenadier, Australian salmon and bearded rock cod, growth rate and reproductive investment appear to have a greater effect on otolith Sr/Ca ratios than temperature (Kalish, 1989; Kalish, 1991). Otolith Sr/Ca ratios in female bearded rock cod correlated significantly with gonadosomatic index and plasma protein concentrations, particularly the relative proportions of albumins and globulins (Kalish, 1991). It was therefore suggested that plasma and endolymph proteins vary in type and prevalence during gonad development, and differences in their metal-binding capacity alter the proportion of free  $\text{Sr}^{2+}$  ions, thus altering availability and uptake of Sr into the otolith. Similarly, otolith Na, K and Sr concentrations were linked to spawning activity in wild red drum (Fuiman and Hoff, 1995) and seasonal fluctuations in otolith Sr/Ca ratios were observed in adult Atlantic salmon held for  $>2$  years in sea-cages, where salinity was almost constant (32-33 psu) (Clarke and Friedland, 2004). Because the changes in otolith Sr/Ca ratios of the caged salmon appeared to lag behind the changes in water temperature, they were attributed to gonad maturation. However, gonad development is often accompanied by reduced feeding, slower growth rates and changes in ambient water temperature, so there are a number of plausible explanations for the observed otolith Sr/Ca fluctuations. Whatever the explanation, such physiological influences on otolith element ratios have the potential to complicate any element-based interpretations of movement patterns and stock discrimination. It remains to be seen whether purely physiological influences on the trace element composition of otoliths

could prove useful. Marked variations in otolith Sr/Ca ratios within fully marine fish might, for example, indicate onset of sexual maturity or provide a quantitative measure of reproductive investment.

### 1.4.3 Practical considerations

In addition to the variety of exogenous and endogenous factors that can affect otolith chemical patterns, analytical artefacts can also play a role. Instrument performance can significantly affect accuracy and precision (Campana *et al.*, 1997), while otolith treatment can contaminate or remove elements from the microstructure (Gauldie *et al.*, 1998; Proctor and Thresher, 1998; Thresher, 1999; Swan *et al.*, 2006).

Instruments are, however, constantly evolving, with the development of improved technologies such as high resolution or sector field inductively coupled plasma mass spectrometry (HR-ICPMS or SF-ICPMS) (Thorrold and Shuttleworth, 2000), and increasing numbers of studies are focusing their attentions on improving decontamination methods (e.g. Campana *et al.*, 2000; Davies *et al.*, 2011).

A significant practical obstacle encountered when attempting to identify movement-related information in otoliths, is the desire to obtain time-resolved chemical data. Current approaches generally achieve this through microsampling or probe-based techniques such as laser ablation ICPMS (LA-ICPMS). Solution analyses can address certain movement-related questions, for example, using whole otolith signatures as

natural tags during brief mixing periods (Campana *et al.*, 2000), however, probe-based techniques take advantage of the otolith chronology and offer the attractive option of targeting specific growth increments and life history stages. The downside to probe-based analyses is that the volume of ablated material is relatively small, reducing detection capabilities and the number of available elements (Campana, 1999).

Given the ever-increasing desire for longer element lists and improved discriminatory capabilities, beam diameter and (or) power might be increased to improve detection limits, but this results in wider, deeper pits and averaging over longer time periods. Thus probe-based techniques face a constant struggle between optimising temporal resolution and instrument performance. Pit depth is rarely reported in the literature, but given the three-dimensional structure of otoliths, could have a significant averaging effect, and artificially inflate apparent time lags between environmental changes and responses within the otolith (Jones and Chen, 2003).

Attempting to use otolith chemistry to infer intra-annual movements of adult fish is particularly difficult, as age-related decreases in growth rate (e.g. Fowler *et al.*, 2005) result in the progressive narrowing of growth increments, often to widths well under 30µm. This clearly limits the spatial and temporal resolution

attainable for multi-elemental otolith analyses. It also means that few validation studies have focused their attentions on adult fish, with most information inferred from wild-caught adults for which environmental histories are not explicitly known (e.g. Kalish, 1989; Fuiman and Hoff, 1995). The vast majority of empirical studies have employed larval or juvenile fish due to easier and cheaper maintenance, faster growth rates and wider otolith increments. However, given age-related changes in physiology and elemental processing, interpretation of otolith signals in adult fish based on observations from young life-history stages should be treated with caution.

Finally, there are also practical considerations regarding the choice of statistical methods used to analyse the complex, often skewed, multivariate data produced by most otolith elemental analyses (Elsdon *et al.*, 2008). Analyses within chemical profiles from individual fish suffer from issues of non-independence, but this can be overcome by using repeated measures of analysis of variance (RM-ANOVA) (e.g. Clarke *et al.*, 2010) or mixed model analyses (e.g. Hamilton and Warner, 2009). Habitat discrimination based on multivariate elemental fingerprints is a common aim among otolith studies. Recent work comparing the classification accuracy of different statistical methods indicated that machine learning methods such as ‘random forest’ exhibited greater classification efficiency with fewer assumptions than equivalent discriminant function analyses (Mercier *et al.*, 2011).

## 1.5 Case studies

To date, though many studies have used otolith chemistry to examine population structure and (or) movements of marine or partially marine fish, few have attempted to corroborate their results with additional, alternative proxies. As discussed by Begg and Waldman (1999), a more ‘holistic approach’ to stock identification instils greater confidence in the results, but also provides support for (or challenges to) the spatial distributions implied by each marker. Here, we present examples of studies that have used otolith microchemistry to infer population structure or movements of adult marine (or partially marine) fish, and attempted to corroborate their results, either directly or indirectly, with additional, alternative proxies.

### 1.5.1 Otolith chemistry vs. genetic tags

Very few studies have directly compared chemical and molecular tags for describing spatial distributions of fish populations. One such study found that both microsatellite DNA and trace element concentrations at the otolith margin (Mg, Mn, Zn, Sr and Ba) inferred c.65% site fidelity for adult *Sebastes melanops*, a value

also independently suggested by mark-recapture studies (Miller *et al.*, 2005). This study provided rare quantitative support for the use of probe-based techniques such as LA-ICPMS to elucidate population structuring in an exclusively marine fish. Possible movement patterns were not explored in this work, but otolith chemical profiles may have indicated temporally-resolved differences between the resident fish and recent immigrants. Microsatellite and otolith elemental markers were also integrated in an attempt to determine dispersal patterns of the anadromous *Osmerus mordax* (Bradbury *et al.*, 2008). While the two techniques were not formally compared, they produced corroborative results with molecular markers indicating high local recruitment and otolith Sr and Ba profiles implying limited dispersal among estuaries.

A number of stock discrimination studies have also anecdotally compared results from otolith chemistry and molecular studies. While none have reported contradictory results, nearly all have observed higher spatial complexity using otolith microchemistry than their genetic equivalent. For example, otolith margin microchemistry (Li, Mg, Mn, Sr and Ba) of *Hyporhamphus melanochir*, an estuarine and nearshore species, inferred 6 'semi-discrete, population components', contrasting with the 2 management units suggested by molecular markers (Steer *et al.*, 2009). The difference was attributed to a 'stepping stone model' of exchange among neighbouring subpopulations, as misclassified fish were generally assigned to adjacent or proximal sites. Similarly, whole otolith fingerprints (Ba, Cd, Cu, K, Pb, Sr, Zn, Mg, Na and S) of *Hoplostethus atlanticus*, a fully marine species, implied stock separations that corroborated those indicated by genetic markers and parasite loads, but inferred an additional grouping within an area previously classified as a single stock (Edmonds *et al.*, 1991). These examples raise an important point – while otolith microchemistry may resolve groups of fish with shared environmental histories and thus reveal spatial structuring undetectable by other methods, these groups may mix on spawning grounds and still be best managed as a single unit. Thus, terming such works 'stock discrimination' can be somewhat misleading, for the point at which groups of fish with shared environmental histories should be considered and managed as separate 'stocks' is difficult to define and depends on a number of factors specific to the system, species and subunits in question (Campana, 2005). Otolith core chemistry has also been used to infer shared (e.g. Fowler *et al.*, 2005) or multiple (e.g. Tanner *et al.*, 2012) spawning grounds in marine species. A significant challenge remains; however, to demonstrate that shared core chemistries reflect common origin, rather than similar water chemistries or physiological overprinting (maternal or intrinsic). Encouragingly, element concentrations in the otolith nuclei of two marine species, *Chaenocephalus aceratus* and *Dissostichus eleginoides*, corroborated population boundaries inferred by a number of additional markers, including growth rates, morphometrics, parasite loadings and genetics, but again, suggested finer scale population structuring than the other methods (Ashford *et al.*, 2006; Ashford *et al.*, 2010).

### 1.5.2 Otolith chemistry vs. otolith shape

While otolith shape has a predominantly genetic basis, it is susceptible to local conditions and, after significant time in contrasting environments, can differ significantly among regions and stocks (Campana and Casselman, 1993). In an estuarine and nearshore species, *Argyrosomus japonicus*, otolith margin Na, Mg, Sr, Ba concentrations classified fish to capture region with high success (94%), while otolith morphometrics produced slightly lower classification scores (83%), but supported the subdivisions suggested by the elemental fingerprints (Ferguson *et al.*, 2011). The relative time periods represented by each marker is of interest, with otolith margin chemistry representing the most recent material and implying short term geographic separation, while the differences in otolith shape implying limited mixing over longer time periods. Similar methods were used to examine spatial distributions of *Coryphaenoides rupestris*, a deep sea macrourid (Longmore *et al.*, 2010). Here, classification scores were considerably lower using shape descriptors (43%) cf. otolith microchemistry (92%), implying possible mixing events prior to the most recent otolith growth. Ontogenetic patterns in otolith Li, Mn, Cu, Zn and Ba concentrations and stable isotopic ratios ( $\delta^{18}\text{O}$  and  $\delta^{13}\text{C}$ ) suggested a shallower larval phase for this deep sea species, which may facilitate longer term regional genetic drift, but further corroborated relatively static population units (Longmore *et al.*, 2011).

### 1.5.3 Otolith chemistry vs. morphometrics

Similar to otolith shape, variations in fish morphometrics can be genetically and (or) environmentally induced (e.g. Silva, 2003). In a study of adult *Helicolenus percoides* in Fiordland, New Zealand, differences in whole otolith microchemistry (Li, Mg, Sr and Ba), morphometric characters, length-at-age and muscle  $\delta^{15}\text{N}$  and  $\delta^{13}\text{C}$  composition implied limited movement between the four fjords under study (Lawton *et al.*, 2010). In the same region, consistent differences in otolith marginal chemistry (Beer *et al.*, 2011) and tissue isotopes (Rodgers and Wing, 2008) of *Parapercis colias* implied even finer scale population structuring, with limited movement between inner and outer fjord habitats, results that were corroborated by mark-recapture studies (Carbines and McKenzie, 2004). In contrast, morphometric variations in *Tenualosa ilisha*, an anadromous species, were not corroborated by patterns in otolith core and margin chemistries (Li, Na, Mg, Al, Mn, Zn, Sr, and Ba) or allozyme markers (Milton and Chenery, 2001a; Salini *et al.*, 2004). Rather, the localised variability in morphometrics was attributed to susceptibility to local conditions, while the widespread variability in chemical and molecular markers was attributed to extensive mixing. While it has been suggested that a lack of detectable differences in otolith microchemistry provides little information (Campana *et al.*, 2000), the authors argued that the areas in question were characterised by significant differences in water

chemistry, and the manner in which the otolith and molecular markers covaried indicated highly mobile individuals and a well-mixed population.

#### 1.5.4 Otolith chemistry vs. applied tags

Mark-recapture studies provide the most irrefutable evidence of individual movement patterns, but to our knowledge, no study has directly compared tag-derived geolocations in a marine species with otolith material deposited during the same period. In Australia, age-related changes in otolith Sr/Ca and Ba/Ca profiles for *Pagrus auratus*, a fully marine species, were related to emigration away from a common spawning ground (Fowler *et al.*, 2005). As water Sr and Ba concentrations were not formally examined, there was the possibility that such shared otolith chemistries reflected intrinsic ontogenetic effects, rather than common origin (Fowler *et al.*, 1995; de Pontual *et al.*, 2003; Tanner *et al.*, 2011). However, substantial differences in oceanographic conditions and terrestrial inputs were predicted among the water masses in question, and the interpretations were supported by behavioural inferences from mark-recapture studies. Meanwhile, in a different part of Australia, the same species was shown to persist in a far more complex set of population units; findings inferred by whole otolith microchemistry, mark-recapture studies, morphometrics and genetics (Edmonds *et al.*, 1989; Edmonds *et al.*, 1995). Such intra-specific plasticity in population structuring emphasise the benefits of using a “toolbox” approach while highlighting the potential hazards of extrapolating observed species distributions to adjacent areas.

To examine movement-related questions, there is a basic need for time-resolved information. Most studies address this using probe-based otolith analyses, but Campana *et al.* (2000) used averaged whole otolith fingerprints (Mg, Sr, Ba, Mn and Li) to track spawning stock aggregations of cod during brief mixing periods. A maximum likelihood-based stock mixture analysis estimated the relative contribution of reference stocks to summer feeding and over-wintering fish, based on the assumption that source signatures would remain identifiable so long as the mixing period was shorter than the time taken for new otolith growth to overprint reference signatures. By repeated sampling over time it was possible to test this assumption, and elemental fingerprints were found to be stable over a 2-3 year period and some elements even over a decade. The results of this study were supported by previous tagging work, but were unambiguous in their own right, taking advantage of substantial sample sizes (~2500 fish) sampled across a large geographic area over a number of years (Campana, 2005). It should be noted that despite efforts to sample similar size ranges, significant relationships between element concentrations and otolith mass were still observed (positive for Sr; negative for Mn and Mg) and needed detrending, again stressing the importance of size and age in otolith studies (Campana *et al.*, 2000).

## 1.6 Discussion

It is encouraging that of most of the studies published so far have reported congruence between the spatial distributions implied by otolith trace element fingerprints and by alternative tags, both natural and artificial (e.g. Miller *et al.*, 2005). By taking advantage of the superior detection capabilities associated with whole otolith solution analyses (e.g. Campana *et al.*, 2000), stock discrimination and mixed stock analyses can be carried out with relative confidence (Campana and Gagne, 1995; Ferguson *et al.*, 2011). In addition, otolith trace elemental profiles and fingerprints have shown good potential to infer ontogenetic and inter-annual changes in the distribution of marine fish stocks and source-sink connectivity patterns (Fowler *et al.*, 2005; Clarke *et al.*, 2010). However, with regards using otolith microchemistry to track the seasonal migration patterns of individual, fully marine fish (e.g. Hunter *et al.*, 2004b), further validation is required. Only very few studies to date have attempted to use intra-annual otolith chemistries to obtain geolocations of individual fish across time and space (e.g. Mercier *et al.*, 2012). As discussed by Elsdon *et al.* (2008), the number of assumptions increases markedly with the spatial complexity of the question being asked. In the marine realm, the low spatial variability among the hard acid cations most likely to be incorporated into the otolith as a function their availability would certainly appear to hinder the widespread application of otolith microchemistry for geolocation. For example, in Patagonian toothfish captured in the open ocean, otolith element concentrations typically varied by just 1-3 standard deviations (Ashford *et al.*, 2007). Once the inherent error and skew found in most trace elemental data has been accounted for, the likelihood for otolith chemical profiles to reveal individual migrations with great precision or accuracy are slim. Other factors too appear discouraging, such as the relatively poor detection capabilities of probe-based analyses and possible confounding effects of temperature, ontogeny and physiology.

Otolith-derived positional information can be further improved by adding stable isotopes (e.g.  $\delta^{13}\text{C}$  and  $\delta^{18}\text{O}$ ) to the chemical fingerprint (Thorrold *et al.*, 2001; Ashford and Jones, 2007; Tanner *et al.*, 2011). However, it is essential that the physicochemical characteristics of the area in question are well described, as subtle differences in salinity can significantly alter water (Harwood *et al.*, 2008) and otolith (e.g. Surge and Walker, 2005)  $\delta^{18}\text{O}$  and  $\delta^{13}\text{C}$  signatures. The geographical and temporal scales of migration are clearly of great importance. Geographic differences in otolith chemistries are often observed among groups of marine fish, implying that even if there is insufficient information to couple element concentrations with specific locations, there may be potential for separating groups of fish with shared migration histories (known as 'contingents', see Secor, 1999; Secor *et al.*, 2001; Elsdon *et al.*, 2008). *In situ* validation studies coupling migration pathways and environmental conditions derived from DST records with concomitant otolith

chemistries will further help to elucidate whether otolith trace element concentrations can successfully reconstruct or infer individual movements in exclusively marine species (e.g. Hunter and Darnaude, 2004).

Interpretation of signals in physiologically-influenced otolith elements, such as Mg and most importantly, Sr, has been identified as an area urgently requiring further investigation. As discussed, otolith composition is influenced by the ambient environment as well as by a suite of physiological processes that may alter the relative abundances of elements between water and their eventual incorporation into the otolith. To better understand these trends, validation experiments examining elemental uptake across realistic temperature regimes and maturity states would be of great use (Walther *et al.*, 2010), as would quantifying the time taken for environmental changes to be reflected in the growing otolith (Miller, 2011). However, stock discrimination studies often include phenotypic traits, such as size and growth rate, to discriminate among groups of fish. If such traits also generate distinctive, reproducible otolith chemistries, their use as population markers can be considered legitimate (Campana *et al.*, 2000). While this assumption may well hold for averaged whole otolith chemical fingerprints, determining the causal effect of intra-annual signals within individual otoliths is particularly complex, and interpretations could easily be confounded by interactions between environment and physiology. However, when attempting to obtain spatial information from any ‘form’ of otolith microchemistry, it must be emphasised that the influence of physiology should be minimised by controlling for sex, size and age when selecting individuals for analysis.

## 1.7 Conclusions

In order to track individual fish migrations using otolith microchemistry, knowledge of the distributions of elements in the region of interest must be balanced with an understanding of the physiological influences on otolith chemistry over the time period of interest. Limited contemporary understanding of the mechanisms controlling elemental incorporation into the otolith restricts the application of elemental data for positioning fish in time and space (Elsdon *et al.*, 2008), while limited environmental variability in the elements most reliably measured in otoliths presents an additional significant challenge for geolocating fully marine species. The otolith elements most likely to act as useful spatial indicators within the open ocean will vary among species, systems and scales, and as detection capabilities of probe-based analyses improves, will be augmented by spatially explicit, low level elements such as rare earths (Arslan and Paulson, 2003). Based on their behaviour as ‘hard’ or ‘intermediate’ acid cations, their potential for environmental heterogeneity, and their positive relationships with ambient concentrations, it seems likely that Ba, and perhaps Mn and Li, will prove to be the most useful and reliable otolith elements in studies of marine fish movements in the coming

years. Nevertheless, the importance of complementing laboratory experiments with *in situ* validation studies cannot be underestimated. Combining otolith trace element profiles with other geolocation tools such as archival tag data and genetics (Begg and Waldman, 1999; Fromentin *et al.*, 2009) will support and greatly extend the overall utility of otolith chemistry for retrospectively describing migrations and mixing patterns of fully marine fish.

## 1.8 Acknowledgements

Anna Sturrock was supported by a Fisheries Society of the British Isles PhD studentship. We would like to express our gratitude to the 2 anonymous reviewers for their constructive criticisms. Defra contract M1102 (Macro-ecology of finfish in UK waters, 2007-2012)



# Chapter 2

---

## *Aquarium experiment: A simple dilution method for multi- elemental analysis of fish blood plasma by HR-ICPMS*

*This chapter has been modified from a paper prepared for submission. Authors include A. Sturrock, E. Hunter, J. A. Milton and C. Trueman. It was written by A. Sturrock, but included feedback from all co-authors, particularly J. A. Milton in Section 2.2.4.*

### 2.1 Introduction

Despite increasing popularity as a natural tag to elucidate the spatial distributions of wild fish, the mechanisms underpinning otolith microchemistry and the incorporation of elements into the otolith are poorly understood. As discussed in Chapter 1, there is considerable debate surrounding the importance of

physiological *vs.* environmental influences on otolith chemistry, particularly in adult marine fish (Kalish, 1991; Friedland *et al.*, 1998; Campana, 1999; Brown and Severin, 2009). To understand the relative importance of the many factors influencing otolith composition, it is important to first consider their initial uptake from the ambient environment into the blood, considering both extrinsic (e.g. temperature) and intrinsic (e.g. condition) influences.

In the current study, a “mensurative experiment” (Hurlbert, 1984) was carried out to examine possible controls on blood plasma and otolith element concentrations in plaice (*Pleuronectes platessa* L.), a fully marine NE Atlantic flatfish. Plaice make an ideal model species for such an experiment, as their spatial dynamics and physiological traits have been the subject of extensive research over many years (e.g. Rijnsdorp and Millner, 1996; Scott *et al.*, 1998). In the North Sea, males tend to become sexually mature at 3-4 years old and females at 4-5 years old (Rijnsdorp, 1989), but in the laboratory, limited food rations and low body condition can induce skipped spawning behaviour (Horwood *et al.*, 1989; Rijnsdorp, 1990). The difference in maturation timing results in sexual dimorphism, with females growing faster and achieving larger maximum body size (Bromley, 2000). The reproductive season in plaice is from December until April, and plaice migrate sometimes hundreds of miles between feeding and spawning grounds (Hunter *et al.*, 2004b). Plaice condition tends to peak at the start of the spawning season (late December) and decline rapidly during spawning. During this period, plaice reduce or stop feeding, even in the presence of food (Rijnsdorp, 1990) and females need to use large quantities of reserves for egg production and energy: 33% and 7% of body protein, and 14% and 50% of body lipids, respectively (Dawson and Grimm, 1980). After feeding resumes in March, female fish attain the “equivalent of the net annual growth increment” in just two months, with any subsequent growth lost during mobilisation of reserves the following winter (Dawson and Grimm, 1980). For this reason, the experiment was designed to begin at the start of June, once study animals had recovered from spawning and had attained their maximum body weight for the forthcoming year.

Based on their detectability and potential for recording environmental conditions within the otolith (Chapter 1), 12 elements were selected for the current study: Li, Mg, K, Ca, Mn, Cu, Zn, Se, Rb, Sr, Ba and Pb. While many aspects of plaice biology have been extensively researched in the past, there have been either few, or no studies examining the behaviour and expression of the selected elements in the blood of plaice. In fact, a comprehensive review of the analytical literature revealed significant under-representation of blood trace element reference ranges in fish in general, particularly for marine species. Also, no studies could be found that had attempted to refine methods for analysing trace element concentrations specifically in fish blood.

Thus, the overall objectives of the study were:

1. to develop satisfactory methods for determining trace element concentrations in plaice blood
2. to describe changes in blood and otolith composition in non-migrating plaice over a full reproductive cycle
3. to determine the physiological and environmental variables driving these patterns
4. to discuss the wider implications of these data in terms of fisheries management and marine fish spatial ecology.

In this chapter, the experimental design is outlined, and a simple dilution procedure is described that allowed the simultaneous determination of the 12 selected elements in the plasma of adult plaice. This is the first study identified to analyse fish blood plasma by inductively coupled plasma mass spectrometry (ICPMS) and includes some of the first reference ranges for trace element concentrations in fish blood.

### **2.1.1 Blood elemental chemistry in marine fish**

Essential trace elements are, by definition, vital to the health and survival of all animals. Concentrations of trace elements in body fluids need to be tightly controlled, given their necessity in many metabolic reactions and their potential toxicity at elevated levels (Versieck and Cornelis, 1989). Precise and accurate reference concentrations are crucial to establish bioindicators of population health and to understand the functionality of elements in biological processes (Folmar *et al.*, 1992). Variations may indicate differences in physiological status among individuals, impaired body function, and/or differences in environmental exposure. All of these are of interest for monitoring wild animal populations, particularly those exploited for food. Despite global importance as a protein resource, both from wild fisheries and increasingly from aquaculture, fish trace elemental chemistry has received relatively little attention compared with their mammalian counterparts (Watanabe *et al.*, 1997). A review of the analytical literature indicated good representation of the major ions ( $\text{Na}^+$ ,  $\text{Cl}^+$ ,  $\text{K}^+$ ,  $\text{Ca}^{2+}$ ) in whole blood (henceforth described simply as 'blood'), serum and plasma, but serious under-representation of most trace elements (Table 2.1).

Table 2.1 Concentrations of 14 elements in serum (S), plasma (P) or whole blood (B) collected from fish inhabiting freshwater (FW) or seawater (SW). Study details provided where relevant, such as when males (M), females (F) and immature or juvenile fish (J) were defined or concentrations represent averages ( $X$ ). All concentrations in  $\mu\text{g g}^{-1}$  and some were extrapolated from graphs. Table updated from S. Campana (pers. comm.)

Taxonomic group	Fish species	Reference	Fraction	Water	Li	Na	Mg	Cl	K	Ca	Mn	Cu	Zn	Sc	Rb	Sr	Ba	Pb	Details
Class Actinopterygii																			
Order Acipenseriformes																			
Family Acipenseridae	<i>Acipenser fulvescens</i>	(LeBreton & Beamish, 1998)	S	FW		2888		4141	94.0	48.0									
	<i>Acipenser naccarii</i>	(Di Marco <i>et al.</i> , 1999)	S	FW <sup>w</sup>		3065		3712		106.0									7 yrs, cannulated
	<i>Ameiurus nebulosus</i>	(Folmar <i>et al.</i> , 1993)	S	FW		2943	46.0	3900	78.2	107.0									
Order Siluriformes	<i>Campostoma oligolepis</i>	(Schmitt <i>et al.</i> , 2007)	B <sup>t</sup>	FW									56.6			0.197	$X$ (2 ref sites)		
	<i>Ictalurus punctatus</i>	(Brumbaugh <i>et al.</i> , 2005)	B <sup>t</sup>	FW									114.0			0.095	$X$ (2 ref sites)		
	<i>I. punctatus</i>	(Kirk, 1974)	P	FW		3150		4396	101.7										
Order Cypriniformes	<i>Catostomus commersoni</i>	(Wiener <i>et al.</i> , 1985)	S	FW					175.3									$X$ (F, 4 sites, $\Delta\text{pH}$ )	
	<i>Hypentelium</i> spp.	(Schmitt <i>et al.</i> , 1984)	B <sup>t</sup>	FW									69.0			0.630			
	<i>Hypentelium nigricans</i>	(Schmitt <i>et al.</i> , 2007)	B <sup>t</sup>	FW									50.5			0.287			
Family Cyprinidae	<i>H. nigricans</i>	(Schmitt <i>et al.</i> , 2009)	B	FW									49.4			0.090	$X$ (protected sites)		
	<i>Cyprinus carpio</i>	(Ayik <i>et al.</i> , 2005)	P	FW		20.0				0.001	0.84	0.7							Anaesthetised, 'Initial concs'
	<i>C. carpio</i>	(Brumbaugh <i>et al.</i> , 2005)	B <sup>t</sup>	FW									52.0			0.290			
	<i>C. carpio</i>	(Field <i>et al.</i> , 1943)	B	FW				1695		0.058									
	<i>C. carpio</i>	(Field <i>et al.</i> , 1943)	S	FW		3000	33.2	4010	246.0	115.0									$X$
	<i>C. carpio</i>	(Houston & Smeda, 1979)	P	FW		3166	30.9	3921	162.6	81.6									$X$
	<i>C. carpio</i>	(Kakuta <i>et al.</i> , 1994)	P	FW		3104	30.0	3470	235.0	85.0		0.10	4.60						Controls
Order Perciformes	<i>Lepomis macrochirus</i>	(Wiener <i>et al.</i> , 1985)	S	FW				200.0										$X$ (M, F)	
	<i>Lepomis megalotis</i>	(Dwyer <i>et al.</i> , 1988)	B	FW												0.030			
	<i>L. megalotis</i>	(Schmitt <i>et al.</i> , 2007)	B	FW									51.7			0.194	$X$ (2 ref sites)		
	<i>Lepomis</i> sp.	(Lohner <i>et al.</i> , 2001)	S	FW		1825		2365	88.0	178.5									$X$ (ref site, 2yr)
	<i>Micropterus salmoides</i>	(Brumbaugh <i>et al.</i> , 2005)	B <sup>t</sup>	FW									53.9			0.100			
	<i>Spicara smaris</i>	(Fleishman <i>et al.</i> , 1986)	P	SW	0.056	3839													
Family Cichlidae	<i>Oreochromis mossambicus</i>	(Bijvelds <i>et al.</i> , 1996)	P	FW <sup>w</sup>			24.1												Control (>8 wk)
	<i>O. mossambicus</i>	(Subash Peter <i>et al.</i> , 2000)	P	FW <sup>w</sup>		3674		4804	106.3										Control
	<i>O. mossambicus</i>	(Vonck <i>et al.</i> , 1998)	S	FW <sup>w</sup>					440.9										F
	<i>O. mossambicus</i>	(Vonck <i>et al.</i> , 1998)	S	FW <sup>w</sup>		3720	34.0	5038	129.0	128.2									M, F (Ca = M)
	<i>O. mossambicus</i>	(Vonck <i>et al.</i> , 1998)	S	SW <sup>w</sup>					384.7										F
	<i>O. mossambicus</i>	(Vonck <i>et al.</i> , 1998)	S	SW <sup>w</sup>		4028	29.2	6180	129.0	144.3									M, F (Ca = M)
Family Istiophoridae	<i>Makaira mazara</i>	(Kai <i>et al.</i> , 1992)	B	SW									0.96						$X$
	<i>Tetrapturus audax</i>	(Kai <i>et al.</i> , 1992)	B	SW									0.80						$X$
Family Moronidae	<i>Dicentrarchus labrax</i>	(Marino <i>et al.</i> , 2001)	S	SW <sup>w</sup>		4198		6044	134.1	172.6									$X$ (ref value)
	<i>Morone saxatilis</i>	(Dawson, 1982)	P	SW <sup>w</sup>		4483			258.0	90.2									
Family Mullidae	<i>Mullus barbatus ponticus</i>	(Fleishman <i>et al.</i> , 1986)	P	SW	0.045	3678													
	<i>Perca fluviatilis</i>	(Valtonen & Laitinen, 1988)	P	FW			42.5			142.8									$X$ (M, F, 2 sites, monthly)

Table 2.1 continued

Taxonomic group	Fish species	Reference	Fraction	Water	Li	Na	Mg	Cl	K	Ca	Mn	Cu	Zn	Se	Rb	Sr	Ba	Pb	Details
Class Actinopterygii																			
Order Perciformes																			
Family Scombridae	<i>Thunnus alalunga</i>	(Hansen <i>et al.</i> , 1978)	B	SW	0.022	2650			2270						0.44				
	<i>Thunnus albacares</i>	(Kai <i>et al.</i> , 1988)	B	SW											42.5				
	<i>T. albacares</i>	(Kai <i>et al.</i> , 1989)	B	SW											38.6		X (M, F)		
	<i>T. albacares</i>	(Kai <i>et al.</i> , 1992)	B	SW											40.8		X		
	<i>Thunnus obesus</i>	(Kai <i>et al.</i> , 1988)	B	SW											41.4				
	<i>T. obesus</i>	(Kai <i>et al.</i> , 1989)	B	SW											44.8		X (M, F)		
	<i>T. obesus</i>	(Kai <i>et al.</i> , 1992)	B	SW											45.2		X		
Family Sparidae	<i>Diplodus annularis</i>	(Fleishman <i>et al.</i> , 1986)	P	SW	0.053	3770													
	<i>Lagodon rhomboides</i>	(Folmar <i>et al.</i> , 1992)	S	SW		4023	42.0	5424	117.3	130.0							X (all months)		
	<i>Pagrus auratus</i>	(Canfield <i>et al.</i> , 1994)	S	SW		4690	41.3	6311	234.6	124.2							Sedated		
	<i>P. auratus</i>	(Wells <i>et al.</i> , 1986)	P	SW		4616		6736	168.1	100.2							Rested, cannulated		
Family Zoarcidae	<i>Lycodes esmarkii</i>	(Graham <i>et al.</i> , 1985)	P	SW		4621	67.6	6559	211.1	110.6									
Order Gadiformes																			
Family Gadidae	<i>Gadus morhua</i>	(Natochin & Shakhamatova, 1996)	S	SW	0.048	3931	23.8		127.9	139.5									
	<i>G. morhua</i>	(Woodhead, 1968)	P	SW						171.9							X (M, F, 1yr)		
Family Lotidae	<i>Lota lota</i>	(Melancon <i>et al.</i> , 2009)	B†	FW		2670	66.4		1970	30.2	0.084		5.78		1.96	0.21	0.37	0.054	
Family Moridae	<i>Antimora rostrata</i>	(Graham <i>et al.</i> , 1985)	P	SW		4115	34.8	5602	89.5	101.8									
	<i>Pseudophycis barbatus</i>	(Kalish, 1991)	P	SW		4213			279.3	71.6					1.10		X (M, F, 8 mo)		
Order Mugiliformes																			
Family Mugilidae	<i>Mugil cephalus</i>	(Nordlie & Whittier, 1983)	P	FW <sup>a</sup>			33.8			101.0							X		
	<i>M. cephalus</i>	(Folmar <i>et al.</i> , 1992)	S	SW <sup>a</sup>		3862	55.0	4963	97.7	120.0							X (all months)		
	<i>M. cephalus</i>	(Nordlie & Whittier, 1983)	P	SW <sup>a</sup>			47.4			95.8							X		
	<i>M. cephalus</i>	(Peterson & Shehadeh, 1971)	P	SW <sup>a</sup>						134.7	2.70						Controls		
Order Pleuronectiformes																			
Family Pleuronectidae	<i>Platichthys flesus</i>	(Larsson <i>et al.</i> , 1981)	P	FW <sup>a,b</sup>		3472	14.6	4680	140.8	96.2									
	<i>P. flesus</i>	(Larsson <i>et al.</i> , 1980)	P	FW <sup>a,b</sup>		3518		4485	82.1								X (1 yr)		
	<i>Kareius bicoloratus</i>	(Mugiya, 1966)	S	SW <sup>a</sup>			19.0			93.0							X (F, all stages)		
	<i>Parophrys verulius</i>	(Johnson & Casillas, 1991)	P	SW <sup>a</sup>			25.4			113.4									
	<i>Pleuronectes platessa</i>	(Cobb <i>et al.</i> , 1973)	S	SW		4012	14.0	5619	162.0	102.0									
	<i>P. platessa</i>	(Harvey, 1978)	S	SW						0.57									
	<i>P. platessa</i>	(Syed & Coombs, 1982)	B	SW						0.67									
	<i>Pseudopleuronectes americanus</i>	(Fletcher, 1975)	P	SW <sup>a</sup>		5081		6807	43.0										
Family Scophthalmidae	<i>Scophthalmus aquosus</i>	(Dawson, 1990)	P	SW		3851			185.7	79.8							X (field, 4 seasons)		

Table 2.1 continued

Taxonomic group	Fish species	Reference	Fraction	Water	Li	Na	Mg	Cl	K	Ca	Mn	Cu	Zn	Se	Rb	Sr	Ba	Pb	Details
Order Salmoniformes																			
Family Salmonidae	<i>Oncorhynchus mykiss</i>	(Daglish <i>et al.</i> , 2004)	P	FW	2457		117.1	76.7		691									Controls.
	<i>O. mykiss</i>	(Houston & Smeda, 1979)	P	FW	3529	17.5	4634	79.4	96.8										M
	<i>O. mykiss</i>	(Korcock <i>et al.</i> , 1988)	P	FW	4370		4056	170.1											X (stunned MS222 treated)
	<i>O. mykiss</i>	(Kucukbay <i>et al.</i> , 2006)	S	FW					0.070	1.30	10.2								
	<i>O. mykiss</i>	(Miller III <i>et al.</i> , 1983)	S	FW		117.2													X
	<i>O. mykiss</i>	(Mugiyia & Takahashi, 1985)	S	FW	3438	22.5	4294	50.0	103.0										X
	<i>O. mykiss</i>	(Mugiyia, 1966)	S	FW		17.0			99.0										X (Jan-Dec)
	<i>O. mykiss</i>	(Parker <i>et al.</i> , 1985)	P	FW				111.0											pH6.62
	<i>O. mykiss</i>	(Shearer, 1984)	B	FW	2941	72.0	812.0	109.0	0.220	0.94	13.0								0.17
	<i>O. mykiss</i>	(Stormer <i>et al.</i> , 1996)	P	FW	3564	17.0	4786	105.6	98.2										
	<i>O. mykiss</i>	(Walker & Fromm, 1976)	P	FW															
	<i>O. mykiss</i>	(Wedemeyer & Chatterton, 1970)	P	FW		3829													X
	<i>O. mykiss</i>	(Zeitoun <i>et al.</i> , 1977)	P	FW	3420	41.0		41.0	256.0		1.25	18.3							X (Controls)
	<i>Oncorhynchus nerka</i>	(Fletcher <i>et al.</i> , 1975)	P	FW <sup>a</sup>							0.85	8.5							X (M, F, spawn)
	<i>O. nerka</i>	(Fletcher <i>et al.</i> , 1975)	P	SW <sup>a</sup>							1.39	23.4							X (M, F)
	<i>Oncorhynchus tshawytscha</i>	(Congleton & LaVoie, 2001)	P	FW	3862		4680	75.9	107.4										J, caudal puncture
	<i>Salmo salar</i>	(Lorentzen & Maage, 1999)	P	FW <sup>a</sup>							1.60	12.8							J, Mn < LOD
	<i>S. salar</i>	(Maage <i>et al.</i> , 2001)	S	FW <sup>a</sup>								22.9							X (4 diets, ΔZn)
	<i>Salmo trutta</i>	(Laitinen & Valtonen, 1995)	P	FW		41.8	5353		192.4										Controls
	<i>S. trutta</i>	(Phillips & Brockway, 1958)	S	FW	3580	23.0	4240	201.0	125.0		2.80								X
	<i>Salvelinus namaycush</i>	(Edsall, 1999)	S	FW			28.0		115.0										
	<i>S. namaycush</i>	(Melancon <i>et al.</i> , 2009)	B	FW	2620	67.8		1990	102.0	0.103		8.8		2.42	0.14	0.25	0.161		
Order Lophiiformes																			
Family Lophiidae	<i>Lophius pectorius</i>	(Palacios <i>et al.</i> , 1972)	P	SW	3816		5859	249.1		0.72									X (J, F, M)
Order Scorpaeniformes																			
Family Cottidae	<i>Myoxocephalus scorpius</i>	(Natochin & Shakhmatova, 1996)	S	SW	0.076														
	<i>Myoxocephalus quadricornis</i>	(Bengtsson & Larsson, 1986)	P	SW <sup>a</sup>	3678	10.9	4396	125.1	97.0										
Family Scorpidae	<i>Scorpaena porcus</i>	(Fleishman <i>et al.</i> , 1986)	P	SW	0.051	3747													
<b>Grand means</b>			<b>FW</b>	-	3216	38.2	4240	381.3	131.3	0.089	77.85	33.5	-	2.19	0.17	0.312	0.193		
<i>(± SEM)</i>					(112)	(5.2)	(145)	(129)	(14.2)	(0.03)	(76.6)	(7.1)		(0.2)	(0.02)	(0.06)	(0.05)		
			<b>SW</b>	0.050	4043	34.2	5875	287.2	128.9	-	1.21	23.38	31.9	0.443	1.10	-	-		
					(0.006)	(109)	(4.9)	(209)	(125)	(14.8)		(0.4)	(-)	(6.8)	(-)	(-)			

† Analyses carried out by ICPMS; <sup>a</sup> Euryhaline species; <sup>b</sup> Brackish water (salinities of 7-7.6)

Accurate and precise measurement of trace and ultra-trace elements in biological fluids presents a number of challenges due to the complex nature of the medium and low detection limits necessary for analysis (Subramanian, 1996). Inductively coupled plasma mass spectrometry (ICPMS) has proven to be the most reliable method for rapid multi-element screening of a variety of complex solutions, but spectral and non-spectral interferences can hinder analyses, particularly for elements close to detection limits. High resolution ICPMS (HR-ICPMS) offers greater sensitivity and can reduce or even eliminate mass interference problems (Bocca *et al.*, 2004). Direct analysis of biological fluids is difficult because the high protein and salt content can block the nebuliser and torch tubes (Subramanian, 1996). This can be overcome through microwave or acid digestion (Rodushkin *et al.*, 2000), but such processes can introduce contamination or cause loss of volatile elements (Vanhoe and Dams, 1994). In addition, strong acids can cause proteins to precipitate out of solution, potentially removing organically-bound elements (Thermo, 2009a). To reduce contamination risk and processing time, simple dilution methods are generally favoured (Subramanian, 1996; Goule *et al.*, 2005; Thermo, 2009b).

While a number of studies have examined optimal dilution methods for the analysis of human biological fluids, none have focused on fish. Marine fish present additional challenges, not least due to a lack of suitable reference materials. Marine fish are hypo-osmotic and continually drink seawater to maintain ionic homeostasis (Campana, 1999). Despite highly evolved excretory mechanisms to remove excess salts, their bloods are characterised by elevated  $\text{Na}^+$  and  $\text{Cl}^-$  concentrations, typically 25-30% higher than freshwater species (Table 2.1) and 20-70% higher than humans (Merck, 2011). Salt loading could have important implications for trace metal analyses and would be augmented in studies such as this, where a sodium-based anticoagulant was used. Otherwise, blood composition is broadly conserved among vertebrates, particularly for essential trace elements such as Zn, Mn and Cu (Table 3.1, Versieck and Cornelis, 1980).

The objective of this work was to modify methods used for the analysis of human plasma and serum to develop a simple preparation procedure for simultaneous, accurate and precise determination of Li, Mg, K, Ca, Mn, Cu, Zn, Se, Rb, Sr, Ba and Pb in plasma from plaice. The elements were chosen as their concentrations in biomineralised fish tissues such as otoliths and scales are frequently used to infer fish movement and stock identities, but metals such as Sr, Ba and Mn are of relatively minor interest in human biomedical studies and are under-represented in the analytical literature. Following a description of the method we present some of the first reference ranges for trace element concentrations in the plasma of a marine fish.

## 2.2 Methods

### 2.2.1 Collection and maintenance of study animals

Study animals were caught by beam and Portuguese high headline trawl on board *CEFAS RV Endeavour* from Liverpool Bay in the Irish Sea (IS) (approx. 53° 23' N, 4° 9' W) between 22<sup>nd</sup> and 27<sup>th</sup> February 2009 (Figure 2.1). Due to a clear male bias (67 males to 13 females) and mortalities encountered during the early stages of the experiment (21 males and 3 females were euthanised after exhibiting symptoms of *Epidermal hyperplasia*), 22 additional females were sourced from the English Channel (EC), near Eastbourne, on August 1<sup>st</sup> 2009 (Figure 2.1). They were held in Sovereign Harbour for 6 days (during which time the water temperature rose to ~20°C). Transport of all fish to the CEFAS Lowestoft aquarium took place in large seawater tanks fed with pure oxygen. For the entire duration of the study, the fish were maintained in a large (9m<sup>3</sup>) outdoor tank, fed with a continuous supply of fresh, coastal seawater. The tank roof was open during daylight hours to establish natural photoperiodism among the study animals, but this did not expose them to direct sunlight. All fish were acclimatised with no handling for three months to ensure common blood parameters had returned to 'normal' levels (Bourne, 1986).

The IS fish were vaccinated against *Vibrio* bacteria two weeks prior to the experiment start date, but issues obtaining the vaccine later in the year resulted in the EC females being introduced to the experiment unvaccinated on 27<sup>th</sup> October 2009. Fish were fed twice weekly with a generous diet, equivalent to 2.5% body weight/day (Horwood *et al.*, 1989), comprising live lugworms (*Arenicola marina*) sourced from a single, local beach. Uneaten food was removed within 24 hours

On the first day of sampling, fish were injected with oxytetracycline (OTC. "Oxytetrin 20 LA" Schering Plough, 200 mg ml<sup>-1</sup>) into the body cavity at a dose rate of 50mg kg<sup>-1</sup> total weight (TW) in order to leave a visible 'start check' on the otolith. The OTC was pre-diluted using a plaice-specific Ringers Solution (8.22mg/ml NaCl in MQ water, after Cobb *et al.*, 1973) to reduce possible effects of osmotic shock, and administered after the initial blood sample had been taken. Passive Integrated Transponder tags ([www.wyremicrodesign.co.uk](http://www.wyremicrodesign.co.uk)) were inserted intramuscularly to provide each fish with a unique ID code.

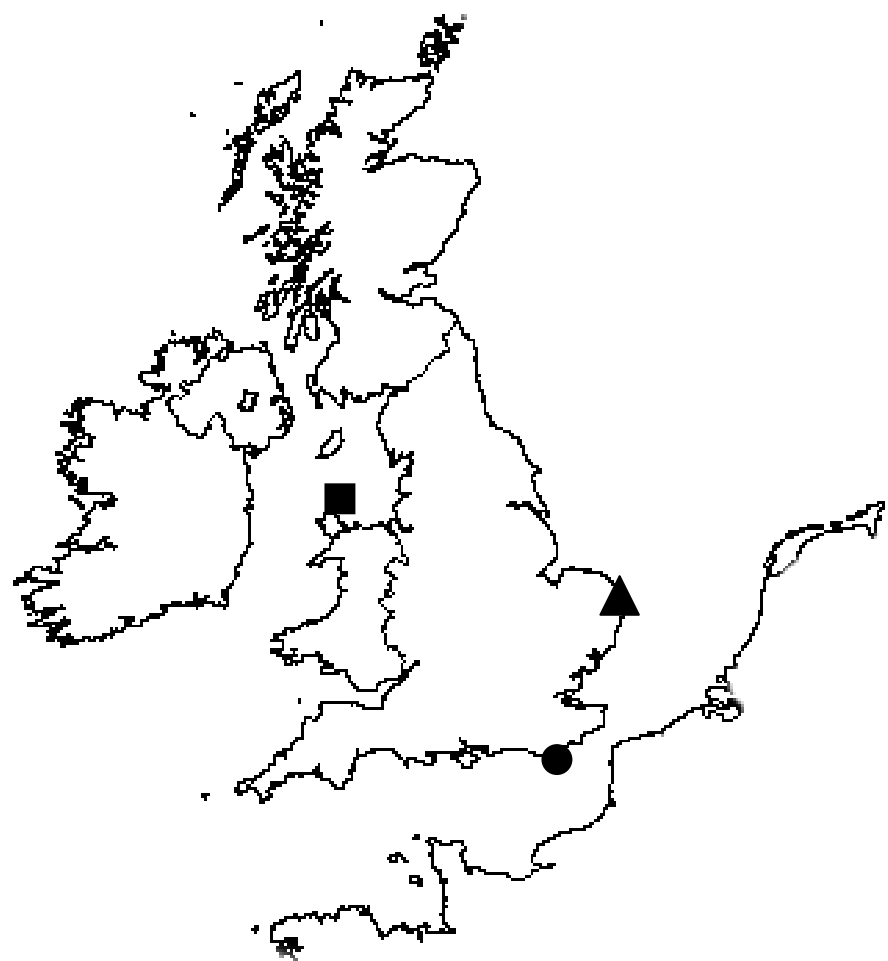


Figure 2.1 Map of the UK showing locations of collection sites in the Irish Sea (square) and English Channel (circle), and the location of the CEFAS aquarium in Lowestoft (triangle)

Captive fish often exhibit some form of reproductive dysfunction, usually due to failure of the pituitary to release the maturation gonadotropin, luteinizing hormone (Zohar and Mylonas, 2001). Plaice are no exception; captive females may fail to undergo final oocyte maturation, ovulation and spawning, while milt production in males is often reduced and of lower quality (Vermeirssen *et al.*, 1998; Scott *et al.*, 1999).

Introducing steroids such as gondotropin releasing hormone (GnRH), can artificially stimulate reproductive processes to overcome such dysfunctions and have been used on captive reared fish for almost a century (Zohar and Mylonas, 2001). To encourage successful spawning events, half of the experimental fish were treated intramuscularly with a 75 $\mu$ g slow-release sGnRHa pellet (Ovaplant) at the start of the spawning season (18<sup>th</sup> January 2010). The pellet is biodegradable, made of natural compounds and has been used to induce spawning in a number of flatfish species (Syndel Laboratories Ltd., 2009).

## 2.2.2 Selection criteria

Given resource limitations it was not possible to analyse blood (and later, otolith) samples from every individual in the experiment. For this reason, fish with otoliths exhibiting clear OTC marks and larger quantities of new growth were favoured. Also, any fish that died from unknown causes prior to the end of the experiment were excluded ( $n = 3$  IS females,  $n = 9$  males,  $n = 2$  EC females). These selection criteria obviously have the potential to bias the results towards healthier, faster growing fish, but given the ultimate aim of the study, it was deemed crucial to ensure sufficient new otolith material to allow repeat sampling across the experimental period. Given the low numbers of IS females remaining ( $n = 8$ ), all were included for further analysis. Six males and six English Channel (EC) females were chosen for otolith analyses, but an additional randomised sample was added to each group ( $n = 4$  and 1, respectively) for blood analysis.

For the purposes of the current chapter, in order to avoid confounding blood elemental reference ranges by including different sampling periods, ages and origins, the EC females were excluded from the reported reference ranges. Similarly, given known spawning effects on blood chemistry (Fletcher *et al.*, 1975; Thompson *et al.*, 2002), which may be augmented in GnRH-treated fish, blood samples collected during the spawning season (January to March) were also excluded.

### 2.2.3 Blood sampling

While serum and plasma are often discussed interchangeably, they are quite different. Serum is acquired after blood coagulation and thus contains no clotting factors and overall lower protein, while plasma is separated from unclotted blood so requires an anticoagulant. Differences in fluid analytes such as glucose, Mg and K have been observed among the two fluid types, particularly in animals with nucleated red blood cells, such as fish (Hrubec and Smith, 1999). It is suggested that the metabolism of blood components during clotting can result in serum being an unreliable recorder of *in vivo* elemental concentrations (Hrubec and Smith, 1999).

Plasma also offers the added benefits of larger volume yield and lower risk of haemolysis (Uges, 1988). However, for trace metal analyses, serum is generally the favoured medium because it avoids contamination from anticoagulants (Versieck and Cornelis, 1989). As such, we attempted to sample without anticoagulants, but clotting time of fish blood is particularly rapid (Wolf, 1959) and the needle often blocked mid-sample. Consequently, we chose to collect plasma, using heparin as the anticoagulant as it has limited effects on common blood parameters (Harvey, 1978; Daglish *et al.*, 2004). A stock solution of heparin (500IU ml<sup>-1</sup>) was prepared using MQ and high purity heparin sodium salt from porcine intestinal mucosa (Sigma Aldrich), and aliquots stored at -20°C. Before each sampling session an aliquot was thawed at 4°C and 0.1ml drawn up the needle (25mm, 25 gauge) and syringe (1ml BD Plastipak) then fully vented. This left 25 ± 2.76mg (mean ± SEM, *n*=17) heparin in each syringe.

Blood samples (one per fish per month) were collected for 12 months (02/06/09-28/05/10) by caudal venipuncture and stored on ice blocks until processing. Sampling took place between 8 and 10am on days before feeding days to avoid diurnal or food-related artefacts. Bloods were centrifuged within 3 hours (15 mins, 2500 rpm, 4°C) and the plasma stored at -20°C. Procedural blanks were collected in the same way, only using MQ in place of blood. For quality control purposes, samples that had clotted or haemolysed were discarded. All processes apart from initial blood collection were carried out in a dedicated Class 100 clean room or Heraeus Class II Safety Cabinet lined with clean plastic sheeting. All consumables except needles and syringes were thoroughly acid cleaned (Kremling, 1999). To avoid blood contamination, subjects were not sedated prior to sampling, but handling time and sample volume were minimised (usually <3 mins and 0.3ml, respectively). All experiments were performed in compliance with Home Office guidelines (Project License no. 80/2260).

## 2.2.4 Analysis methods

### 2.2.4.1 Instrumentation

Analyses were carried out on a Thermo Fisher Scientific Element 2 XR HR-ICPMS (Bremen, Germany). Low-resolution (LRM,  $m/\Delta m$  300), medium-resolution (MRM,  $m/\Delta m$  3000) and high-resolution modes (HRM,  $m/\Delta m$  7500) were utilised to avoid spectral interferences (Table 2.2). Sample introduction was achieved via autosampler (ESI SC2, Omaha, US) using a pumped micro PFA nebuliser into a peltier cooled PFA cyclonic spray chamber (ESI PC3). Additional Ar add gas was ported into the spray chamber to improve sensitivity and signal stability. The instrument used the standard torch, sapphire injector and guard electrode. Using this configuration and adjusting ion lens settings to maximise sensitivity, the instrument was tuned to achieve sensitivity of around  $1 \times 10^6$  cps in LRM  $1 \text{ ng g}^{-1}$   $^{115}\text{In}$ . Oxide formation was minimised using the  $^{238}\text{U}^{16}\text{O}^+ / ^{238}\text{U}^+$  ratio.

### 2.2.4.2 Reagents and solutions

Multi-element stock solutions were prepared using 2% nitric acid ( $\text{HNO}_3$ ) and single element standards (Inorganic Ventures, Lakewood, USA, and Romil, Cambridge, UK). These were diluted to produce five-point calibration curves in physiologically relevant ranges (Table 2.3). MilliQ water (MQ,  $>18.2 \text{ M}\Omega$ ) and trace metal grade  $\text{HNO}_3$  (Fisher Scientific, UK), further purified by sub-boiling (sb.) distillation in a Savillex Teflon still, were used throughout. Seronorm Human Trace Elements Serum L-1 (Batch 0608414, Nycomed, Norway) was used as the certified reference material (CRM), but required separate calibration due to differences in its composition. Samples and calibration standards were diluted using mixtures previously developed for human biological fluids (Table 4), spiked with internal standards ( $^9\text{Be}$  at  $20 \mu\text{g l}^{-1}$ ;  $^{103}\text{Rh}$  and  $^{185}\text{Re}$  at  $10 \mu\text{g l}^{-1}$ ). Both diluents are weakly acidic and contain Triton-X 100 (Sigma Aldrich, UK) to form a stable emulsion and avoid build up of organic residues, and butan-1-ol ( $\geq 99.5$  Fisher Scientific, UK) to ensure efficient ionisation of Se (Thermo, 2009a).

### 2.2.4.3 Dilution method

To determine optimal diluent mixture and dilution factor, plasma and Seronorm samples were serially diluted 10, 20, 30, 50, 100, 250, 600 and 1000-fold; their exact dilution factor determined by wet weight. Samples were analysed sequentially from the least to the most concentrated (operating conditions in Table 2.2). Internal standard-spiked “acid blanks”, sb. 2%  $\text{HNO}_3$  and “diluent blanks” (mixtures outlined in Table 2.4) were analysed at the start and end of each batch to correct for instrument drift and to calculate limits of detection (LOD, 3 s.d. of diluent blanks). The optimal preparation was defined as the diluent mixture and dilution factor that minimised signal suppression while producing concentrations  $>\text{LOD}$ .

Table 2.2 Isotopes, resolutions and operating conditions for HR-ICPMS

RF power (W)	1200		
Sample uptake rate (ml min <sup>-1</sup> )	0.15, pumped		
Ar gas flow rates (l min <sup>-1</sup> )			
Coolant	15.0	Nebuliser	0.7 (via nebuliser)
Auxiliary	0.95	Add gas	0.3 (ported into spray chamber)
Nebuliser		ESI PFA ST	
Spray chamber		ESI PFA cyclonic, peltier cooled	
	LRM	<sup>7</sup> Li, <sup>9</sup> Be <sup>a</sup> , <sup>45</sup> Sc <sup>a</sup> , <sup>85</sup> Rb, <sup>88</sup> Sr, <sup>103</sup> Rh <sup>a</sup> , <sup>137</sup> Ba, <sup>185</sup> Re <sup>a</sup> , <sup>208</sup> Pb	
Resolution	MRM	<sup>9</sup> Be <sup>a</sup> , <sup>24</sup> Mg, <sup>44</sup> Ca, <sup>45</sup> Sc <sup>a</sup> , <sup>55</sup> Mn, <sup>63</sup> Cu, <sup>66</sup> Zn, <sup>103</sup> Rh <sup>a</sup>	
	HRM	<sup>39</sup> K, <sup>45</sup> Sc <sup>a</sup> , <sup>77</sup> Se, <sup>78</sup> Se, <sup>103</sup> Rh <sup>a</sup>	
Acquisition mode		E-scan, Mode 1, 12 scans per resolution	
Mass window (%) <sup>b</sup>		50 (LRM), 125 (MRM and HRM)	
Search window (%) <sup>b</sup>		25 (LRM), 60 (MRM and HRM)	
Integration window (%) <sup>b</sup>		20 (LRM), 60 (MRM and HRM)	
No. of samples per peak		50 (LRM), 20 (MRM and HRM)	

<sup>a</sup> Internal standards (<sup>45</sup>Sc later excluded)

<sup>b</sup> Percent of peak width

Table 2.3 Concentration ranges (in ng g<sup>-1</sup>) for external calibration of fish plasma and Seronorm at 150-fold dilution

	Fish plasma		Seronorm	
	Min	Max	Min	Max
Li	0.012	1.396	17.381	83.755
Mg	5.92	698.29	60.51	291.60
K	10.34	1220.08	375.32	1808.63
Ca	24.78	2925.10	317.35	1529.26
Mn	0.009	1.112	0.030	0.145
Cu	0.221	26.091	4.036	19.451
Zn	2.329	274.892	4.088	19.700
Se	0.099	11.645	0.199	0.961
Rb	0.002	0.205	0.011	0.055
Sr	0.198	23.347	0.086	0.416
Ba	0.0024	0.2806	0.4207	2.0274
Pb	0.0001	0.0078	0.0099	0.0478

<sup>a</sup> Internal standards (<sup>45</sup>Sc later excluded);

<sup>b</sup> Percent of peak width

Table 2.4 Contents of the dilution mixtures (v/v)

	Mix 1 (Thermo, 2009a; b)	Mix 2 (Goulle <i>et al.</i> , 2005)
Nitric acid	0.05%	1% <sup>a</sup>
Triton X-100	0.10% <sup>b</sup>	0.01%
Butanol	3%	0.50%

<sup>a</sup> This refers to 1% of concentrated HNO<sub>3</sub> (usually around 65%)

<sup>b</sup> ‘TAMA SC’ was replaced with Triton X-100

#### 2.2.4.4 Memory effects

Memory effects were informally assessed by analysing replicate 2% HNO<sub>3</sub> washes after plasma and Seronorm samples. Generally, counts had returned to background levels by the second wash (equivalent to ~3.5 mins), so wash times were set to 4 mins. Even with this extended wash time, Seronorm Li (almost 100x higher than fish plasma Li) remained elevated in subsequent samples, so to avoid cross-contamination Seronorm-based samples and their calibration standards were analysed only at the end of runs.

#### 2.2.4.5 Sample preparation, analysis and calculations

All solutions were weighed to the nearest 0.00001g and concentrations calculated by weight. The following steps were taken to improve matrix matching among blanks, calibration standards and samples:

1. Volumes of Be-, Rh- and Re-spiked diluent mixture were matched among all tubes (2.5ml).
2. MQ was used in place of plasma or Seronorm in the blank and calibration tubes (20 $\mu$ l).
3. All tubes were spiked with an equal volume (480 $\mu$ l) of 2% HNO<sub>3</sub> or 2% HNO<sub>3</sub> based standard, increasing the HNO<sub>3</sub> concentration in each tube by ~0.3%.

‘Procedural standards’ were prepared in the same manner, scaled up to larger volumes to allow repeat-sampling within and across runs. Even with our efforts to improve matrix matching, internal standard behaviour indicated susceptibility to matrix changes mid-sequence, so the instrument was ‘conditioned’ at the start of each run by repeat-analysis of a stock bottle of diluent mixture for c.45 mins. Also, while sample order was randomised, blanks, calibrations and Seronorm samples were analysed only at the start or end of runs. “Procedural blanks” and “laboratory blanks” were both analysed, their only difference being the source of the added MQ (transferred among heparinised syringes and multiple tubes then frozen, or direct from the lab).

Interferences and low ionisation efficiency on Se can preclude its accurate quantification by ICPMS, but through use of HRM and careful setting of mass offsets it was possible to separate Se from the <sup>40</sup>Ar<sup>37</sup>Cl<sup>+</sup> and <sup>40</sup>Ar<sup>38</sup>Ar<sup>+</sup> peaks. There was good agreement between concomitant <sup>77</sup>Se and <sup>78</sup>Se measurements ( $r^2 = 0.99$ ,  $n = 59$ ), so <sup>78</sup>Se was used as it is the more abundant isotope.

After the analysis run, raw counts were blank and drift-corrected offline, and concentrations quantified by direct calibration (sample calibration curves  $r^2 > 0.999$  except for Pb, which ranged from 0.954 to  $>0.999$ ). Differences between procedural and laboratory blanks were tested by ANOVA following log transformation if data were heterogeneous (Brown-Forsythe test, JMP 8.0). Concentrations <LOD were excluded. As no CRM for fish serum or plasma is currently available, accuracy was gauged using ‘acceptable ranges’ for

Seronorm, while internal and external precision was assessed using relative standard deviation (%RSD). External precision was represented by intra- and inter-assay replicates of ‘procedural standards’ (single tubes repeatedly analysed to indicate instrument and/or calibration error) and multiple tubes prepared from a single sample (preparation, instrument and/or calibration error).

## 2.3 Results and Discussion

### 2.3.1 Dilution method

In all cases, ion yield for the internal standards was greater using Mix 2 as the diluent (Figure 2.2), probably due to signal suppression from the butanol, so Mix 1 was excluded from further investigation. Signal suppression of Be, Rh and Re was also greatest in the most concentrated samples, but appeared negligible at 100 to 250-fold dilution (Figure 2.2). However, at 250-fold dilution, plasma Mn, Ba and Pb concentrations were close to or below LOD, so 150 was chosen as the dilution factor for all future analyses. The relatively high dilution factor resulted in almost no cases of nebuliser blockage, even during long runs of more than 100 analyses, and there was also only minor instrument drift. A high dilution factor also helps to circumvent issues relating to low sample volume, which is crucial in serial sampling experiments such as this one, both in terms of animal welfare and to ensure blood samples are representative of a healthy, minimally stressed population.

### 2.3.2 Calibrations and blanks

$^{45}\text{Sc}$  was excluded as an internal standard due to erratic behaviour during the run, which appeared to indicate its presence in the blood samples. Blank subtractions were carried out using laboratory blanks due to unexpected patterns in Ba. Raw counts did not differ between procedural and laboratory blanks for any other elements ( $p > 0.05, n = 36$ ), but procedural blanks contained significantly higher Ba ( $F_{1,34} = 73.2, p < 0.0001$ ) and concentrations almost an order of magnitude higher than associated plasma samples (averages of 0.5 and  $0.07\text{ ng g}^{-1}$ , respectively). Given the identical treatment of plaice blood and procedural blank MQ, this appears to indicate a source of Ba in the heparin, syringe or needle that is not transferred to (or is highly suppressed in) the plasma, possibly remaining in the pellet following separation of plasma from whole blood. The final Ba concentrations should therefore be taken with some caution.

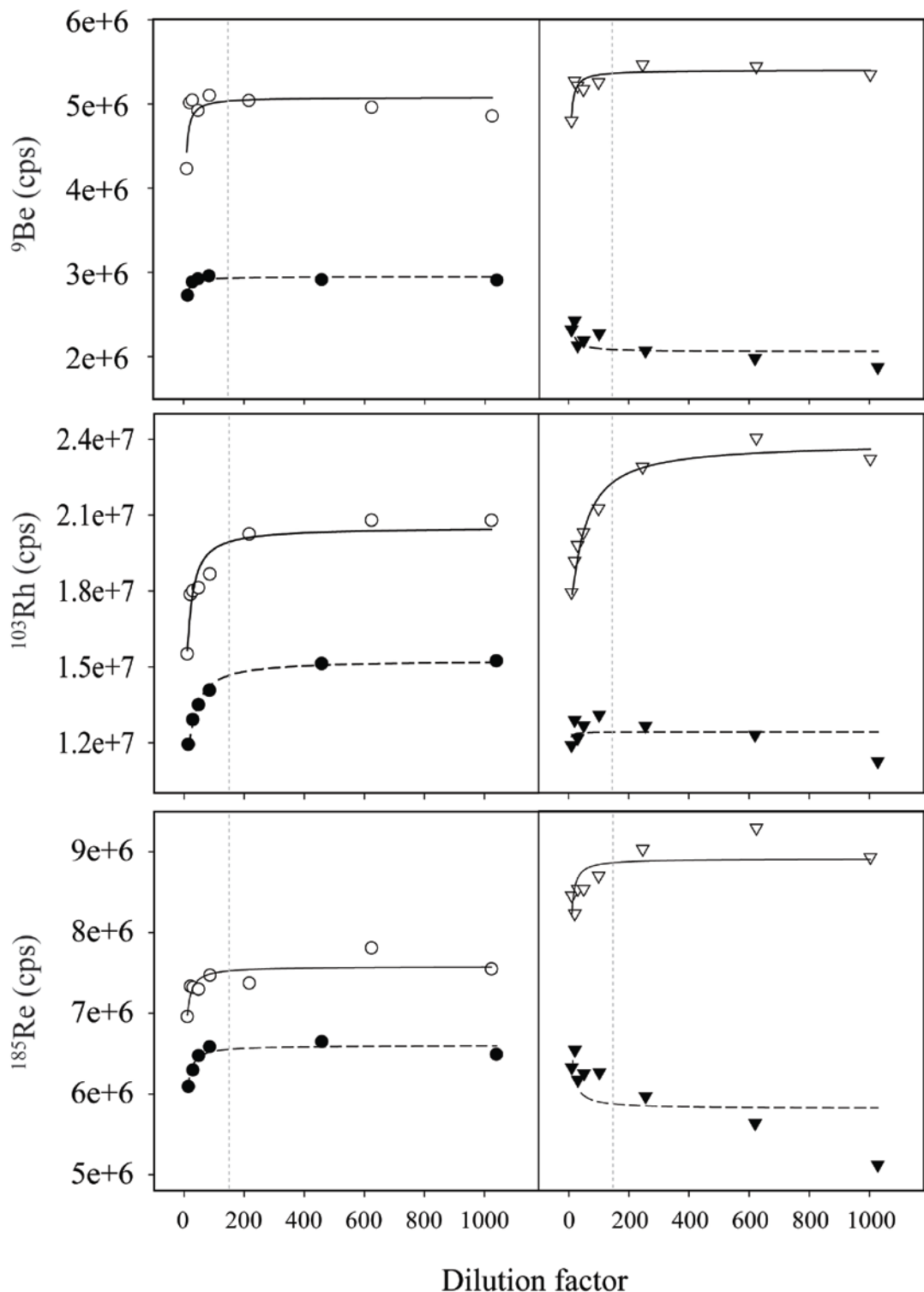


Figure 2.2 Internal standard counts (Be, Rh, and Re) in fish plasma (circles) and Seronorm (triangles) diluted with Mix 1 (solid symbols, dashed line) and Mix 2 (open symbols, solid line). The vertical grey lines show the dilution factor chosen for subsequent analyses. Unexpected patterns were observed for the 'Seronorm + Mix 1' combination, but these particular analyses were at the start of the sequence and coincided with a shift in instrument performance, so should be treated with caution. Subsequent samples were drift corrected using subsequent, unaffected blanks

### 2.3.3 Precision and detection limits

With the exception of Pb and Ba, internal precision was consistently better than 3% and similar for single tubes analysed repeatedly within runs (Table 2.5). Error relating to sample processing resulted in higher RSD values for intra-assay repeats of multiple sample preparations, but precision was still generally around 3%, except for Ba (6.6%) and Pb (13.6%). The most conservative measure of external precision (inter-assay replicates of multiple preparations encompassing preparation, calibration and instrument-related errors) affected Pb measurements the most (23%), but produced RSD values 10% or less for all other elements. The elements closest to detection limits, Ba and Pb, exhibited the lowest overall precision, although the former appeared to be dominated by handling error, as indicated by elevated RSD for multiple sample preparations and high levels in the procedural blanks, while the latter appeared to be hampered more by calibration errors, as indicated by the lower  $r^2$  values of calibration curves and higher inter-assay RSD values.

On the whole, precision was superior for Seronorm analyses and generally <5%. Some of the differences in precision can be explained by the composition of the two blood fractions. Concentrations of Li, K and Ba were higher in Seronorm, sometimes by orders of magnitude (Table 2.6), and as a result, exhibited higher precision. However, Mn, Zn, Se and Sr were generally higher in fish plasma, but were rarely accompanied by higher precision. Overall lower precision in plasma analyses most likely relates to the sample matrix and treatment. Serum contains no clotting factors. Whilst any clotted and heterogeneous plasma samples were rejected, some had a slightly cloudy appearance, and any protein precipitation could affect matrix viscosity and behaviour. Also, once prepared, Seronorm aliquots were stored <1 month prior to analysis, while plasma samples were stored for up to 24 months. Inter-assay sample degradation may have contributed to the reduced precision for plasma analyses, however even for tubes prepared from a single sample >3 months apart, precision was still generally better than 10%, implying that any such effect was relatively minor.

Table 2.5 Average detection limits (LOD, in  $\text{ng g}^{-1}$ ) and precision (%RSD) for plaice plasma and Seronorm analyses. Internal precision is represented by the mean instrument (intra-analysis) error for all plasma samples ran over 5 days. External precision is represented by the mean RSD of intra- and inter-day repeat analyses of single (S) or multiple (M) preparations of a given sample. Analysis numbers are shown in parentheses.

Element	LOD (30)	Plaice plasma			Seronorm		
		Internal precision (380)	S (8)	Intra M (25)	Inter M (12)	Intra M (3)	Inter M (6)
Li	0.021	1.8	2.7	3.0	9.9	0.9	2.5
Mg	0.332	0.9	1.4	2.7	5.2	0.8	1.9
K	2.079	1.0	1.1	2.0	5.4	1.2	2.2
Ca	11.12	0.9	2.1	3.6	5.1	0.7	2.8
Mn	0.009	1.3	1.0	3.2	5.1	2.0	3.5
Cu	0.071	1.0	0.7	3.0	4.5	0.2	1.3
Zn	3.583	0.8	0.9	3.1	6.0	0.1	1.5
Se	1.003	2.6	2.7	3.2	8.1	5.4	5.9
Rb	0.0007	2.1	2.2	3.5	5.6	1.0	3.6
Sr	0.018	1.5	0.5	2.8	4.1	4.7	2.3
Ba	0.035	3.1	2.3	6.6	10.0	1.0	1.2
Pb	0.011	5.5	5.1	13.6	23.3	5.2	21.2

### 2.3.4 Accuracy

Owing to the lack of commercially available fish plasma reference materials, external accuracy was assessed using Seronorm, a human serum. As mentioned above, there are substantial differences in NaCl content of human and marine fish blood, but there were also differences in other elemental concentrations, particularly Li and Sr (Table 6). However, if one assumes broadly similar behaviour among blood types, accuracy was deemed satisfactory, as measured Seronorm concentrations were generally within certified ranges. Se was the exception, for which half the measurements were slightly out of range, producing an average concentration  $0.0002\mu\text{g g}^{-1}$  higher than the maximum accepted value. Ba concentrations were also at the upper end of the range, although individual measurements were all within certified limits.

Agreement between reference ranges and previously published concentrations (Table 2.1 and Table 2.6) provides some additional corroboration for the method and values presented herein. Generally, where available, measured concentrations agreed with those reported in the literature (e.g. Li, Mg, Ca, Cu), particularly when comparing analogous blood fractions. However there is substantial variability in the literature, so exceptions and noteworthy patterns are discussed below. Note that here, whole blood is referred to simply as 'blood'.

Table 2.6 Measured concentrations and reference ranges for 12 elements in male and female plaice plasma and Seronorm. All results in  $\mu\text{g g}^{-1}$

Element	Plaice plasma			Plaice plasma			%RSD	Mean	'Certified acceptable range'
	All analyses (n = 157 <sup>a</sup> )	Males (n = 85)	Females (n = 72)	(n = 157 <sup>a</sup> )					
Li	100	0.0653	0.0632	0.0509 - 0.0740	0.0665	0.0549 - 0.0770	10.9	5.36	4.78 - 5.62
Mg	100	26.608	26.801	19.377 - 40.683	26.499	21.278 - 45.300	26.2	18.48	17.10 - 19.50
K	100	42.600	44.803	13.972 - 110.007	40.939	12.872 - 101.572	62.1	116.86	100.00 - 124.00
Ca	100	126.77	123.92	107.77 - 148.57	136.73	112.25 - 190.42	16.2	98.24	85.10 - 100.00
Mn	100	0.0210	0.0166	0.0089 - 0.0413	0.0242	0.0112 - 0.0495	49.6	0.0095	0.0071 - 0.0011
Cu	100	0.7363	0.7664	0.4887 - 1.0926	0.7124	0.4522 - 1.0227	24.8	1.116	1.010 - 1.330
Zn	100	12.495	13.100	9.094 - 16.561	11.539	7.109 - 16.891	21.2	1.320	1.100 - 1.340
Se	100	0.3677	0.3747	0.2344 - 0.5158	0.3612	0.2317 - 0.4753	22.9	0.0650	0.0536 - 0.0648
Rb	100	0.0064	0.0070	0.0019 - 0.0155	0.0063	0.0021 - 0.0151	64.0	0.0030	0.0027 - 0.0039
Sr	100	1.0303	0.9981	0.7643 - 1.2839	1.0784	0.8584 - 1.3977	16.0	0.0261	0.0228 - 0.0280
Ba	100	0.0078	0.0082	0.0026 - 0.0234	0.0073	0.0029 - 0.0254	70.3	0.1549	0.0920 - 0.1560
Pb	84.5	0.00032	0.00027	0.00010 - 0.00066	0.00044	0.00011 - 0.00134	87.2	0.0026	0.0025 - 0.0033

<sup>a</sup> 157 blood samples from 18 fish (8F, 10M), taken monthly for 1 year, but excluding the spawning period (January - March); <sup>b</sup> 5th - 95th percentile

## Potassium

All studies in which the concentration of K has been reported to exceed 800  $\mu\text{g g}^{-1}$  (Table 2.1) used blood as the analysis medium. Concentrations in the current study were in keeping with those determined in serum and plasma of other species, albeit at the lower end of the spectrum. It has been suggested that the release of K from cells and platelets during blood coagulation result in unnaturally elevated K concentrations in serum (Hrubec and Smith, 1999). On the other hand, in a study examining optimal treatment of salmon blood, plasma K was significantly reduced in samples stored for extended periods (8.5 hrs) prior to centrifugation, potentially due to movement of K<sup>+</sup> ions into erythrocytes (Clark *et al.*, 2011). While this may help to explain our low K concentrations, our pre-centrifugation periods were less than half those used in the latter experiment, and our median value was almost identical to the concentration reported for a closely related flatfish (Fletcher, 1975) (42.6 cf. 43  $\mu\text{g g}^{-1}$ ).

## Manganese

Measurements in the current study were approximately five times lower than Mn concentrations reported for blood from four freshwater species. This implies an effect of blood fraction and an association between Mn and erythrocytes, and the same pattern has also been observed among human blood fractions (Goulli *et al.*, 2005). However, there is considerable variation in the reported Mn concentrations among a very limited

number of studies to measure Mn in fish blood, plasma or serum (Table 2.1), making it difficult to draw useful conclusions.

### **Zinc**

Measured Zn concentrations were in similar ranges to previously reported values for marine and freshwater species, but approximately four times lower than those reported in blood. Similarly, Zn was about six times lower in human serum than in blood, again implying erythrocyte binding (Barany *et al.*, 2002). However, given overlap in Zn concentrations among blood fractions in Table 2.6, the differences noted are more likely due to sample contamination (Versieck and Cornelis, 1989), physiological status (Thompson *et al.*, 2002) and/or environmental exposure, with waterborne Zn tending to follow a nutrient type distribution (Bruland and Lohan, 2003).

### **Selenium**

Measured Se concentrations were similar to those measured in the blood of two marlin species, but an order of magnitude lower than levels found in tuna blood in the same study (Kai *et al.*, 1992). The discrepancy may be related to tuna-specific elemental processing as a result of its unique metabolism (Dickson, 1995).

### **Rubidium**

Rb concentrations in the blood of two freshwater species and one marine species (Hansen *et al.*, 1978; Melancon *et al.*, 2009) were approx. 400 and 70 times higher than those measured in the current study, respectively. Some of this variation could be due to blood fraction, with human blood exhibiting Rb concentrations approximately 12 times higher than equivalent serum samples (Barany *et al.*, 2002). However, given the magnitude of the differences and the fact that Rb concentrations are generally conserved with salinity (Bruland and Lohan, 2003), the elevated concentrations reported for the freshwater species are most likely an effect of sample treatment.

### **Strontium**

Measured Sr concentrations were almost identical to those previously reported in the plasma of another marine species (Kalish, 1991), but almost an order of magnitude higher than concentrations reported in the blood of three freshwater species (Shearer, 1984; Melancon *et al.*, 2009). Sr is a conservative element and concentrations are similarly elevated in the biomineralised tissues of marine species (Campana, 1999), implying an effect of environmental availability rather than blood fraction, sample treatment or analysis method.

## **Barium**

Even with the concerns for potential Ba contamination in the present study, measured Ba was approximately 30 times lower than those reported in the blood of two freshwater fish species (Melancon *et al.*, 2009). The discrepancy is unlikely due to fluid type as human plasma Ba levels were, if anything, higher than equivalent blood samples (Goule *et al.*, 2005). The differences are more likely the result of ambient concentrations, with Ba generally more abundant and bioavailable in freshwater systems (Bruland and Lohan, 2003; Elsdon and Gillanders, 2005b).

## **Lead**

Pb concentrations determined in the present study were approximately 500 times lower than those determined in the blood of a number of freshwater species. This may not simply be due to contamination, although Pb contamination is notoriously difficult to avoid (Versieck and Cornelis, 1989). In humans, Pb has been found to be 56 and 420 times higher in blood than serum (Barany *et al.*, 2002) and plasma (Goule *et al.*, 2005), respectively. Such results imply that the majority of blood Pb exists bound to erythrocytes and other components, such as platelets.

### **2.3.5 Reference ranges**

An investigation into the intrinsic and extrinsic influences on blood composition of plaice is beyond the scope of the current study. Reproductive events in teleost fish are coupled with major changes in blood chemistry (Kalish, 1991), so samples collected during the spawning period were excluded from the reference ranges. Even with this step in place, there was considerable variation in measured concentrations, as indicated by the RSD values in Table 2.5. Plaice are sexually dimorphic, exhibiting sex-related differences in life history traits such as reproductive investment and growth (Rijnsdorp, 1989). These traits will almost certainly affect blood composition, so reference ranges are displayed for males and female fish separately. Indeed, the results indicate that plasma Ca, Mn, Sr and Pb concentrations were generally higher in the female fish, while Cu, Zn and Se concentrations were generally higher in the males.

## 2.4 Conclusions

The results here indicate that a suite of trace and minor elements can be simultaneously quantified in fish plasma using simple dilution methods. To date, most studies examining fish blood elemental chemistry have focused on major elements, freshwater species and/or whole blood. To our knowledge, no previous study has measured Mn, Ba or Pb in any blood fraction of a marine fish species nor determined Rb, Pb or Se in serum or plasma fractions of any fish species, and none have previously analysed fish plasma or serum by ICPMS or HR-ICPMS. Also no previous studies have investigated analysis methods for this unique biological fluid, characterised by particularly elevated protein and salt concentrations. For serial sampling experiments such as ours, it is crucial to use low sample volumes to minimise stress and maintain a healthy population. The lower yield obtained using serum over plasma (Uges, 1988), and the potential for reworking of blood components during coagulation, particularly for fish (Hrubec and Smith, 1999), make plasma the preferred biofluid for such experiments. By heparinising syringes using standardised, low volume procedures and a high purity preparation, we found that procedural blanks were not significantly higher than laboratory blanks in any of the measured elements except Ba. However, whatever the source of the Ba contamination, it did not appear to transfer significantly into the blood samples.

While HR-ICPMS is an excellent tool for multi-element analyses, combining high sensitivity with a capability to separate analyte peaks from spectral interferences, it is particularly susceptible to salt loading and matrix changes. By carefully tuning the instrument, using the highest possible dilution factor and matrix matching among samples, blanks and standards where possible, such effects were minimised in this study. The simple dilution procedure described here produced precise and accurate results for almost all elements in question, however Pb and Ba concentrations were at, or close to, detection limits, so a slightly lower dilution factor would be recommended for studies prioritising these metals.

An area that would greatly benefit from improved understanding of blood elemental behaviour is biomimetic microchemistry (Campana, 1999). Otoliths ('earstones') are acellular calcium carbonate structures, common to all bony fish, that grow incrementally incorporating chemical markers from the environment and producing a time-resolved natural tag that can infer stock identity and individual movements (Campana, 1999). They represent a valuable resource in fish ecology and management, but the mechanisms underpinning elemental fractionation from water to the blood, blood to endolymph, and finally into the otolith, are poorly understood, hindering progress within this field. Accurate and precise determination of element concentrations in multiple biological tissues, including plasma, is key to understanding the behaviour of ions in metabolic reactions and their movements across biological membranes.

It is also crucial that reliable blood reference ranges are determined across a wide range of species and systems. These concentrations can improve clinical diagnosis and provide crucial biomarkers of population health, both of which are increasingly important for the fast-growing aquaculture sector. Currently, few studies have attempted multi-elemental analysis of fish blood, while some of the variations among published concentrations imply contamination issues and/or incompatibilities among biofluids and analytical techniques. The production of accurate and precise measurements of trace element concentrations in a range of fish species, blood fractions and physiological states will allow a better understanding of natural and anthropogenic variations. A key objective in the field of fish trace elemental chemistry should be the development of a CRM for fish blood and plasma, and inter-study standardisation of sample treatment and analytical techniques

## 2.5 Acknowledgements

The research was funded (partially) by Defra contract M1102 MEMFISH (Macroecology of marine finfish in UK waters) and an FSBI studentship to AMS. Particular thanks go to CEFAS staff for their help with animal husbandry and sample collection and to S. Campana for his help with reference sourcing.



# Chapter 3

---

## *Experimental results: Environmental and physiological influences on blood element chemistry*

### 3.1 Introduction

In order to understand potential physiological influences on incorporation of ions into the otolith, and thus to determine how closely otolith composition reflects ambient conditions, it is essential to first consider ion fractionation between the environment and the blood. Elemental uptake is likely to be regulated for all elements, as the persistence of internal homeostasis is vital to the health and survival of all organisms, and the circulatory system integral to maintaining ion balance (Evans, 1993). Fish blood is in constant flux, with elements assimilated from the gills, gut and via tissue turnover, and removed by excretion and storage in various tissues. Around half of the blood fluid is comprised of plasma, which contains proteins, glucose, dissolved ions, hormones, platelets, blood cells and waste products such as carbon dioxide and urea (Thermo, 2009b). Blood proteins play a number of crucial roles, but it is their role as a transport molecule that has the greatest implications in the field of otolith microchemistry (Kalish, 1991). Protein binding influences the

rate of elemental turnover and exerts a major influence on the proportion of dissolved free ions in the blood and their ability to pass across membranes via passive diffusion or active ion pump channels. While it is unlikely that proteins are able to move freely from blood to endolymph, some proteins and free amino acids are likely to form the precursor molecules for assembly of the otolith organic matrix (OM) by the saccular epithelial cells (Payan *et al.*, 2004a). Thus, even predominantly 'bound' metal ions may still enter the endolymph and become incorporated into the otolith crystals or OM. While representing only a small fraction of the total otolith mass, the OM plays a vital role in otolith biomineralisation and structure, thought to regulate crystal morphologies and growth rates (Campana, 1999; Tomás *et al.*, 2004).

In the current study, a "mensurative experiment" (Hurlbert, 1984) was carried out examining seasonal changes in blood and otolith elemental composition in plaice (*Pleuronectes platessa*). Monitoring seasonal changes in teleost blood chemistry is not new, but few previous studies have described within-fish blood trace element concentrations over time and even fewer have attempted to link blood and otolith elemental composition. In fact, the most rigorous example of such a study was carried out over two decades ago (Kalish, 1991). In this study, blood and endolymph Na, K, Sr, Ca and otolith edge Na/Ca, K/Ca, Sr/Ca and S/Ca concentrations were described in wild bearded rock cod (*Pseudophysis barbatus*), an exclusively marine species. Blood and otolith element concentrations were linked to temperature and a variety of biological parameters. Using total length (TL), condition, gonadosomatic index (GSI), age and plasma Sr and Ca, more than 80% of the variance in female otolith Sr/Ca ratios could be explained. For otolith Sr/Ca ratios with both sexes combined, endolymph protein and total weight (TW) were amongst the most important predictors. This was the first concerted attempt to explain physiological effects on otolith microchemistry, and while extremely thorough there were some caveats. While water elemental concentrations were not formally measured, salinity was, but it was not included as a possible predictor variable, so any potential contribution to plasma, endolymph and otolith concentrations could not be determined. Also, as the study was based on single measurements from wild caught fish, there was no way of partitioning individual variation vs. temporal variation, and there was the possibility that subjects had recently immigrated to the study site from areas of different physicochemical conditions. Aside from Kalish (1991) and experimental work examining pathways of major ions from plasma to endolymph and otoliths (e.g. Payan *et al.*, 2002; Payan *et al.*, 2004b), most studies have focused on *in vitro* experiments (e.g. Tohse and Mugiyama, 2001; Payan *et al.*, 2002) or the relationship between manipulated conditions and otolith concentrations (e.g. Geffen *et al.*, 1998; Bath *et al.*, 2000; Walther and Thorrold, 2006; Ranaldi and Gagnon, 2008). These are clearly very important, but the removal of an animal from its natural environment could result in changes in elemental processing, so should be complemented by mensurative experiments as well as field observations. In a more

recent study by Melancon *et al.* (2009), average water, blood, endolymph and otolith concentrations of Na, Mg, Ca, K, Mn, Zn, Ba, Sr and Pb (and Fe and Rb for water and blood) were compared in two freshwater species, burbot (*Lota lota*) and lake trout (*Salvelinus namaycush*). Given different collection years for the endolymph and otolith cf. water and blood samples, some of the reported 'partition coefficients' should be taken with caution, however, this represents the only other study to have related sub-ppm elemental concentrations between water, blood and otoliths.

While plaice blood hormone and major ion concentrations have been well described (e.g. Cobb *et al.*, 1973; Scott *et al.*, 1998), no previous study has examined their blood trace element concentrations. In the current chapter, seasonal changes in blood plasma elemental concentrations are described for an experimental population of plaice, and the main environmental and physiological influences examined by means of mixed effects models.

## 3.2 Methods

Experimental design and blood analysis methods were described in Chapter 2, but in brief, plaice were maintained under natural, but monitored, conditions for 7-12 months and their blood elemental chemistry analysed each month. The main group of plaice were sourced from the Irish Sea (IS) in February 2009 and sampled 02/06/09 - 28/05/10, while a second group of plaice (7 females) were sourced from the English Channel (EC) in August 2009 and introduced to the same tank and sampling regime on 27/10/09. On 18/01/10, approximately half of the fish were treated with gonadotropin-releasing hormone (GnRH) to encourage spawning and an additional sampling date was added at the start of February. Otherwise, blood sampling was carried out once per month. The sampling and analysis methods used to collect the suite of 'environmental' and 'physiological' data are described in full below.

At the end of the experiment, otoliths were removed and ages determined by counting translucent growth bands on transverse sections. Fish were selected based on their otolith growth characteristics and the clarity of the OTC mark. Any that had died prior to the end of the experiment were excluded. These selection criteria obviously have the potential to bias the results towards healthier, faster growing fish, but given the ultimate aim of the study, it was deemed essential to ensure sufficient new otolith material to allow repeat sampling across the experimental period. Nineteen fish were selected for blood and otolith analyses (6 males, 7 IS females, 6 EC females) and five additional fish selected at random for the blood analyses (4 males, 1 IS female, 1 EC female). The results presented in the current chapter apply only to this subset of fish ( $n = 25$ ).

### 3.2.1 Environmental variables

To examine environmental effects on otolith and blood trace element composition, water temperature, salinity and element concentrations were monitored throughout the experiment (Table 3.1).

Table 3.1 Collection details for the environmental variables measured during the aquarium study

Variable	Sampling method	Details	Frequency and resolution
Temperature	Aquarium staff took temperature measurements each morning	Ambient but capped at approx. 14°C	Daily
Salinity	Aquarium staff overfilled brown glass bottles in Raceways A, that were later analysed in the CEFAS nutrient laboratory.	Ambient	Weekly
Water elemental chemistry (Li, Mg, K, Ca, Mn, Cu, Zn, Se, Rb, Sr, Ba, Pb)	For blanks, an acid-cleaned plastic syringe was flushed 3 times with MQ water, then 7ml MQ pushed through an acid cleaned filter (Millex <sup>®</sup> nylon membrane, 0.2µm) into a pre-acidified (HNO <sub>3</sub> ) bottle. The same syringe, filter and procedure was immediately used to collect a seawater sample direct from the plaice tank. All water samples were stored at -20°C	Ambient. Procedural blanks also taken each sampling event	Weekly

#### 3.2.1.1 Water elemental analysis

Seawater samples from the experimental tank (collection details in Table 3.1) were analysed by ICPMS and concentrations calculated by external calibration. Initially, samples were diluted 1000-fold and analysed for 12 elements (Li, Mg, K, Ca, Mn, Cu, Zn, Se, Rb, Sr, Ba and Pb) by quadrupole ICPMS (X-series, Thermo Fisher scientific). Most of the lower level elements were below detection limits so the same samples were analysed for all elements except majors (Mg, K and Ca) at 15-fold dilution on an Element 2 high resolution ICPMS (HR-ICPMS; Thermo, Bremen, Germany). Element isotopes and instrument operating conditions are provided in Table 3.2. Multi-element parent solutions were prepared using 3% HNO<sub>3</sub> and single element standards (Inorganic Ventures and Romil). Samples and standards were spiked with internal standards (<sup>9</sup>Be at 10 ng g<sup>-1</sup>; <sup>115</sup>In and <sup>185</sup>Re at 5 ng g<sup>-1</sup>) to correct for instrument drift and signal suppression, and NASS-5 (Seawater Reference Material for Trace Metals, NRC) was used as a seawater 'base' in the calibration series to improve matrix matching among standards and samples. NASS-5 is characterised by low heavy metal content, but it was diluted 1.2 times to ensure there were some points below the unknowns in each 5-point calibration curve. All solutions were weighed to the nearest 0.00001g and concentrations calculated by weight. Attempts to reduce possible matrix effects were made by (1) analysing blanks and calibration series only at the start or end of the sequence, (2) 'conditioning' the instrument after blanks using

repeat analysis of appropriately diluted seawater, and (3) randomising sample order. To estimate external precision and accuracy, CASS-4 (Nearshore Seawater Reference Material, NRC) and a randomly chosen seawater sample ('procedural standard') were analysed repeatedly throughout the run.

Raw counts were drift corrected and blank subtracted offline. Concentrations in the NASS-5 'base' were determined by standard addition and accounted for in the external calibration curves ( $r^2$  values all  $>0.999$ ). Ideally one would measure all elements on the same instrument in the same run, but the orders of magnitude differences between trace and major element concentrations in seawater meant that this was not possible. As such, the results from the 1000-fold dilution X-Series run were used only to quantify elements at the ppm level (Mg, K, Ca and Sr) and the 15-fold dilution Element 2 run used for sub-ppm elements. Concentrations were presented as absolute concentrations but also converted into molar ratios to Ca for comparisons with otolith concentrations. Measurements of Li, Rb and Sr were highly correlated among instruments, but absolute concentrations were, on average, 5.7%, 5.5% and 3.8% higher on the HR-ICPMS, respectively (Figure 3.1). The reason for this slight offset was not clear, but while absolute values for concentrations and ratios were slightly different, temporal patterns were not changed.

Limits of detection (LOD, 3 standard deviations [s.d.] of blank analyses) and estimates of precision are displayed in Table 3.3. With the exception of Zn and Mn (55% and 2%  $<\text{LOD}$  respectively), all sample analyses were above detection limits. All Zn measurements in CASS-4 were  $<\text{LOD}$  but all other elements  $>\text{LOD}$ . With the inclusion of sub-LOD Zn measurements, the average measured concentration in CASS-4 was just slightly below the certified acceptable range (Table 3.3). As the method for setting LOD is somewhat arbitrary and can lead to the loss of potentially valuable information, some studies have purposely included sub-LOD values (e.g. Ben-Tzvi *et al.*, 2007). In the current study, it was impossible to obtain matrix-matched blanks, leading to some uncertainty in the LOD. Also, given the fact that Zn is a highly mobile element (Versieck and Cornelis, 1989), exclusion of sub-LOD values may just bias the dataset towards contaminated samples. For these reasons, all Zn measurements were retained. Congruence among temporal patterns in the 'soft acid' metals (Zn, Cu, Pb in particular) implied that the sub-LOD Zn measurements were reliable; however, results should clearly be taken with some caution. Accuracy was otherwise deemed satisfactory, with Cu, Mn and Pb measurements within certified ranges (Table 3.3). Outliers, defined as concentrations greater than the 'median + 3 s.d.' were excluded and samples containing 2 or more outliers were considered contaminated and excluded from the dataset ( $n=1$ ).

Table 3.2 Isotopes and operating conditions for seawater analyses on the X-Series ICPMS and Element 2 HR-ICPMS. Operating conditions for the Element 2 were otherwise identical those described in Table 1.2

**X-Series ICPMS:**

RF power (W)	1400
Sample uptake rate ( $\mu\text{l min}^{-1}$ )	700
Ar gas flow rates ( $\text{l min}^{-1}$ ):	
Coolant	13.0
Auxiliary	0.8
Nebuliser	0.88
Sampling depth	165
Spray chamber	Peltier cooled cyclonic/impact bead-type
Sample cone / Skimmer	Standard Ni Xt
Scanning mode	Peak jumping
Dwell time (ms)	10
Sweeps	50
Isotope list	$^7\text{Li}$ , $^9\text{Be}^a$ , $^{24}\text{Mg}$ , $^{39}\text{K}$ , $^{44}\text{Ca}$ , $^{55}\text{Mn}$ , $^{63}\text{Cu}$ , $^{66}\text{Zn}$ , $^{78}\text{Se}$ , $^{85}\text{Rb}$ , $^{88}\text{Sr}$ , $^{115}\text{In}^a$ , $^{137}\text{Ba}$ , $^{185}\text{Re}^b$ , $^{208}\text{Pb}$

**Element 2 HR-ICPMS:**

LRM	$^7\text{Li}$ , $^9\text{Be}^a$ , $^{85}\text{Rb}$ , $^{86}\text{Sr}$ , $^{115}\text{In}^a$ , $^{118}\text{Sn}^b$ , $^{137}\text{Ba}$ , $^{185}\text{Re}^b$ , $^{208}\text{Pb}$
MRM	$^9\text{Be}^a$ , $^{55}\text{Mn}$ , $^{65}\text{Cu}$ , $^{66}\text{Zn}$ , $^{115}\text{In}^a$ , $^{185}\text{Rh}^a$
HRM	$^{77}\text{Se}$ , $^{78}\text{Se}$ , $^{115}\text{In}^a$ , $^{185}\text{Re}^a$
Acquisition mode	E scan, Mode 1, 3 runs 3 passes [9 scans], 2m40s analysis
Mass window (%) <sup>c</sup>	50 (Li and Be in LRM), 20 (rest of LRM), 125 (MRM), 150 HRM
Search window (%) <sup>c</sup>	50 (Li and Be in LRM), 0 (rest of LRM), 100 (MRM and HRM)
Integration window (%) <sup>c</sup>	80 (LRM), 50 (MRM), 60 (HRM)
No. of samples per peak	100 (LRM), 40 (MRM) 60 (HRM)
Sample time (ms)	10 (LRM), 20 (MRM and HRM)

<sup>a</sup> Internal standards <sup>b</sup> In case of interference on  $^{115}\text{In}$  <sup>c</sup> Percent of peak width

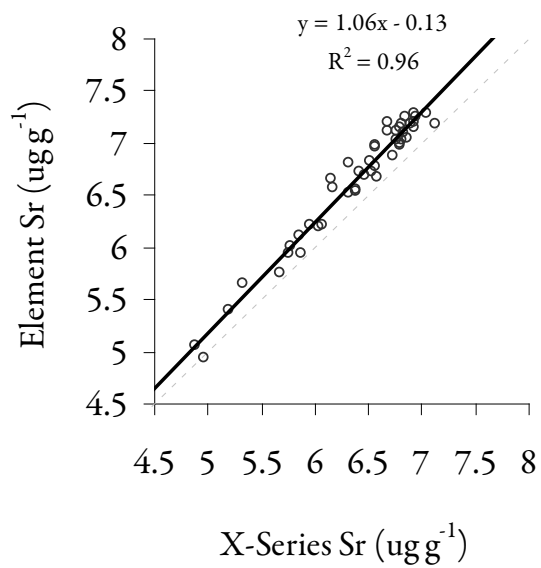
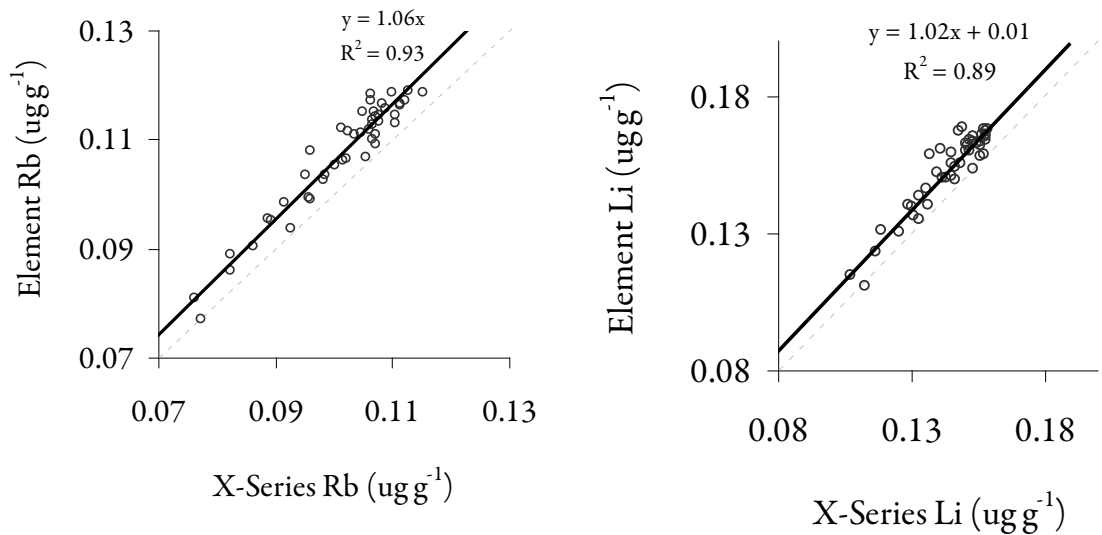


Figure 3.1 Concentrations of Li, Rb and Sr for the same samples measured on the X-Series ICPMS (1000-fold dilution) and the Element 2 HR-ICPMS (15-fold dilution). The 1:1 reference line is displayed as a dashed grey line

Table 3.3 Detection limits (LOD) and average internal and external precision for seawater analyses carried out on the X-Series ICPMS (1000-fold dilution) and Element 2 HR-ICPMS (15-fold dilution). Zn was <LOD in the consistency sample and CASS-4, but were included in the dataset. Accuracy was assessed using certified ranges for the CASS-4 reference material where available. All except Zn were within range.

	LOD (ng g <sup>-1</sup> )	Internal	External precision	Mean measured	Certified conc.
		precision (%RSD) n= 56	(%RSD) Consistency sample (n)	conc. (ng g <sup>-1</sup> ) CASS-4 n=4	range (ng g <sup>-1</sup> ) CASS-4 n=4
X-series	Mg	7.1 x 10 <sup>-5</sup>	0.98	1.81 (4)	1.115 x 10 <sup>6</sup>
	K	1.5 x 10 <sup>-3</sup>	1.06	1.81 (4)	3.34 x 10 <sup>5</sup>
	Ca	1.8 x 10 <sup>-3</sup>	1.56	0.77 (4)	3.44 x 10 <sup>5</sup>
	Sr	1.3 x 10 <sup>-6</sup>	0.62	0.76 (4)	6.31 x 10 <sup>3</sup>
Element 2	Li	0.0163	1.84	0.46 (3)	152.78
	Mn	0.0082	3.02	2.87 (3)	2.93
	Cu	0.0027	1.98	2.82(3)	0.631
	Zn	0.3565	4.51	15.43 (3)	0.308
	Se	0.0011	1.76	3.17 (3)	0.063
	Rb	0.0007	1.31	1.05 (3)	110.92
	Ba	0.0032	1.00	0.68 (3)	6.84
	Pb	0.0035	2.69	1.16 (3)	0.0097

### 3.2.1.2 Smoothing of environmental data

While physiological sampling was carried out at least once per month, there was substantial variability in the sampling date within each month. As such, 'Local Polynomial Regression Fitting' smoother (LOESS, R software) was used to predict temperature, salinity, elemental concentrations and element/Ca ratios for each specific sampling date. LOESS fits a polynomial model using a weighted least squares linear regression and a window size ( $\alpha$  or 'span') determined by the user. For example, a span of 0.3 would give a fit at point x based on a window containing 30% of the data, weighted by distance from x (Cleveland *et al.*, 1992). For temperature and salinity, which were sampled more frequently and exhibited lower variability over time, a narrower window was used (span = 0.25). Elemental concentrations and ratios to Ca were generally more variable over time. It was assumed that some of this variability was the result of sampling, processing and instrument artefact, but also that elemental processing and the ultimate expression of environmental effects in the fish would incorporate some biological lag and natural smoothing. As such, a span of 0.5 was used for all water concentrations except for elements close to detection limits (Mn, Zn and Se), for which a span of 0.6 was used to avoid over-fitting noisy data. The smoothing effect can be visually examined in the plots presented in Section 3.3.2.1 and resulted in local smoothing of temperature and salinity data across c. weekly time frames, while elemental data was smoothed over c.monthly time frames.

### 3.2.2 Physiological variables

On each blood sampling day, fish length and weight were recorded (Table 3.4), photographs were taken of the females for GSI estimation (Section 3.2.2.1) and blood samples were collected by caudal venipuncture. Full details of blood treatment and elemental analyses are provided in Chapter 2, but in brief, blood samples were centrifuged within 3 hours of collection and the plasma aliquoted for protein (Section 3.2.2.2) and elemental analyses. Blood plasma was stored at -20°C.

Table 3.4 Details of the physiological variables measured each month during the aquarium study

Variable	Details
Total length (TL)	to 0.1 cm*
Total weight (TW)	to 0.1 g
Fulton's Condition Factor ( $K$ )	$TW/TL^3 \times 100$
Daily growth rate	$mm\ day^{-1} (TL_2 - TL_1 / \text{no. days})^{\dagger}$
Gonadosomatic index (GSI)	Ovary mass/TW $\times 100$
Total plasma protein	g dL $^{-1}$

\* It was assumed that, in lieu of physical tail damage, fish cannot decrease in length, so if TL decreased between months but tail damage was not visible in associated images, the previous TL was carried forward.

$\dagger$  Month 1 was thus always assigned a growth rate of zero.

#### 3.2.2.1 Gonadosomatic index (GSI)

GSI in the female fish was estimated over the course of the experiment using the methods of Kennedy *et al.* (2008). Photographs were taken of the fish on a lightbox, and the area of the ovary shadow, posterior to the body cavity, was measured using ImageJ freeware (Abramoff *et al.*, 2004) (Figure 3.2). Due to the position and small size of the testes, it was not possible to use this method to estimate male GSI. Training was carried out using photographs and measurements from the study by Kennedy *et al.* (2008) and via email discussion (J. Kennedy pers. comm., 2009). Ovary area ( $O_a$ ) was measured three times per calibration image, without knowledge of the fish or month. The relationship between average  $O_a$  and ovary mass ( $O_m$ ) was calibrated using ovaries from any females that died mid-study or were sacrificed on completion of the experiment and used to estimate  $O_m$  values, which were then used to calculate GSI (Table 3.4). Given that no females died during the spawning season, six gravid plaice from the study of Kennedy *et al.* (2008) were used to constrain the upper end of the calibration curve. Otherwise GSI values could exceed 60%, which is highly unlikely. Overall, ovary mass exhibited a strong ( $r^2 = 0.98$ ) non-linear relationship with ovary area, best described by a two-order polynomial curve (Figure 3.3).

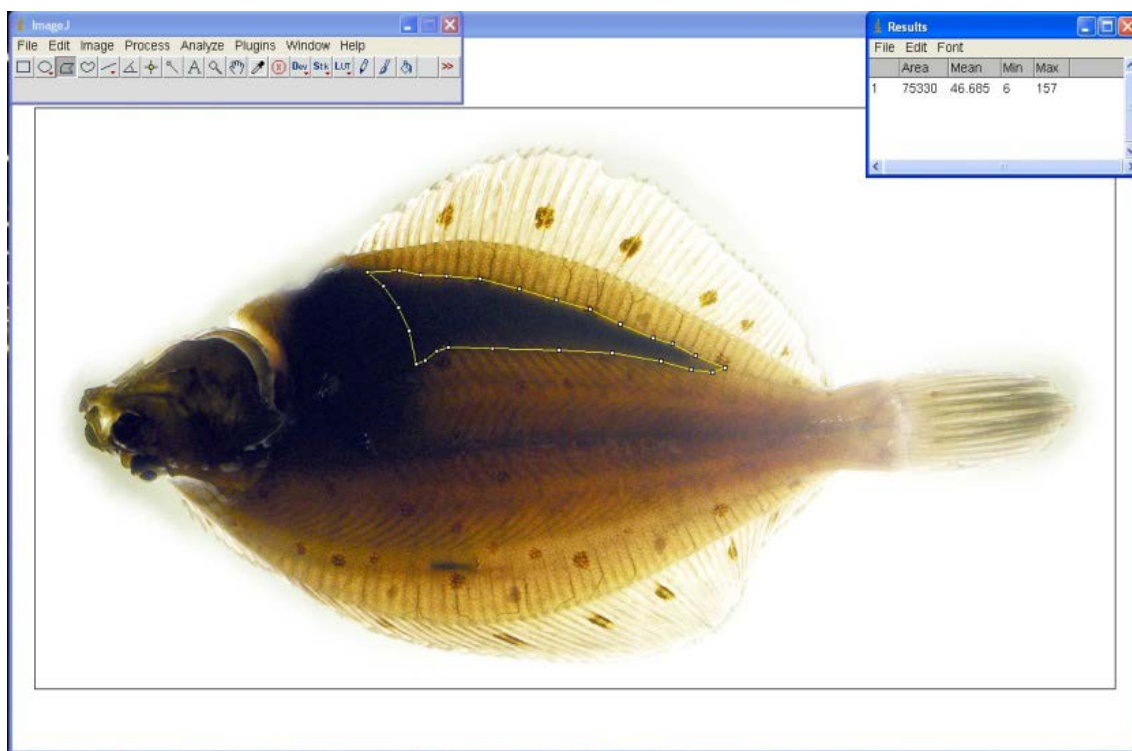


Figure 3.2 Method for measuring the area of the ovary shadow using ImageJ software, in order to estimate ovary mass and GSI non-destructively (after Kennedy *et al.*, 2008)

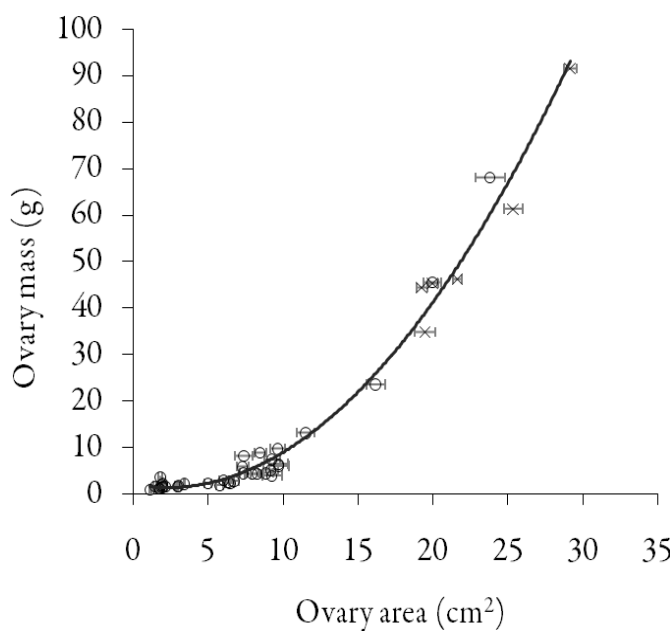


Figure 3.3 Relationship between ovary area and mass ( $y = 0.1267x^2 - 0.5782x + 2.0286$ ,  $r^2 = 0.98$ ), used to predict GSI in female plaice during the experiment. Ovary area is represented by the mean ( $\pm$  SEM) of three repeat measurements taken from the final available image of females in the current study (circles) and six from Kennedy *et al.* (2008) (crosses).

The percentage error for measured vs. predicted GSI on the final sampling day was 24.6%. It should be noted that this comparison was made post-spawning, when GSI was generally <3% and this particular measure of GSI is more relative than absolute. On the whole, however, estimated GSI values were within realistic ranges (0.33-30.4%), with measured GSI in American plaice (*Hippoglossoides platessoides*) up to ~37% (Maddock and Burton, 1998).

### 3.2.2.2 Blood proteins

Blood plasma was analysed for total protein using the Biuret test (Wedemeyer and Yasutake, 1977). Standards were made in replicate using Bovine Serum Albumin (Sigma-Aldrich) and concentrations calculated by volume, using direct calibration and 'Standard Curve' software.

When blood sampling was less successful and only low volumes of plasma obtained, element analyses were prioritised over protein. This resulted in occasional missing protein values in the final dataset ( $n=12$  out of 282). For statistical purposes the missing values were replaced with the average of the previous and subsequent measurements within fish; otherwise the missing value resulted in exclusion of the entire row.

### 3.2.2.3 Blood element concentrations

As described in Chapter 2. Prior to statistical analysis, concentrations greater than the 'median + 5s.d.' were deemed 'contaminated' and excluded ( $n = 3$ , Pb;  $n = 1$ , Mg, Ba and Rb).

## 3.2.3 Data analysis

### 3.2.3.1 Summary of the variables included in the current chapter

Given the large number of parameters measured in the current study, a full list of the response and predictor variables are presented in Table 3.5. Note that throughout the text, concentrations are denoted 'El<sub>X</sub>' for element 'El' concentrations in medium 'X', where 'X' is defined as water (W), blood (B) or otolith (O).

### 3.2.3.2 Distribution coefficients (D)

Distribution coefficients from seawater to blood ( $D_{El(B/W)}$ ) were calculated using equation 1

$$D_{El(B/W)} = [Element]_{(blood)} / [Element]_{(water)} \quad (1)$$

Table 3.5 Physiological and environmental variables measured as possible controls on plaice blood elemental concentrations. Element concentrations (response variables) are divided among broad chemical groups. Note that TW was later excluded from the model selection criteria, as it was highly correlated with TL, and TL and condition factor were considered more appropriate measures of fish size and 'fatness', respectively.

Response variables ( $El_B$ )			Predictor variables	
Group I	Group II	'Soft' ions	'Physiological'	'Environmental'
$^{7}\text{Li}$	$^{24}\text{Mg}$	$^{55}\text{Mn}$	Sex	Time (Day number)
$^{39}\text{K}$	$^{44}\text{Ca}$	$^{63}\text{Cu}$	GnRH treatment (Y/N)	Water temperature
$^{85}\text{Rb}$	$^{88}\text{Sr}$	$^{66}\text{Zn}$	Origin (IS/ EC)	Salinity
	$^{137}\text{Ba}$	$^{78}\text{Se}$	Plasma protein concentration	$El_w$
		$^{208}\text{Pb}$	Fulton's condition factor	
			Growth rate	
			TL	
			TW	
			Age	
			GSI (females only)	

### 3.2.3.3 Data exploration and Pearson correlations

Initial data exploration was carried out in R, examining data distributions and pairwise Pearson correlations among variables. Pearson product-moment correlation coefficients (PCCs) and conditioning plots ('coplots', R) were used to explore broad relationships among variables. Coplots provide a simple means to visualise relationships and interactions across groups under specified conditions. Given that correlations were carried out on longitudinal, non-independent data, p-values could not be used to gauge the strength of the relationships, but PCC values greater than 0.6 were (arbitrarily) deemed 'strong'. Some of the predictor variables and elemental concentrations were  $\log_{10}$ , natural log (Ln) or square root (SQRT) transformed to meet assumptions of homogeneity and normally distributed residuals in the mixed effects models.

### 3.2.3.4 Linear mixed-effects models

Linear mixed effects models (lmer function, lme4 package) were carried out in R to examine which combination of physiological and/or environmental variables best explained variations in blood element concentrations. Mixed effects models allow for non-independence and autocorrelation of the response variable by inclusion of a 'random effect', in this case, 'fish'. The model was built so that the random effect allowed for different intercepts for individual fish (Crawley, 2007; Zuur *et al.*, 2009). To model each response variable, a systematic model selection and assessment process was carried out, as described below.

## 1) Global model

Initially, for each elemental response variable, a ‘global model’ was built (equation 2), including all single fixed effects and their first order interactions (indicated by the “^2” command below). Variables classified as categorical ‘factors’ are underlined.

$$El_B = (\underline{\text{sex}} + GSI^{\dagger} + \underline{\text{treatment}} + \underline{\text{origin}} + \underline{\text{spawner}} + \text{temperature} + \text{salinity} + El_W + \text{day} + [\text{protein}] + \text{condition} + \text{growth rate} + \text{overall growth rate} + TL + \text{age})^2 + (1|\text{fish}) \quad (2)$$

<sup>†</sup> GSI was only included in the female only model, when ‘sex’ was also removed

## 2) Initial model reduction

Due to computational restrictions, it was not possible to run the global model through the full model selection procedure, so the number of interactions were reduced by running the global model using maximum likelihood (ML) methods, then analysing it by Analysis of Deviance (‘Anova’ function. Note the capital A; Anova is not sensitive to the order of terms in the model, ‘anova’ is). While *p*-values are generally incompatible with mixed effects models due to lack of an underlying F distribution (Bates, 2006), they can still provide useful information about the importance of individual terms. As such, only highly significant (*p* < 0.01) interactions were included in the reduced model, as well as any that made particular biological sense. All single terms were included. The reduced model was then ‘standardized’ (‘arm’ package) to centre and scale predictor and response variables and analysed using restricted maximum likelihood estimation (REML) methods.

## 3) Multi-model inference (‘MuMIn’)

‘Dredge’ (MuMIn package) was then to find the most parsimonious model(s). Dredge builds all possible models using inputted terms, then ranks them by Akaike information criterion (AIC). AIC is also known as a ‘penalised log-likelihood’ and effectively measures model fit whilst penalising for the number of terms (Crawley, 2007).

## 4) Model selection and assessment

Usually there was a single ‘top model’ that clearly performed better than the others (indicated by a drop in AIC of about 2), but in certain cases there were multiple ‘top models’ with similarly low AIC values. All top models were assessed for multicollinearity (‘vif < 5’, ‘kappa’ < 30) and the residuals checked for normality, homogeneity and autocorrelation. The importance of each term within the model was inferred by Chi-squared statistics and *p* values using Analysis of Deviance, and the model performance judged using

Nagelkerke pseudo  $r^2$  values (code from Richard Inger, pers. comm.). In cases where the dredge output included multiple 'top models', the final model was selected by means of the following criteria: (i) improved homogeneity and normality of the residuals, (ii) reduced autocorrelation of the residuals, (iii) reduced multicollinearity, (iv) higher pseudo  $r^2$  value and (v) if it seemed more biologically sensible. Any subjectivity in the final model was highlighted for discussion.

Blood element concentrations were modelled for all fish and samples, however, as GSI values were only available for the females, it was necessary to run a separate model for females only, including GSI.

### 3.3 Results

#### 3.3.1 Physiological conditions

Generally, the male fish were smaller and older than the females, and the EC females larger and younger than the IS fish (Table 3.6). Over the 12 month experiment, TL increased by  $2.5\text{cm} \pm 0.62\text{ SE}$  in the IS females (paired t-test:  $t(7) = 4.01 p = 0.005$ ) and by  $2.7\text{cm} \pm 0.47\text{ SE}$  in the males ( $t(9) = 5.80 p < 0.001$ ), as did TW (by  $102.1\text{g} \pm 21.5\text{ SE}$ ,  $t(7) = 4.74 p = 0.002$  and by  $72.8\text{g} \pm 11.4\text{ SE}$ ,  $t(9) = 6.37 p < 0.001$ , respectively). The EC females were introduced to the experiment later on, and while average TL increased by  $1.11\text{cm}$  (3.4%) and TW by  $17.71\text{g}$  (5.0%) during the 7 month period, these changes were not significant ( $p > 0.05$ ). Overall daily growth rates were not significantly different among groups, but on average, fastest in the males and slowest in the EC females (Table 3.6). Based on Figure 3.4, somatic growth was fastest from mid-October to mid-December in the IS fish, and slowed mid-December onwards. During the spawning season the IS females generally grew more slowly than the males and exhibited no growth in the latter half of February. The EC females exhibited slower growth than the IS fish during the pre-spawning period, but similar average growth from January onwards, only with greater variation among individuals.

On termination of the experiment, condition was not significantly different ( $p > 0.05$ , ANOVA) between males, IS and EC females (Table 3.6). Over time, condition and plasma protein concentration followed broadly similar trends, increasing from June then falling from December until the experiment termination (Figure 3.4). Overall, IS females exhibited slightly higher plasma protein than the males, while EC females exhibited the lowest condition, protein and GSI.

The average age of the IS males and females was about 5 years old (Table 3.6), but the range was greater in the males (3-12 years cf. 4-6 years). Despite their larger sizes, the EC females were younger (3-5 years) and

primarily immature (Figure 3.4), with significantly lower GSI than the IS females in March (5.1% cf. 15.4%,  $F_{1,13} = 6.27, p = 0.026$ ). Three EC females exhibited some signs of ovary development, but only one was observed to have spawned. Macroscopic examination of ovaries in June 2010 revealed no sign of post-ovulatory follicles (POFs) in any fish, but one EC female still had ovaries full of unhydrated eggs. This 4 year old fish had been treated with GnRH in mid-January and until this point had shown little sign of ovary development. Given that fish were sacrificed well after the usual spawning season, it is likely these eggs would have eventually been resorbed by atresia. While the hormone treatment was applied randomly among 'males' and 'females', of the eight IS females, only two were not treated. Of these two, both showed signs of ovary development but only one definitely spawned. Of the treated IS females, five of the six fish spawned, while the remaining individual (4 years old), showed no ovary development and was deemed immature.

Table 3.6 Average ( $\pm$ SD) total length (TL), total weight (TW), growth rate, Fulton's condition factor, gonadosomatic index (GSI) and age of subject animals presented in the current chapter at the end of the experiment (28/05/10)

Origin	Sex	<i>n</i>	TL (cm)	TW (g)	Overall growth rate (mm day <sup>-1</sup> )	Condition	GSI (%)	Age (years)
IS	M	10	27.22 (2.38)	208.6 (51.01)	0.075 (0.041)	1.02 (0.08)	n/a	5.4 (2.5)
IS	F	8	30.84 (2.01)	293.3 (67.84)	0.069 (0.049)	0.98 (0.05)	3.18 (2.12)	5.0 (0.76)
EC	F	7	33.54 (1.75)	370.7 (95.00)	0.052 (0.064)	0.97 (0.13)	2.76 (4.06)	3.4 (0.79)

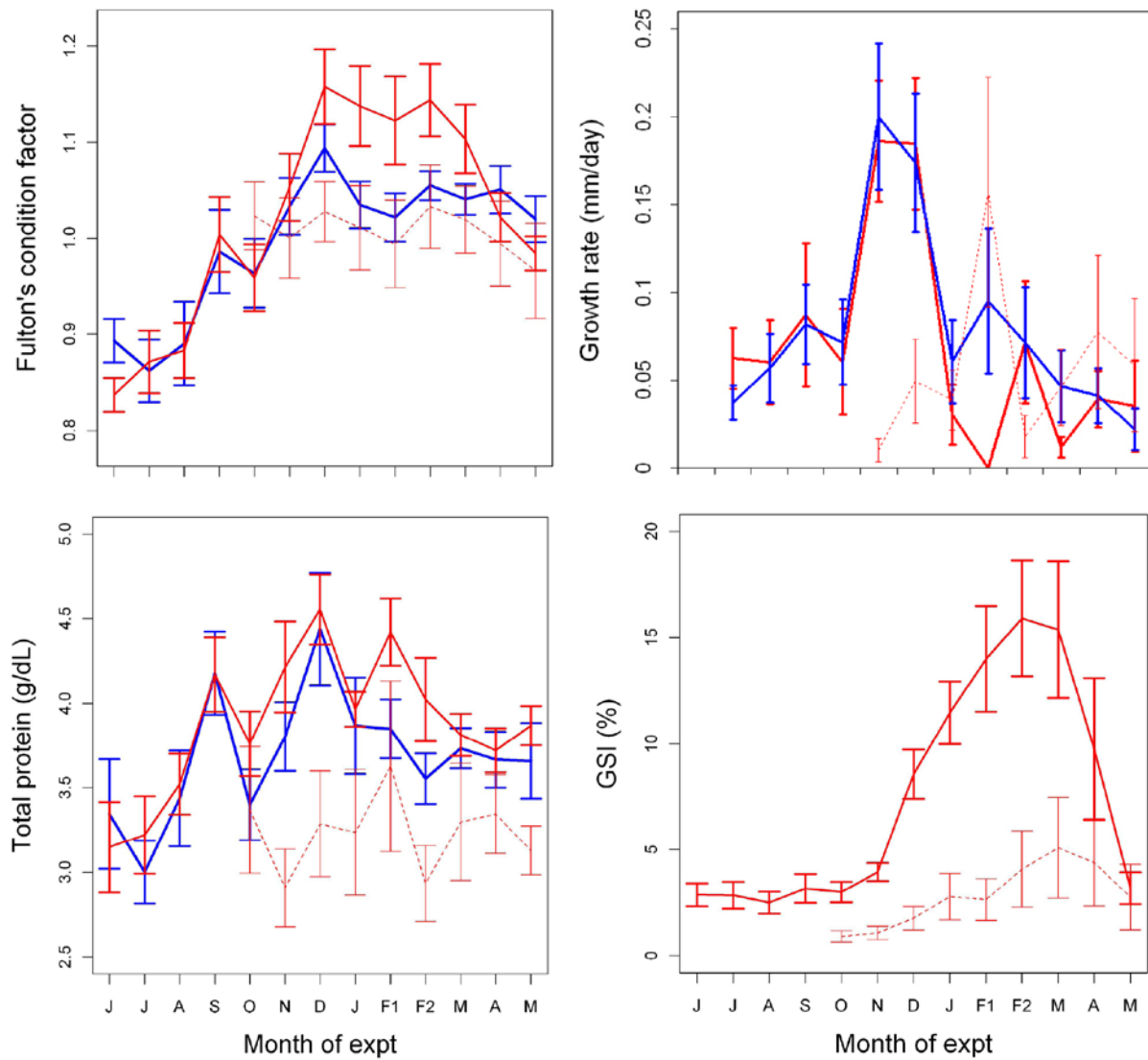


Figure 3.4 Monthly average condition, somatic growth rate, blood protein and gonadosomatic index (GSI) of plaice sampled from 02/06/09 to 28/05/10 (males = blue, Irish Sea females = red, solid line, English Channel females = red, dashed line). Note that sampling was carried out twice in February 2010 (F1 and F2), GSI estimates are not available for the male fish, and growth rates were based on  $TL_{month2} - TL_{month1}$ , so no values were assigned to the first sampling month for each group. Error bars are SEM (as opposed to SD) to improve graph clarity

### 3.3.1.1 Correlations among physiological variables

As illustrated by Figure 3.5, many of the physiological variables were highly correlated, particularly protein and condition, growth rate and GSI, TW and condition, TL and TW, while temperature was negatively correlated with GSI, TW and condition. To improve homogeneity and distribution of the data, age and GSI were log transformed and growth rate  $\ln(x+0.1)$  transformed.

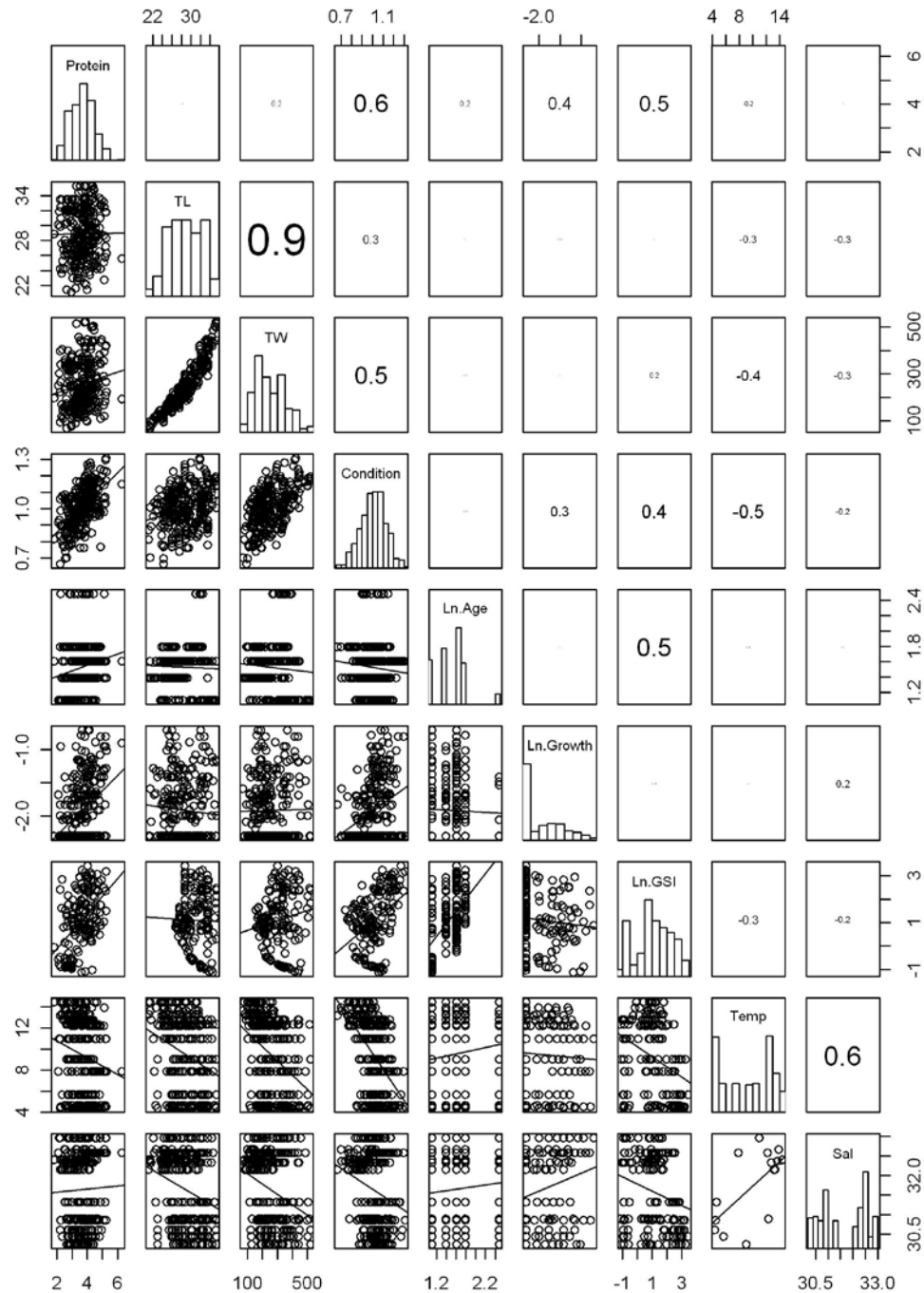


Figure 3.5 Distributions, scatterplots and Pearson pairwise correlations among physiological variables (natural log transformed data indicated by Ln), temperature and salinity

### 3.3.2 Environmental conditions

#### 3.3.2.1 Salinity, temperature and seawater element concentrations over time

The CEFAS Lowestoft aquarium sources its seawater direct from the Norfolk coast, so the tank water temperature and salinity varied with ambient conditions. The 2009/2010 winter was relatively cold with air temperature frequently falling below 0°C from January onwards. The aquarium water temperature began to decrease in October, but fell rapidly from November 1<sup>st</sup> (day 150) until reaching a minimum temperature of 3.8°C in February 2010. While cooling systems tried to maintain summer temperatures below 14°C, water temperatures reached a maximum of 14.9°C in June 2009. Based on DST records, such temperatures are typical of those experienced by wild North Sea plaice. Salinity in this coastal region is relatively low and ranged from 30.1 to 33.3, generally following the same trend as temperature, but lagged by 1-2 months (Figure 3.6).

Seawater minor and trace element concentrations generally followed similar trends to salinity, reaching a minimum in early February (~ day 250). In Figure 3.7 and throughout the remainder of this chapter, elements are organised into the following broad chemical groupings: Group I, Group II and 'soft' (see Chapter 1) elements. Concentrations of the conservative Group I elements (Li, Rb, K) varied with salinity, fluctuating in a sinusoidal manner and returning to almost exactly the same concentration as they were one year previous. Concentrations of the Group II conservative (Mg) and quasiconservative (Ca, Sr, Steele *et al.*, 2009) elements also varied with salinity, resulting in little temporal variation in element/Ca ratios. Ba<sub>W</sub> and concentrations of nearly all the 'soft' elements (Mn, Cu, Zn, Se and Pb), exhibited similar sinusoidal cycles, but over a proportionally greater amplitude, reflected in clearer cycles after Ca normalisation. Concentrations of Mn, a scavenged element, were more difficult to interpret due to a low instrumental signal:noise ratio, but temporal trends in Mn concentrations did contrast with the other elements, with generally low concentrations until late 2009, increasing until the experiment termination.

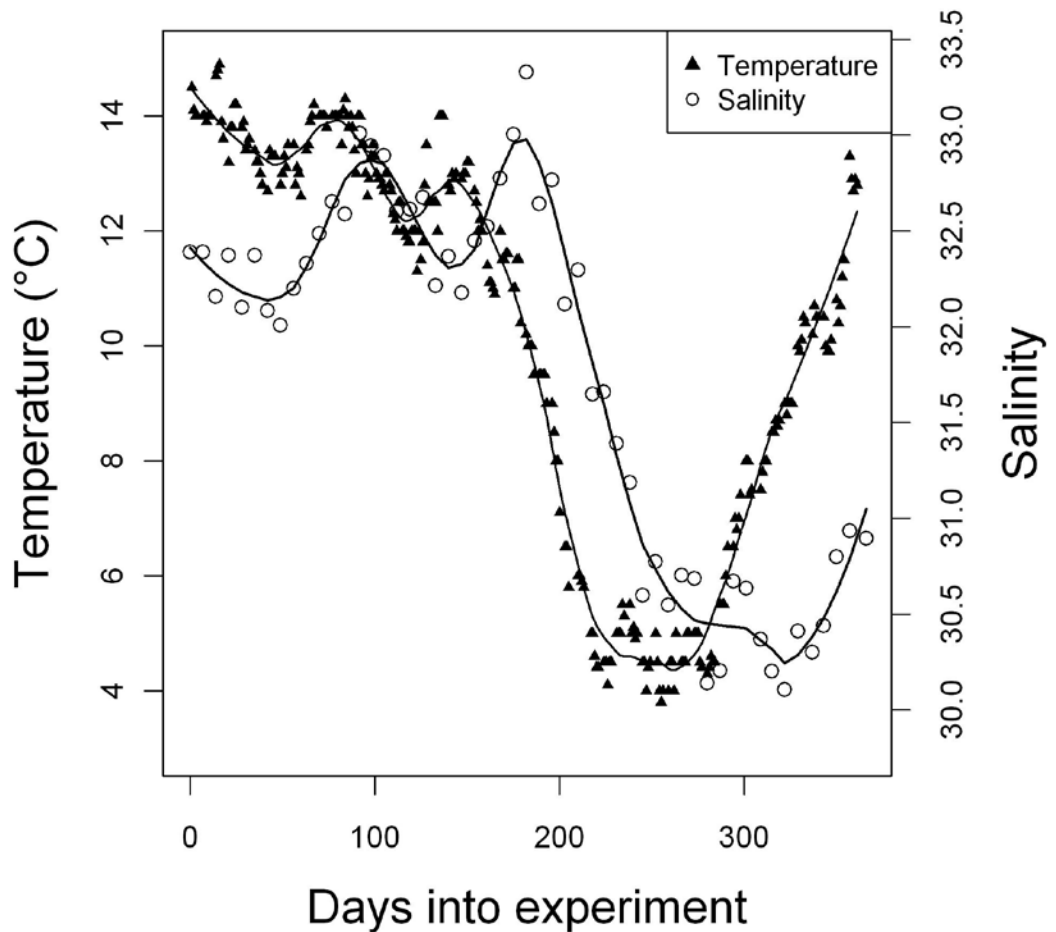


Figure 3.6 Temperature (triangles) and salinity (circles) of the CEFAS aquarium seawater over the experimental period. For reference, Day 1 = 02/06/09, Day 200 = 18/12/09 and Day 361 = 28/05/10.

### 3.3.2.2 Correlations between water element concentrations and environmental variables

Environmental variables were highly correlated with seawater element concentrations, with Pearson product-moment correlation coefficients (PCCs) generally greater than 0.6 (Table 3.7). Mn was a clear outlier, as it was negatively correlated with salinity and negatively correlated (if at all) with all other elements, while Se and Pb exhibited generally lower and more variable PCCs than the other elements.

Table 3.7 Pearson product-moment correlation coefficients (PCCs) for pairwise comparisons between temperature, salinity and seawater element concentrations. Correlations were carried out on the fitted values for all blood sampling days ( $n=15$ ), predicted by LOESS smoothers.

	Sal	Temp	Li	K	Rb	Mg	Ca	Sr	Ba	Mn	Cu	Zn	Se
Sal	1												
Temp	0.66	1											
Li	0.87	0.89	1										
K	0.89	0.85	0.99	1									
Rb	0.82	0.93	0.99	0.97	1								
Mg	0.90	0.83	0.99	1.00	0.96	1							
Ca	0.88	0.84	0.99	1.00	0.98	0.99	1						
Sr	0.89	0.84	0.99	1.00	0.97	1.00	1.00	1					
Ba	0.79	0.73	0.93	0.94	0.92	0.94	0.96	0.94	1				
Mn	-0.60	0.12	-0.22	-0.29	-0.13	-0.32	-0.30	-0.30	-0.27	1			
Cu	0.69	0.95	0.90	0.85	0.94	0.83	0.86	0.85	0.80	0.00	1		
Zn	0.55	0.91	0.85	0.81	0.91	0.78	0.83	0.80	0.83	0.18	0.94	1	
Se	0.40	0.44	0.58	0.58	0.61	0.56	0.62	0.58	0.79	0.00	0.55	0.70	1
Pb	0.68	0.89	0.78	0.70	0.81	0.70	0.70	0.71	0.58	0.05	0.87	0.77	0.40

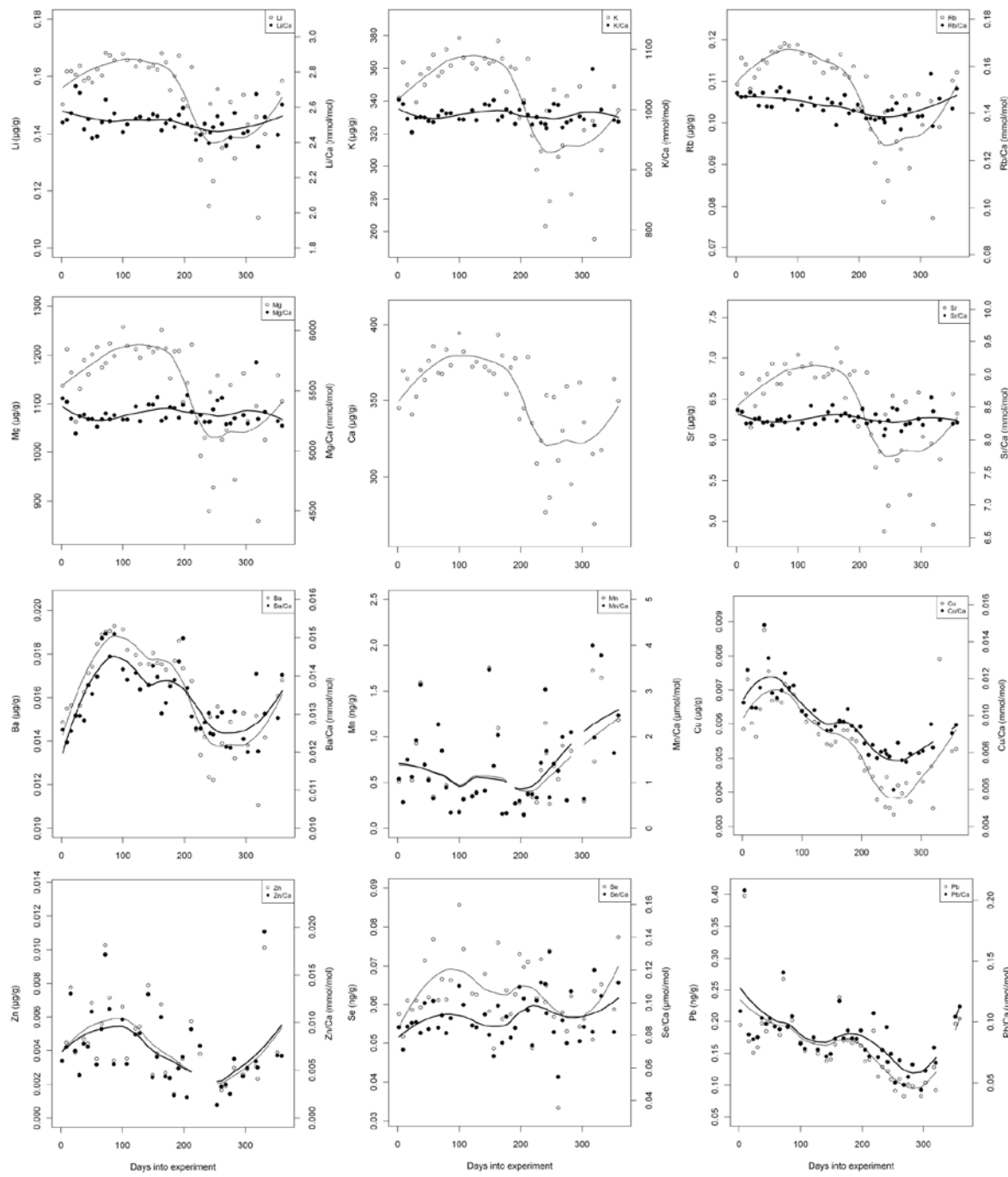


Figure 3.7 Element concentrations (open circles,  $\mu\text{g g}^{-1}$  or  $\text{ng g}^{-1}$ ) and element/Ca ratios (closed circles,  $\text{mmol/mol}$  or  $\mu\text{mol/mol}$ ) in seawater samples collected every 1-2 weeks during the experimental period. For reference, Day 1 = 02/06/09, Day 200 = 18/12/09 and Day 361 = 28/05/10. The elements are ordered by mass and broad elemental groupings: conservative Group I, Group II, then 'soft' (Chapter 1) elements. Mg, K, Ca and Sr were analysed by ICPMS and Li, Mn, Cu, Se, Rb, Ba and Pb by HR-ICPMS. LOESS smoothers are displayed and were used to predict concentrations and element/Ca molar ratios for specific blood sampling days.

### 3.3.2.3 Description of blood element concentrations over time

As presented in Figure 3.8 and discussed on an element by element basis below, blood element concentrations often varied over time and between the males, females, IS and EC fish, despite exposure to the same ambient concentrations, temperatures and diets throughout.

#### Trends in $\text{Li}_B$

$\text{Li}_B$  values did not exhibit clear temporal trends, but, aside from a drop in August, were generally lower during winter months. There was potentially some enrichment of  $\text{Li}_B$  values in the females compared with the males between October and March, but initial and terminal  $\text{Li}_B$  values were similar for all groups of fish.

#### Trends in $\text{Rb}_B$ and $\text{K}_B$

$\text{Rb}_B$  and  $\text{K}_B$  values have been grouped due to similar behaviours. Unlike most of the other elements, initial and terminal  $\text{K}_B$  and  $\text{Rb}_B$  values were clearly different, with final concentrations lower due to a gradual decline over time in all groups. Aside from this,  $\text{K}_B$  and  $\text{Rb}_B$  values exhibited limited temporal variability and no major differences between the sexes, although there was a dip in  $\text{K}_B$  values around November in the IS females and a dip in  $\text{K}_B$  and  $\text{Rb}_B$  values in January in the males.

#### Trends in $\text{Mg}_B$

Excluding the initial measurement (June 2009),  $\text{Mg}_B$  values appeared to vary in a roughly sinusoidal manner, peaking from September to January then falling in February and remaining low during the winter spawning season.  $\text{Mg}_B$  values exhibited no clear difference between the males, females, IS or EC fish.

#### Trends in $\text{Ca}_B$ and $\text{Sr}_B$

$\text{Ca}_B$  and  $\text{Sr}_B$  values have been grouped due to similar behaviours. Unlike the other Group II metals  $\text{Ca}_B$  and  $\text{Sr}_B$  values exhibited clear changes over time and among groups of fish. Concentrations of both elements were generally highest during the spawning season, however, the main peak in  $\text{Ca}_B$  values was two months earlier than  $\text{Sr}_B$  values (December cf. February). There was also divergence among the groups of fish, with the highest peaks exhibited by the IS females, only a small rise in  $\text{Ca}_B$  values apparent in the males, lower  $\text{Sr}_B$  values in the EC fish and a delayed  $\text{Ca}_B$  peak in the EC females in early February. On termination of the experiment,  $\text{Ca}_B$  and  $\text{Sr}_B$  values were generally similar to their starting concentrations.

#### Trends in $\text{Ba}_B$

There was limited temporal variability in  $\text{Ba}_B$  values except for a dip in December that was exhibited by all groups of fish. There were no obvious differences in  $\text{Ba}_B$  values between males, females, IS and EC fish.

### **Trends in Mn<sub>B</sub>**

Mn<sub>B</sub> values were lowest at the start and end of the experimental period and exhibited peaks in July and November. In the IS fish Mn<sub>B</sub> values then remained elevated from January to April while the EC fish exhibited a third shorter peak in March to April. Generally Mn<sub>B</sub> values were higher in the females and initial and terminal concentrations were similar.

### **Trends in Cu<sub>B</sub>**

In the IS fish, Cu<sub>B</sub> values increased from June to December then dropped rapidly through the spawning season. Apart from the first and last samples, the males exhibited higher Cu<sub>B</sub> values than the IS females. The EC females exhibited high but variable Cu<sub>B</sub> values when introduced to the experiment, but concentrations decreased rapidly until late February and were, for the majority of the experiment, considerably lower than the IS fish. Both sets of females exhibited increasing Cu<sub>B</sub> values towards the end of the experiment. Terminal Cu<sub>B</sub> values were lower than initial Cu<sub>B</sub> values in the EC females, but higher in the IS fish.

### **Trends in Zn<sub>B</sub>**

Zn<sub>B</sub> values decreased during the spawning season in all fish, but had returned to initial Zn<sub>B</sub> values by the end of the experiment. From October (IS females) and November (EC females) onwards, Zn<sub>B</sub> values exhibited clear divergence among the sexes, with the females exhibiting lower concentrations than the males. During peak spawning (January-March) Zn<sub>B</sub> values were lower in the IS females than the EC females or the males.

### **Trends in Se<sub>B</sub>**

Cu<sub>B</sub> and Se<sub>B</sub> concentrations exhibited relatively similar patterns, with lower concentrations in the EC females and maximum concentrations between August and December in the IS fish. Following onset of spawning, Se<sub>B</sub> values decreased in the IS fish and began to rise from March onwards in all groups. The IS fish exhibited higher Se<sub>B</sub> values than the EC females throughout the experiment, although the divergence between them was less by the end of the experiment. Terminal Se<sub>B</sub> values were higher than initial values for all groups of fish.

### **Trends in Pb<sub>B</sub>**

Pb<sub>B</sub> values in the males exhibited a slight but consistent decrease over time, not shared by either other group. While fairly variable, Pb<sub>B</sub> values in IS females exhibited similar patterns to Ca<sub>B</sub> values, being higher than the males from September until May, and peaking in December. Pb<sub>B</sub> values in the EC females were similar to the males apart from a small peak in January to early February. Terminal and initial Pb<sub>B</sub> values were similar among the females.

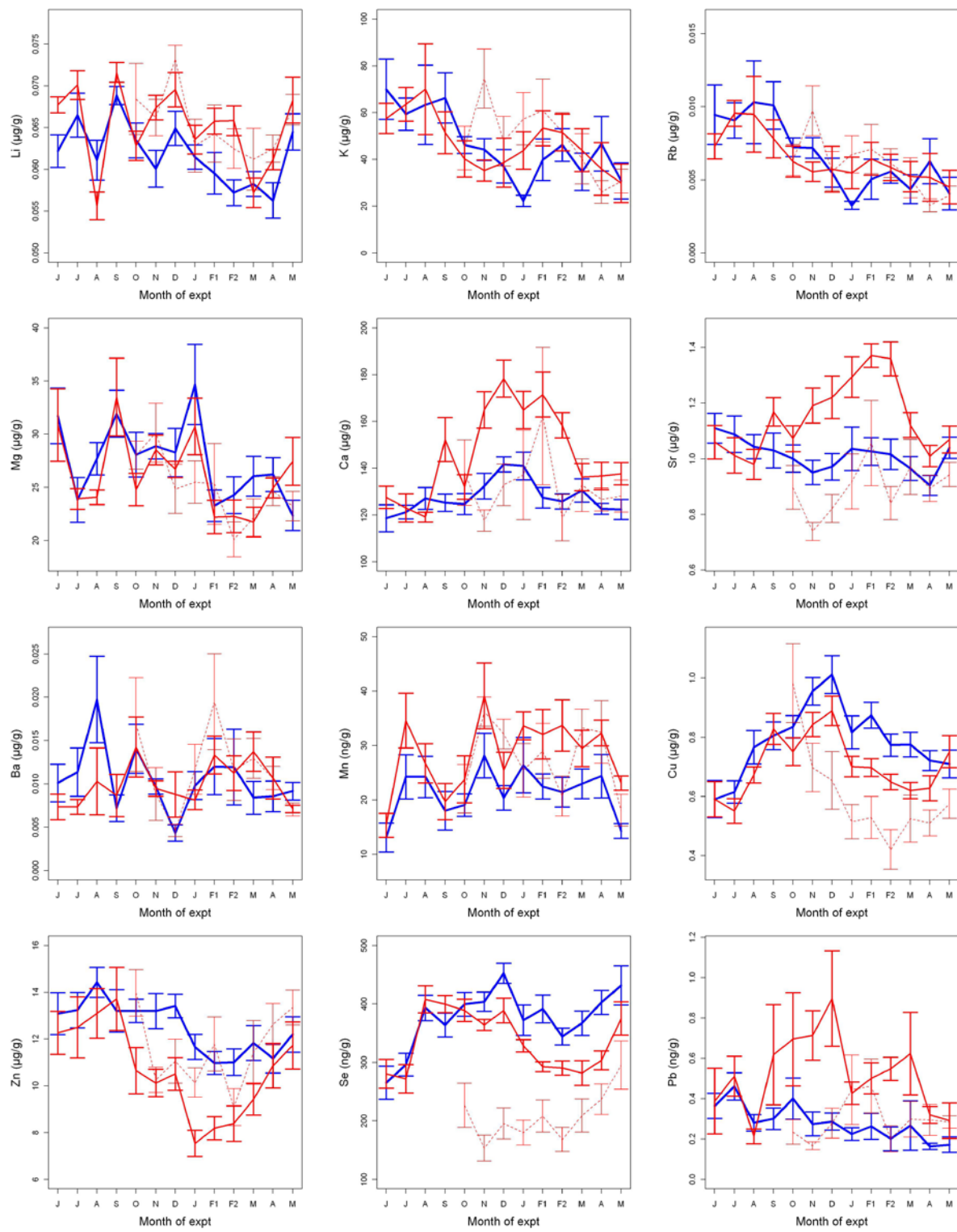


Figure 3.8 Monthly average blood elemental concentrations in plaice sampled from 02/06/09 to 28/05/10 (males = blue, Irish Sea females = red, solid line, English Channel females = red, dashed line). Note that sampling was carried out twice in February 2010 (F1 and F2). Note the units on the plots; all are in  $\mu\text{g/g}$  except Mn, Se and Pb, which are in  $\text{ng/g}$ . Error bars are SEM (as opposed to SD) to improve graph clarity

### 3.3.2.4 Correlations among blood elemental concentrations and distribution coefficients

Blood concentrations and distribution coefficients ( $D_{Ei(B/W)}$ ) were generally less correlated within ‘chemical groupings’ than seawater concentrations (Table 3.7 cf. Table 3.8).  $K_B$  and  $Rb_B$  and  $D_{K(B/W)}$  and  $D_{Rb(B/W)}$  were almost perfectly correlated, but appeared unrelated to other conservative and quasiconservative elements.

$Ca_B$  and  $Sr_B$  were also highly correlated, but only weakly correlated with  $Mg_B$  and  $Li_B$ , both in terms of concentrations and distribution coefficients. Blood concentrations were weakly correlated with salinity, if at all, and  $D_{Ca(B/W)}$  and  $D_{Sr(B/W)}$  were negatively correlated with temperature.  $Ba_B$  and  $D_{Ba(B/W)}$  were not correlated with any other elements, temperature or salinity. Among the ‘soft’ elements,  $Cu_B$ ,  $Zn_B$  and  $Se_B$  and their distribution coefficients were positively correlated, and  $D_{Cu(B/W)}$  and  $D_{Zn(B/W)}$  negatively correlated with temperature. Relationships across ‘groups’ were most apparent among the divalent ions  $Ca^{2+}$ ,  $Sr^{2+}$  and  $Pb^{2+}$ , while  $D_{Ca(B/W)}$  was also positively correlated with  $D_{Mn(B/W)}$ ,  $D_{Cu(B/W)}$  and  $D_{Zn(B/W)}$ .

Table 3.8 PCCs for pairwise comparisons of temperature, salinity and (A) blood element concentrations and (B) blood/seawater distribution coefficients, defined here as  $D_{Element}$ . Correlations were carried out on predicted temperature and salinity values for all blood sampling days ( $n=15$ ) and blood concentrations across all samples ( $n = 282$ ).

<b>A</b>	Sal	Temp	Li	K	Rb	Mg	Ca	Sr	Ba	Mn	Cu	Zn	Se
Sal	1												
Temp	0.60	1											
Li	0.28	0.19	1										
K	0.19	0.15	0.13	1									
Rb	0.29	0.26	0.11	0.96	1								
Mg	0.31	0.17	0.23	-0.08	-0.04	1							
Ca	0.01	-0.27	0.23	-0.26	-0.26	0.26	1						
Sr	-0.03	-0.10	0.18	-0.02	-0.03	0.29	0.60	1					
Ba	-0.06	-0.03	-0.13	0.00	0.01	-0.10	-0.06	-0.04	1				
Mn	-0.05	-0.21	-0.08	-0.20	-0.18	-0.02	0.41	0.11	-0.02	1			
Cu	0.30	0.06	0.08	-0.13	-0.06	0.28	0.30	0.17	-0.08	0.05	1		
Zn	0.27	0.43	0.13	-0.11	-0.03	0.23	0.08	-0.08	-0.05	-0.10	0.28	1	
Se	0.13	0.17	-0.15	-0.22	-0.11	0.20	0.21	0.20	-0.09	-0.09	0.59	0.35	1
Pb	0.15	0.00	0.17	-0.05	-0.03	0.14	0.46	0.38	0.06	0.21	0.07	-0.16	-0.02
<b>B</b>	Sal	Temp	D.Li	D.K	D.Rb	D.M	D.Ca	D.Sr	D.Ba	D.M	D.Cu	D.Zn	D.Se
Sal	1												
Temp	0.60	1											
D.Li	-0.27	-0.38	1										
D.K	0.10	0.05	0.08	1									
D.Rb	0.20	0.16	-0.03	0.97	1								
D.Mg	0.09	-0.03	0.16	-0.14	-0.13	1							
D.Ca	-0.27	-0.50	0.39	-0.24	-0.28	0.30	1						
D.Sr	-0.29	-0.35	0.33	-0.01	-0.06	0.31	0.67	1					
D.Ba	-0.14	-0.10	-0.09	0.12	0.11	-0.12	-0.03	-0.01	1				
D.Mn	0.27	-0.26	0.04	-0.13	-0.11	0.10	0.42	0.12	-0.04	1			
D.Cu	-0.14	-0.52	0.14	-0.18	-0.19	0.23	0.42	0.29	-0.04	0.22	1		
D.Zn	-0.33	-0.67	0.24	-0.13	-0.19	0.15	0.44	0.23	0.05	0.17	0.55	1	
D.Se	0.05	0.08	-0.27	-0.25	-0.14	0.20	0.17	0.17	-0.08	-0.08	0.47	0.14	1
D.Pb	-0.07	-0.19	0.14	-0.03	-0.05	0.08	0.38	0.31	0.04	0.20	0.07	0.04	-0.10

### 3.3.2.5 Blood:water distribution coefficients

Blood:water distribution coefficients ( $D_{Ei(B/W)}$ ) varied by more than five orders of magnitude among the 12 measured elements, ranging from 0.01 ( $D_{Rb(B/W)}$ ) to  $>8500$  ( $D_{Se(B/W)}$ ). Coefficients greater than 1.0 indicate enrichment of the blood relative to ambient concentrations. This was the case for all 'soft' elements, but for Group I and II elements, average  $D_{Ei(B/W)}$  values were consistently  $<1.0$  (Table 3.9).  $D_{Ba(B/W)}$  was an intermediary with occasional values  $>1$ , particularly during winter. There were substantial differences between  $D_{Ei(B/W)}$  values from this study and those reported for two freshwater species (Melancon *et al.*, 2009) (Table 3.9), particularly among the conservative elements due to the differences in ambient concentrations.  $D_{K(B/W)}$  and  $D_{Rb(B/W)}$ , for example, differed by four orders of magnitude among studies. Differences in other  $D_{Ei(B/W)}$  values may also be due differences in environmental or dietary concentrations, but some could be due to differences between plasma and whole blood or sample treatment (Chapter 2).

If patterns in blood plasma concentrations were varying with ambient concentrations,  $D_{Ei(B/W)}$  would remain constant over time. However, patterns in  $D_{Ei(B/W)}$  were broadly similar to those exhibited by the absolute blood concentrations (Figure 3.9), implying that elemental fractionation was largely occurring in spite of, rather than as a function of, ambient concentrations. The decreases in ambient concentrations during winter were almost always accompanied by relative enrichment of the blood during the spawning period, but particularly in Ca, Sr, Mn and Cu, and Li and Pb in the females. Also, while  $Zn_B$  decreased in all groups of fish during winter,  $Zn_W$  decreased during the same period, resulting in unchanging (IS females) or increasing (EC females and males)  $D_{Zn(B/W)}$  during this period.  $D_{Mg(B/W)}$  and  $D_{Ba(B/W)}$  exhibited no clear differences between the sexes and remained relatively constant over time

Table 3.9 Average distribution coefficients ( $D_{Ei(B/W)}$ ) for blood plasma vs. water element concentrations for all samples in the current study ( $n = 282$ ), and whole blood vs. water element concentrations for two freshwater species (Melancon *et al.*, 2009)

Element	$D_{Ei(B/W)}$ (this study)	$D_{Ei(B/W)}$ (Burbot)	$D_{Ei(B/W)}$ (Lake trout)
Li	0.423	n/a	n/a
K	0.140	1,560	1,590
Rb	0.061	2,590	3,190
Mg	0.024	10.2	10.4
Ca	0.391	3.03	3.85
Sr	0.165	1.63	1.07
Ba	0.684	20.0	13.7
Mn	41.38	161	197
Cu	142.8	n/a	n/a
Zn	3363	4,790	7,250
Se	5214	n/a	n/a
Pb	2.836	500	1,490

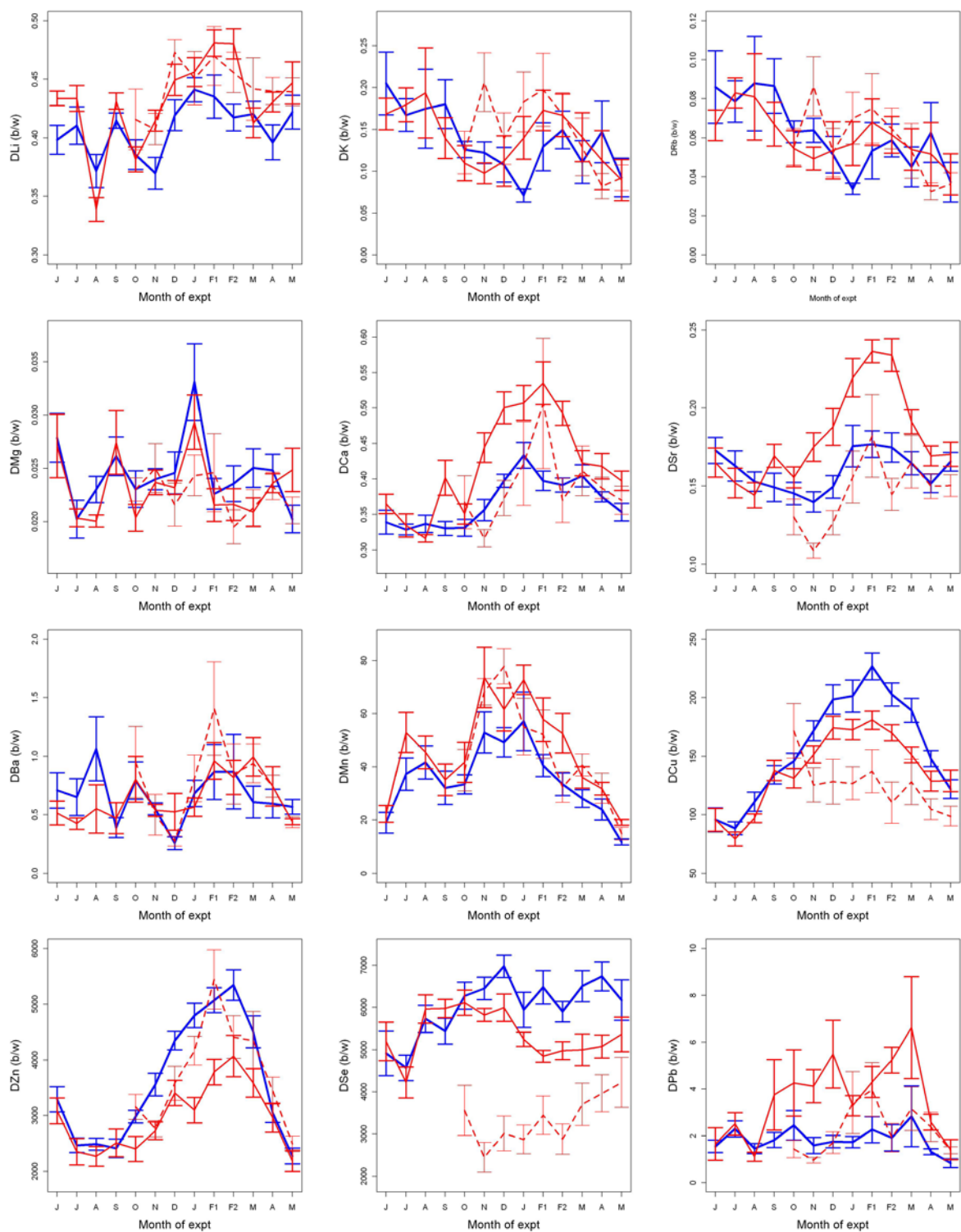


Figure 3.9 Monthly average distribution coefficients ( $D = [\text{element}]_{\text{blood}} / [\text{element}]_{\text{water}}$ ) in plaice sampled from 02/06/09 to 28/05/10 (males = blue, Irish Sea females = red, solid line, English Channel females = red, dashed line). Note that sampling was carried out twice in February 2010 (F1 and F2). Error bars are SEM (as opposed to SD) to improve graph clarity

### 3.3.3 What are the primary influences on blood element concentrations?

#### 3.3.3.1 Relationship between blood and ambient concentrations

Many otolith microchemistry applications assume that elemental concentrations in the otolith vary with concentrations in the ambient water (although not necessarily in a common or linear fashion). A basic linear model was initially used to summarise the relationships between elemental concentrations in blood and water (Table 3.10). The strongest positive correlations were for Zn, Se Li, Rb and Mg concentrations, while concentrations of Ca, Sr and Ba in blood were negatively (if at all) correlated with water concentrations, particularly in the females. Concentrations of Cu in the blood were negatively correlated with  $Cu_W$  in the males, positively correlated in the EC females and unrelated in the IS females. Blood Pb concentrations, on the other hand, were positively correlated with ambient concentrations in the males, negatively correlated in the IS females, and unrelated in the EC females.

It should be stressed that due to the almost bimodal distribution of the seawater concentrations, few if any of these datasets fully satisfy requirements of homogeneity of variance and dispersion, so correlation coefficients are illustrative only.

Table 3.10 Pearson's product Correlation Coefficients (PCC) for pairwise comparisons of blood and water elemental concentrations and the data transformations used in the remainder of the statistical analyses. Blood samples were collected at c. monthly intervals from 25 fish for one year: 10 Irish Sea (IS) males, 8 IS females and 7 English Channel (EC) females. Water concentrations were fitted to each blood sampling day using LOESS smoothers (Figure 3.7).

Element	Data transformation		Pearson's product Correlation Coefficient (otolith vs. water)			
	SW	Blood	Males <i>n</i> = 120	Females <i>n</i> = 162	IS females <i>n</i> = 102	EC females <i>n</i> = 160
Li	-	-	0.37	0.25	0.21	0.35
K	-	Ln	0.31	0.08	0.06	0.12
Rb	-	$\text{Log}_{10}$	0.40	0.20	0.23	0.12
Mg	-	$\text{Log}_{10}$	0.19	0.32	0.26	0.38
Ca	-	$\text{Log}_{10}$	-0.05	-0.11	-0.24	-0.06
Sr	-	$\text{Log}_{10}$	0.07	-0.15	-0.32	-0.25
Ba	-	$\text{Log}_{10}$	0.08	-0.19	-0.15	-0.25
Mn	Ln	Ln	-0.16	-0.03	-0.03	-0.09
Cu	-	SQRT	-0.25	0.21	-0.04	0.46
Zn	-	SQRT	0.32	0.48	0.57	0.44
Se	-	-	0.34	0.36	0.55	0.26
Pb	Ln	Ln	0.29	-0.06	-0.21	-0.03

### 3.3.3.2 Modelling blood element concentrations using environmental and physiological variables

Linear mixed effect models were carried out to examine which physiological and/or environmental variables best explained blood element concentrations, using 'fish' as a random effect. For each element, a model was built for all fish and for females only (thus including GSI). The model outputs are displayed in Table 3.11. Note that due to collinearity between temperature and many of the seawater concentrations, as well as near-bimodal distribution of both terms, it was often impossible to separate their effects using models alone. Such cases are highlighted below, along with a description of the model outputs and the main observed trends. Unless otherwise stated, the same terms were selected for the 'full' and the 'female only' models.

#### **Li<sub>B</sub>**

Overall, Li<sub>B</sub> values were best explained by sex (F>M) and environmental effects. Overall, Li<sub>B</sub> values were positively correlated with temperature and salinity, however, at the highest and lowest salinities the correlation between Li<sub>B</sub> values and temperature appeared negative (Figure 3.10). Both full and female only models exhibited a moderate fit ( $r^2 > 0.25$ ), with almost no variation explained by the random effect.

#### **K<sub>B</sub> and Rb<sub>B</sub>**

K<sub>B</sub> and Rb<sub>B</sub> values were primarily explained by day number, resulting from their general decrease over time (Figure 3.11). A negative effect of protein concentrations was also significant in both models. K<sub>B</sub> values were partly explained by a positive effect of temperature. Similar to Li<sub>B</sub>, there was a positive overall relationship between K<sub>B</sub> and Rb<sub>B</sub> values and salinity, but it was not significant. Unlike Li<sub>B</sub>, neither K<sub>B</sub> or Rb<sub>B</sub> values differed among the sexes. Model fit was poor to moderate ( $r^2 = 0.21-0.28$ ) with around 20% of the variation explained by the fixed effects.

#### **Mg<sub>B</sub>**

Mg<sub>B</sub> values were primarily explained by a positive relationship with salinity (or temperature, Figure 3.12). Unlike the monovalent ions discussed above, protein concentrations were positively correlated with Mg<sub>B</sub> values. There was also a slight effect of GnRH treatment, with treated fish exhibiting higher Mg concentrations. Mean Mg<sub>B</sub> was also higher in treated females, but treatment was not significant in the female only model, with greater proportion of the variance explained by blood protein concentrations. Overall model fits were relatively poor ( $r^2 = 0.17$  and 0.21), but very little was explained by the random effect implying similar responses among fish.

Table 3.11 Summary of linear mixed effects model outputs predicting blood element concentrations in 25 experimental plaice sampled c.monthly for one year. Outputs include Analysis of Deviance Chi square statistic, degrees of freedom (df) and p values; Nagelkerke pseudo  $r^2$  for whole model, fixed effects (FE) and random effects (RE)

Element	Fixed effects (Full model)	Effect	Chi sq. statistic	df	p value <sup>†</sup>	$r^2$	FE (RE)	Fixed effects (Female only model)	Chi sq. statistic	df	p value <sup>†</sup>	$r^2$	FE (RE)			
Conservative and quasi conservative elements																
<b>Li<sub>2</sub></b>	Sex	F>M	11.586	1	0.0007	***	0.26	0.24	Salinity	11.0872	1	0.0009	***	0.28	0.28	
	Temp	+ve (n.s.)	0.821	1	0.3650			(0.02)	Temp	0.0233	1	0.8787			(0.00)	
	Salinity	+ve	16.528	1	<0.0001	***			Salinity*Temp	9.6975	1	0.0018	**			
	Temp*Salinity	S +ve at low T	11.490	1	0.0007	***										
<b>K<sub>2</sub>S</b>	Day	-ve	48.473	1	<0.0001	***	0.21	0.18	Day	36.382	1	<0.0001	***	0.28	0.20	
	Protein	-ve	13.784	1	0.0002	***		(0.03)	Protein	13.398	1	0.0003	***		(0.08)	
	Temp	+ve	5.224	1	0.0223	*			Temp	14.518	1	0.0001	***			
<b>Rb<sub>8</sub></b>	Day	-ve	62.980	1	<0.0001	***	0.23	0.21	Day	31.947	1	<0.0001	***	0.24	0.17	
	Protein	-ve	8.580	1	0.0034	**		(0.02)	Protein	7.8939	1	0.0050	**		(0.07)	
<b>Mg<sub>2</sub></b>	Protein	+ve	15.287	1	<0.0001	***	0.17	0.15	Protein	19.397	1	<0.0001	***	0.21	0.20	
	Salinity	+ve	33.953	1	<0.0001	***		(0.02)	Salinity	22.947	1	<0.0001	***		(0.02)	
	Treatment	Treated>N.T.	4.622	1	0.0316	*			Treatment	n.s.						
<b>Ca<sub>8</sub></b>	Temp	-ve	14.28	1	0.0002	***	0.62	0.50	Temp	11.385	1	0.0007	***	0.71	0.61	
	Sex	F>M	47.351	1	<0.0001	***		(0.12)	Protein	271.046	1	<0.0001	***		(0.10)	
	Protein	+ve	291.383	1	<0.0001	***										
	Sex:Protein	F = more +ve	56.1	1	<0.0001	***										
<b>Sr<sub>8</sub></b>	Sex	n.s.	0.079	1	0.7790		0.51	0.23	GSI (+ve)	25.847	1	<0.0001	***	0.66	0.40	
	Growth	-ve	19.172	1	<0.0001	***		(0.28)	Protein	62.665	1	<0.0001	***		(0.26)	
	Protein	+ve	49.213	1	<0.0001	***										
	Sex*Protein	+ve F, -ve M	66.376	1	<0.0001	***										
Ba and thiophilic elements	<b>Ba<sub>2</sub></b>	Ba/Caw	n.s.	0.363	1	0.5469		0.18	0.18	Ba/Caw	0.8688	1	0.3513		0.27	0.27
		Temp	n.s.	0.475	1	0.4906			(0.00)	Temp	2.7234	1	0.0989			(0.00)
		Ba/Caw*Temp	-ve at low T, +ve(?) at high T	21.948	1	<0.0001	***			Ba/Caw*Temp	8.9574	1	0.0028	**		
	<b>Mn<sub>2</sub></b>	Sex	F>M	10.3518	1	0.0010	**	0.43	0.20	Growth	4.6821		0.0305	*	0.30	0.18
		Growth	+ve	8.9304	1	0.0030	**		(0.23)	Condition	17.7066		<0.0001	***		(0.12)
		Condition	+ve	27.5493	1	<0.0001	***									
	<b>Cu<sub>2</sub>S</b>	Protein	+ve	56.829	1	<0.0001	***	0.61	0.42	Protein	43.405	1	<0.0001	***	0.60	0.47
		Condition	+ve	21.881	1	<0.0001	***		(0.19)	Condition	21.845	1	<0.0001	***		(0.13)
		Temp	+ve	25.917	1	<0.0001	***			Temp	23.966	1	<0.0001	***		
		Sex	M>F	7.401	1	0.0065	**			GSI (-ve)	16.542	1	<0.0001	***		
		Temp*Sex	+ve F, -ve M	30.021	1	<0.0001	***									
	<b>Zn<sub>2</sub>S</b>	Znw	+ve	60.047	1	<0.0001	***	0.77	0.65	Znw	34.7478	1	<0.0001	***	0.80	0.74
		Protein	+ve	42.073	1	<0.0001	***		(0.12)	Protein	27.4814	1	<0.0001	***		(0.06)
		Condition	-ve	16.945	1	<0.0001	***			Condition	5.6307	1	0.0177	*		
<b>Se<sub>2</sub>S</b>	Origin	IS>EC	33.478	1	<0.0001	***	0.71	0.42	Origin	49.535	1	<0.0001	***	0.71	0.44	
	Sex	M>F	11.577	1	0.0007	***		(0.29)	Min	40.766	1	<0.0001	***		(0.27)	
	Protein	+ve	62.972	1	<0.0001	***			Min	25.558	1	<0.0001	***			
	Sew	+ve	59.375	1	<0.0001	***			GSI (-ve)	15.272	1	<0.0001	***			
	Condition	n.s.	0.5065	1	0.4766		0.34	0.23	Growth	13.176	1	0.0003	***	0.40	0.26	
<b>Pb<sub>2</sub>S</b>	Sex	F>M	7.9314	1	0.0049	**		(0.11)	Protein	10.051	1	0.0015	**		(0.14)	
	Growth	+ve	7.7312	1	0.0054	**			GSI (+ve)	9.842	1	0.0017	**			
	Protein	+ve	11.324	1	0.0008	***										
	Condition*Sex	+ve for F, -ve for M	44.8459	1	<0.0001	***										

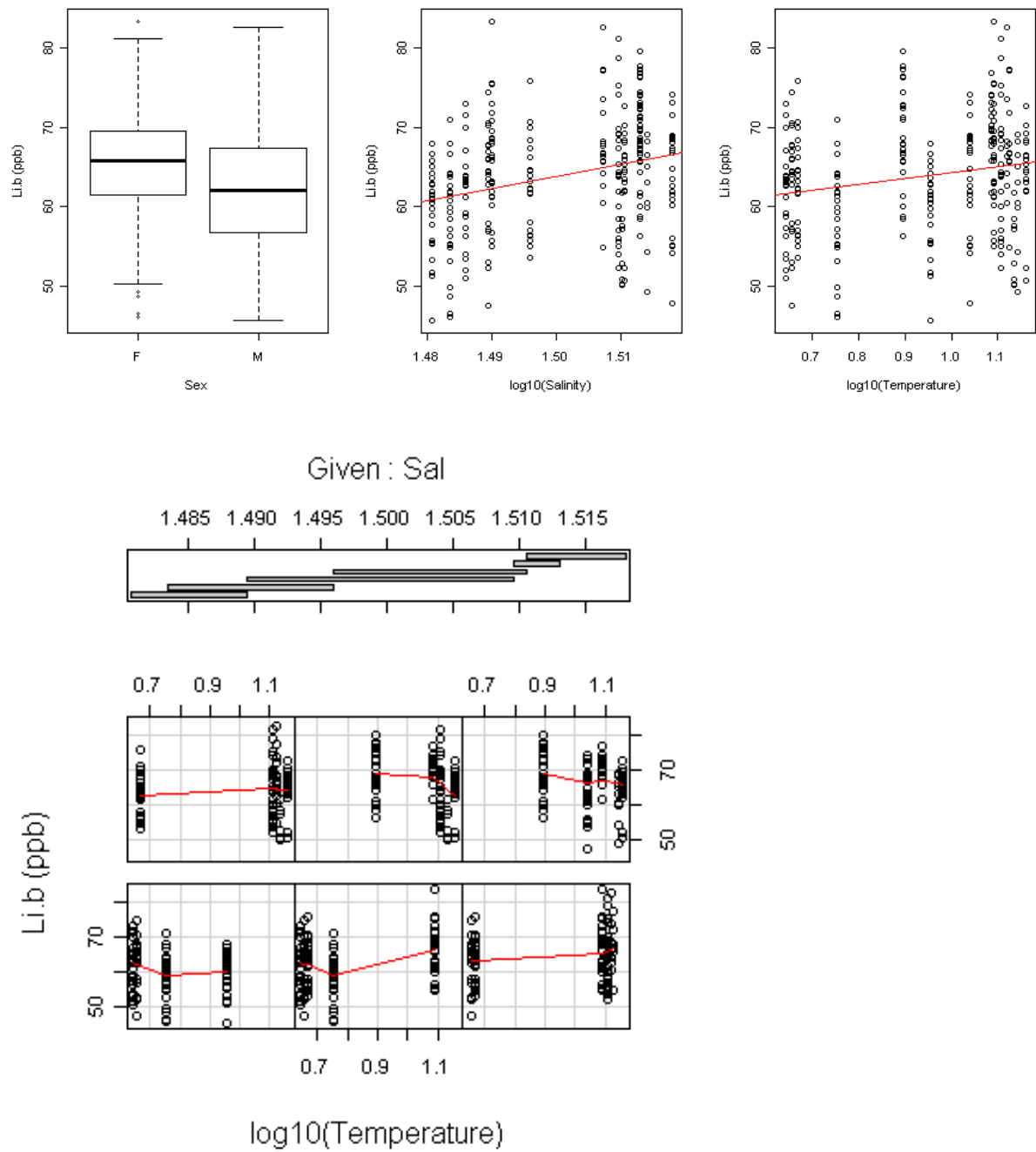


Figure 3.10 Patterns in Li<sub>B</sub>. Note that in the ‘coplot’ on the bottom row, plot order relates to the salinity ranges defined above (starting bottom left, moving left to right; salinity and temperature  $\log_{10}$  transformed). The boxplot whiskers extend 1.5 times the inter-quartile range from the 25<sup>th</sup> and 75<sup>th</sup> quartiles (lower and upper ranges of the box, respectively), while the bold line indicates the median

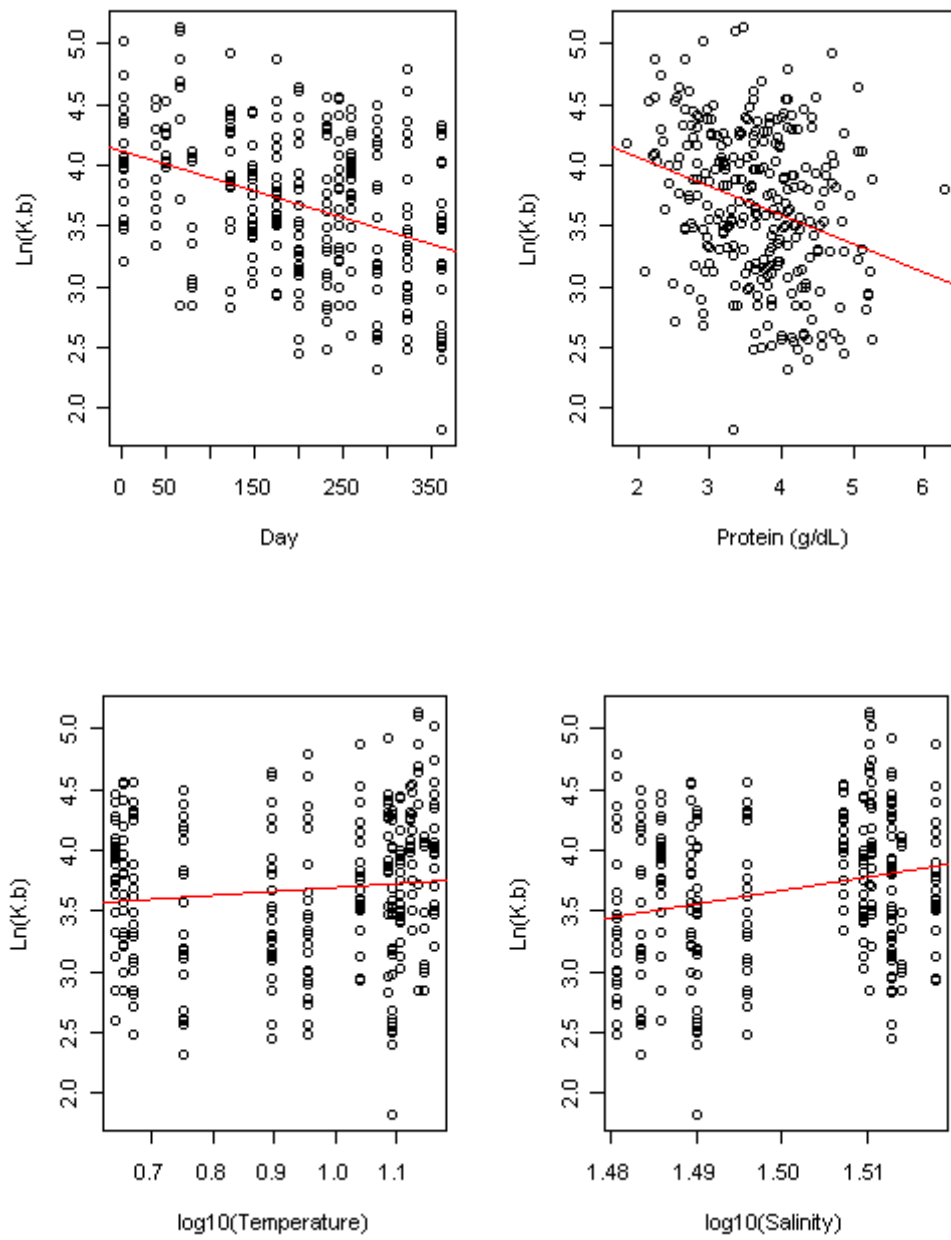


Figure 3.11 The relationship between the number of days into the experiment, blood protein concentrations, temperature ( $\log_{10}$  transformed, in  $^{\circ}\text{C}$ ), salinity ( $\log_{10}$  transformed) and  $\text{K}_\text{B}$  values ( $\text{Ln}$  transformed concentrations in ppm). Plots were near identical for  $\text{Rb}_\text{B}$ , so are not displayed. Note that the relationship with temperature was weaker and non-significant for  $\text{Rb}_\text{B}$  values and the relationship with salinity was only significant for either element if temperature was excluded

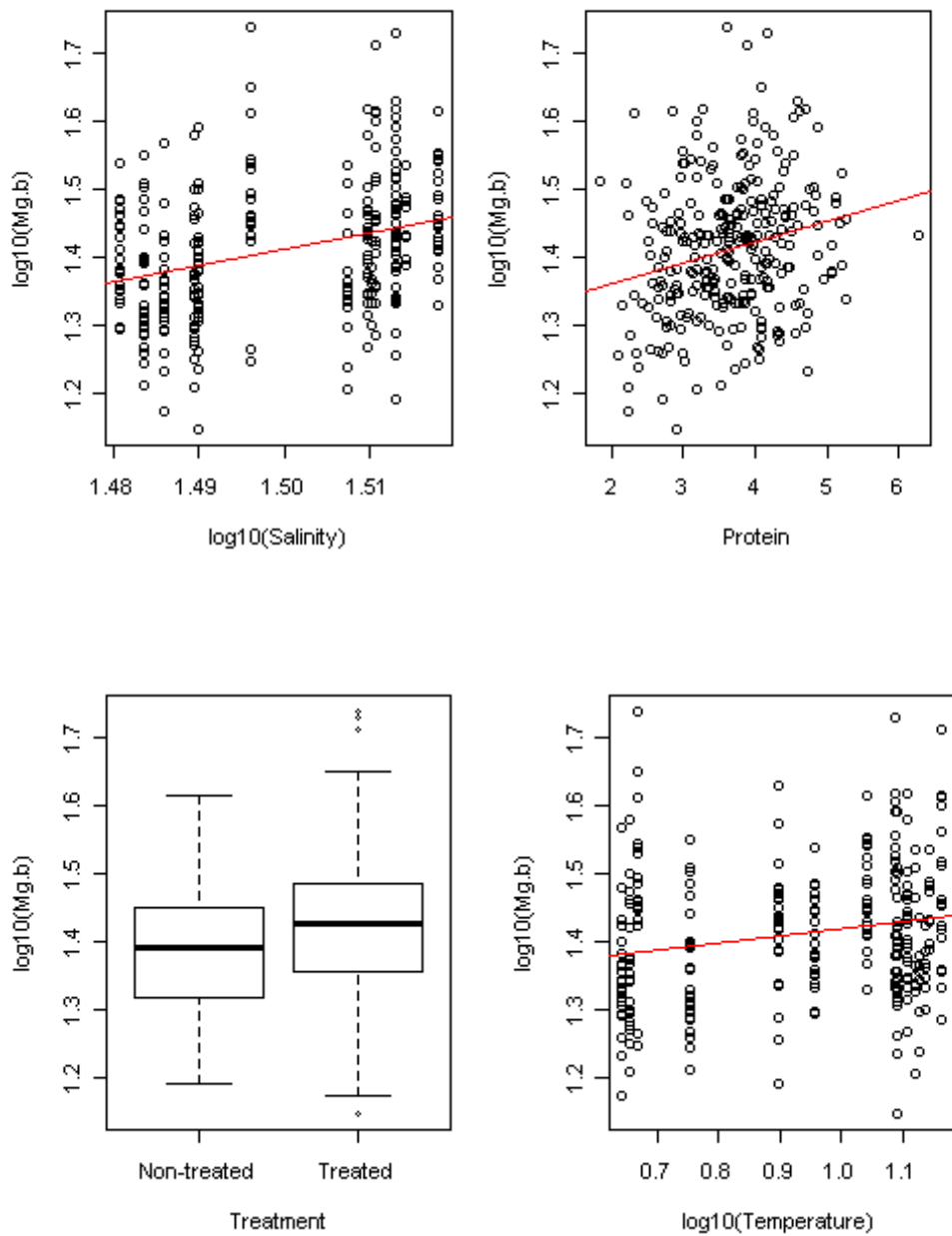


Figure 3.12 The relationship between salinity ( $\log_{10}$  transformed), blood protein concentrations (in g/dL), temperature ( $\log_{10}$  transformed, in  $^{\circ}\text{C}$ ) and  $\text{Mg}_B$  values ( $\log_{10}$  transformed concentrations in ppm). Note that the relationship with treatment was non-significant in the female only model and the relationship with temperature was only significant if salinity was excluded. The boxplot whiskers extend 1.5 times the inter-quartile range from the 25<sup>th</sup> and 75<sup>th</sup> quartiles (lower and upper ranges of the box, respectively), while the bold line indicates the median

### **Ca<sub>B</sub>**

Ca<sub>B</sub> values were almost entirely explained by a positive relationship with blood protein concentrations, however the slope differed between the sexes, with proportionally more Ca<sub>B</sub> per unit increase in protein in the females (Figure 3.13). This resulted in higher overall concentrations in the females. There was also a relatively weak negative relationship between Ca<sub>B</sub> values and temperature. The female only model was the same, only with slightly better fit ( $r^2 = 0.7$  vs. 0.6). Approximately 10% of the variance in Ca<sub>B</sub> was explained by the random effect.

### **Sr<sub>B</sub>**

Sr<sub>B</sub> values were largely explained by an interaction between protein and sex, with a positive relationship between Sr<sub>B</sub> and blood protein concentrations in the females and a weakly negative relationship in the males (Figure 3.14). There was also a negative relationship between Sr<sub>B</sub> values and somatic growth rate (GR), although it was not significant in the female only model. While mean Sr<sub>B</sub> was slightly higher in the females, the difference was not significant. Model fit was good, but better in the female only model ( $r^2 = 0.66$  vs. 0.51). In both cases, >25% of the variation was explained by the random effect, indicating among-fish differences in Sr<sub>B</sub> values.

While not specifically part of the Sr<sub>B</sub> model outputs, it is important to note that there was a clear difference in the relationship between Ca<sub>B</sub> and Sr<sub>B</sub> in the males and females. It was similar to Sr<sub>B</sub> vs. protein concentrations, with a strong positive correlation in the females but no relationship in the males (Figure 3.15).

### **Ba<sub>B</sub>**

The interaction between Ba/Ca<sub>W</sub> values and temperature was highly significant in both models, but model fits were relatively poor ( $r^2 = 0.18-0.27$ ). Based on the coplot in Figure 3.16, the effects of the interaction were somewhat ambiguous, but seemed to indicate a weakly positive effect of Ba/Ca<sub>W</sub> on Ba<sub>B</sub> values at high temperatures but a non significant or negative effect at all other temperatures. The same effect was observed using Ba<sub>W</sub> values, just with a slightly poorer model fit. No variation in Ba<sub>B</sub> values was explained by the random effect.

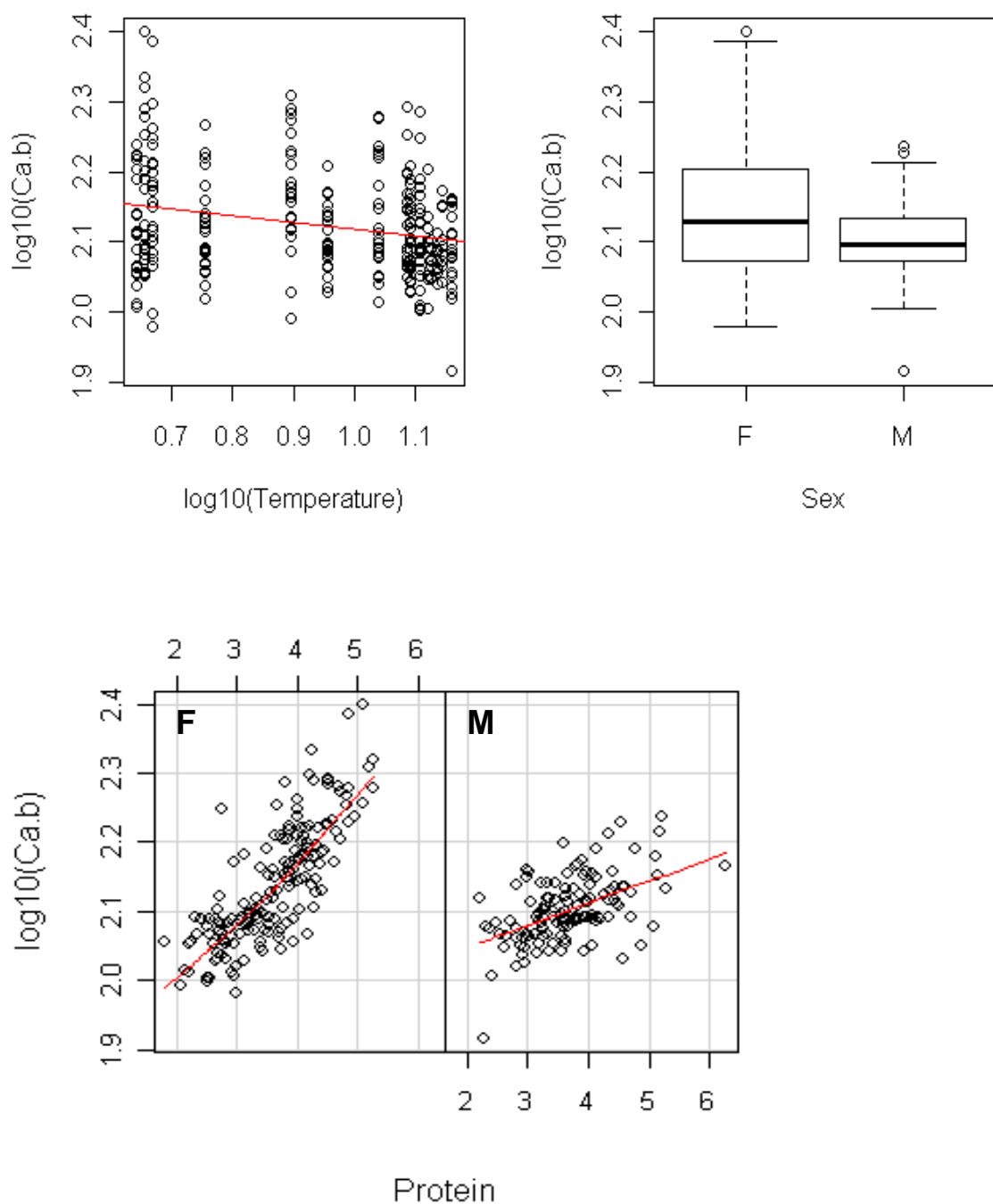


Figure 3.13 The relationship between temperature ( $\log_{10}$  transformed, in  $^{\circ}\text{C}$ ), sex and protein (in g/dL) and  $\text{Ca}_\text{b}$  values ( $\log_{10}$  transformed concentrations in ppm). The coplot on the bottom row indicates the relationship between  $\text{Ca}_\text{b}$  and protein for females (F) and males (M) separately. The boxplot whiskers extend 1.5 times the inter-quartile range from the 25<sup>th</sup> and 75<sup>th</sup> quartiles (lower and upper ranges of the box, respectively), while the bold line indicates the median

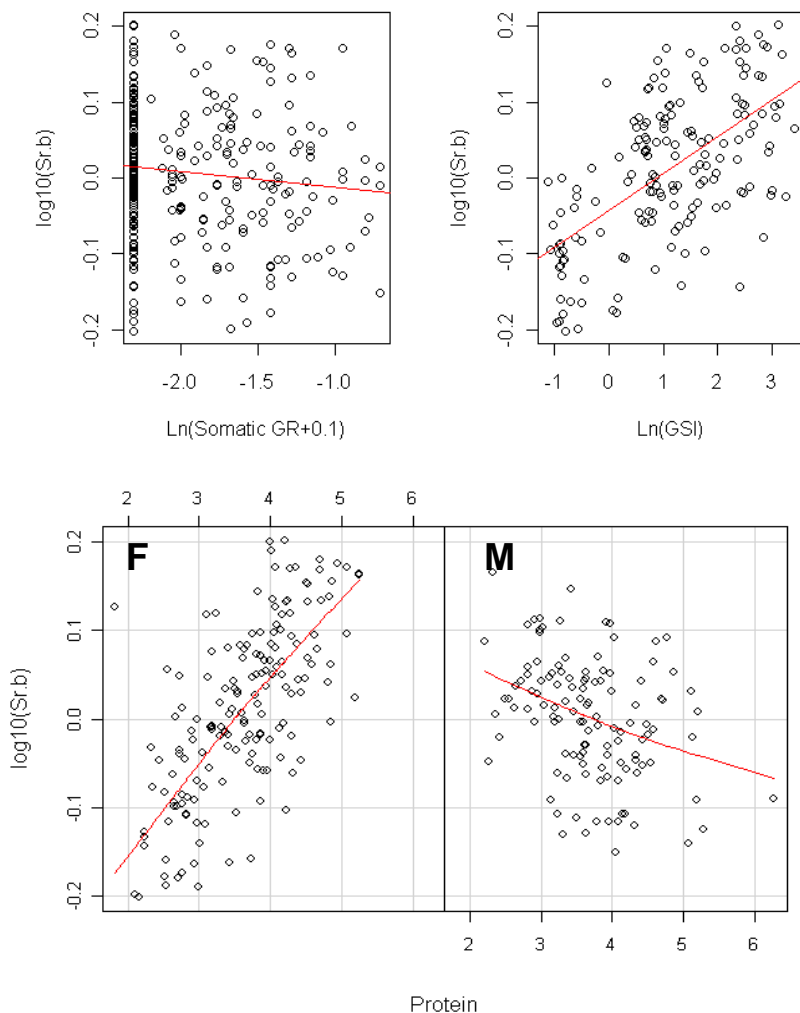


Figure 3.14 The relationship between somatic growth rate (GR;  $\text{Ln}(x+0.1)$  transformed, in mm/day), GSI (Ln transformed, in %), blood protein concentrations (in g/dL) and  $\text{Sr}_B$  values ( $\log_{10}$  transformed concentrations in ppm). The coplot on the bottom row indicates the relationship between protein and  $\text{Sr}_B$  for females (F) and males (M)

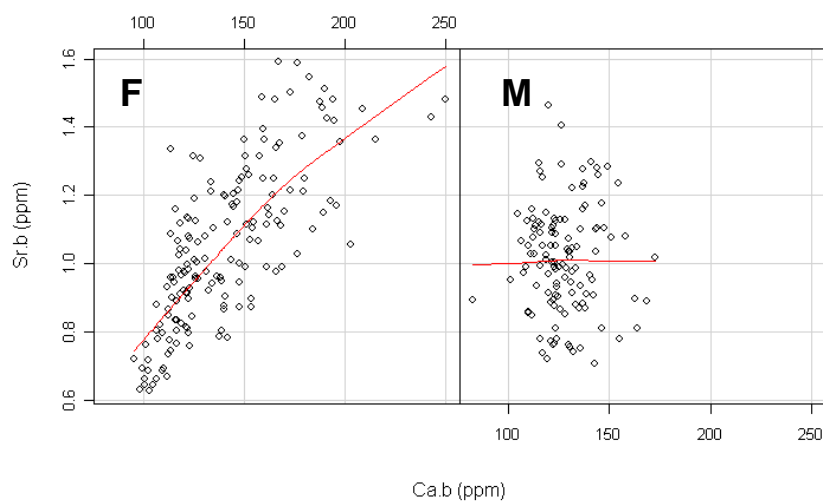


Figure 3.15 Coplot to show the relationship between  $\text{Ca}_B$  and  $\text{Sr}_B$  concentrations in females (F) and males (M)

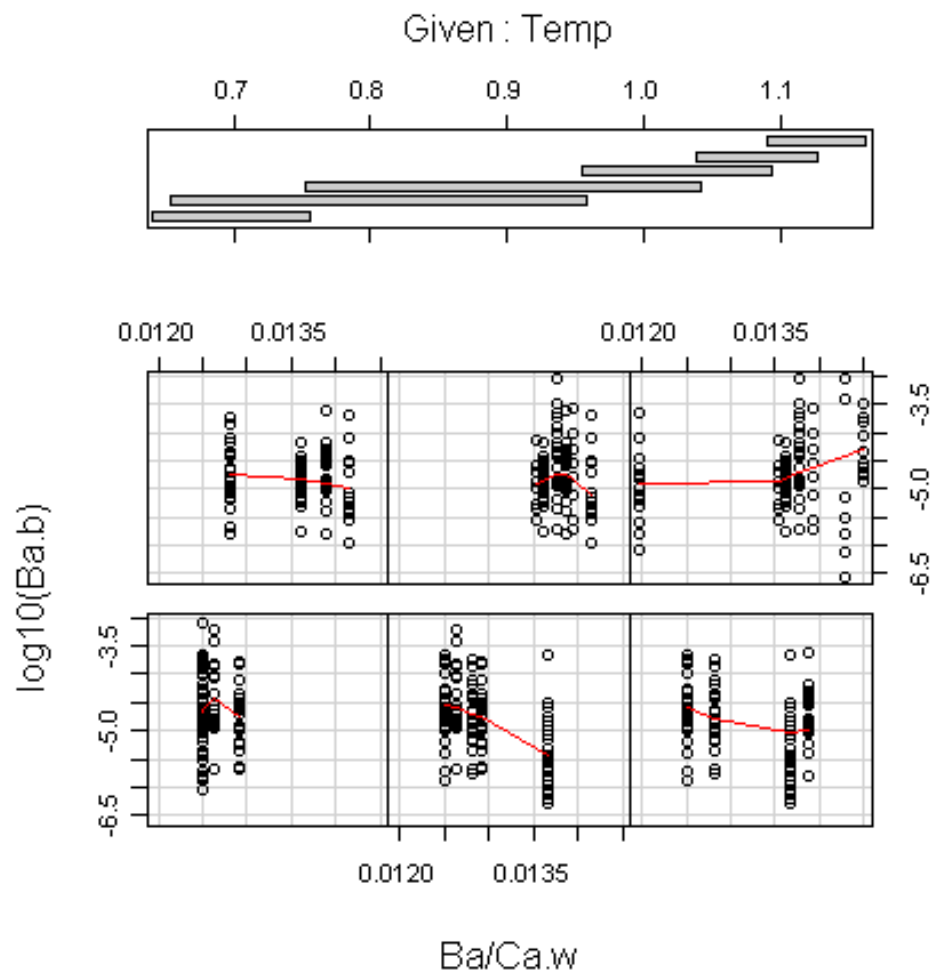


Figure 3.16 Coplot to show the relationship between Ba/Ca<sub>W</sub> (mmol/mol) and Ba<sub>B</sub> (log<sub>10</sub> transformed concentrations in ppb) at different temperatures (log<sub>10</sub> transformed, in °C). Note that plot order relates to the temperatures defined above (starting bottom left, moving left to right)

### **Mn<sub>B</sub>**

Mn<sub>B</sub> values were mainly explained by a positive effect of condition (Figure 3.17). There was also a positive effect of growth rate and concentrations were higher in the females than the males. A negative relationship with temperature was almost significant and there was a similarly weak negative relationship with Mn<sub>W</sub>. There was no difference in the female only model, only a slightly poorer fit ( $r^2 = 0.30$  vs. 0.43). For both models the variation explained was divided almost equally amongst the fixed and random effects.

### **Cu<sub>B</sub>**

Explaining patterns in Cu<sub>B</sub> values was more complex due to its correlation with many of the physiological and environmental terms. However, common across all models was a main positive effect of blood protein concentrations (Figure 3.18). Cu<sub>W</sub> and temperature were almost perfectly correlated (PCC = 0.95), so it was impossible to fully discriminate among them. There was potentially a significant interaction between Cu<sub>W</sub> values and origin, with EC females exhibiting a positive relationship with ambient concentrations, while IS fish exhibiting no or even a negative relationship (Figure 3.18). However, the interaction was excluded from the model as there were no representative ‘high Cu<sub>W</sub>’ values for the EC females given their delayed introduction to the experiment. Note that even when the interaction was included, ‘origin’ was not significant, with the lower Cu<sub>B</sub> values in the EC females explained by their lower protein concentrations and condition. The significant interaction between sex and temperature resulted from a generally positive relationship between Cu<sub>B</sub> values and temperature in the females and non-linear, negative relationship in the males (Figure 3.18).

The female only model also included a negative effect of GSI, which was most apparent in the EC females, and while the ‘origin\*GSI’ interaction was significant ( $p = 0.02$ ), it did not improve model performance (based on AIC or  $r^2$ ), so was not added to the final model. For both models, overall fit was good ( $r^2 = 0.6$ ), with 13-19% explained by the random effect.

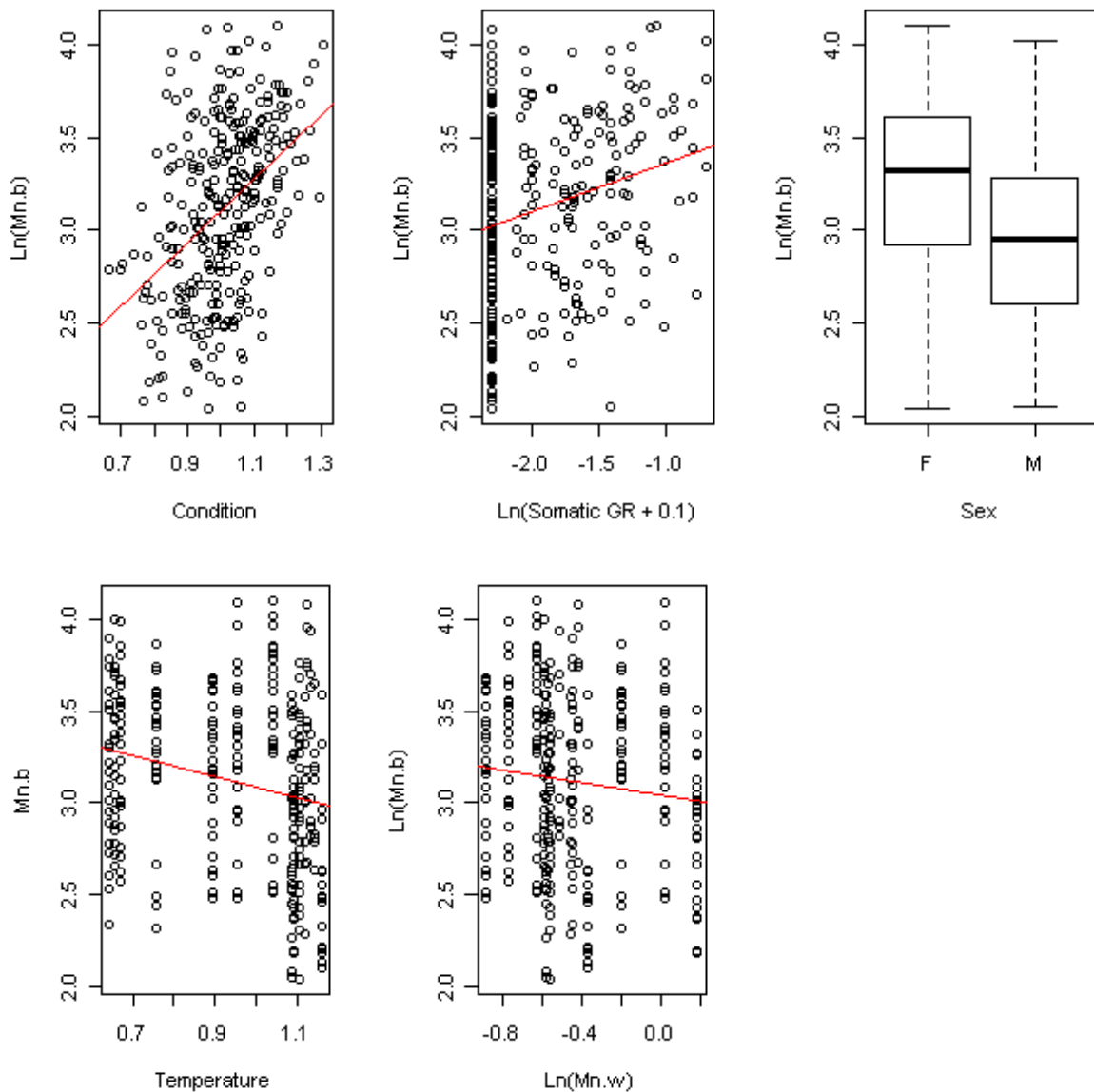


Figure 3.17 The relationship between condition, somatic growth rate (GR;  $\text{Ln}(x+0.1)$  transformed, in mm/day), sex, temperature ( $\log_{10}$  transformed, in  $^{\circ}\text{C}$ ),  $\text{Mn}_W$  ( $\text{Ln}$  transformed, in ppb) and  $\text{Mn}_B$  values ( $\text{Ln}$  transformed concentrations in ppb). Note that the relationships with temperature and  $\text{Mn}_W$  were not significant but are displayed for discussion. The boxplot whiskers extend 1.5 times the inter-quartile range from the 25<sup>th</sup> and 75<sup>th</sup> quartiles (lower and upper ranges of the box, respectively), while the bold line indicates the median

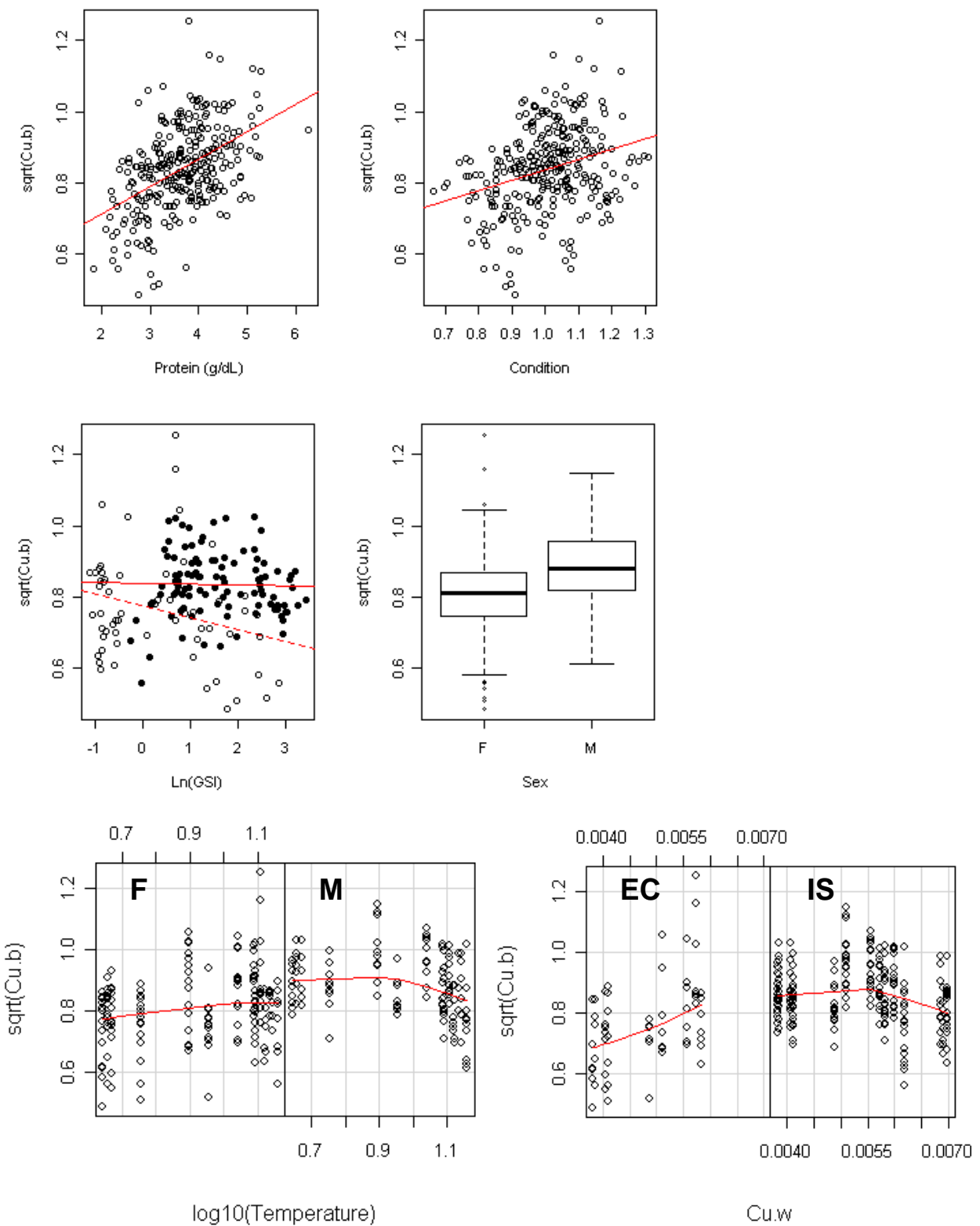


Figure 3.18 Patterns in  $\text{Cu}_B$  (SQRT transformed concentrations in ppb). Note that the interaction between origin (EC = English Channel, IS = Irish Sea) and  $\text{Cu}_w$  (in ppm) indicated by the coplot (bottom, right) was excluded from the final model due to lack of representative 'high  $\text{Cu}_w$ ' data in the EC females. In the GSI (Ln transformed, in %) vs.  $\text{Cu}_B$  plot, EC females are indicated by open circles and a dashed line; IS females by solid circles. The boxplot whiskers extend 1.5 times the inter-quartile range from the 25<sup>th</sup> and 75<sup>th</sup> quartiles (lower and upper ranges of the box, respectively), while the bold line indicates the median

### **Zn<sub>B</sub>**

Zn<sub>B</sub> values were primarily explained by a positive relationship with ambient concentrations or temperature (Figure 3.19). In the female only model, the fit was 6% higher using Zn<sub>W</sub> than temperature, hence its selection in the final models presented. However, inclusion of either term produced models with  $r^2$  values above 0.7. The positive effect of protein and the negative effect of condition on Zn<sub>B</sub> values were significant in both models, and in the female only model, the negative effect of GSI was also highly significant. In both cases, most of the variance was explained by the fixed effects, but particularly in the female only model.

### **Se<sub>B</sub>**

Similar to Zn<sub>B</sub>, Se<sub>B</sub> values were largely explained by positive relationships with protein and ambient concentrations or temperature, however, inclusion of temperature in place of Se<sub>W</sub> reduced model fit by about 10%. There was also a significant origin and sex effect, with Se<sub>B</sub> concentrations lower in the EC fish than the IS fish, and lower in the females than the males (Figure 3.20). Similar to Zn<sub>B</sub> and Cu<sub>B</sub>, a negative effect of GSI was also significant in the female only model. Overall model fits were good ( $r^2 > 0.7$ ) but the random effect explained 27-29% of the variation in both cases.

### **Pb<sub>B</sub>**

Pb<sub>B</sub> values behaved in a broadly similar manner to Ca<sub>B</sub> and Sr<sub>B</sub>, and the most important predictor was an interaction between condition and sex, with a positive relationship between condition and Pb<sub>B</sub> values in the females but a negative relationship in the males (Figure 3.21). Unlike Sr<sub>B</sub>, Pb<sub>B</sub> varied in a positive manner with growth rate, but like Ca<sub>B</sub> and Sr<sub>B</sub> exhibited a positive correlation with blood protein concentrations, and was higher in the females. The female only model included GSI instead of condition and exhibited better overall fit  $r^2 = 0.40$  vs. 0.34), but a slightly larger random effect.

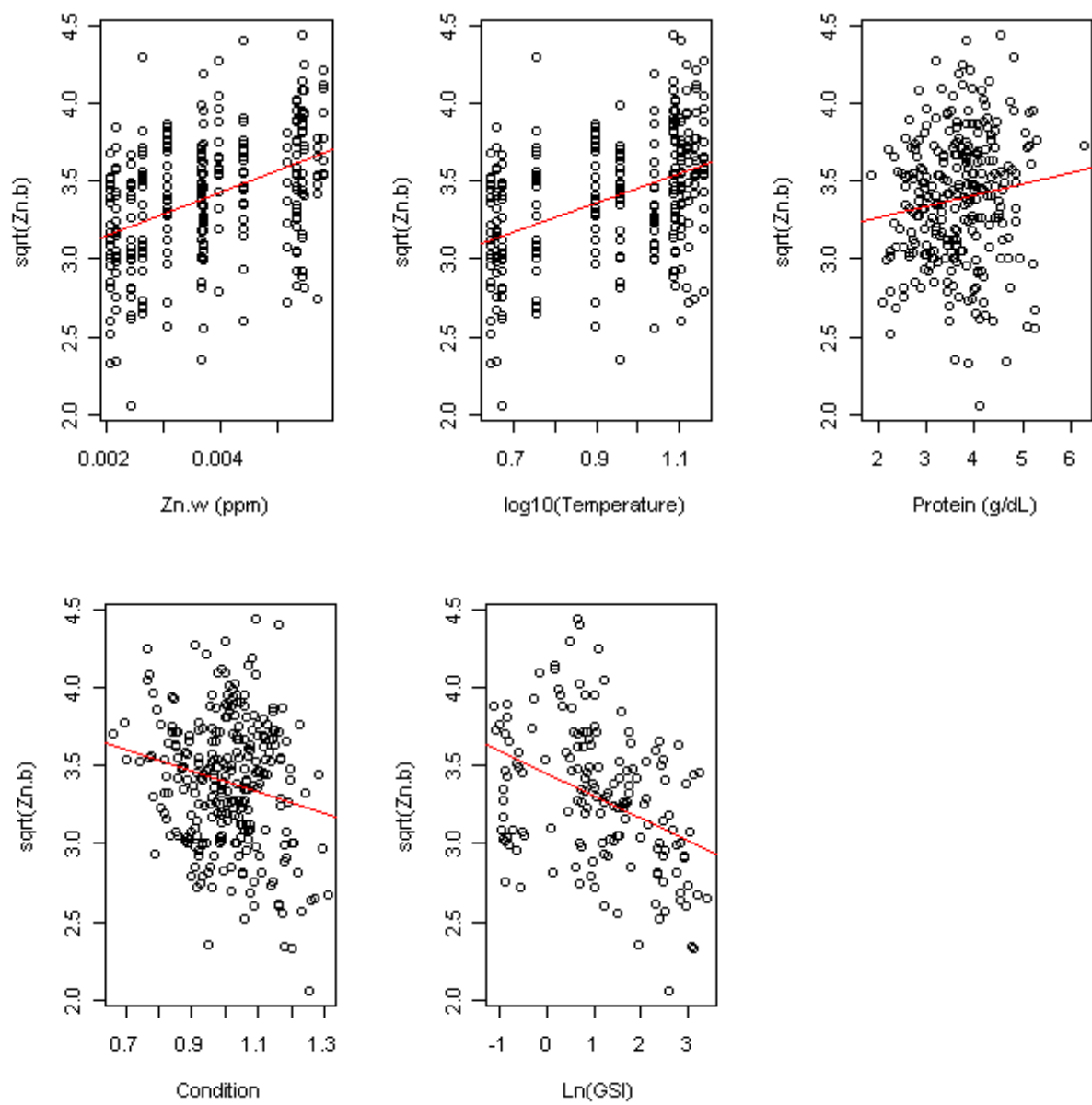


Figure 3.19 Patterns in  $\text{Zn}_B$  values (SQRT transformed concentrations in ppm). Note that the relationship with  $\text{Zn}_W$  was 'interchangeable' with temperature, but  $\text{Zn}_W$  produced a slightly better model fit.

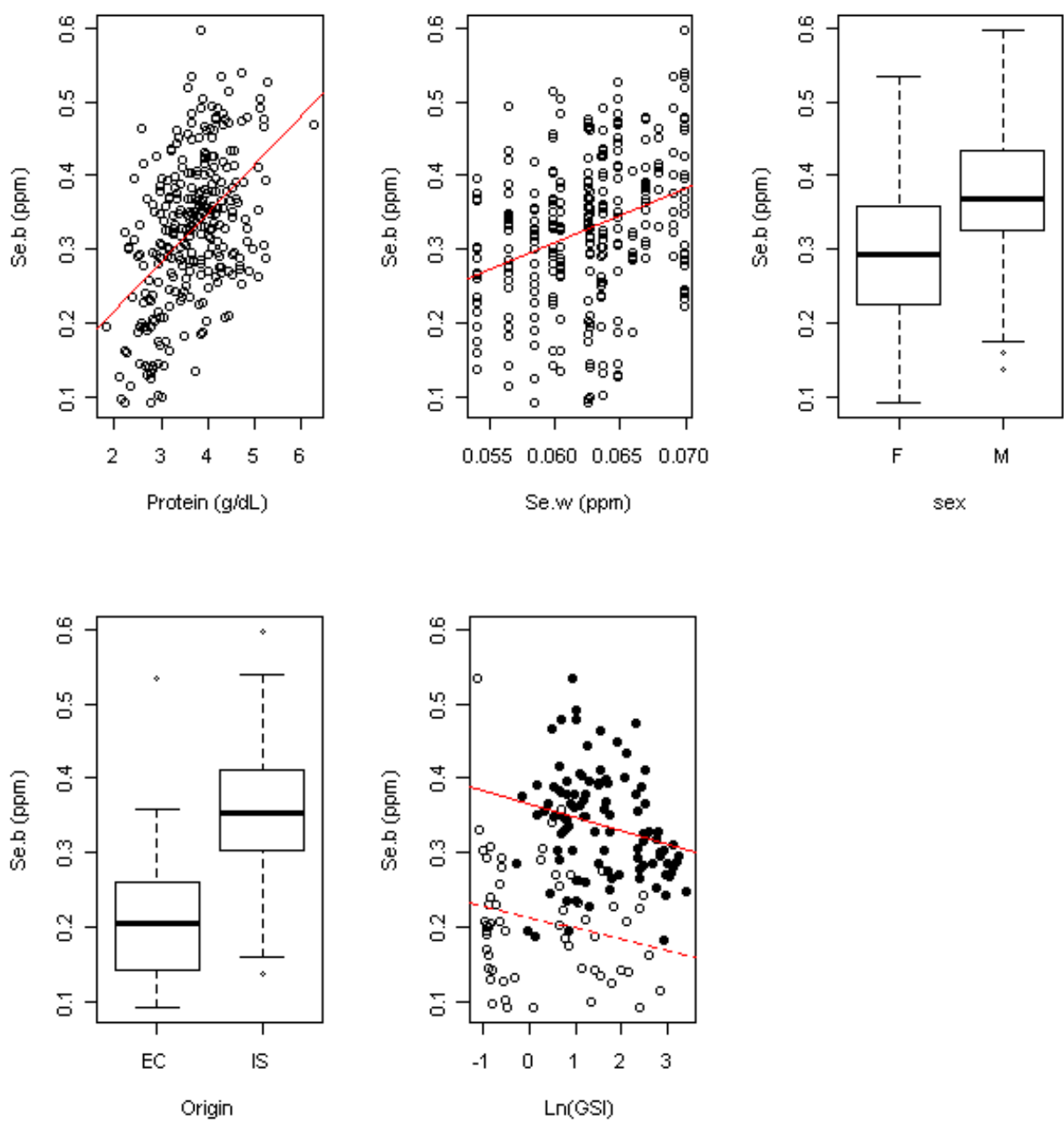


Figure 3.20 Patterns in  $Se_B$  values. In the plot showing GSI vs.  $Se_B$ , EC females are indicated by open circles and the dashed line, while IS females are indicated by solid circles and a solid line. The boxplot whiskers extend 1.5 times the inter-quartile range from the 25<sup>th</sup> and 75<sup>th</sup> quartiles (lower and upper ranges of the box, respectively), while the bold line indicates the median

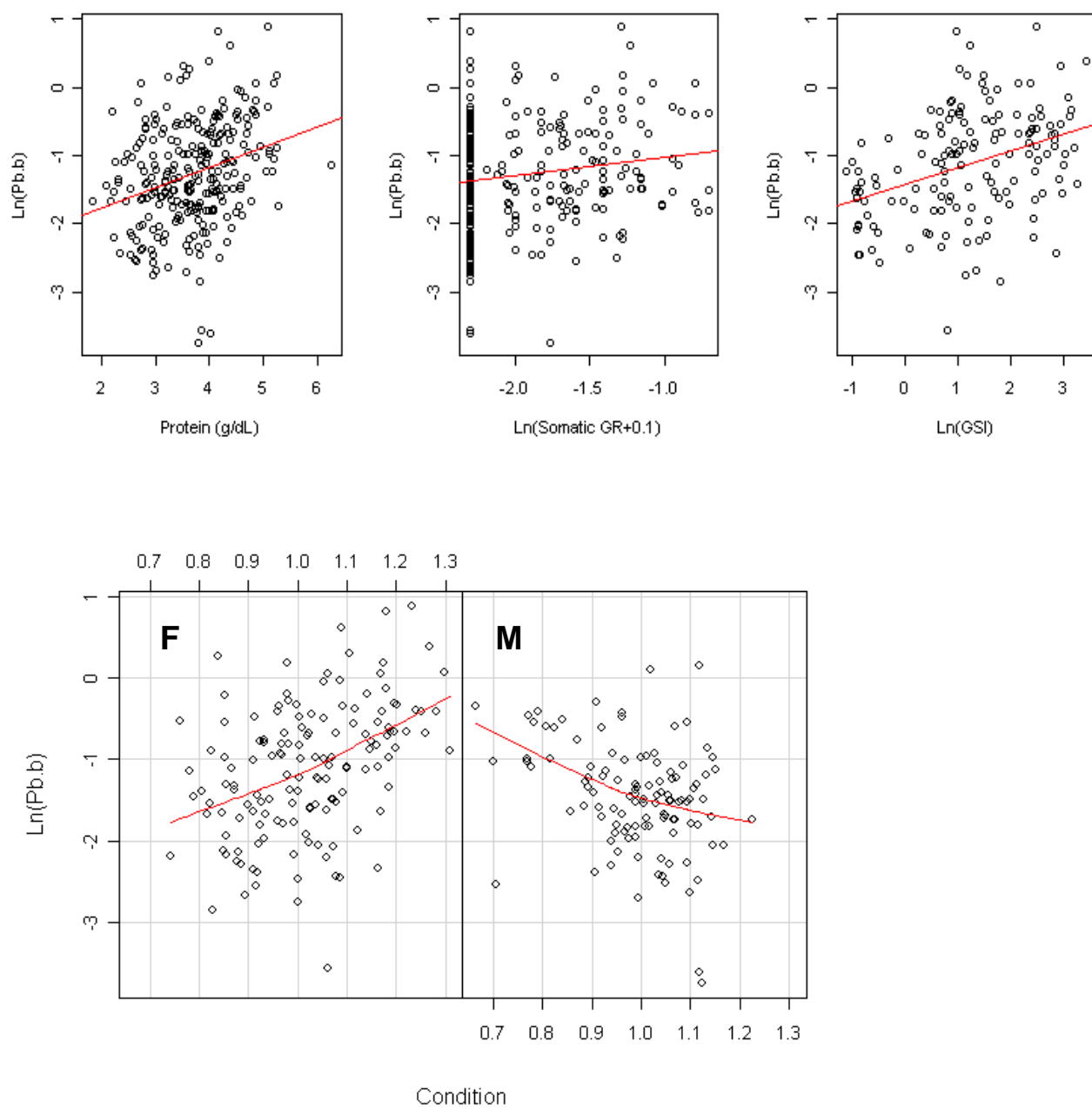


Figure 3.21 Relationship between blood protein concentrations, somatic growth rate (GR;  $\ln(x+0.1)$  transformed, in mm/day), GSI ( $\ln$  transformed, in %) and  $\text{Pb}_B$  values ( $\ln$  transformed concentrations in ppb). The coplot in the bottom row indicates the relationship between  $\text{Pb}_B$  and condition for females (F) and males (M) separately.

### 3.4 Discussion

Fish blood represents the major intermediary step between the environment and the otolith. Thus in order to understand element incorporation into the otolith it is important to appreciate their fractionation from water to blood. Clearly, blood is a highly regulated medium, with few elements exhibiting strong, if any, relationship with ambient concentrations, and this sets a first order limit on the sensitivity of otolith chemistry to fluctuations in ambient water chemistry. Variations in blood elemental concentrations over time and among the three 'groups' of fish indicated major physiological influences and complicated the relationship between ambient and blood element concentrations. Such influences were greatest for the softer, thiophilic elements (Mn, Cu, Zn, Se and Pb) and the quasiconservative elements (Sr and Ca). Apart from Sr and Ca, the 'hard' elements (Li, Mg, K, Rb, Ba) were less affected by physiology, with lower overall temporal variation and only minor differences among the sexes observed for  $\text{Li}_B$ . Overall, blood protein content was the single most important explanatory term and was included in all mixed effects models except Li, Ba and Mn, although the  $\text{Mn}_B$  model did include both condition and growth rate, which were both highly correlated with protein concentrations. This emphasises the importance of protein-binding in regulating blood element concentrations, and it is likely that other physiological variables influence blood chemistry via modifications to blood protein composition and concentrations.

Before further discussion, it is important to highlight the caveats associated with this type of experiment. By attempting to reproduce 'natural' conditions to encourage natural physiological behaviour, the 'experiment' becomes inherently uncontrolled and complex. Without fully factorial experimental design, such an experiment cannot lend itself to formal hypothesis testing. While controlled empirical studies are crucial for disentangling extrinsic influences on blood and otolith chemistry, unfortunately it is not possible to control and manipulate the physiological status of an organism while maintaining 'natural' conditions. Thus, any studies attempting to disentangle such effects face inevitable challenges. In the current study, multicollinearity was an issue, with many of the model terms covarying with season. This was particularly apparent among seawater chemistry and temperature. Dilution of the tank water by increased precipitation in winter provides the most plausible explanation for the correlated, but lagged, trend in temperature and salinity, but the greater congruence of temperature and seawater element concentrations (e.g. PCC of 0.95 between temperature and  $\text{Cu}_W$ ) may also reflect seasonal changes in primary productivity. While increasing model complexity almost always improved its fit, the use of AIC-based model selection resulted in the selection of the most parsimonious models using the lowest number of terms. This helped to reduce multicollinearity in a non-subjective manner, and allow inferences to be made as to the most important terms; however, 'correlation is not causation', and given the collinearity among variables, it remains a

possibility that some of the significant terms played no active role in the expression of the response variable. Another caveat associated with the modelling carried out in the current study, was the assumption of linear relationships among variables. Much of the data required transformation in order to meet the model assumptions and even then, some non-linear relationships are apparent in the plots presented above. It is sometimes argued that data transformation can remove or modify true relationships among variables (Zuur *et al.*, 2009), however, it was vital to ensure homogeneity and normality of model residuals. While using non linear modelling will often improve the model fit and accuracy of predictions, it also greatly increases model complexity. Given our aim to explore 'main effects' governing blood element concentrations, a linear approach that allowed modification of the intercept but not the slope, was deemed to be the most robust. Whatever the 'true' underlying mechanisms controlling the blood elements studied, it is key to remember that the observed variations between individuals, males and females, IS and EC fish were irrefutable, and occurred despite exposure to identical conditions, diet and sampling regimes.

Another caveat to consider is how representative the study animals were of a randomly sampled wild population. While the experimental fish did not endure the physiological stresses associated with spawning migrations and foraging, the handling and repeat blood sampling of them would have almost certainly resulted in higher stress levels than their wild equivalents. The effect of the sampling regime was unknown, but may have affected physiological parameters and elemental expression in the blood. Indeed, net confinement of flounder and turbot resulted in elevated plasma cortisol, osmolality, monovalent ion concentrations and(or) protein (Waring *et al.*, 1992; 1996). While it is not possible to rule these out, it is reassuring that the growth rates, condition and GSI values of the experimental population were similar to those reported for wild plaice (Rijnsdorp, 1989; Maddock and Burton, 1998; Bromley, 2000) and blood element concentrations were broadly similar to those reported for other marine species, where available (Chapter 2).

Seawater element concentrations were highly correlated within chemical groups and even across groups, with the lowest concentrations consistently observed during winter. This implies a significant precipitation/dilution effect, however, it is important to note that  $El/Ca_w$  ratios remained relatively constant in the conservative elements, but were more variable in the softer elements, such as  $Cu/Ca_w$ . Blood element concentrations and blood/water distribution coefficients were less correlated within chemical groups than seawater concentrations, implying element-specific uptake and processing mechanisms. Despite this variability, there were still broad similarities among the hard and soft acid ions, so patterns in blood elemental concentrations will be discussed according to the following three subdivisions: (i) 'hard elements', (ii) 'Sr and Ca' and (iii) 'soft' elements.

### 3.4.1 ‘Hard’ elements

K and Rb concentrations behaved almost identically in both the seawater and in the blood. In the blood, concentrations decreased gradually over time. Accordingly, the single most important term explaining their concentrations was ‘Day’, implying the presence of an additional, temporally structured variable. In flounder, plasma K<sup>+</sup> concentrations were significantly elevated following net confinement, indicating its expression as a stress response (Waring *et al.*, 1992). Given that the experimental plaice were not handled for three months prior to the first sampling event in June 2009, K concentrations in the initial samples may have been unnaturally elevated due to stress, and the gradual decrease over time the result of habituation to the handling and sampling regime. Studies measuring Rb<sub>B</sub> in fish blood are rare (Chapter 2), but its behaviour was so tightly correlated with that of K that is likely to be controlled by the same mechanisms. In the IS females, blood K<sub>B</sub> and Rb<sub>B</sub> values to a certain extent, decreased in November, approximately three months prior to the start of the spawning season. A dip in plasma K concentrations also occurred about three months prior to spawning in bearded rock cod (Kalish, 1991) and American plaice (Audet *et al.*, 1993), while in sockeye salmon, whole ovary K concentrations increased during early maturation then decreased rapidly with increasing GSI (Shearer, 1984). North Sea plaice ovaries begin to develop in July, but ovary mass only starts to appreciably increase in October (Rijnsdorp, 1989), around the same time GSI began to increase in the current study. These findings suggest that K may be removed from the blood and utilised for the early stages of ovarian development; specifically when the ovaries begin to increase in mass about three months prior to spawning.

Both Li<sub>B</sub> and Mg<sub>B</sub> values were positively related to salinity and(or) temperature, although for Li<sub>B</sub>, there was a significant temperature\*salinity interaction, where at extreme salinities the temperature effect appeared to be negative. The reliability of such interactions is difficult to determine given heterogeneity in the environmental data and little published on Li concentrations in fish blood. Li<sub>B</sub> was also significantly higher in the females than the males, although this difference was only really apparent from October onwards. Li<sub>B</sub> values were generally lower during winter, but D<sub>Li(B/W)</sub> indicated relative enrichment relative to ambient concentrations, implying a regulatory effect. D<sub>Li(B/W)</sub> was higher in the females during this time, however, given congruence among the mature (IS) and immature (EC) females, such enrichment is unlikely to be related to ovary development. The patterns might, however, be related to size or growth rates, with the females consistently larger than the males and tending to grow more slowly during the spawning period.

Blood Mg concentrations have received considerable attention in the literature, although controls on its concentration are still not clear, with some studies suggesting elevation of blood Mg concentrations during spawning (e.g. Valtonen and Laitinen, 1988), but other studies reporting fluctuations out of phase with reproductive cycles (e.g. Mugiya, 1966; Folmar *et al.*, 1992). Mg was found to be elevated in the ovaries of winter flounder (Fletcher and King, 1978) and rainbow trout (Shearer, 1984), implying some Mg requirement for ovarian development. In support of this, in the current study Mg<sub>B</sub> values dropped sharply at the height of the spawning season (February–March), however GSI was not a significant explanatory variable in the female-only model and there was no significant difference in Mg<sub>B</sub> values between the sexes. Unlike the monovalent ions discussed above, Mg<sub>B</sub> values were positively correlated with protein concentrations and slightly higher in GnRH treated fish. It is tempting to associate these observations with the correlation between Ca<sup>2+</sup> and protein concentrations (Urist and Schjeide, 1961). If, for example, increased Ca<sup>2+</sup> requirement resulted in ‘accidental’ increases in other divalent ions this might explain positive correlations between blood Mg concentrations and protein levels. However, if this were the case, one would expect greater concentrations of Mg<sub>B</sub> in the females during the hypercalcaemic period (November – February) and this was not the case. The highest concentrations of blood Mg and protein were exhibited during the first half of the experiment, when plaice were actively feeding, and water temperatures were at their highest. Assuming this period also corresponded to elevated metabolic activity, this may have resulted in greater Mg uptake, as Mg<sup>2+</sup> is essential in almost every major metabolic pathway (Kaim and Schwederski, 1994).

There were no clear patterns in Ba<sub>B</sub> or differences among groups of fish, and the interaction between temperature and Ba/Ca<sub>W</sub> appeared relatively weak. However, significant interactions between salinity and temperature on Ba concentrations in otoliths have been observed in a number of studies (e.g. Elsdon and Gillanders, 2002; de Vries *et al.*, 2005; Miller, 2011). Unfortunately there was lower confidence in the Ba<sub>B</sub> data, because, as discussed in the previous chapter, the procedural blanks contained higher Ba than almost all of the blood samples, implying a source of Ba contamination that was not (or only partially) transferred to the plasma, possibly remaining in the pellet after centrifugation. Caution must therefore be applied to all Ba<sub>B</sub> measurements. However, concentrations were still around 20–40 times lower than those reported for burbot and lake trout (Melancon *et al.*, 2009). This was despite similar ambient concentrations, suggesting that any potential contamination effects were minor. In the otolith literature, positive relationships between Ba<sub>W</sub>, Ba/Ca<sub>W</sub> and Ba<sub>O</sub> are common and suggest that Ba uptake in marine fish is linearly related to ambient concentrations, with some additional effects of temperature (e.g. Elsdon and Gillanders, 2003b; Miller, 2009). Such experiments have manipulated ambient concentrations to ranges far greater than those exhibited in the current study, essentially mimicking gradients that may be observed during diadromous migrations.

Miller (2009), for example, used Ba/Ca<sub>W</sub> treatments ranging from ~20 to 230  $\mu\text{mol/mol}$ , whilst Ba/Ca<sub>W</sub> in the current study ranged from ~12 to 15  $\mu\text{mol/mol}$ . Importantly, for both Mg and Ba, there were no differences in their concentrations among the sexes or among EC and IS fish.

### 3.4.2 Calcium and strontium

Ca<sub>B</sub> and Sr<sub>B</sub> were clear outliers among the ‘conservative’ elements, as concentrations of these elements in blood were strongly related to blood protein concentrations. D<sub>Ca(B/W)</sub> and D<sub>Sr(B/W)</sub> values indicated enrichment of Ca and Sr in blood in the IS females from October onwards, while GSI began to appreciably increase from November onwards. Ovaries in North Sea plaice begin to develop as early as July, but ovary mass only begins to increase from October onwards (Rijnsdorp, 1989), consistent with the timing of the observed increase in Ca<sup>2+</sup> concentrations in blood. In a study by Dawson and Grimm (1980), the maximum ovary dry weight was attained immediately prior to spawning in February–March, of which 85% was protein. Blood protein concentrations were highly correlated with Ca<sub>B</sub> and Sr<sub>B</sub>, although particularly Ca<sub>B</sub>, for which protein levels alone explained almost 50% of the variation. The relationships between blood hypercalcaemia, hyperproteinemia and reproductive investment in teleost fish are well recognised, with females from oviparous species mobilising large quantities of protein and Ca<sup>2+</sup> for egg yolk production (Urist and Schjeide, 1961). Mechanistically, it is possible that the concentration of blood proteins (especially albumins with relatively high glutamate contents) is increased in order to bind additional Ca. The observed increase in total blood Ca concentrations could be a result of increased recovery of Ca through the gut lining, through increased residence time of protein-bound Ca compared to free Ca (Williams, 1971) or through demineralisation of bones and breakdown of soft tissues during the non-feeding period (Kacem *et al.*, 2000). The associated pre-spawning increase in blood Ca has been observed in a range of marine, euryhaline and freshwater species, including *P. barbatus* (Kalish, 1991), Arctic cod (*Gadus morhua*) (Woodhead, 1968), pinfish (*Lagodon rhomboides* L.), striped mullet (*Mugil cephalus* L.) (Folmar *et al.*, 1992), rainbow trout (*Oncorhynchus mykiss*) (Mugiya, 1966; Shearer, 1984), stone flounder (*Kareius bicoloratus*) (Mugiya, 1966) and perch (*Perca fluviatilis*) (Valtonen and Laitinen, 1988). While hypercalcemia was far greater in the mature females, it was also observed in the immature females and males, an observation shared by other studies (Kalish, 1991; Folmar *et al.*, 1992).

Strontium is thought to be a largely ‘nonessential’ element (Underwood, 1977) and little is known about its function(s) in fish metabolism and reproduction. In the current study, GSI was positively correlated with Sr<sub>B</sub> and the peak in Sr<sub>B</sub> occurred at the height of spawning in mid-February, slightly later than the main peak in

$\text{Ca}_B$ . These patterns were similar to those reported in Kalish (1991) and corroborate positive correlations between ovary Ca and Sr concentrations and GSI in rainbow trout (Shearer, 1984). In the latter study, the author suggests such correlations likely indicate a functional requirement for Sr to transfer somatic Ca to the ovaries. However, it is also likely that the proportional uptake of Sr, Ca and protein in the females (but not the males), might simply be artefact of the similar atomic radius and electronegativity of  $\text{Sr}^{2+}$  and  $\text{Ca}^{2+}$  ions (Chapter 1) and the elevated  $\text{Ca}^{2+}$  and protein requirements during egg production (Urist and Schjeide, 1961). Comparing  $\text{Sr}_B$  and  $\text{Ca}_B$  models, the higher amount of variation attributed to the random effect in the former indicates greater among-fish variation in  $\text{Sr}_B$  values, which would presumably be less likely if  $\text{Sr}_B$  were fulfilling an essential bodily role. The negative relationship between growth rate and  $\text{Sr}_B$  values implies that the positive relationship between  $\text{Sr}_B$  and protein in the females was almost entirely explained by the period of hyperproteinemia around the spawning period.

### 3.4.3 The 'soft' elements

In vertebrates, Zn, Cu and Se are essential micronutrients, Mn is required in respiratory development and bone formation, and Pb is highly toxic (Williams, 1971; Kaim and Schwederski, 1994). As such, concentrations of all five elements are likely to be tightly regulated in the blood. Indeed, all 'soft' elements exhibited enrichment of blood concentrations relative to water concentrations with average  $D_{\text{El(B/W)}}$  varying from 2.8 (Pb) to 3363 (Zn), although given its toxicity to fish (Martinez *et al.*, 2004) the elevated  $\text{Pb}_B$  values likely reflect inability to regulate the ion, rather than active enrichment. Overall, the soft elements exhibited the largest differences between the males, females, IS and EC fish and for all of the elements in this group, a significant positive effect of protein and(or) condition was observed. Based on these correlations and observations in the literature (e.g. Pentreath, 1973; Pentreath, 1976; Fletcher and Fletcher, 1980; Ranaldi and Gagnon, 2008), it is likely that the soft element ions discussed here are almost entirely protein-bound in blood and largely sourced from the diet.

In the experimental plaice,  $\text{Mn}_B$  values were elevated in the females and positively correlated with growth rate and condition, which might explain the increase in the first few months of the experiment and peaks in November when growth rates were highest. There is evidence to suggest that concentrations of Mn in plaice tissue is derived almost entirely from the diet (Pentreath, 1973; 1976), but blood concentrations remained steady and enriched throughout the non-feeding period (~December to March), implying additional waterborne and(or) recycled sources from bone demineralisation and/or tissue breakdown. Apart from the lower concentrations in the initial and terminal blood samples,  $\text{Mn}_B$  concentrations remained relatively

constant throughout the experiment, suggesting strong regulation. This was corroborated by the large decrease in  $D_{Mn(B/W)}$  at the end of the experiment, where blood concentrations fell in spite of rising  $Mn_w$ .

Concentrations of Cu, Zn and Se in blood were broadly similar and largely explained by a positive effect of blood protein levels and ambient concentrations or temperature, and a negative effect of GSI in the females. All three elements exhibited a drop in concentrations during or just before the spawning period and an increase in concentrations towards the end of the experiment. This pattern was clearly exaggerated in the females and likely due to ovary maturation, with reproductive investment in female plaice approximately twice that of males (Bromley, 2000). The removal and utilisation of blood Cu and Zn for egg production is well documented, and appears broadly conserved among the vertebrates (Fletcher *et al.*, 1975; Fletcher and Fletcher, 1980; Versieck and Cornelis, 1989; Tamura *et al.*, 2000; Thompson *et al.*, 2002). Plasma Cu is strongly bound to ceruloplasmin (85-90%) and more loosely bound to albumin (~10%), with very low levels existing in the ultrafiltrable form (Fletcher and Fletcher, 1980; Versieck and Cornelis, 1989). During human pregnancy, Cu is mobilised from the liver and plasma concentrations increase as a function of ceruloplasmin and drop immediately after parturition. Very similar patterns were observed in the current study, however, the increase in  $Cu_B$  up until the spawning season was similar for both IS males and females, implying a common cause, such as feeding and body condition, rather than the oestrogen-mediated effects suggested for  $Cu_B$  increases in pregnant women (e.g. Versieck and Cornelis, 1989). Similar pre-spawning patterns were also observed in  $Se_B$  values and the main divergence between the males and females for both metals was most apparent during the height of the spawning season (January-March). This contrasted with  $Zn_B$ , which was noticeably depleted in the IS females from October onwards, concurrent with the early stages of plaice ovary development. Vitellogenin is a female-specific Zn-binding protein thought to be expressed in all oviparous species during egg production (Fletcher and Fletcher, 1980) and its upregulation during this period to transport Zn to the ovaries is likely to explain the earlier decreases in  $Zn_B$  values in the mature females. These subtle differences in the timing of variations in  $Cu_B$  and  $Zn_B$  values were reflected in their positive and negative correlations with condition, respectively, and emphasise the subtle but important differences among the blood protein, condition and GSI model terms.

The importance of plasma Se in human reproduction is well established (Versieck and Cornelis, 1989; Bedwal and Bahuguna, 1994), but this is the first time seasonal changes in  $Se_B$  concentrations have been described in a fish.  $Se_B$  behaved in a similar way to  $Cu_B$ , and their models contained almost identical terms and exhibited almost identical fits. However,  $Se_B$  was the only model to include a separate 'origin' term, suggesting that the lower blood protein in these fish could not fully explain the depleted Se concentrations in

the EC fish compared to the IS fish. Given that the EC fish were fed a similar diet during the acclimatisation period immediately prior to their introduction to the experiment, the ~100% difference between  $Se_B$  in the IS and EC fish in October and November could not be explained simply by diet. That said, the strong relationship between  $Cu_B$  and  $Se_B$ , blood protein concentrations and condition imply some dietary component in their expression. It is likely that the differences between EC and IS fish were driven primarily by differences in their maturity status, age, and(or) length-at-age, with the EC females generally immature, younger and larger than the IS females. While it cannot be ruled out, intrinsic, population-level differences in elemental processing (Clarke *et al.*, 2011) was unlikely to have caused the differences between EC and IS fish as there is no evidence for genetic differentiation among North Sea and Irish Sea plaice stocks (Hoarau *et al.*, 2004; Watts *et al.*, 2004).

The positive relationships between ambient concentrations (or temperature) and Cu, Zn and Se concentrations in blood were largely driven by the common decrease in blood concentrations during the spawning period. As discussed above, utilisation of these thiophilic elements in ovary development can explain much of this effect in the females, but the decreases also exhibited by the males and immature EC females imply additional factors. Asides from spawning effects and possibly direct effects caused by decreases in temperature and ambient concentrations, the fall in  $Cu_B$ ,  $Zn_B$  and  $Se_B$  also coincided with the period when plaice stop feeding, even in the presence of food (Rijnsdorp, 1990). While volumes of uneaten food were not formally quantified in the current study, they certainly increased during the spawning period, potentially leading to an additional 'dietary effect' during this period. It was assumed that 'dietary effects' in blood element concentrations would primarily be caused by feeding-related changes blood protein levels and condition; both of which were monitored throughout the experiment. However, possible temporal changes in diet composition were not quantified in the current study. Given that marine fish constantly drink seawater to maintain ionic homeostasis, it is assumed that the majority of the hard metal cations are sourced from the surrounding water (Walther and Thorrold, 2006), however, experiments involving labelled isotopes in plaice have suggested that tissue Mn, Cu and Zn concentrations are primarily sourced from the diet (Pentreath, 1973; 1976). Lugworms were sourced from a single, local beach throughout the experiment to attempt to minimise variability in dietary contributions, however, some of the observed variations in blood element concentrations might be explained by seasonal fluctuations in the diet. Lugworm soft element concentrations appear to be predominantly controlled by sediment chemistry (Casado-Martinez *et al.*, 2009) and there is some suggestion of seasonal changes in lugworm Cu composition, however the data are scant (Everaarts, 1986). Even if lugworm element concentrations had been measured, without knowledge of which body parts were digested by the fish, it would be impossible to fully partition dietary vs. waterborne sources.

Finally, while  $Pb_B$  values were more variable, given concentrations close to detection limits, there were clear differences between the males and females.  $Pb_B$  was positively correlated with  $Ca_B$  ( $PCC = 0.46$ ), and exhibited broadly similar patterns over time, with elevated concentrations in the mature IS females during the pre-spawning period (October to December) and a second smaller peak in March. Similar to the significant interaction between protein and sex in the  $Ca_B$  model,  $Pb_B$  was largely explained by an interaction between condition and sex, being positively related to condition in the females but not the males. In the female only model, condition was 'replaced' with a significant positive effect of GSI and in both models, a positive effect of growth rate was also observed. These data imply that upregulation of protein and associated increases in blood Ca concentrations, potentially due to bone demineralisation (Kacem *et al.*, 2000) or increased assimilation through the gut (Williams, 1971), also results in increased uptake of  $Pb_B$ . It is unlikely that the observed patterns indicate an actual function for Pb in reproduction, given its well documented toxicity (e.g. Martinez *et al.*, 2004), but similar to  $Sr^{2+}$ , the observed patterns could result from similar binding chemistries between  $Ca^{2+}$ ,  $Sr^{2+}$  and partially,  $Pb^{2+}$  ions.

In summary, the results of the current study indicate clear seasonal changes in blood elemental concentrations and significant differences among males, females, IS and EC plaice. These differences were largest in the soft acid ions ( $Cu^{2+}$ ,  $Zn^{2+}$ ,  $Se^{2+}$ ,  $Pb^{2+}$ ),  $Ca^{2+}$  and  $Sr^{2+}$ . Almost all of the major patterns in blood elemental concentrations were explained by changes in or different responses to blood protein concentrations. Multicollinearity in the data limited the extent to which terms could be discriminated amongst using mixed effects modelling, however, in most cases, covarying variables were within 'categories' (e.g. temperature and salinity; protein and condition). Thus the relative importance of 'environmental' vs. 'physiological' terms could be assessed with relative confidence. Even without a fully factorial experiment to test which variables were controlling blood elemental concentrations, the results indicate temporal, sex and possibly maturity-related variations in blood elemental processing that have important implications in the field of blood and otolith microchemistry.



# Chapter 4

---

## *Experimental results: Environmental and physiological influences on otolith microchemistry in a marine, adult flatfish*

### 4.1 Introduction

The incorporation of elements into otoliths is potentially controlled by both environmental and physiological factors, yet there are many examples where otolith microchemistry has been successively applied to separation of wild fish stocks (reviewed in Chapter 1). The cause of such differences among groups of fish is generally attributed to different environmental conditions, however, based on the literature and results in Chapter 4, it would appear that physiological conditions play a major role in element uptake and uptake within the fish. This could confound interpretations of otolith microchemistry, particularly for studies attempting to use the elemental fingerprint to retrospectively position fish in time and space. For this, it is necessary to appreciate the spatial and temporal characteristics of the relevant environment(s) and to understand how environmental conditions manifest within the otolith. A key first step is the uptake of elements from the environment, which could be water, diet and (or) sediments. Marine fish need to

constantly hypo-osmoregulate to avoid water loss by osmosis and passive gain of major ions. To do this, they continually drink seawater and absorb most of the fluid in the intestine, excreting the remainder as 'rectal fluid' (Smith, 1930). This behaviour means the hard metal cations such  $\text{Sr}^{2+}$  and  $\text{Ba}^{2+}$  are thought to be mainly sourced from the surrounding seawater (Walther and Thorrold, 2006). The main sources of other elements are largely unknown; studies often point towards diet being the primary source of softer metal cations such as  $\text{Zn}^{2+}$  and  $\text{Mn}^{2+}$  (Pentreath, 1973; Ranaldi and Gagnon, 2008), although one experiment indicated a significant positive effect of water Cu levels on otolith concentrations (Milton and Chenery, 2001b).

In the previous chapter, very few of the studied elements exhibited strong, if any, correlations between water and blood, however it is important to note that these represented total concentrations and included free, complexed and protein bound fractions. They might, therefore not reflect concentrations available for uptake into the blood or otolith. Any such effect is likely to be less in the water than in the blood because blood contains proportionally more available ligands, especially complex organic ligands, than seawater. Indeed, Mugiya (1966) observed greater enrichment of total serum Ca than diffusible serum Ca around the spawning season, but very little divergence of diffusive Ca concentrations in the plasma vs. endolymph. If total blood concentrations are a poor proxy for 'available' concentrations, then otolith composition may still record ambient concentrations when blood concentrations did not. Similarly, in the previous chapter, fractionation of elements between water and blood were discussed in terms of absolute concentrations, but it is likely that element/Ca ratios have greater control over otolith concentrations, and possibly even blood concentrations. This possibility will be explored further below.

In the current chapter, patterns in otolith growth and elemental concentrations are explored in context with the physiological and environmental data presented in the previous chapter. The fractionation of elements from water to otolith and blood to otolith are discussed. Similar to the previous chapter, linear mixed effects models are used to explore patterns amongst variables, here, reporting on the variables that best explained variations in otolith elemental concentrations as well as otolith:blood distribution coefficients. The ultimate aim of the current chapter was to identify the major controls on otolith element incorporation, focusing on eight of the twelve elements presented in previous chapters (Li, K, Mg, Sr, Ba, Mn, Cu and Zn).

## 4.2 Methods

The sampling and analysis methods used to collect blood, 'environmental' and 'physiological' data were described in full in Chapters 2 and 3, but in brief, plaice were maintained under natural, but monitored, conditions for 7-12 months and their blood elemental chemistry analysed each month. The main group of plaice were sourced from the Irish Sea (IS) in February 2009 and sampled from 02/06/09 to 28/05/10, while a second group of plaice (7 females) were sourced from the English Channel (EC) in August 2009 and introduced to the same tank and sampling regime on 27/10/09. All fish were injected with oxytetracycline (OTC) on their introduction to the experiment to leave a visible 'start check' on the otolith to guide analyses. On 18/01/10, approximately half of the fish were treated with gonadotropin-releasing hormone (GnRH) to encourage spawning and an additional sampling date added at the start of February. Otherwise, blood sampling was carried out once per month.

Individuals were selected based on their otolith growth rate and clarity of the OTC mark. Any that had died prior to the end of the experiment were excluded. A total of 19 fish were selected (7 IS females, 6 English Channel (EC) females and 6 males) and the data presented from here on in refers only to this subset of fish.

### 4.2.1 Otolith analyses

#### 4.2.1.1 Cleaning and mounting procedures

On termination of the experiment, study animals were humanely euthanased using 'Schedule 1' procedures and the sagittal otoliths were removed using Teflon-coated or plastic forceps. Immediately following their removal, otoliths were placed in acid washed, racked pipette tips and rinsed in Milli-Q water (MQ), then dried for at least 24 hours in a laminar flow cabinet and stored in acid cleaned Eppendorf tubes. The official 'cleaning protocol' used methods adapted from A. Darnaude (pers. comm. 2009) and all steps (apart from no. 7) were carried out in a dedicated Class 100 clean laboratory:

1. Sonicate otolith (5 mins) in an ultrasonic bath filled with MQ.
2. Pour into an acid-washed petri dish, pipette off water and replace with new MQ.
3. Scrub (1 min) with an acid-washed toothbrush.
4. Triple-rinse with MQ.
5. Sonicate for 3 mins in MQ.
6. Pour into acid cleaned tissue culture trays and replace MQ.
7. Photograph under reflected and transmitted light.
8. Rinse 3 more times with MQ in clean lab.
9. Air-dry (at least 24 hours) in trays inside a clean cell
10. Store in same trays, taped shut and in new plastic bags.

The left otolith from each pair was embedded in a small 'tear drop' of Buehler EpoThin™ epoxy resin on parafilm inside a laminar flow cabinet to try to reduce contamination of the otolith edge. The resin was put under vacuum to force bubbles out, then cured at 36°C. 'Tear-dropped' otoliths were embedded in the CEFAS otolith laboratory using moulds and a stereomicroscope specifically designed to help locate and line up otolith cores. Transverse thin sections (c. 500µm thick) were cut using a Buehler Isomet Low Speed Saw with a diamond wafering blade and used to age the fish. The remaining half was cut and/or ground down using 600 grit silicon carbide paper and MQ to expose the frontal plane (longest point from core to rostrum). Due to the faster growth rates at the rostrum, the frontal plane provides maximum spatial and temporal resolution across the otolith, particularly in the left, more asymmetrical, otolith (Figure 4.1). Otolith sections (frontal 'blocks' unless unavailable or poor quality, in which case transverse sections were used) were set in round 24.5mm epoxy resin mounts with University of Wisconsin Calcite (UWC) standard at the centre. The mounts were cured under pressure (2.5 bar, N<sub>2</sub>) to remove bubbles while avoiding amine blush, then polished with 0.3 µm aluminium oxide paste, rinsed in MQ, dried then gold coated. Careful sample preparation is extremely important to maximise quality and resolution of SIMS analyses. Surfaces must be flat with no imperfections (e.g. bubbles, scratches) and samples need to be within 0.5cm of the centre of the mount, however, due to the lengthy vacuum pump-down time, it was also important to maximise the number of samples within each mount (further details available here:

[www.geos.ed.ac.uk/facilities/ionprobe/](http://www.geos.ed.ac.uk/facilities/ionprobe/)). Mounts were imaged under reflected light and using a 450nm filter with Hg-vapour lamp to record the position of growth bands and OTC marks. As OTC degrades in light, efforts were made to ensure samples were exposed to as little light as possible throughout the process.

Because of the sensitivity of SIMS to sample surface imperfections, SIMS analyses were carried out first, resulting in the need for gold-coat removal prior to any laser ablation-ICPMS (LA-ICPMS) analyses. On completion of SIMS analyses, mounts were re-imaged and the gold coat removed using a brief (<10 s) wipe with propanol-soaked KimWipes™ then rinsed with MQ. The mounts were then polished briefly (c.20s) on a polishing wheel loaded with 1 µm diamond paste then rinsed with MQ. The SIMS ablation pits (typically 2-5µm depth (Fairchild *et al.*, 2001)) were still clearly visible after this process, providing some confidence that the same otolith plane was sampled by both techniques. Prior to LA-ICPMS analysis, mounts were cleaned in a dedicated Class 100 clean room using MQ water only: (1) rinsed thoroughly then placed in acid washed polypropylene containers, (2) sonicated for 15 minutes, (3) rinsed 3 times, (4) air dried for 24 hours inside a clean cell, (5) stored dry in clean containers inside Ziplock© bags.

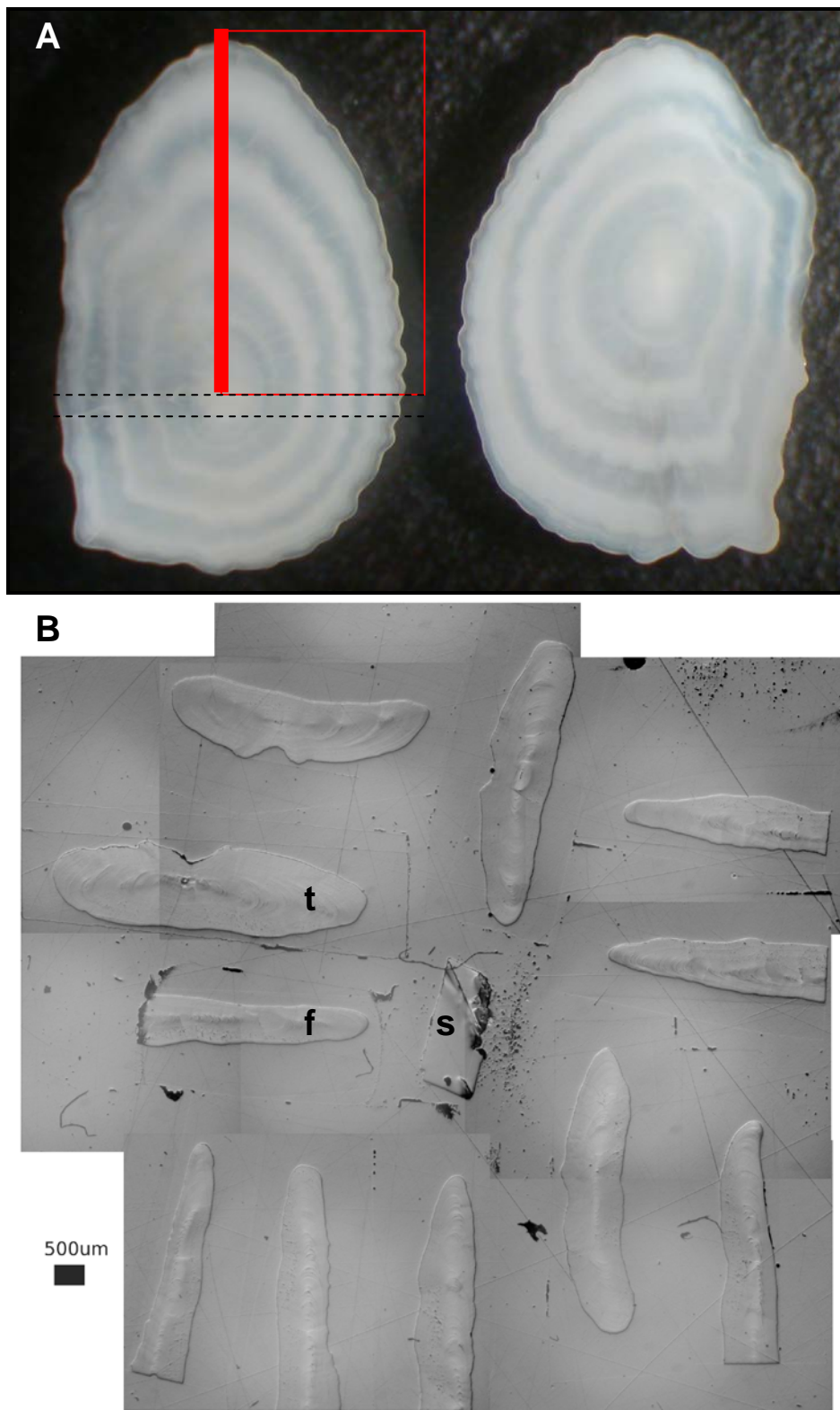


Figure 4.1 A - Plaice sagittae, with the left otolith showing the cutting lines used to produce transverse (dotted lines) and frontal sections (red box, the thick line representing the plane used for analyses) B - Frontal (f) and transverse (t) sections, and UWC standard (s) mounted for SIMS and ICPMS analysis. Note that the 500 $\mu$ m scale bar is scaled to Figure 4.1B only.

#### 4.2.1.2 $\delta^{18}\text{O}$ analysis by SIMS (Cameca 1270)

As the seasonality of opaque-translucent banding is known to vary for this species (Van Neer *et al.*, 2004) and environmental and physiological measurements were recorded on a monthly basis, an intra-annual timeline was added to each section using oxygen isotopic ratios ( $\delta^{18}\text{O}$ ). Analyses were carried out on a CAMECA-IMS-1270 ion microprobe (Cameca, Gennevilliers, France) at the Edinburgh Ion Microprobe Facility (EIMF), using a  $\sim 5$  nA primary  $^{133}\text{Cs}^+$  beam. Secondary ions were extracted at 10 kV, and  $^{16}\text{O}$  (approx.  $3 \times 10^9$  cps) and  $^{18}\text{O}$  (approx.  $6 \times 10^6$  cps) were monitored simultaneously on dual Faraday cups (L'2 and H'2). Spot analyses comprised a pre-sputtering time of 50 s, then automatic centring of the secondary beam and entrance slit. Data collection occurred in two blocks of five cycles, resulting in a total count time of 40 s. A beam size of  $20\mu\text{m}$  diameter was used and analyses were carried out at  $30\text{--}40\mu\text{m}$  intervals along transects, perpendicular to growth bands from the otolith edge to a point past the OTC mark. Unless the otolith had grown uncharacteristically fast during the experimental period, two parallel, offset transects were analysed so that measurements were obtained at  $\sim 20\mu\text{m}$  resolution across the period of interest. Ablation depth was between  $0.78$  and  $2.7\mu\text{m}$  (J. Craven, pers. comm.). A reference material (University of Wisconsin calcite, UWC-1) was analysed every c.10 otolith analyses to calibrate raw counts (bulk data from J. Valley pers. comm.) correct for instrument drift and to assess precision. Internal precision was on average, 0.014%, but there was a shift between sampling periods, with values generally  $< 0.01\%$  for the first set of analyses and about 0.02% for the second batch of analyses (Figure 4.2). External precision (s.d. of repeated UWC-1 measurements) was  $0.24\text{\textperthousand}$  ( $n = 453$ ). Within-day external precision was, on average,  $0.20\text{\textperthousand}$ .  $\delta^{18}\text{O}_{\text{otolith}}$  is reported relative to Vienna PeeDee Belemnite (VPDB) after Coplen (1996).

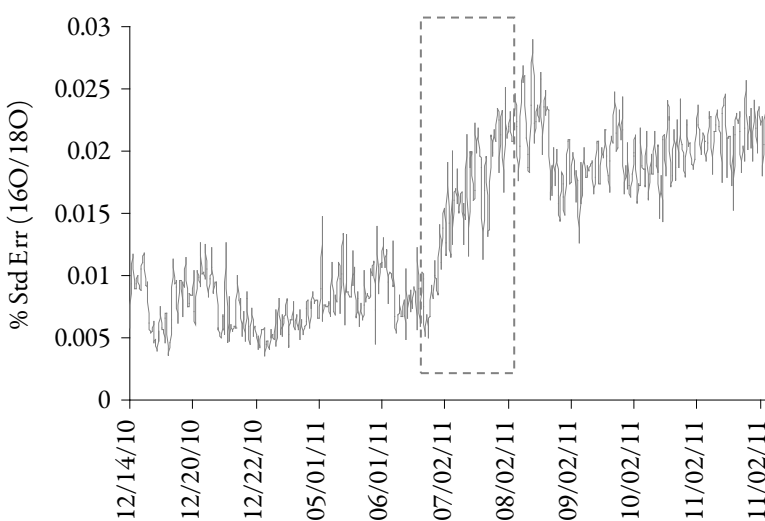


Figure 4.2 Internal precision of SIMS  $\delta^{18}\text{O}$  analyses over time. Data collected on 07/02/11 (dotted box) were discarded due to variability in the UWC-1 measurements and a clear shift in instrument performance

#### 4.2.1.3 Elemental analysis by SIMS (Cameca 4f)

Otolith trace metal SIMS analyses were carried out on a CAMECA-IMS-4f ion microprobe (Cameca, Gennevilliers, France) at EIMF. A primary negative ion ( $O^-$ ) beam from a duoplasmatron source bombarded the sample surface, sputtering positively charged secondary ions which were detected by an electron multiplier. Analyses were carried out in step scan mode, analysing the sample at  $\sim 10 \mu\text{m}$  intervals along a transect parallel to the 1270 marks. A c. $20 \mu\text{m}$  beam size was used with a c. $8 \mu\text{m}$  analysis window to provide greater surface cleaning efficiency whilst maintaining finescale ( $< 10 \mu\text{m}$ ) resolution across the period of interest (R. Hinton, pers. comm.). Each spot analysis included a pre-sputtering time equivalent to 37 s, then data collection over three cycles and a total count time of 78 s. The count time was divided amongst six elements, with a longer count time attributed to lower level elements:  $^7\text{Li}$  (15 s),  $^{26}\text{Mg}$  (15 s),  $^{41}\text{K}$  (6 s),  $^{48}\text{Ca}$  (6 s),  $^{88}\text{Sr}$  (6 s) and  $^{138}\text{Ba}$  (30 s). Ablation depth was not formally measured, but is typically 2-5  $\mu\text{m}$  for such analyses (Fairchild *et al.*, 2001).

Raw counts were averaged across the three cycles then normalised to Ca. Concentrations were calibrated against a 2-3 point calibration curve using 3 calcite standards: M93, Haxby and Oka (Treiman and Essene, 1985). Standards were analysed in the morning of 6 consecutive days in March 2011 and used to estimate external precision (Table 4.1). Concentrations were then converted into element/Ca molar ratios. The calibration curve was not as well defined for Ba, and heavily influenced by the high concentrations in Oka (Figure 4.3). Also, external precision for Ba was relatively poor for Oka (14.7%) and M93 (19.9%).

Table 4.1 Standard bulk concentrations for three calcite reference materials, Oka, Haxby and M93 in  $\mu\text{g g}^{-1}$ . External inter-day precision are provided in parentheses (%RSD)

Element	M93	Haxby	Oka
	Coral (n = 45)	Coral (n = 55)	Carbonatite (n = 51)
Li	0.36 (16.2)	2.52 (11.1)	-
Mg	1246 (17.1)	17869 (7.0)	688 (10.4)
K	152* (34.8)	127* (6.8)	-
Sr	7189 (7.0)	2276 (4.6)	11967 (6.5)
Ba	3.52 (19.9)	16.74 (6.9)	1296 (14.7)

\* Because of greater uncertainty in the K bulk measurements the mean of these two values ( $139.5 \mu\text{g g}^{-1}$ ) was used for both standards

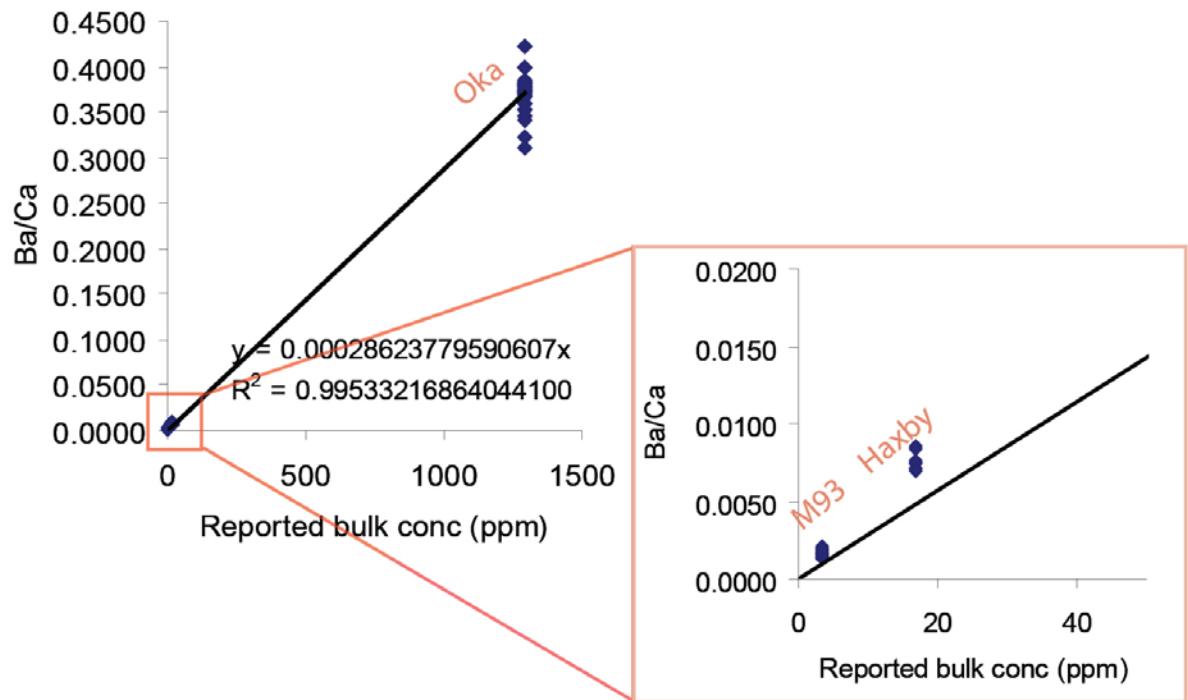


Figure 4.3 Graph showing the calibration curve for Ba/Ca concentrations vs. Ba/Ca counts per second (cps) based on three standards (M93, Haxby and Oka). As indicated by the close up inset image, the calibration was heavily influenced by the much higher Ba concentrations in Oka. Note that otolith Ba concentrations measured in the current study were usually around 5 ppm

#### 4.2.1.4 Elemental analysis by HR-ICPMS

Analyses were carried out on an Element 2 HR-ICPMS (Thermo). Initial method development indicated minor but heterogeneous Zn contamination on the section surface, so samples were pre-ablated prior to analysis (details provided in Table 4.2). The dwell time was kept relatively short for each spot analysis (16s) to avoid deep ablations that averaged over extended time periods. Given that many of the elements of interest (namely Mn, Cu, Zn and Se) are subject to spectral interferences, they were analysed in MRM or HRM for Se. Smaller spot sizes and higher resolution modes are unfortunately paired with lower sensitivity, and early on it was clear that Pb and Se concentrations were almost always <LOD, and Zn and Cu close to detection limits. As such, the element list was reduced, excluding most of the elements already analysed by SIMS (Li, Mg, K), Rb as it was deemed likely to covary with K, and the elements likely to be consistently <LOD (Pb and Se). Also, to avoid wasting time shifting between resolutions, all analyses were carried out in MRM.

Otolith sections were analysed in a random order using a 35  $\mu\text{m}$  spot size, moved in 40  $\mu\text{m}$  steps along transects parallel to SIMS analyses. Isotopes, operating conditions and analytical details are provided in Table 4.2. Background counts were collected for 40-50 seconds prior to every ablation of which the first  $\sim$ 20 seconds of data was excluded to allow full ‘wash out’ from the previous ablation. Each ‘sample’ analysis (otoliths and standards) corresponded to a ‘data block’ comprising 4 rows (time slices) by 16 columns (masses) per element. Rows corresponding to the very start and end of ablations, indicated by increasing or decreasing Ca and Sr counts, were excluded. Reference standard NIST612 (National Institute of Standards and Technology) was analysed every  $\sim$ 30 otolith ablations and NIST614 every  $\sim$ 60 otolith ablations.

Concentrations were determined offline using R and Excel. First, raw counts were filtered to remove transient spikes. Each sample and background ‘data block’ was treated individually and values greater than the ‘median + 3sd + 200’ were excluded. The process was done iteratively to allow removal of multiple large spikes within single data blocks. The value of 200 was added to avoid filtering out high variation at low background count rates (Ba and Zn in particular), similar to the methods used by Beer *et al.* (2011). This process removed 2.12% (Ca), 0.21% (Mn), 0.15% (Cu), 0.10% (Zn), 0.33% (Sr) and 0.07% (Ba) of the data. Second, drift correction was applied to all data using time-resolved linear interpolation between NIST612 analyses. Third, counts within each ‘data block’ were averaged and samples blank subtracted using the average preceding background count.

Otolith concentrations were calibrated using the standard closest to the sample concentration and the most recent determined values for NIST (Jochum *et al.*, 2011). Concentrations were normalised to Ca to correct

for ablation yield and matrix effects, assuming a concentration of 388 000  $\mu\text{g g}^{-1}$  (Yoshinaga *et al.*, 2000).

Average LOD (3 s.d. of the blanks) and external precision, based on repeat analyses of NIST glass, are presented in Table 4.3. Relatively few measurements were below LOD (8.5% and 0.1% of Zn and Cu, respectively) so all data was retained, similar to the seawater concentrations (Chapter 3) and the methods used in other otolith microchemistry studies (e.g. Ben-Tzvi *et al.*, 2007; Beer *et al.*, 2011). Concentrations were converted into molar ratios relative to Ca when comparing with seawater and blood El/Ca ratios.

Table 4.2 Analysis and operating details used for LA-HR-ICPMS analyses of frontal otolith sections

	Preablation	Spot analyses
Spot size ( $\mu\text{m}$ )	100	35
Spacing ( $\mu\text{m}$ )	N/A (continuous)	40
Moving speed ( $\mu\text{m s}^{-1}$ )	20	N/A
Power (%)	55	95
Frequency (Hz)	10	7
Dwell time per ablation (s)	N/A	16
Isotopes (resolution)	N/A	$^{44}\text{Ca}$ , $^{55}\text{Mn}$ , $^{63}\text{Cu}$ , $^{66}\text{Zn}$ , $^{186}\text{Sr}$ , $^{137}\text{Ba}$ (all MRM)
Mass window (%) <sup>b</sup>	N/A	40
Search window (%) <sup>b</sup>	N/A	40
Integration window (%) <sup>b</sup>	N/A	40
No. of samples per peak	N/A	40
Dwell time per sample (ms)	N/A	20

Table 4.3 Detection limits (LOD, 3sd of gas blanks) and external precision for LA-HR-ICPMS analyses

	<i>n</i>	Mn	Cu	Zn	Sr	Ba
LOD ( $\mu\text{g g}^{-1}$ )	837	0.019	0.019	0.093	0.679	0.024
Precision	NIST612	134	1.744	2.235	3.531	3.149
(%RSD)	NIST614	54	3.841	6.796	10.649	7.213

## 4.2.2 Otolith timelines, growth rates and opacity

The  $\delta^{18}\text{O}$  measurements produced by the SIMS analyses were compared with the  $\delta^{18}\text{O}$  values predicted by water temperature and salinity, using a temperature-dependent fractionation equation developed for juvenile Atlantic cod (Hoie *et al.*, 2004). Profile shape and inflection points were ‘wiggle matched’ using Analyseries 2.0 (Paillard *et al.*, 1996) to produce a calendar date estimation for each  $\delta^{18}\text{O}$  spot analysis. While the method is somewhat subjective, correlation coefficients for predicted vs. measured  $\delta^{18}\text{O}$  values following ‘temporal corrections’ were generally  $>0.8$ . An example is shown in Figure 4.4 and all plots provided in Appendix 1.1. Temporal alignment of the Cameca-4f and Element 2 ablations was carried out visually by overlaying images and referencing pit positions to the OTC mark and the centre of the Cameca-1270 pit marks, following the axis of growth marks. An example (using the fish featured in Figure 4.4) is provided in Figure 4.5. This multi-stage process provided a start date and a number of intra-annual “anchor points” within each otolith. Dates were assigned to trace elemental analyses between anchor points using linear interpolation. Following assignment of a date to each analysis, LOESS smoothers were used to fit a curve through the data points and predict a value for each individual sampling day. Smoothed elemental data are provided in Appendix 1.2.

Otolith overall growth rate was calculated as the maximum distance from the OTC mark to the otolith edge, perpendicular to growth bands, divided by the number of experimental days (361 for IS fish, 213 for EC fish). Otolith growth rates at each 4f spot were calculated as the distance from the previous spot divided by the difference in ‘ $\delta^{18}\text{O}$  assigned days’. Individual blood sampling days were assigned the growth rate associated with the closest previous 4f spot.

An opacity score was assigned to each 4f spot, as these were the most high frequency measurements carried out. Opacity was scored using a coarse measure of 1 (opaque) or 0 (translucent), estimated visually under reflected light. While opaque and translucent zones were treated as separate entities, there were gradations in opacity that will not be accounted for in the scoring system used. Given the potential subjectivity, only pure white, reflective bands were assigned a ‘1’ (e.g. Figure 4.5) and any areas exhibiting intermediary opacity were assigned a ‘0’. The opacity scores were then allocated to sampling days; where sampling days fell during a transitional period between opaque and translucent zones, they were assigned a score of 0.5.

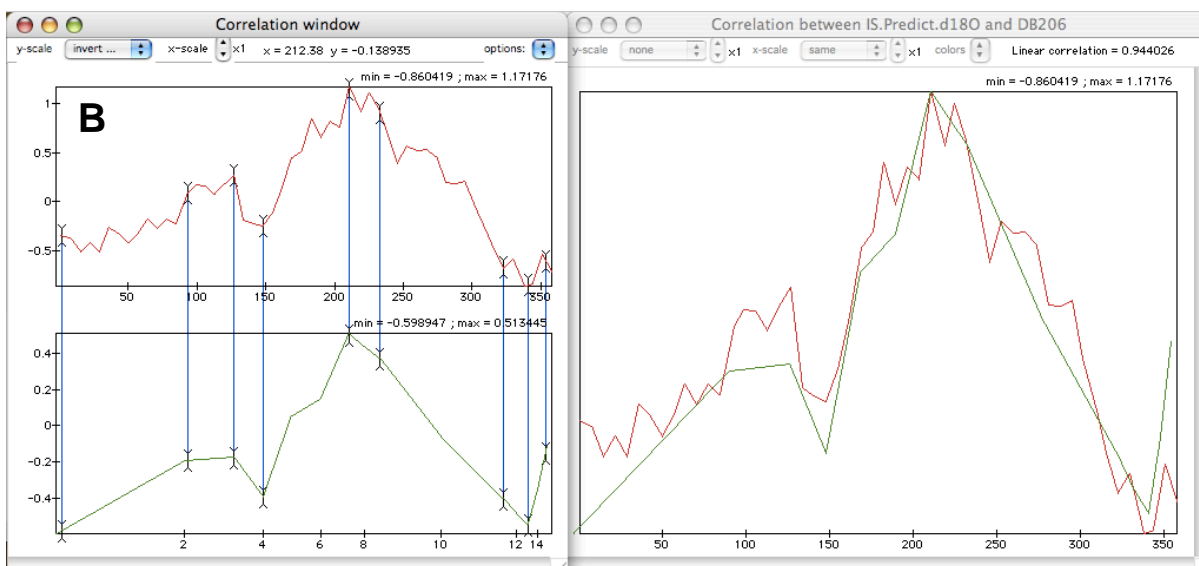
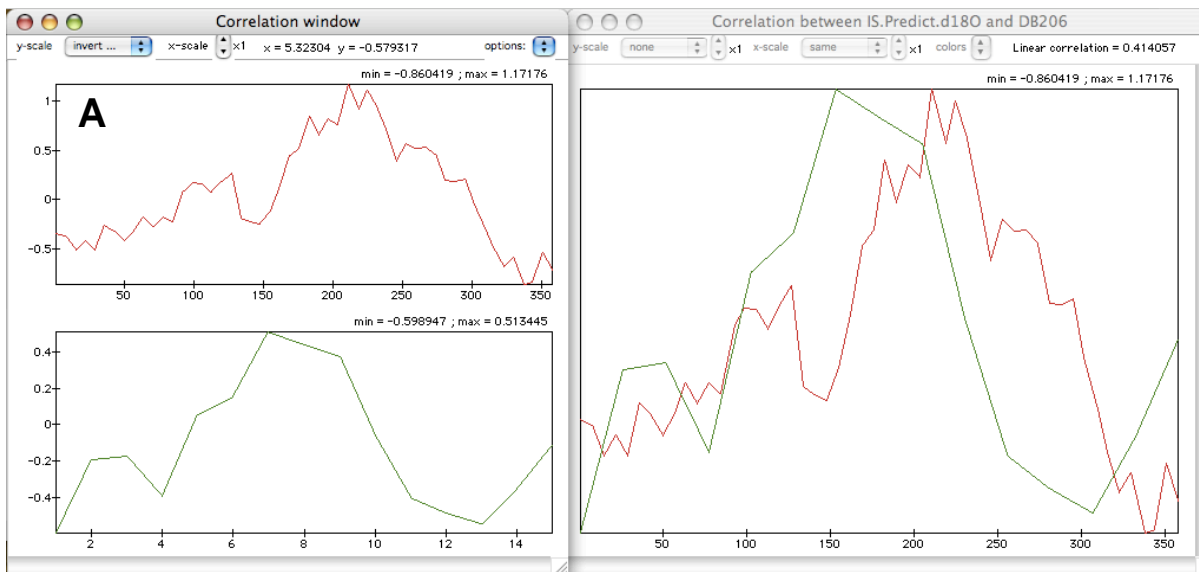


Figure 4.4 An example of the "wiggle matching" carried out in AnalySeries 2.0. Predicted (red) and measured (green)  $\delta^{18}\text{O}$  profiles are displayed, with panel 'A' showing the raw data and panel 'B' showing the wiggle matched profiles, with the blue vertical lines showing anchor points and the plot on the right showing the correlation between the two profiles. In this particular case the absolute values were lower in the measured profile compared with the predicted profile, but the correlation coefficient was 0.94.

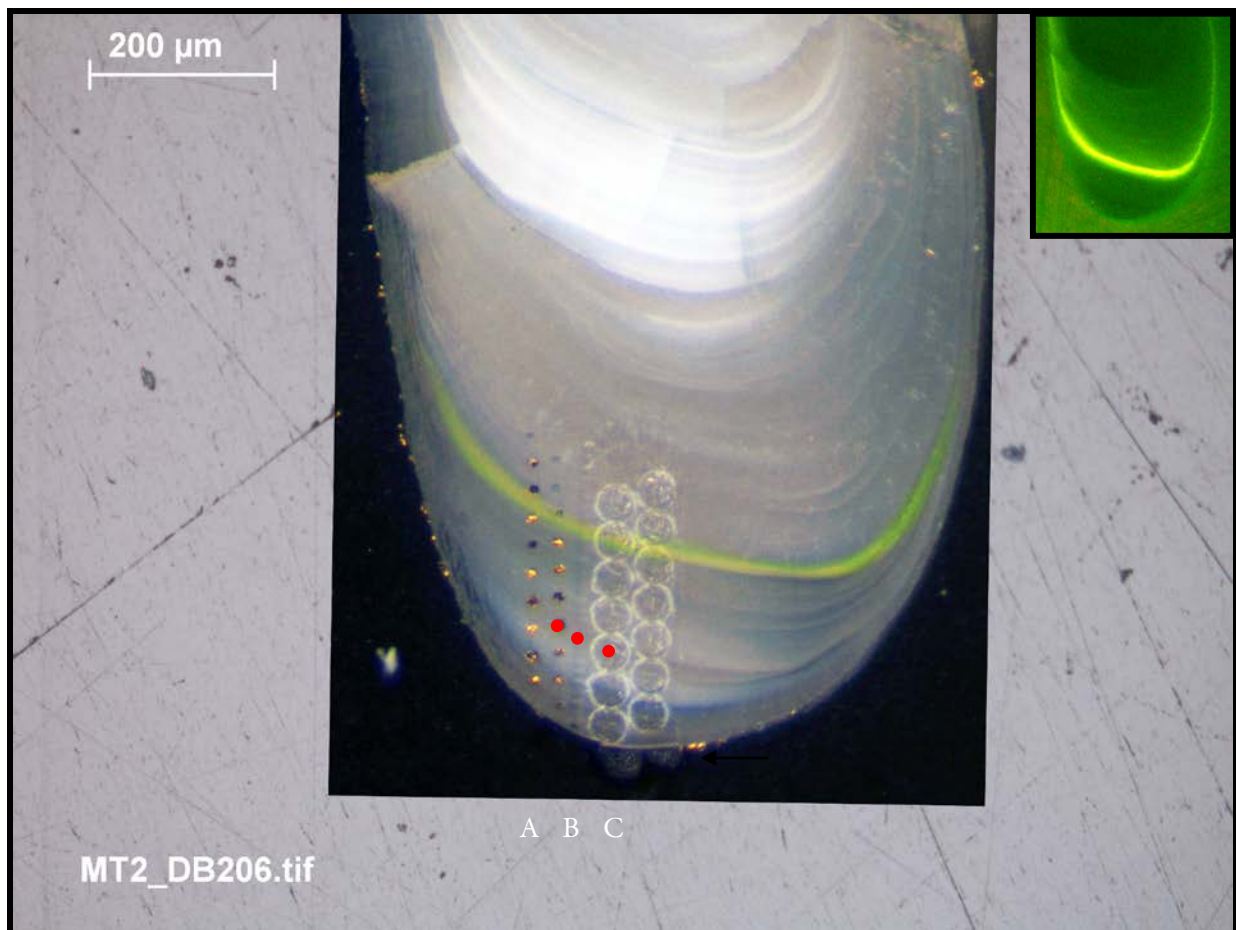


Figure 4.5 Photograph of a frontal otolith section under reflected light showing pits left from the three types of analyses used in the current study, labelled (A) two offset lines of SIMS  $\delta^{18}\text{O}$  spots (Cameca 1270,  $\sim 20\mu\text{m}$  beam diameter), (B) single line of SIMS elemental analyses (Cameca 4f,  $\sim 8\mu\text{m}$  beam, Li, Mg, K, Ca, Sr, Ba) and (C) two offset lines of HR-LA-ICPMS trace elemental analyses (Element 2,  $35\mu\text{m}$  beam, Mn, Cu, Zn, Sr, Ba). The red spot indicates an example of where a spot from each analysis type has been visually matched by following growth band axes. The opaque band (defined '1') is indicated by an arrow. Inset image shows the same otolith under blue light (450nm filter) to visualise the OTC mark (which has then been overlaid onto the main image)

## 4.2.3 Data analysis

### 4.2.3.1 Distribution coefficients (D)

Distribution coefficients (D) from blood to otolith and seawater to otolith were calculated using equations 1-4 below.

$$D_{El(O/B)} = [Element]_{(otolith)} / [Element]_{(blood)} \quad (1)$$

$$D_{El(O/W)} = [Element]_{(otolith)} / [Element]_{(water)} \quad (2)$$

$$D_{El/Ca(O/B)} = [Element/Ca]_{(otolith)} / [Element/Ca]_{(blood)} \quad (3)$$

$$D_{El/Ca(O/W)} = [Element/Ca]_{(otolith)} / [Element/Ca]_{(water)} \quad (4)$$

The final list of variables examined in the current chapter is displayed in Table 3.5. Note that TW was excluded from the model selection criteria as it was highly correlated with TL, and TL and condition factor were considered more appropriate measures of fish size and relative 'fatness', respectively.

Throughout the text, concentrations will be denoted as  $El_X$  for concentrations of element 'El' in medium 'X', where 'X' is defined as water (W), blood (B) or otolith (O). Similarly, distribution coefficients are denoted as  $D_{El(X1/X2)}$  and  $D_{El/Ca(X1/X2)}$ .

Table 4.4 Elemental, physiological and environmental variables examined in the current study. The elements are divided among broad chemical groups and the method used to determine their concentrations in the otoliths indicated by 'S' (SIMS) or 'L' (LA-ICPMS). Note that these elements formed the response variables in the models both as absolute otolith concentrations and otolith:blood distribution coefficients ( $D_{El/Ca(O/B)}$ )

Elements measured in water, blood plasma and otoliths of plaice		Predictor variables	
Group I & II	'Soft' elements	'Physiological'	'Environmental'
Li (S)	Mn (L)	Sex	Time (Day number)
K (S)	Cu (L)	GnRH treatment (Y/N)	Water temperature
Mg (S)	Zn (L)	Origin (IS/ EC)	Salinity
Ca (S & L)		Plasma protein concentration	$El_w$
Sr (S & L)		Fulton's condition factor	$El/Ca_w$
Ba (S & L)		Growth rate by sampling day	
		Growth rate over the whole experiment	
		TL	
		Age	
		$El_B$	
		$El/Ca_B$	
		Otolith growth rate by sampling day	
		Otolith growth rate over the whole experiment	
		Otolith opacity (0 / 0.5 / 1)	
		GSI (females only)	

#### 4.2.3.2 Linear mixed effects modelling

Initially, for each otolith element ( $El_O$ ) and otolith:blood distribution coefficient ( $D_{El(O/B)}$ ), a ‘global model’ was built (equations 5 and 6), including all single effects and their first order interactions (indicated by the “ $^2$ ” command in R). Variables classified as ‘factors’ (i.e. categorical) are underlined. Modelling the distribution coefficient provided a means to examine the factors governing element fractionation specifically from blood to otolith, and allowed removal of seawater and blood concentration terms, thus reducing some of the model complexity.

$$El_O = (\underline{\text{sex}} + GSI^{\dagger} + \underline{\text{treatment}} + \underline{\text{origin}} + \underline{\text{spawner}} + \underline{\text{opacity}} + \text{temperature} * \text{salinity} + El_w + El/Ca_w + El_b + El/Ca_b + \text{day} + [\text{protein}] + \text{condition} + \text{growth rate} + \text{overall growth rate} + TL + \text{age} + \text{otolith growth rate} + \text{overall otolith growth rate})^2 + (1|\text{fish}) \quad (5)$$

$$D_{El(O/B)} = (\underline{\text{sex}} + GSI^{\dagger} + \underline{\text{treatment}} + \underline{\text{origin}} + \underline{\text{spawner}} + \underline{\text{opacity}} + \text{temperature} + \text{day} + [\text{protein}] + \text{condition} + \text{growth rate} + \text{overall growth rate} + TL + \text{age} + \text{otolith growth rate} + \text{overall otolith growth rate})^2 + (1|\text{fish}) \quad (6)$$

<sup>†</sup> GSI was only included in the female only model, when ‘sex’ was also removed

Given the large number of variables, it was computationally impossible to use exactly the same model selection methods as the previous chapter. Thus, while global models were still ran through Anova to identify any highly significant interactions, only a selection of these were included in the ‘reduced model’, based on the validity of their effects (visualised using ‘conditioning plots’ or ‘coplots’ in R) and whether they were deemed biologically sensible. The “temperature\*salinity” interaction was included in all reduced models and where there were highly collinear terms, such as ‘growth rate’ and ‘overall growth rate’, the term most correlated with the response variable was included only. Following this initial model simplification process, model selection followed the same procedures described in Chapter 3.

## 4.3 Results

### 4.3.1 Physiological conditions

Average values for the main physiological parameters for the fish presented in the current chapter are provided in Table 4.5.

Table 4.5 Average ( $\pm$ SD) total length (TL), total weight (TW), somatic and otolith growth rate, Fulton's condition factor, gonadosomatic index (GSI) and age of subject animals presented in the current chapter at the end of the experiment (28/05/10)

Origin	Sex	n	TL (cm)	TW (g)	Overall growth rate (mm day <sup>-1</sup> )	Overall otolith growth rate ( $\mu$ m day <sup>-1</sup> )	Condition	GSI (%)	Age (years)
IS	M	6	26.68 (1.98)	206.17 (45.3)	0.099 (0.034)	0.797 (0.389)	1.069 (0.047)	n/a	4.33 (1.03)
IS	F	7	30.83 (2.17)	296.71 (72.5)	0.072 (0.052)	0.672 (0.521)	0.994 (0.044)	2.99 (2.21)	4.86 (0.69)
EC	F	6	33.55 (1.91)	377.83 (102.0)	0.061 (0.065)	0.943 (0.384)	0.982 (0.136)	2.87 (4.44)	3.50 (0.84)

### 4.3.2 Otolith growth rates and opacity

Overall otolith and somatic growth rates were positively correlated ( $r^2 = 0.39, n = 19$ ), but growth rates for each blood sampling day exhibited much lower correlations, particularly in the males (Table 4.6). Average otolith growth rates peaked in June, October/November and May, with the lowest growth rates exhibited by the IS females, particularly during the spawning season (Figure 4.7). The EC females exhibited highest otolith growth rates at the start and end of the experiment. In the males, the proportion of opaque to translucent otolith 'inferred edges' (based on  $\delta^{18}\text{O}$  timelines) increased from June to December then decreased rapidly. Opacity remained generally low in the IS females and almost non-existent in January and February. Otolith inferred edge opacity increased in the EC females from their introduction in October until January, then remained higher than the IS fish before decreasing from March onwards. On completion of the experiment all females exhibited translucent material at their (true) otolith margins.

Table 4.6 Correlation coefficients for pairwise comparisons of somatic and otolith daily growth rates for all experimental plaice, males, females, Irish Sea (IS) females and English Channel (EC) females averaged over the entire experiment per fish (total difference in TL or distance from OTC mark to otolith edge divided by no. of days,  $n = 19$ ) and for individual sampling days ( $n = 212$ )

	All	M	F	F (IS)	F (EC)
Overall growth rates	0.63	0.57	0.68	0.72	0.86
Growth rate at each sampling day	0.16	-0.06	0.26	0.31	0.25

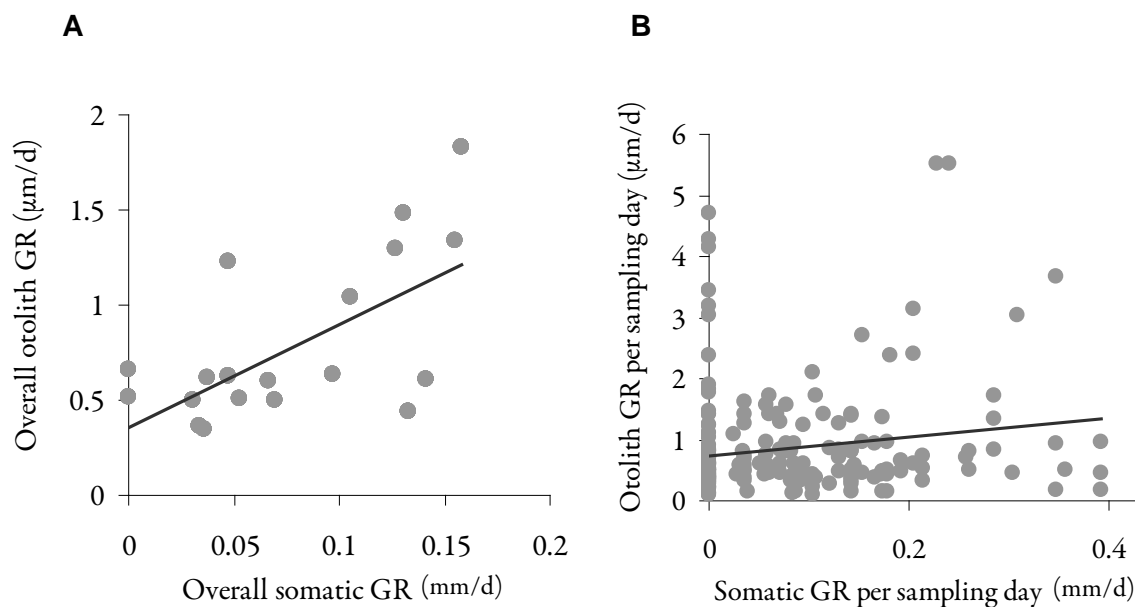


Figure 4.6 Somatic vs. otolith daily growth rates (GR) for (A) experimental plaice over the entire experiment ( $n = 19$ ), or (B) fitted to each sampling day ( $n = 212$ ). Overall GR was calculated as the total difference in TL over the experimental period or distance from OTC mark to otolith edge divided by the total no. of days ( $r^2 = 0.39, n = 19$ ). Somatic GR per sampling day was calculated as the difference in TL between sampling days divided by the no. of days, while otolith GR per sampling day was based on the GR for the nearest previous 4f spot (which had, in turn, been calculated by the distance from the previous spot divided by the difference in ' $\delta^{18}\text{O}$  assigned days')

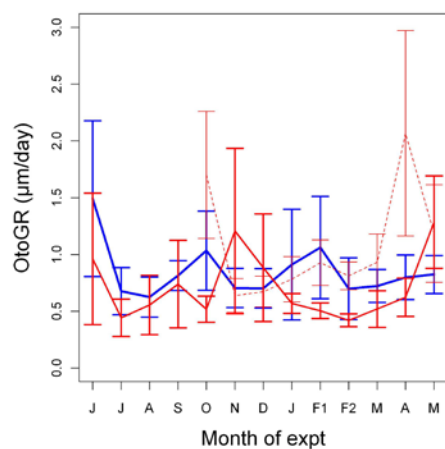
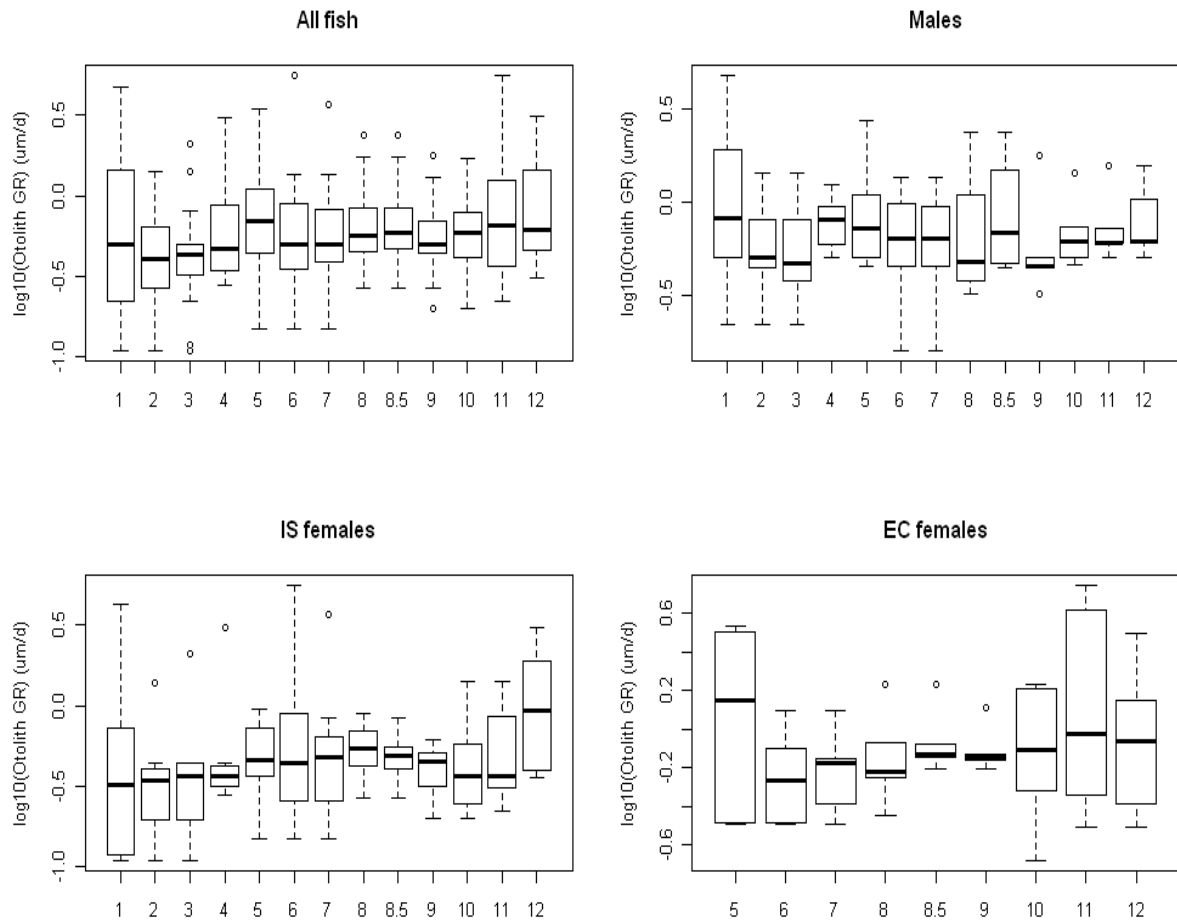
**A****B**

Figure 4.7 (A) Average otolith growth rate in plaice sampled from 02/06/09 to 28/05/10 (males = blue, Irish Sea females = red, solid line, English Channel females = red, dashed line). Note that sampling was carried out twice in February 2010 (F1 and F2). Error bars are SEM to improve graph clarity  
 (B) Boxplots showing median and distribution of  $\log_{10}$  transformed otolith growth rates over the course of the experiment (where month 1 = June 2009, F1 = 8.5 and F2 = 9). The boxplot whiskers extend 1.5 times the inter-quartile range from the 25<sup>th</sup> and 75<sup>th</sup> quartiles (lower and upper ranges of the box, respectively), while the bold line indicates the median

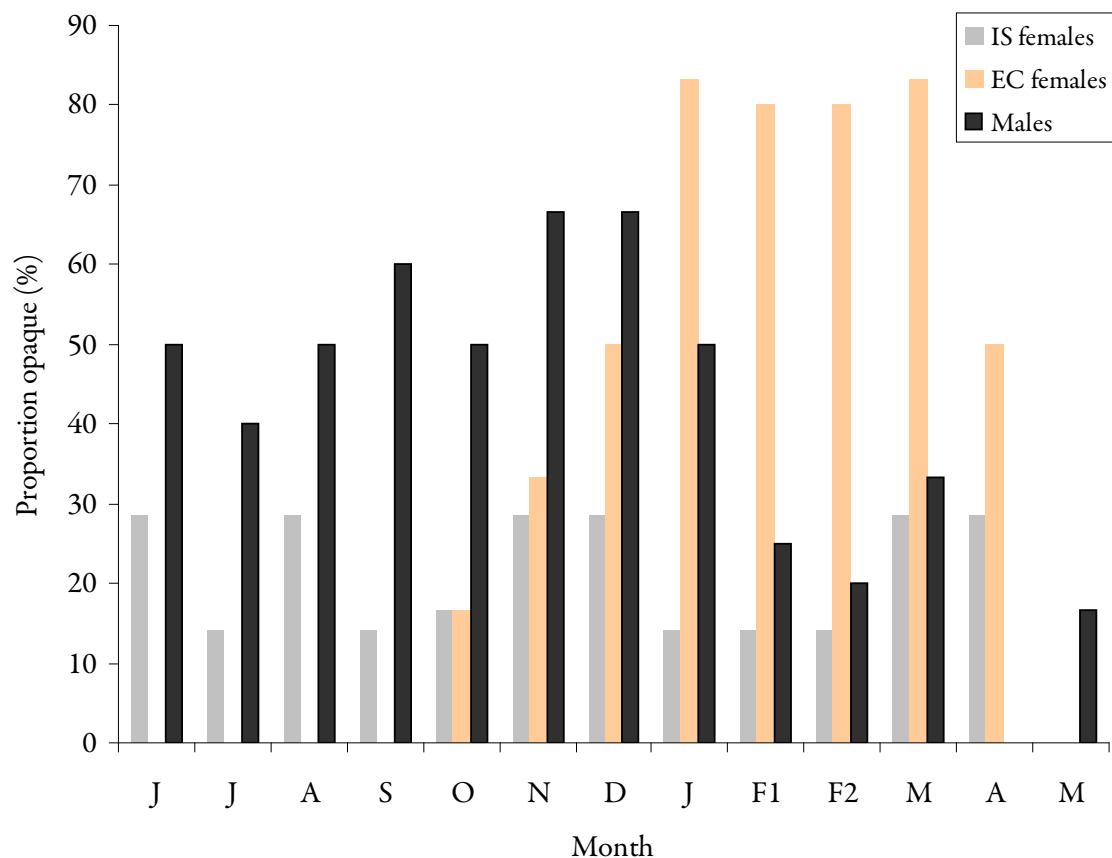


Figure 4.8 Monthly proportion of otoliths exhibiting opaque growth in plaice sampled from 02/06/09 to 28/05/10 (Irish Sea females = pale grey, English Channel females = orange, males = dark grey). Note that sampling was carried out twice in February 2010 (F1 and F2).

### 4.3.3 Patterns among otolith elements

The most highly correlated otolith element concentrations were Ba<sub>o</sub> and Sr<sub>o</sub>, both within and among analysis types (SIMS and LA-ICPMS). This indicates congruence between the ‘timelines’ assigned to each transect. Cu<sub>o</sub> and Zn<sub>o</sub> were weakly correlated with most of the other elements. Additional positive correlations included Li<sub>o</sub> vs. K<sub>o</sub>, Mn<sub>o</sub> vs. Mg<sub>o</sub>. Negative correlations included Sr<sub>o</sub> vs. Mg<sub>o</sub> and Sr<sub>o</sub> vs. Mn<sub>o</sub>. Correlations among measured element concentrations within SIMS or LA-ICPMS spots (i.e. no potential error due to assigned timelines, data transformation or LOESS smoothing) indicated similar patterns to those displayed in Table 4.7. The main exceptions included Mg<sub>o</sub> vs. Sr<sub>o</sub>, which was more negative within SIMS analyses (PPC = -0.32 as opposed to the -0.21 exhibited in Table 4.7) and weaker relationships between Zn<sub>o</sub> and Cu<sub>o</sub> and most other elemental concentrations, presumably due to the reduction in noise caused by smoothing and transforming the data.

Table 4.7 Correlation coefficients for pairwise comparisons of otolith element concentrations (determined by SIMS ‘S’, or LA-ICPMS, ‘L’), using raw values ‘fitted’ to each blood sampling day.

	Li (n = 211)	K (n = 211)	Mg (n = 210)	Sr (S) (n = 211)	Sr (L) (n = 209)	Ba (S) (n = 211)	Ba (L) (n = 209)	Mn (n = 209)	Cu (n = 208)	Zn (n = 207)
Li	1									
K	0.82	1								
Mg	0.40	0.28	1							
Sr (S)	0.11	0.18	-0.21	1						
Sr (L)	0.05	0.11	-0.25	0.82	1					
Ba (S)	0.19	0.25	0.17	0.75	0.59	1				
Ba (L)	0.17	0.24	0.11	0.62	0.72	0.82	1			
Mn	0.29	0.38	0.67	-0.24	-0.19	0.04	0.09	1		
Cu	0.43	0.40	0.13	0.33	0.43	0.34	0.41	0.06	1	
Zn	0.35	0.34	0.27	0.11	0.09	0.23	0.27	0.33	0.40	1

### 4.3.4 Time matching using $\delta^{18}\text{O}$ values

As described in the methods, an intra-annual timeline was added to each section using predicted vs. measured oxygen isotopic ratios ( $\delta^{18}\text{O}$ ). Generally, measured otolith  $\delta^{18}\text{O}$  values followed a similar pattern to those predicted by temperature and salinity measurements (Hoie *et al.*, 2004) (Figure 4.9). Correlation coefficients for predicted vs. measured  $\delta^{18}\text{O}$  profiles were usually  $>0.8$  (see Appendix 1.1), however, it is immediately obvious from Figure 4.9 that there was also considerable noise around individual measurements, although measurements were usually within  $\pm 0.5\text{‰}$  of the predicted line. Importantly, had constant growth been assumed for the otolith featured in Figure 4.10 and a timeline assigned to the section using linear interpolation between OTC mark and otolith edge, the otolith elemental concentrations would have been mismatched with environmental and physiological samples by more than three months.

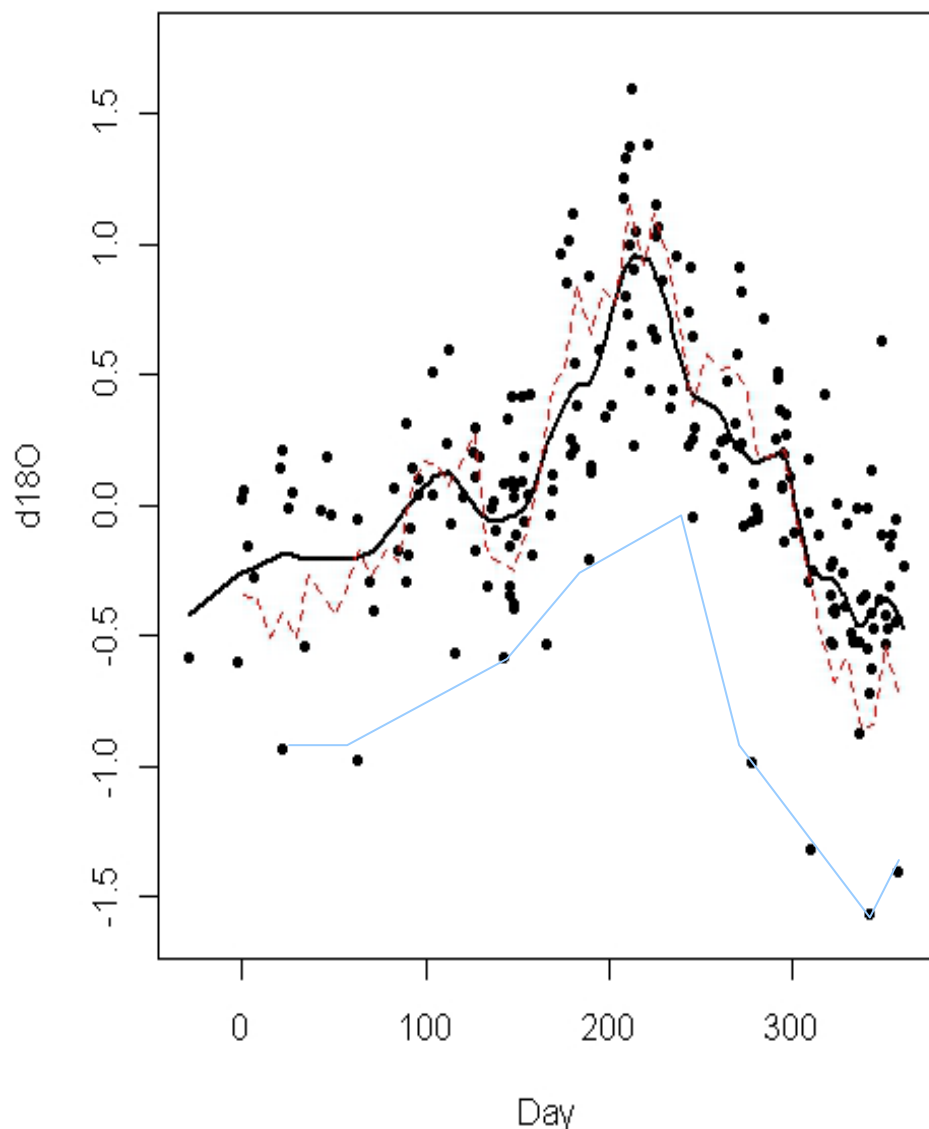


Figure 4.9 Plot showing measured (black spots and line) vs. predicted (red dashed line)  $\delta^{18}\text{O}$  measurements from experimental plaice maintained under ambient, but monitored conditions for 12 months. The black line represents a LOESS smoother through the measured values, while the predicted line was calculated based on weekly water salinity and temperature measurements. The outlier otolith (blue line) was still included because it exhibited the same pattern, just offset by  $\sim 0.7\text{‰}$ , implying some kind of calibration artefact.

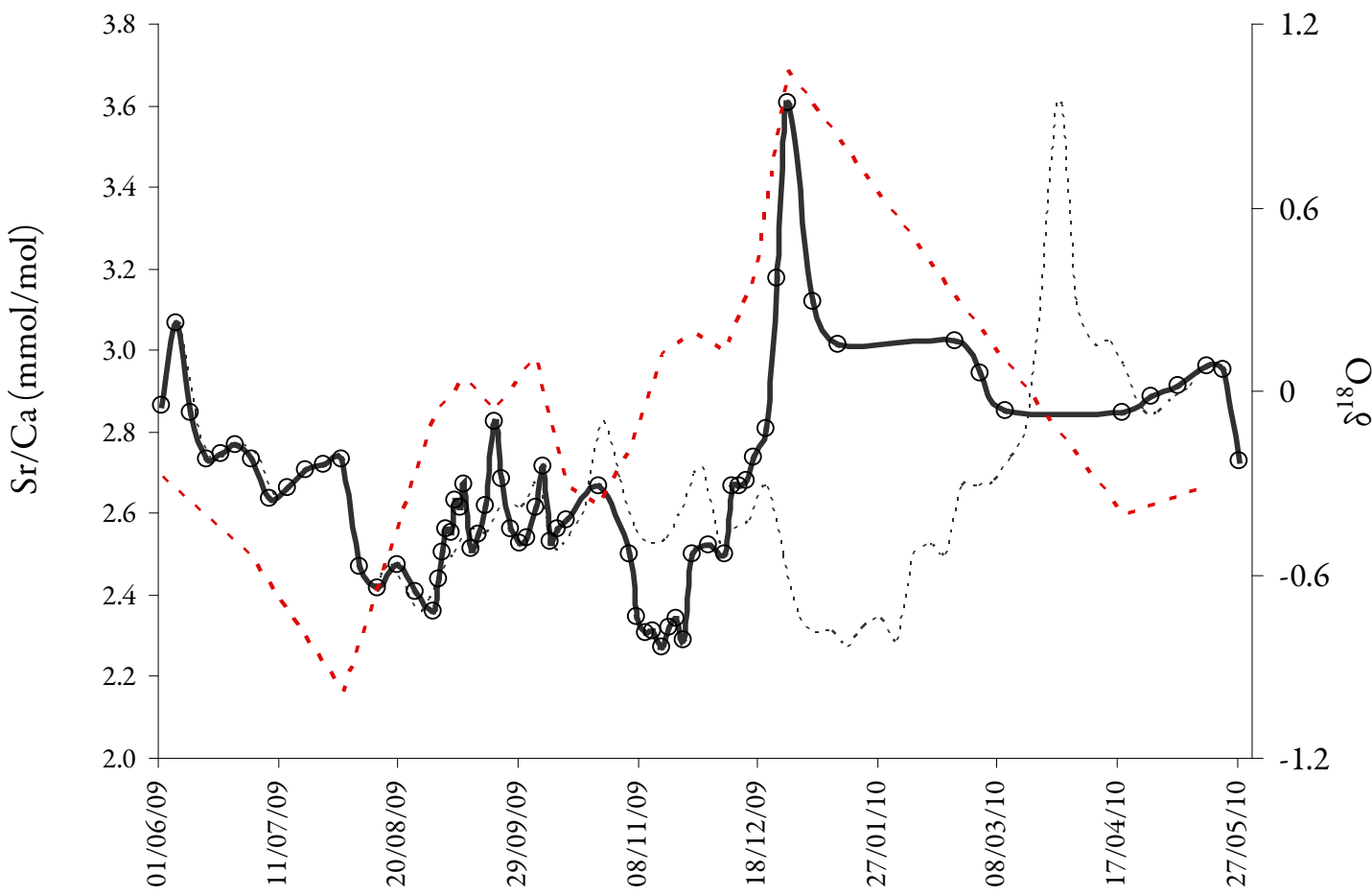


Figure 4.10 Example of an otolith (“DC062”, mature IS female) for which growth was elevated in the first half of the experiment. Wiggle matching of the  $\delta^{18}\text{O}$  profile (red dashed line) resulted in the corrected otolith Sr/Ca profile (thick black line) peaking three months earlier than it would have done had constant growth rate been assumed.

#### 4.3.5 Descriptions of otolith elemental concentrations over time

Otolith elemental concentrations exhibited clear temporal variations as well as some differences between the males and females, IS females and EC females (Figure 4.11). The relationship between SIMS and LA-ICPMS measured  $\text{Sr}_\text{O}$  was good ( $\text{PCC} = 0.8$ ), although SIMS measured Sr concentrations were lower on average. The correlation between  $\text{Ba}_\text{O}$  measurements was similar, but SIMS generally produced concentrations  $\sim 1 \mu\text{mol/mol}$  higher than those determined by LA-ICPMS (Figure 4.11). As discussed above, the Ba calibration curve for SIMS was not so well resolved and SIMS-measured Ba and Sr exhibited lower external precision than the LA-ICPMS analyses. The main argument for using SIMS over LA-ICPMS measurements was its superior temporal resolution; however, given relatively fast otolith growth in the experimental plaice, the resolution offered by LA-ICPMS was sufficient for the current chapter. Accordingly, only LA-ICPMS-measured  $\text{Ba}_\text{O}$  and  $\text{Sr}_\text{O}$  are presented for the remainder of this chapter. A brief description of the patterns in otolith concentrations displayed in Figure 4.11 is provided below.

$\text{Li}_\text{O}$  and  $\text{K}_\text{O}$  exhibited similar temporal trends, gradually increasing over time, particularly in the first half of the experiment. The males had higher average concentrations than the IS females, but the difference lessened over time as concentrations plateaued in the males from January onwards, but continued to rise in the IS females until March.  $\text{Li}_\text{O}$  and  $\text{K}_\text{O}$  in the EC females followed similar trends to the IS females, only at higher concentrations.  $\text{Mg}_\text{O}$  decreased from June to January then increased until the end of the experiment. There was no clear difference between the groups of fish, although, like  $\text{Li}_\text{O}$  and  $\text{K}_\text{O}$ , average concentrations tended to be similar in the males and EC females and lower in the IS females.

$\text{Sr}_\text{O}$  followed a clear sinusoidal pattern over time that was common to all groups of fish and common to measurements carried out by SIMS and LA-ICPMS. The lowest concentrations occurred in September to November, while highest concentrations were found in peaks that occurred in January to March. During the minima and maxima, average  $\text{Sr}_\text{O}$  tended to be higher in the IS females than the males. This was particularly apparent during February to March in the LA-ICPMS measurements.  $\text{Ba}_\text{O}$  also followed an approximately sinusoidal pattern, particularly in the IS fish. Concentrations were relatively low and stable for the first half of the experiment, with minimum average  $\text{Ba}_\text{O}$  occurring in November for all IS fish. Male  $\text{Ba}_\text{O}$  peaked in January to early February then fell in March, while IS female  $\text{Ba}_\text{O}$  peaked slightly later.  $\text{Ba}_\text{O}$  in the EC females increased from their introduction in October until January and remained at relatively steady concentrations, slightly lower than the IS females, until falling in the final month.  $\text{Ba}_\text{O}$  in the EC females exhibited the clearest divergence among the two techniques, with SIMS measurements indicating an earlier rise in  $\text{Ba}_\text{O}$  to concentrations higher than those exhibited by the IS females.

Among the ‘soft elements’,  $Mn_O$  followed generally similar patterns to  $Mg_O$ , decreasing slightly from the experiment outset until October in the females and until January in the males, then increasing towards the end of the experiment in all groups. Male  $Mg_O$  was generally higher than the IS females, but lower than the EC females, particularly towards the end of the experiment.  $Cu_O$  followed a similar pattern to  $Mn_O$  and  $Mg_O$  at the start of the experiment, decreasing slightly from concentrations exhibited at the experiment outset, and higher on average in the males than the IS females. In the latter half of the experiment,  $Cu_O$  patterns were more pronounced, indicating clear, but temporally offset, peaks during the winter spawning season.  $Cu_O$  in the females peaked at the end of February, although concentrations began to rise earlier in the EC females than the IS females, while  $Cu_O$  in the males peaked earlier, increasing rapidly from November to January before dropping to concentrations almost half of those exhibited at the start. Finally,  $Zn_O$  was also lower in the IS females than the males, particularly during a peak exhibited by the males in July and a second, larger peak in January to February, which occurred around the same time the females reached their  $Zn_O$  minima.  $Zn_O$  in the EC females followed a similar trend to the IS females, only offset by approximately  $+0.5\mu\text{mol/mol}$  throughout, decreasing from their introduction in October until January, then increasing to concentration maxima towards the end of the experiment.

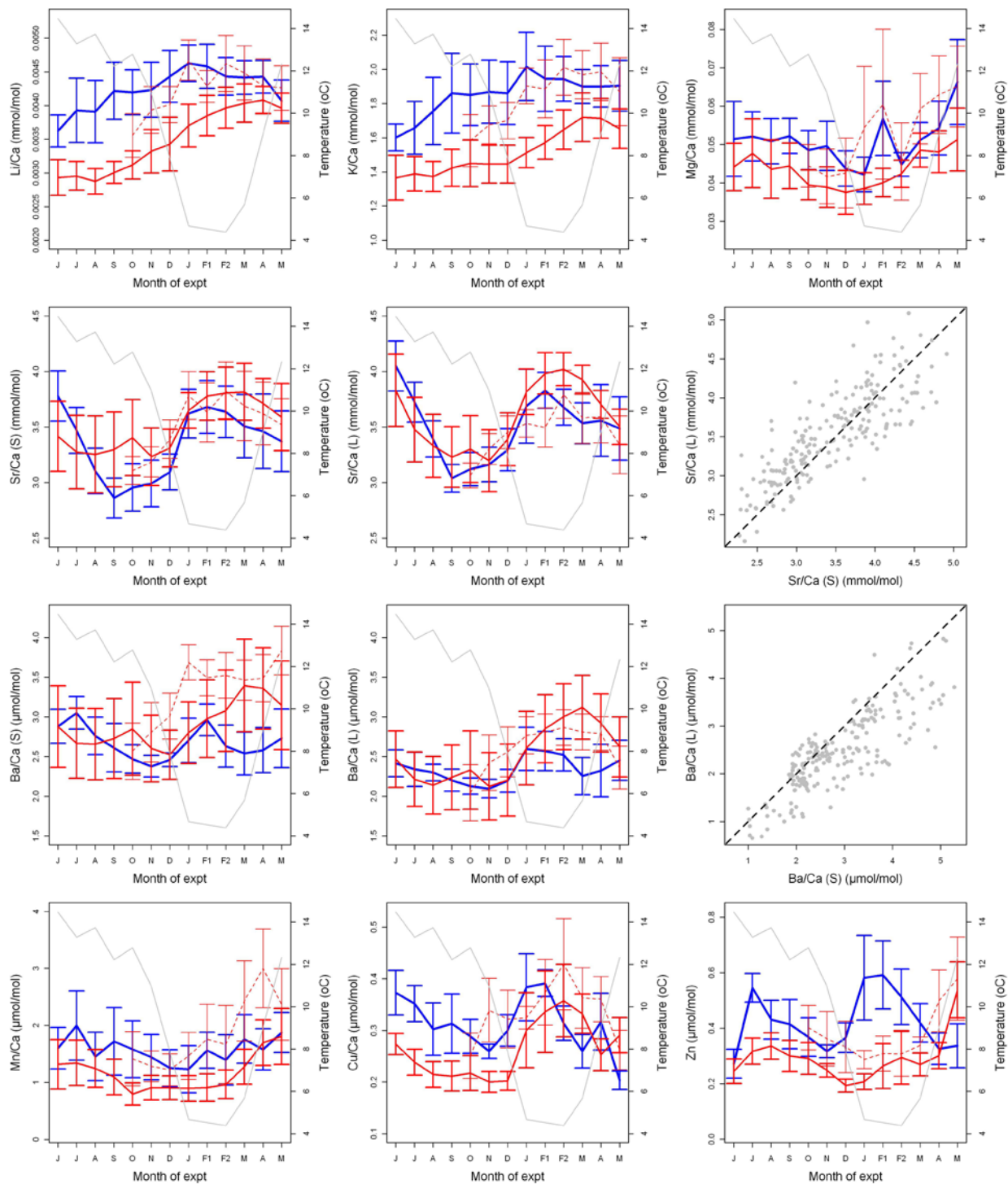


Figure 4.11 Monthly average otolith element concentrations for 19 experimental plaice sampled from 02/06/09 to 28/05/10 (males = blue, Irish Sea females = red, solid line, English Channel females = red, dashed line). Water temperature is also displayed as a thin grey line. There are two plots for Sr/Ca and Ba/Ca, displaying measurements carried out on SIMS (S) and LA-ICPMS (L). The relationships between measurements carried out on the two instruments is also displayed, with the 1:1 line indicated as a dashed line. Note that sampling was carried out twice in February 2010 (F1 and F2). Error bars are SEM (as opposed to SD) to improve graph clarity

## 4.3.6 Element fractionation from blood to otolith and water to otolith

### 4.3.6.1 Patterns in distribution coefficients

To examine fractionation of elements between the blood and otolith, and the water and otolith, the ratio between absolute concentrations and element/Ca ratios were examined (here denoted  $D_{El(O/B)}$ ,  $D_{El/Ca(O/B)}$ ,  $D_{El(O/W)}$  and  $D_{El/Ca(O/W)}$  respectively). Distribution coefficients greater than 1 indicate relative enrichment in the otolith. Comparing otolith and blood concentrations, otoliths were relatively enriched in Li, K, Sr, Ba and Mn, while comparing otolith and water concentrations, otoliths were enriched in all elements apart from Mg (Table 4.8). Also displayed are the  $D_{El(O/W)}$  values provided in Melancon *et al.* (2009), where available. These were for burbot, a freshwater species, and indicate accordingly greater enrichment of the hard acid cations (K, Mg, Sr and Ba) and Zn relative to ambient concentrations, but less enrichment of Mn. Given that otoliths are composed almost entirely of calcium carbonate, absolute concentrations can be calculated by ‘referencing’ to Ca (here, producing concentrations in  $\mu\text{g/g}$ ) or ‘normalised’ to Ca (here, producing ratios in  $\text{mmol/mol}$  or  $\mu\text{mol/mol Ca}$ ). As such, it is important to consider changes in element/Ca ratios among ‘compartments’. Distribution coefficients based on Ca-normalised concentrations indicate relative depletion of all otolith El/Ca ratios, except for  $D_{Sr/Ca(O/B)}$  and  $D_{Mn/Ca(O/W)}$ .

Table 4.8 Average and range (in parentheses) for distribution coefficients (D) for element concentrations and element/Ca ratios between otoliths and blood (O/B), and otoliths and seawater (O/W). For comparison,  $D_{El(O/W)}$  values are also displayed for burbot, a freshwater species (Melancon *et al.*, 2009)

Element	$D_{El(O/B)}$	$D_{El(O/W)}$	$D_{El(O/W)}$ Melancon <i>et al.</i> (2009)	$D_{El/Ca(O/B)}$	$D_{El/Ca(O/W)}$
Li	4.29 (2.01-7.16)	1.81 (0.94-3.02)	n/a	0.00146 (0.00064-0.00337)	0.001557 (0.000837-0.00246)
K	21.8 (2.2-124.8)	2.0 (0.97-3.26)	289	0.00756 (0.00066-0.04088)	0.001718 (0.000849-0.00278)
Mg	0.47 (0.17-1.31)	0.011 (0.004-0.030)	1.80	0.00016 (0.00005-0.00082)	0.000009 (0.000004-0.000024)
Sr	3114.7 (1637.8-5693)	492.64 (274.4-715.4)	5300	1.039 (0.535-1.709)	0.424 (0.258-0.606)
Ba	492.8 (30.1-3192.5)	220.0 (50.82-481.98)	513	0.1683 (0.0089-0.9159)	0.188 (0.048-0.386)
Mn	36.37 (0.58-192.65)	1242.0 (19.13-3960.59)	310	0.01186 (0.00021-0.04856)	1.069 (0.015-3.722)
Cu	0.301 (0.07-1.641)	38.53 (9.32-129.8)	n/a	0.000101 (0.000021-0.000478)	0.0333 (0.0088-0.1032)
Zn	0.0201 (0.0029-0.0624)	68.37 (9.63-277.85)	1140	0.0000068 (0.0000009-0.0000209)	0.0587 (0.0084-0.227)

Comparing measured  $D_{\text{El/Ca(O/W)}}$  values with those reported in the literature indicated similar  $D_{\text{Ba/Ca(O/W)}}$ ,  $D_{\text{Mn/Ca(O/W)}}$  and  $D_{\text{Sr/Ca(O/W)}}$  values, but towards the lower end of published  $D_{\text{Mg/Ca(O/W)}}$  values.

Table 4.9 Table showing average distribution coefficients for element/Ca ratios between otolith and water ( $D_{\text{El/Ca(O/W)}}$ ) for the current study alongside values from the literature. Reproduced in part from Melancon *et al.* (2009) and Miller (2009)

Study	Species	$\text{H}_2\text{O}^*$	$D_{\text{Ba/Ca(O/W)}}$	$D_{\text{Sr/Ca(O/W)}}$	$D_{\text{Mg/Ca(O/W)}}$	$D_{\text{Mn/Ca(O/W)}}$	Experiment type (temperature °C)
(Bath <i>et al.</i> , 2000)	Spot croaker	S	0.06	0.182			Laboratory (20)
(Milton and Chinery, 2001b)	Barramundi	S	0.03	0.16			Laboratory (28-30)
(Wells <i>et al.</i> , 2003)	Cutthroat trout	F	0.04	0.4			Field
(Elsdon and Gillanders, 2003b)	Black bream	S	0.099	0.131		0.683	Laboratory (20)
(de Vries <i>et al.</i> , 2005)	Black bream	B	0.058	0.463			Laboratory (22)
(de Vries <i>et al.</i> , 2005)	Black bream	S	0.136	0.287			Laboratory (22)
(Elsdon and Gillanders, 2005a)	Black bream	S	0.27	0.28			Laboratory (20)
(Elsdon and Gillanders, 2005a)	Black bream	S	0.26	0.52			Field
(Dorval <i>et al.</i> , 2007)	Spotted seatrout	B	0.31	0.23		14.8	Field
(Melancon <i>et al.</i> , 2009)	Burbot	F	0.034	0.35		0.021	Field
(Melancon <i>et al.</i> , 2009)	Lake trout	F	0.0037	0.28		0.054	Field
(Martin and Wuenschel, 2006)	Juvenile grey snapper	E	0.044 -0.450	0.21- 0.38	0.00000765 -0.0000891	0.018- 1.020	Laboratory
(Forrester, 2005)	Juvenile mudsucker	E				0.39	Field
(Martin and Thorrold, 2005)	Larval & juvenile spot	E	0.37		0.00014 – 0.0010	0.196	Laboratory
(Miller, 2009)	Juvenile Black rockfish	S	0.32			0.409	Field (13)
Present study	Adult plaice	S	0.188	0.424	0.000009	1.069	Laboratory (3-14)

\* E = euryhaline, S = saltwater, F = freshwater, B = brackish water

#### 4.3.6.2 Element fractionation: blood to otolith

To consider elements available for uptake to otolith, it is important to consider both total blood concentrations as well as element/Ca ratios. Monthly  $El_B$  concentrations were presented in Chapter 3, but  $El/Ca_B$  values for the current group of fish ( $n = 19$ ) are presented in Figure 4.12. Generally,  $El/Ca_B$  exhibited similar trends to  $El_B$ , however the effect of hypercalcaemia between November and February, particularly in the IS females, resulted in often depleted  $El/Ca$  ratios during this period. For Li, Mn and Mg, absolute blood concentrations were higher on average in the females (significantly so for  $Mn_B$ ), however, when normalised to Ca, there was either no clear difference among the sexes or slight enrichment in the males. For  $Sr/Ca_B$  the similar trends in  $Sr_B$  and  $Ca_B$  resulted in a 'dampening' of the  $Sr_B$  peak between October and March, although there was still clear  $Sr/Ca_B$  enrichment in the IS females in March and April.

Distribution coefficients showing fractionation of elements from blood to otolith indicated similar trends using absolute concentrations or element/Ca ratios (Figure 4.13). The largest difference was between  $D_{Sr(O/B)}$  and  $D_{Sr/Ca(O/B)}$ , where  $D_{Sr(O/B)}$  indicated depletion of  $Sr_O$  relative to  $Sr_B$  in the IS females from November to March (when their  $Ca_B$  concentrations were at their highest), and concurrent enrichment of  $Sr_O$  in the males and EC females. When normalised to Ca,  $D_{Sr/Ca(O/B)}$  were similar among fish and followed analogous trends to  $Sr/Ca_O$  over time, with relatively enriched  $Sr/Ca_O$  in all fish between December and April (Figure 4.11). If otolith concentrations were faithfully tracking  $El_B$  or  $El/Ca_B$ , the distribution coefficients would remain constant over time. The elements that exhibited the most constant  $D_{El(O/B)}$  and  $D_{El/Ca(O/B)}$  values over time and among groups of fish were Mg and Ba (Figure 4.13).

#### 4.3.6.3 Element fractionation: seawater to otolith

Distribution coefficients showing fractionation of elements between otolith and water exhibited almost identical trends using absolute concentrations or element/Ca ratios (Figure 4.14). All elements apart from Ba and Sr exhibited greater enrichment in the otoliths of the males compared with the IS females, particularly during the first half of the experiment for Li, K and Mn. With the exception of  $D_{Ba(O/W)}$  and  $D_{Zn(O/W)}$ , relative elemental uptake from the environment was more similar between the males and EC females than between the two groups of females. The clear exception was for Zn, where the increase  $Zn_O$  in the males during winter (Figure 4.11) coincided with the period of minimum water concentrations and thus accompanied by a large increase in  $D_{Zn(O/W)}$ . The cyclical patterns in  $D_{Sr(O/W)}$  and  $D_{Ba(O/W)}$  indicated enrichment in the otolith during the spawning season, particularly in the IS females, however, the cycles were inversely related to changes in ambient concentrations and temperature, with the period of maximum otolith enrichment occurring when water concentrations and temperatures were at their annual minimum.

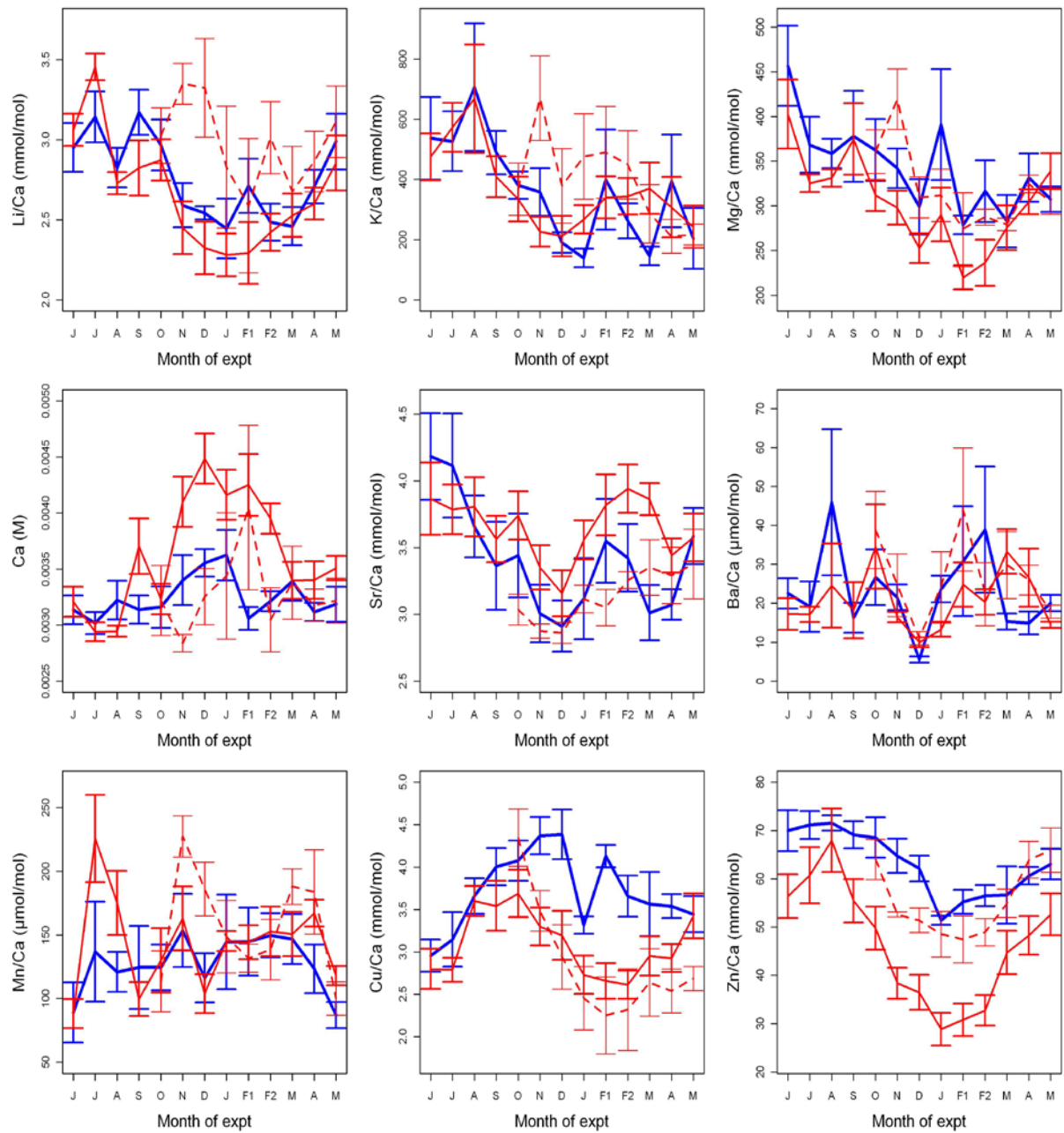
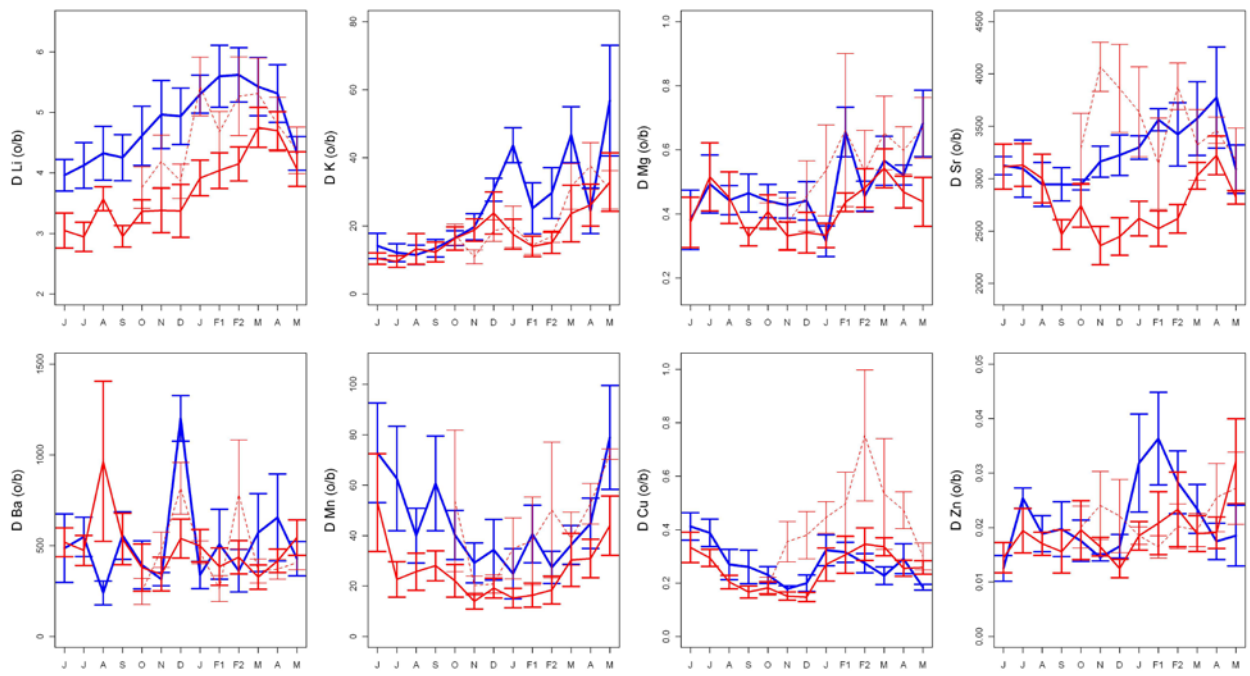


Figure 4.12 Monthly average blood El/Ca ratios for 19 plaice sampled from 02/06/09 to 28/05/10 (males = blue, Irish Sea females = red, English Channel females = red, dashed line). Note that sampling was carried out twice in February 2010 (F1, F2) and blood Ca concentrations are displayed for reference. Error bars are SEM (as opposed to SD) to improve graph clarity

D [El] (otolith:blood)



D [El/Ca] (otolith:blood)

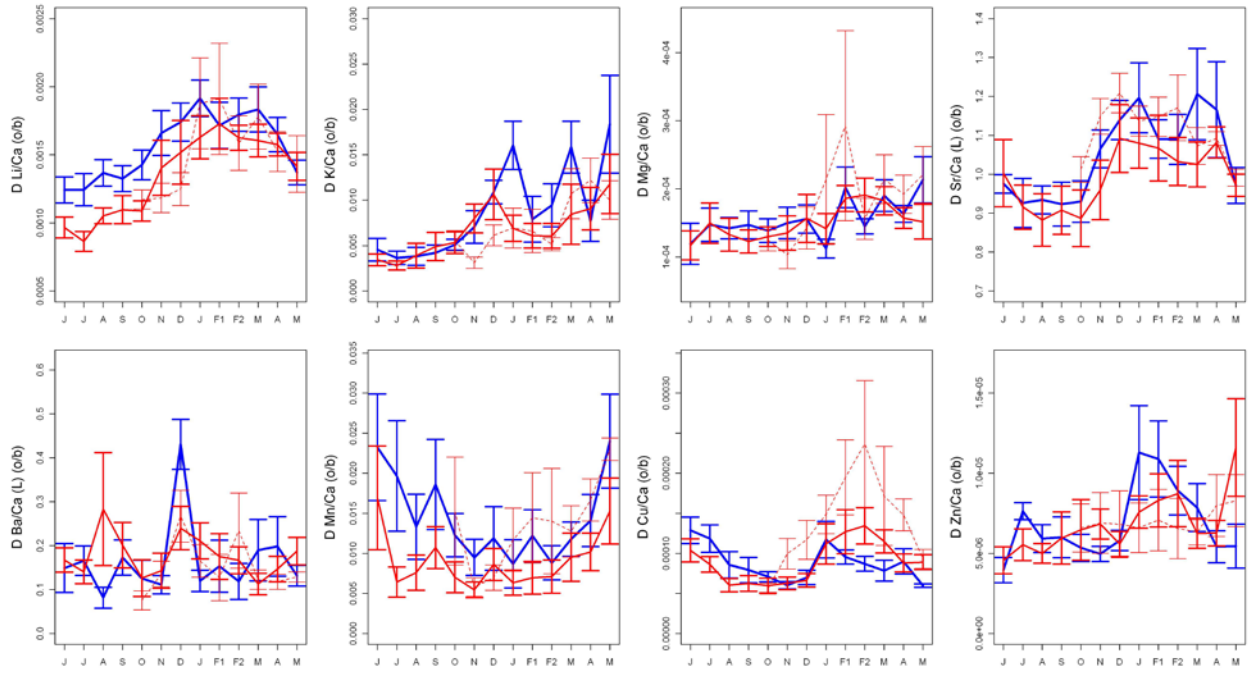
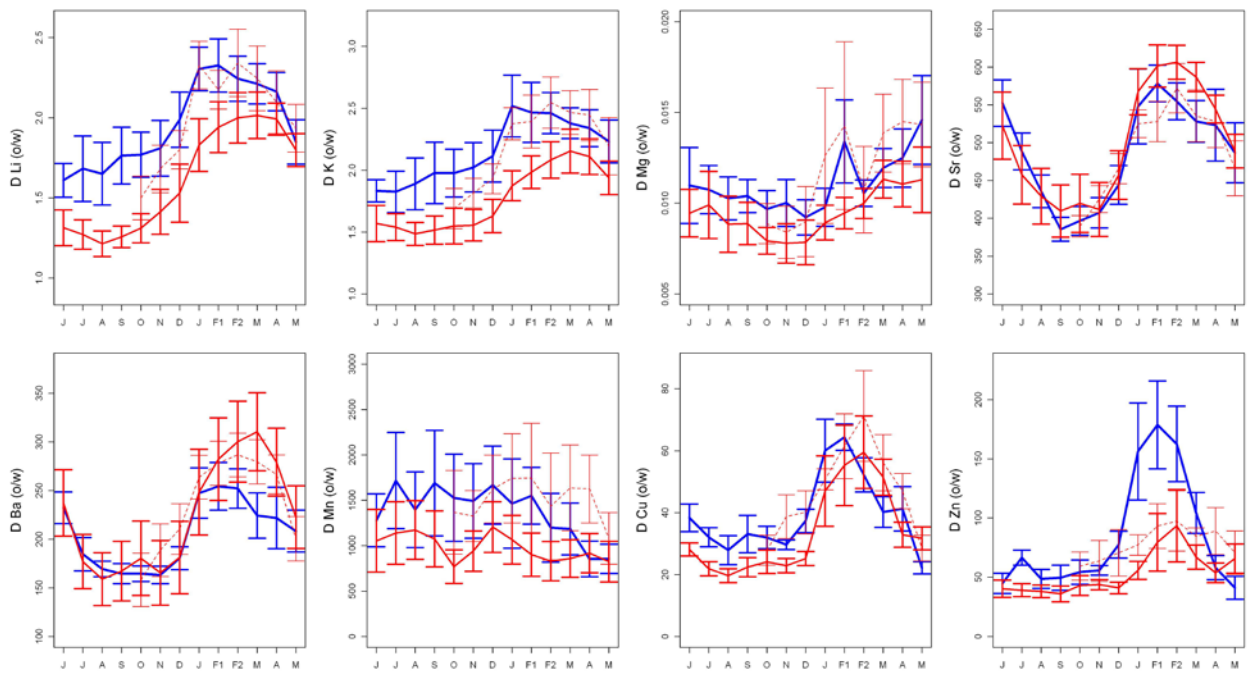


Figure 4.13 Monthly average distribution coefficients for otolith:blood element concentrations and element/Ca ratios ( $D_{El(o/b)}$  and  $D_{El/Ca(o/b)}$ , respectively) for 19 experimental plaice sampled from 02/06/09 to 28/05/10 (males = blue, Irish Sea females = red, solid line, English Channel females = red, dashed line). Note that sampling was carried out twice in February 2010 (F1 and F2). Error bars are SEM (as opposed to SD) to improve graph clarity

### D [El] (otolith:water)



### D [El/Ca] (otolith:water)

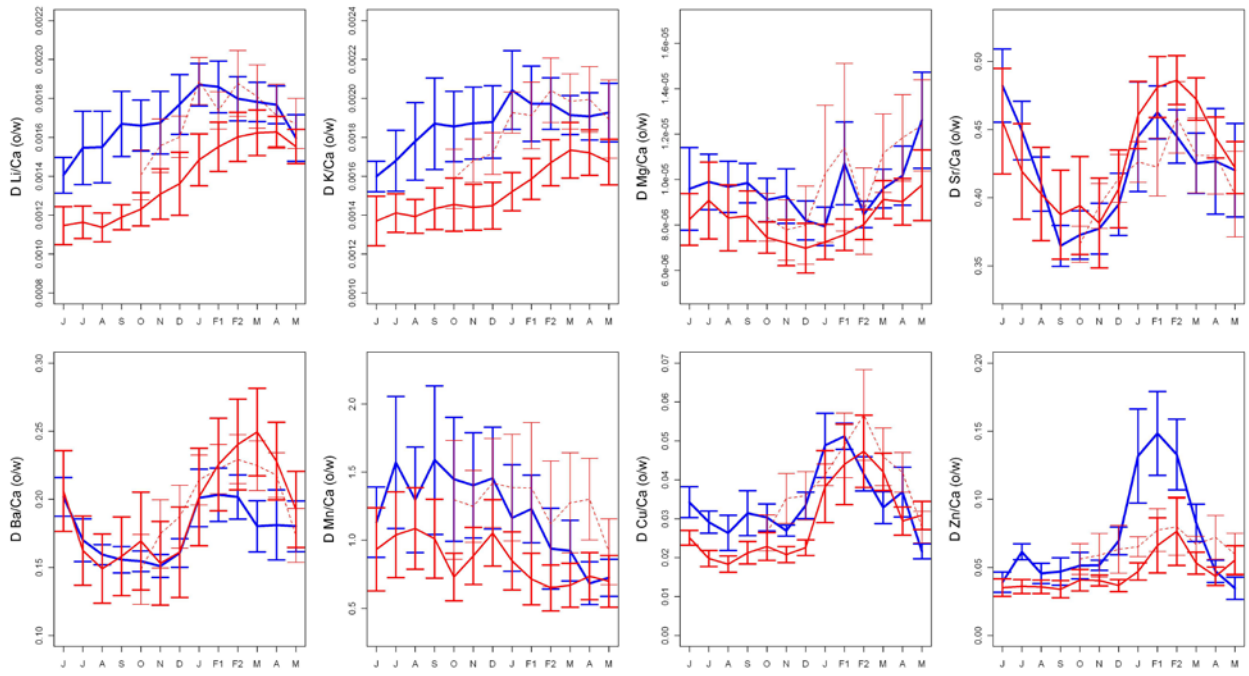


Figure 4.14 Monthly average distribution coefficients for otolith:seawater element concentrations and element/Ca ratios ( $D_{El(o/b)}$  and  $D_{El/Ca(o/b)}$ , respectively) for 19 experimental plaice sampled from 02/06/09 to 28/05/10 (males = blue, Irish Sea females = red, solid line, English Channel females = red, dashed line). Note that sampling was carried out twice in February 2010 (F1 and F2). Error bars are SEM (as opposed to SD) to improve graph clarity

## 4.3.7 Modelling otolith elemental concentrations

### 4.3.7.1 Were otolith element concentrations correlated with ambient water and/or blood concentrations?

Before attempting to model the data, simple pairwise correlations were carried out between otolith, blood and seawater elemental concentrations and element/Ca ratios, as well as between otolith element concentrations and temperature. It was immediately clear that very few otolith elements exhibited positive (if any) correlation with ambient concentrations or element/Ca ratios (Table 4.10). The only exceptions were Mn and Mn/Ca for which positive correlations were observed among all groups of fish, and Zn and Zn/Ca for which positive correlations were observed in the females only.

Table 4.10 Pearson product-moment correlation coefficients for fitted otolith element concentrations and concomitant concentrations in the water and blood for all observations for the experimental plaice ( $n = 19$ : 6 males (M), 7 Irish Sea (IS), 6 English Channel (EC) females). Given that correlations were carried out on longitudinal non-independent data, the  $p$  values are invalid, so to help to identify any potential relationships, weaker relationships (coefficients  $<0.2$ , arbitrarily chosen) are displayed in grey.

	Otolith vs. seawater				Otolith vs. blood			
	All	M	IS	EC	All	M	IS	EC
Li	-0.36	-0.24	-0.37	-0.47	-0.16	-0.05	-0.21	-0.13
K	-0.26	-0.15	-0.32	-0.38	-0.09	-0.10	-0.15	0.18
Mg	-0.09	-0.02	-0.08	-0.18	0.03	0.02	0.06	0.02
Sr	-0.37	-0.33	-0.42	-0.39	0.37	0.45	0.45	0.12
Ba	-0.29	-0.23	-0.29	-0.37	0.03	-0.11	0.11	-0.13
Mn	0.27	0.17	0.25	0.42	0.11	0.09	0.14	0.24
Cu	-0.25	-0.06	-0.30	-0.34	-0.17	-0.22	0.00	-0.30
Zn	0.12	-0.19	0.27	0.32	0.23	-0.18	0.20	0.26
Li/Ca	-0.33	-0.33	-0.28	-0.38	0.01	0.04	-0.06	0.01
K/Ca	-0.11	-0.10	-0.09	-0.23	-0.02	-0.06	-0.16	0.25
Mg/Ca	-0.12	-0.15	-0.09	-0.17	-0.05	0.02	0.06	-0.41
Sr/Ca	-0.18	-0.12	-0.17	-0.33	0.47	0.58	0.37	0.61
Ba/Ca	-0.25	-0.19	-0.35	-0.27	-0.02	-0.07	0.05	-0.22
Mn/Ca	0.26	0.15	0.24	0.43	0.14	0.11	0.19	0.12
Cu/Ca	-0.21	0.03	-0.26	-0.32	-0.12	-0.17	-0.08	-0.28
Zn/Ca	0.13	-0.20	0.30	0.35	0.29	-0.01	0.26	0.13

#### 4.3.7.2 Which variables best explain variation in otolith elemental concentrations and otolith:blood distribution coefficients?

Linear mixed effect models were carried out to examine which physiological and/or environmental variables best explained variations in (i) otolith element concentrations and (ii) otolith:blood distribution coefficients ( $D_{El(O/B)}$ ), using 'fish' as a random effect in both cases. For each response variable, a model was built for all fish and for females only (thus including GSI). Note that for modelling the distribution coefficients,  $El_B$ ,  $El/Ca_B$ ,  $El_W$  and  $El/Ca_W$  were not included as potential explanatory variables. The model outputs are displayed in Table 4.11 and Table 4.12. Note that due to collinearity between temperature and many of the seawater concentrations, as well as near-bimodal distribution of both terms, it was often impossible to separate their effects using the models alone. Such cases are highlighted below, along with a brief description of the model outputs and the main observed trends. Unless otherwise stated, the same terms were selected for the 'full' and 'female only' models.

#### Lithium and potassium

Given similar patterns in the otolith,  $Li_O$  and  $K_O$  will be discussed together. Otolith concentrations of both elements were primarily driven by a positive effect of opacity, a negative effect of TL, a negative effect of ambient concentrations (or temperature), and a weak sex effect (M>F). Note that these effects were often the opposite to those exhibited by blood concentrations, for example, with  $Li_B$  values largely explained by a positive effect of salinity and higher concentrations in the females than the males. The positive effect of 'Day' was almost significant in both models. Model fits were good, but better for  $K_O$  than  $Li_O$  ( $r^2 = 0.79-0.81$  vs.  $0.57-0.60$  respectively). However, in all models, around 30% of the variation was explained by the random effect, indicating among-otolith differences in Li and K concentrations.

$D_{Li(O/B)}$  and  $D_{K(O/B)}$  values were primarily explained by a positive effect of day, but otherwise the models were quite different. A positive effect of otolith opacity and a negative effect of temperature were important for explaining variations in  $D_{Li(O/B)}$  values, while positive effects of otolith growth rate and blood protein concentrations explained more of the variation in  $D_{K(O/B)}$  values (Figure 4.16). Model fit was better for explaining  $D_{Li(O/B)}$  than  $D_{K(O/B)}$  values ( $r^2 > 0.7$  vs.  $0.3$ , respectively), however, the amount of variation explained by the fixed effects was not much higher ( $r^2 \sim 0.35$  vs.  $0.25$ , respectively), indicating smaller among-fish variation in  $D_{K(O/B)}$  values.

Table 4.11 Linear mixed effects model outputs (Analysis of Deviance *p* values, Nagelkerke pseudo-*r*<sup>2</sup>) for otolith element concentrations of 19 experimental plaice

All fish (n = 212)									Females only (n = 212)								
		Pseudo r <sup>2</sup>							Pseudo r <sup>2</sup>								
Fixed effects		Effect?	Chi Sq statistic	df	p value	Whole model	FE (RE)	Notes	Fixed effects		Chi Sq statistic	df	p value	Whole model	FE (RE)	Comments	
Li	Opacity	+ve	48.180	2	<0.0001	***	0.57	0.25	Temp in place of Liw, FE r <sup>2</sup> = 0.19	Opacity	10.730	2	0.0047	**	0.60	0.32	Temp in place of Liw, FE r <sup>2</sup> = 0.24
	Liw	-ve	21.960	1	<0.0001	***	(0.31)	FE r <sup>2</sup> = 0.19		Liw	23.570	1	<0.0001	***	(0.28)	Temp in place of Liw, FE r <sup>2</sup> = 0.24	
	TL	-ve	27.150	1	<0.0001	***				TL	27.810	1	<0.0001	***			
	Sex	M>F	14.810	1	0.0001	***											
K	Opacity	+ve	40.730	2	<0.0001	0.79	0.48	Temp in place of Sal, FE r <sup>2</sup> = 0.42	Opacity	9.476	2	0.0088	**	0.81	0.51	Temp in place of Sal, FE r <sup>2</sup> = 0.37	
	Salinity	-ve	21.390	1	<0.0001	(0.30)	FE r <sup>2</sup> = 0.42			Salinity	34.039	1	0.0000	***	(0.31)	Temp in place of Sal, FE r <sup>2</sup> = 0.37	
	TL	-ve	8.220	1	0.0002					TL	19.501	1	0.0000	***			
	Sex	M>F	16.680	1	<0.0001												
Mg	O.otolith GR	+ve	26.466	1	<0.0001	***	0.65	0.25	CoxSnell r <sup>2</sup> values	Oto.o.GR	26.466	1	<0.0001	***	0.65	0.26	
	Growth	+ve	6.113	1	0.0134	*	(0.39)	FE r <sup>2</sup> = 0.37		Growth	6.113	1	0.0134	*	(0.39)		
	Salinity	-ve	59.494	1	<0.0001	***				Salinity	59.494	1	<0.0001	***			
	Temperature	+ve	31.273	1	<0.0001	***				Temperature	31.273	1	<0.0001	***			
Sr	Sr/Ca <sub>w</sub>	+ve	18.958	1	<0.0001	***	0.67	0.50	Temp in place of Sr <sub>w</sub> , FE r <sup>2</sup> = 0.37	Sr/Ca <sub>s</sub>	13.945	1	0.0002	***	0.78	0.66	Temp in place of Sr <sub>w</sub> , FE r <sup>2</sup> = 0.55
	Otolith GR	-ve	8.324	1	0.0039	**	(0.17)	FE r <sup>2</sup> = 0.37		Otolith GR	7.504	1	0.0062	**	(0.12)		
	Sr <sub>w</sub>	-ve	67.589	1	<0.0001	***				Sr <sub>w</sub>	49.680	1	<0.0001	***			
	TL	-ve	5.708	1	0.0169	*				TL	14.717	1	0.0001	***			
	Condition	n.s.	0.000	1	0.9871					Condition	1.440	1	0.2301				
	Treatment	n.s.	1.191	1	0.2752					Treatment	8.938	1	0.0028	**			
Ba	Condn*Treatmt	treated+ve	9.405	1	0.0022	**				Condn*Treatmt	25.037	1	<0.0001	***			
	Salinity	-ve	25.581	1	<0.0001	***	0.70	0.28		Salinity	25.902	1	<0.0001	***	0.75	0.38	
	Temperature	-ve (n.s.)	3.781	1	0.0518	.	(0.42)	Temp+GR		Temperature	5.098	1	0.0240	*	(0.37)	+ Treatment	
Mn	Mn <sub>w</sub>	+ve	78.542	1	<0.0001	***	0.71	0.35	Temp in place of Mn <sub>w</sub> , FE r <sup>2</sup> = 0.13	Mn <sub>w</sub>	64.694	1	<0.0001	***	0.73	0.42	Temp in place of Mn <sub>w</sub> , FE r <sup>2</sup> = 0.17
	Somatic GR	+ve	8.994	1	0.0027	**	(0.36)	FE r <sup>2</sup> = 0.13		Somatic GR	10.823	1	0.0010	**	(0.31)		
	O.otolith GR	+ve	17.829	1	<0.0001	***				O.otolith GR	10.391	1	0.0013	**			
Cu	Condition	-ve	14.083	1	0.0002	***	0.54	0.40	Temp in place of Cu <sub>w</sub> , FE r <sup>2</sup> = 0.23	Condition	5.107	1	0.0238	*	0.43	0.33	Temp in place of Cu <sub>w</sub> , FE r <sup>2</sup> = 0.21
	Cu <sub>w</sub>	-ve	31.499	1	<0.0001	***	(0.14)	FE r <sup>2</sup> = 0.23		Cu <sub>w</sub>	24.311	1	<0.0001	***	(0.11)		
	Sex	n.s.	1.489	1	0.2224												
	Cu <sub>w</sub> *sex	F-ve	6.809	1	0.0091	**											
Zn	Zn/Ca <sub>w</sub>	+ve	18.066	1	<0.0001	***	0.39	0.24	Temp in place of Zn.w, FE r <sup>2</sup> = 0.17	Zn/Ca <sub>w</sub>	13.781	1	0.0002	***	0.36	0.28	Temp in place of Zn.w, FE r <sup>2</sup> = 0.17
	Temp	+ve	13.762	1	0.0002	***	(0.15)	FE r <sup>2</sup> = 0.17		Temp	8.171	1	0.0043	**	(0.09)		
	Spawner	Sp<nonsp	5.043	1	0.0247	*				Spawner	3.081	1	0.0792	.			
	Sex	M>F	6.217	1	0.0127	*				GSI	1.970	1	0.1605				
	Zn/Ca <sub>w</sub> *Sex	F+ve, M-ve at Zn.w	18.577	1	<0.0001	***		GSI*Spawner	4.864	1	0.0274	*			Spawner -ve		

Table 4.12 Linear mixed effects model outputs (Analysis of Deviance p values, Nagelkerke pseudo- $r^2$ ) for otolith:blood distribution coefficients ( $D_{El(o/b)}$ ) for 19 experimental plaice

		All fish ( $n = 212$ )					Females only ( $n = 212$ )								
		Fixed effects	Effect	Chi Sq statistic	df	p value <sup>†</sup>	Pseudo r <sup>2</sup>		Fixed effects	Chi Sq statistic	df	p value <sup>†</sup>	Pseudo r <sup>2</sup>		
							Whole model	FE (RE)					Whole model	FE (RE)	
$D_{Li(o/b)}$	Day	+ve	41.50	1	<0.0001	***	0.75	0.38	Day	48.343	1	<0.0001	***	0.71	0.34
	Opacity	+ve	30.80	2	<0.0001	***		(0.37)	Opacity	8.146	2	0.0170	*		(0.37)
	Temp	-ve	19.84	1	<0.0001	***			Temp	11.354	1	0.0008	**		
	Sex	M>F	6.02	1	0.0141	*									
$D_{K(o/b)}$	Otolith GR	-ve	5.60	1	0.0179	*	0.33	0.28	Otolith GR	5.85	1	0.0156	*	0.32	0.22
	Protein	-ve	7.13	1	0.0076	**		(0.05)	Protein	3.85	1	0.0497	*		(0.10)
	Day	+ve	62.36	1	<0.0001	***			Day	31.26	1	<0.0001	***		
$D_{Mg(o/b)}$	O. otolith GR	+ve	20.65	1	<0.0001	***	0.53	0.12	O. otolith GR	14.90	1	0.0001	***	0.54	0.12
	Treatment	NT>T	8.28	1	0.0040	**		(0.41)							(0.43)
	Origin	EC>IS	7.75	1	0.0054	**									
	TL	+ve	11.73	1	0.0006	***									
$D_{Sr(o/b)}$	Protein	-ve	61.53	1	<0.0001	***	0.51	0.36	Protein	63.86	1	<0.0001	***	0.63	0.47
	Treatment	T>NT	13.42	1	0.0002	***		(0.15)	Treatment	14.93	1	0.0001	***		(0.16)
	Condition	-ve	11.02	1	0.0009	***			Condition	1.24	1	0.2663			
	Treatm*Condn	-ve (NT)	8.79	1	0.0030	**			Treatmt*Condn	21.42	1	<0.0001	***		
	Sex	M>F	4.79	1	0.0286	*									
	Protein*Sex	-ve (F)	29.10	1	<0.0001	***									
$D_{Ba(o/b)}$	Otolith GR	-ve	2.84	1	0.0920		0.09	0.01 (0.09)	Otolith GR	6.70	1	0.0096	**	0.17	0.04 (0.13)
$D_{Mn(o/b)}$	Day	+ve	21.773	1	<0.0001	***	0.66	0.21	Day	12.868	1	0.0003	***	0.62	0.16
	Temp	+ve	23.237	1	<0.0001	***		(0.45)	Temp	12.539	1	0.0004	***		(0.46)
	Condition	-ve	10.361	1	0.0013	**			Condition	4.462	1	0.0347	.		
	O. otolith GR	+ve	8.607	1	0.0033	**			O. otolith GR	5.846	1	0.0156	*		
$D_{Cu(o/b)}$	Temp	-ve	45.61	1	<0.0001	***	0.41	0.30	Temp	41.29	1	<0.0001	***	0.42	0.31
	Protein	-ve	16.32	1	0.0001	***		(0.11)	Protein	15.29	1	0.0001	***		(0.11)
	Condition	-ve	16.49	1	<0.0001	***			Condition	5.54	1	0.0186	*		
	Sex	n.s.	0.00	1	0.9638										
	-ve F, +ve (?) M		12.81	1	0.0003	***									
	Sex*Temp														
$D_{Zn(o/b)}$	Temp	-ve	5.820	1	0.0158	*	0.23	0.06	Temp	41.29	1	<0.0001	***	0.42	0.31
	Sex	n.s.	0.173	1	0.6775			(0.17)	Protein	15.29	1	0.0001	***		(0.11)
	-ve in M (at low T),		8.297	1	0.0040	**			Condition	5.54	1	0.0186	*		
	Temp*Sex		n.s. in F												

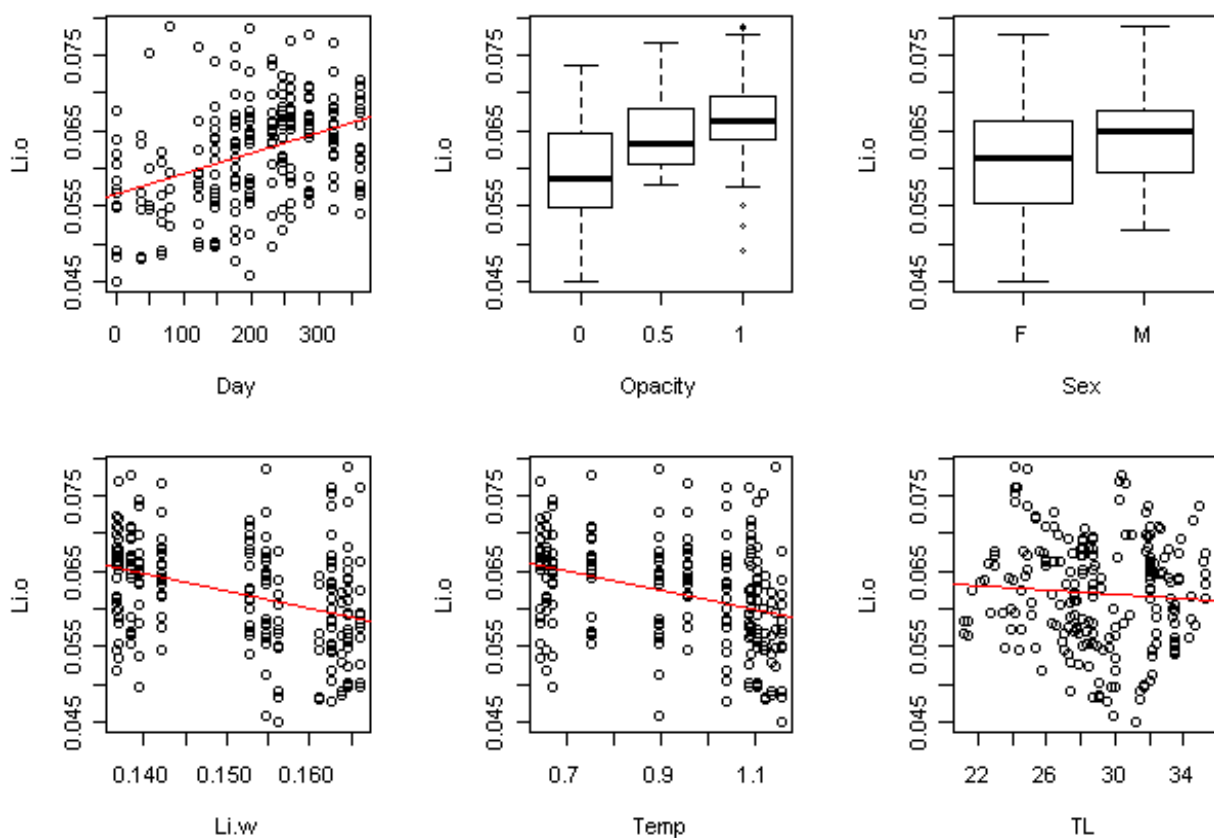


Figure 4.15 Relationships between number of days into the the experiment, otolith opacity (0 = translucent, 1 = opaque), sex,  $Li_W$  (in ppm), temperature ( $\log_{10}$  transformed, in  $^{\circ}C$ ), total length (TL, in cm) and  $Li_O$  values (SQRT transformed Li/Ca concentrations in mmol/mol). Note that the relationships were near identical for  $K_O$  and for  $D_{Li(O/B)}$ , so are not displayed. Temperature was only significant in the  $D_{Li(O/B)}$  model. The boxplot whiskers extend 1.5 times the inter-quartile range from the 25<sup>th</sup> and 75<sup>th</sup> quartiles (lower and upper ranges of the box, respectively), while the bold line indicates the median

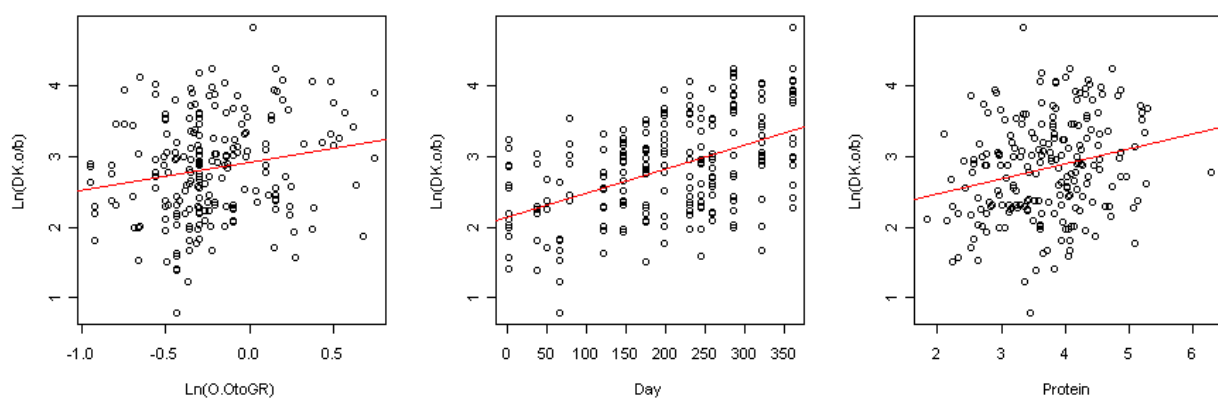


Figure 4.16 Relationships between overall otolith growth rate (O.OtoGR, Ln transformed, in  $\mu m/day$ ), number of days into the the experiment, blood protein (in g/dL) and  $D_{K(O/B)}$  values (Ln transformed)

## **Magnesium**

The most parsimonious model for explaining  $Mg_O$  values included salinity, temperature, otolith and somatic growth rates (Figure 4.17). Unlike  $Mg_B$  values,  $Mg_O$  concentrations were negatively correlated with salinity, although the effect was relatively weak and driven largely by the increase in  $Mg_O$  values at the end of the experiment, when salinity remained low. Similar to the  $Mg_B$  model, the effect of temperature on  $Mg_O$  values was positive. Model fit was almost identical for all fish pooled and females only ( $r^2 = 0.65$ ), however the majority of the variation was explained by the random effect, with only 25% explained by the fixed effects.

$D_{Mg(O/B)}$  values were best explained by a negative effect of treatment (while  $Mg_B$  values had been, in part, explained by a positive treatment effect), a positive effect of TL and, as for  $Mg_O$ , a positive effect of otolith growth rate (Figure 4.17). Possibly related to the 'size effect', EC fish exhibited significantly higher  $D_{Mg(O/B)}$  values than the IS fish, exhibiting slightly higher concentrations in the otoliths despite similar levels in the blood. The full and female only models explained similar amounts of variation, but the latter only included otolith growth rate. Model fits were quite good ( $r^2 > 0.5$ ), but the majority of the variation was attributed to the random effect, with only 12% explained by the fixed effects.

## **Strontium**

The  $Sr_O$  model was the most complex of the models presented herein, however,  $Sr_O$  values were largely explained by two variables:  $Sr_W$  and  $Sr/Ca_B$ . The significant negative relationship with  $Sr_W$  values contradicts the results of many empirical studies; however, with temperature in place of  $Sr_W$ , the  $r^2$  value for the fixed effects fell by 13%. The relationship between  $Sr_O$  and  $Sr/Ca_B$  values was strong and positive, and there was a negative effect of otolith growth rate and TL. Finally, a highly significant interaction between condition and treatment was observed, with  $Sr_O$  values positive correlated with condition in the treated fish, but negatively correlated in the non-treated fish (Figure 4.18). Model fits were good ( $r^2 = 0.67-0.78$ ) and a relatively low proportion was explained by the random effect. In the female only model, while GSI was positively correlated with  $Sr_O$  values, the effect was not significant, however the condition\*treatment interaction was again, highly significant.

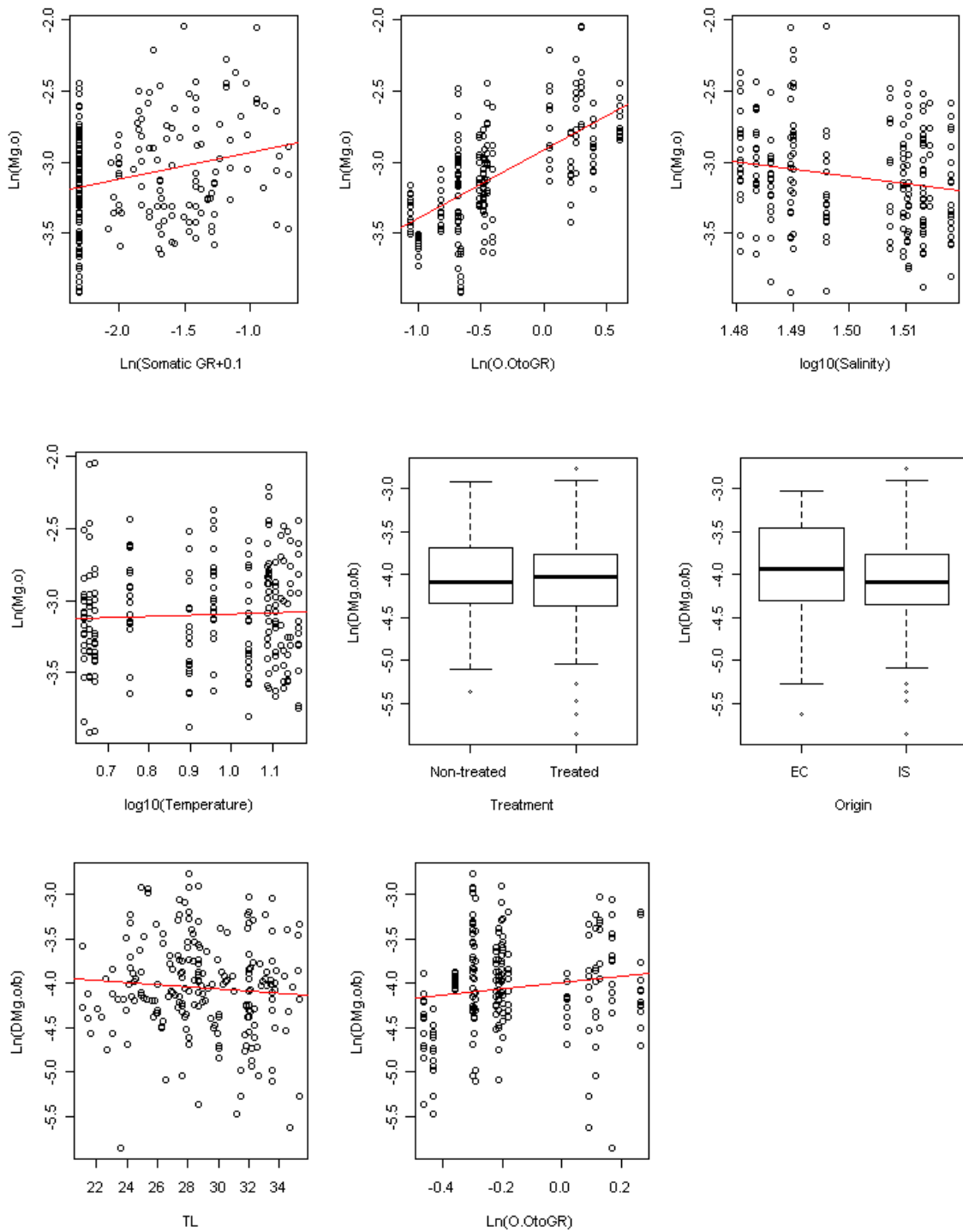


Figure 4.17 Relationships between somatic growth rate (GR,  $(x+0.1)\ln$  transformed, in cm/day), overall otolith growth rate ( $O.OtoGR$ ,  $\ln$  transformed, in  $\mu\text{m}/\text{day}$ ), salinity ( $\log_{10}$  transformed), temperature ( $\log_{10}$  transformed, in  $^{\circ}\text{C}$ ), treatment (GnRH treated/non treated), origin (EC = English Channel, IS = Irish Sea), total length (TL, in cm) and  $Mg_O$  and  $D_{Mg(O/B)}$  values. The boxplot whiskers extend 1.5 times the interquartile range from the 25<sup>th</sup> and 75<sup>th</sup> quartiles (lower and upper ranges of the box, respectively), while the bold line indicates the median

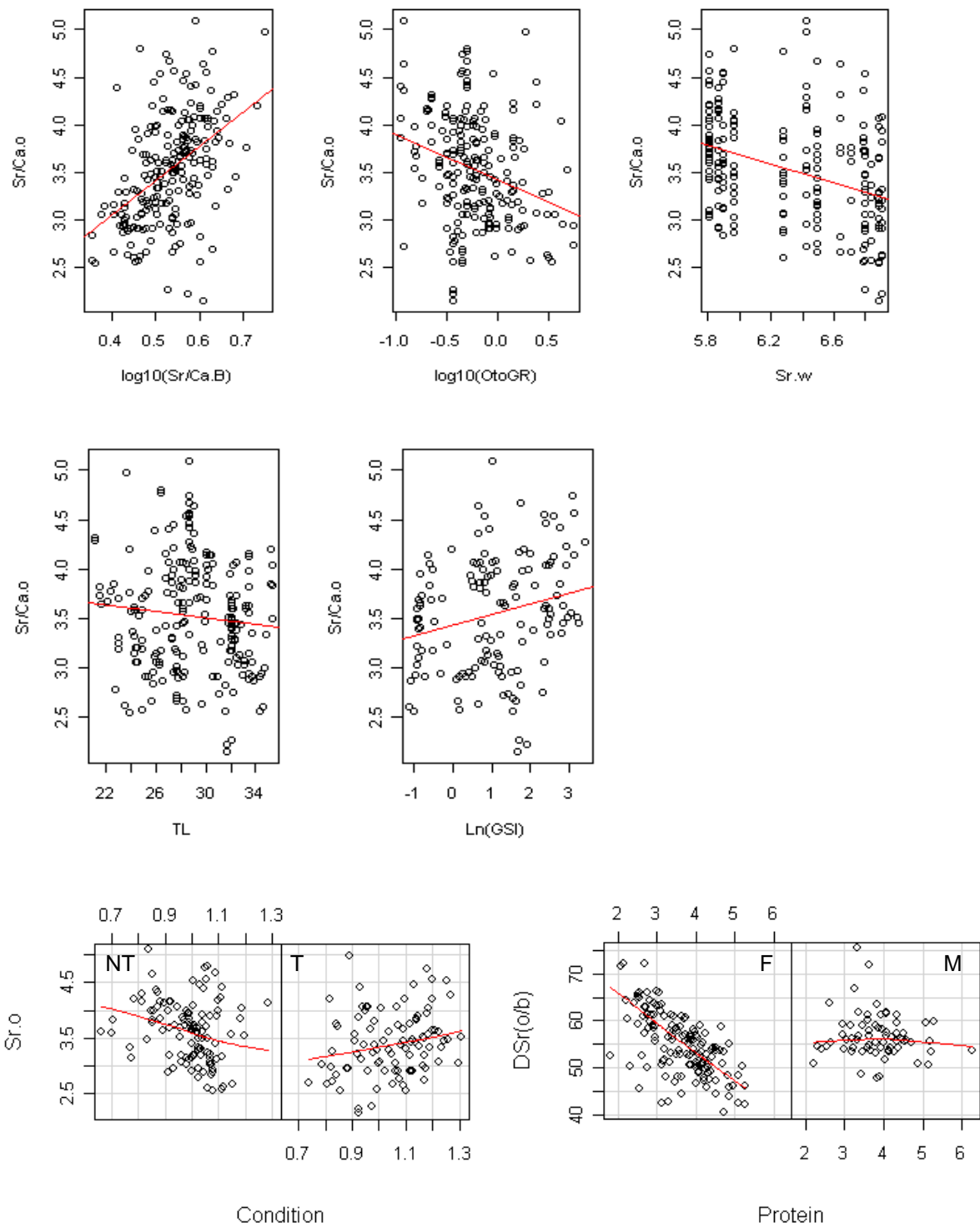


Figure 4.18 Relationships between blood Sr/Ca ratios ( $\log_{10}$  transformed in mmol/mol), otolith growth rate ( $\log_{10}$  transformed, in  $\mu\text{m}/\text{day}$ ),  $\text{Sr}_W$  (in ppm), total length (TL, in cm), GSI ( $\ln$  transformed, in %) and  $\text{Sr}_O$  (Sr/Ca ratios in mmol/mol) and  $D_{\text{Sr(O/B)}}$  (SQRT transformed) values. Note that the interaction between condition and treatment (NT = non-treated, T = GnRH treated) was also highly significant in the  $D_{\text{Sr(O/B)}}$  model, but produced a similar plot to that for  $\text{Sr}_O$ , so is not displayed.

## Barium

The best  $\text{Ba}_\text{O}$  models included a negative effect of salinity and temperature (Figure 4.19), although temperature was only significant in the female only model. Model fit was good ( $r^2 > 0.7$ ), but about 40% was explained by the random effect. If seawater concentrations were excluded from the model selection criteria, the next best model included negative effects of temperature and somatic growth rate. The best model for explaining  $D_{\text{Ba(O/B)}}$  values was based only on a weak negative relationship with otolith growth rate, with greater enrichment in the otolith occurring during periods of slow growth. However, model fit was very poor, with only 1-4% of the variation explained by the fixed effect and the growth rate term was only significant in the female only model.

## Manganese

$\text{Mn}$  was the only element to exhibit a significant positive relationship between water and otolith concentrations. However, this was primarily explained by the increase in  $\text{Mn}_\text{O}$  and  $\text{Mn}_\text{W}$  in the final three months of the experiment and it should be noted that there was no relationship between  $\text{Mn}_\text{B}$  and  $\text{Mn}_\text{W}$  values (Chapter 3). The next most important terms included positive effects of otolith and somatic growth rates, patterns that were also observed for  $\text{Mn}_\text{B}$ . Model fit was good ( $r^2 > 0.7$ ), but like most of the otolith models, around 30% of the variation was explained by the random effect. The female only model exhibited slightly more variation explained by the fixed effects.

Similar to the  $\text{Mn}_\text{O}$  and  $\text{Mg}_\text{O}$  models, there was a positive effect of otolith growth rate on  $D_{\text{Mn(O/B)}}$  values, but also positive effects of day and temperature, largely resulting from the concomitant increases in  $\text{Mn}_\text{O}$  and temperature at the end of the experiment. The negative effect of condition on  $D_{\text{Mn(O/B)}}$  values might partially explain why otolith and blood concentrations were not well correlated, as condition and  $\text{Mn}_\text{B}$  values were significantly positively correlated.

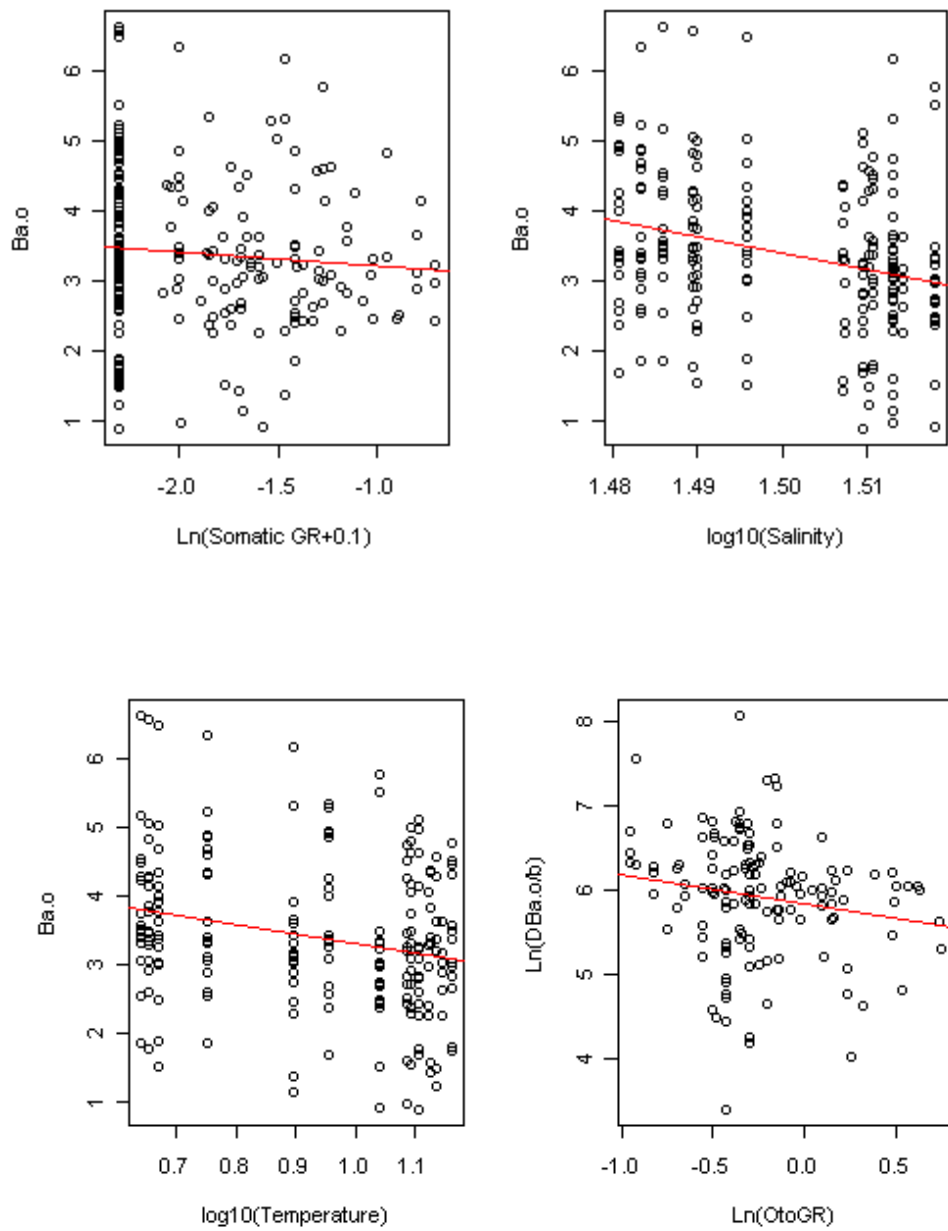


Figure 4.19 Relationships between somatic growth rate (GR,  $(x+0.1)\ln$  transformed, in  $\text{cm/day}$ ), salinity ( $\log_{10}$  transformed), temperature ( $\log_{10}$  transformed, in  $^{\circ}\text{C}$ ) and Ba<sub>O</sub> values (Ba/Ca in  $\mu\text{mol/mol}$ ). Note that somatic growth rate (GR) was not significant, while otolith growth rate (OtoGR,  $\ln$  transformed, in  $\mu\text{m/day}$ ) was only significant in the female only  $D_{\text{Ba(O/B)}}$  model, so only the females are displayed in the bottom right hand plot.

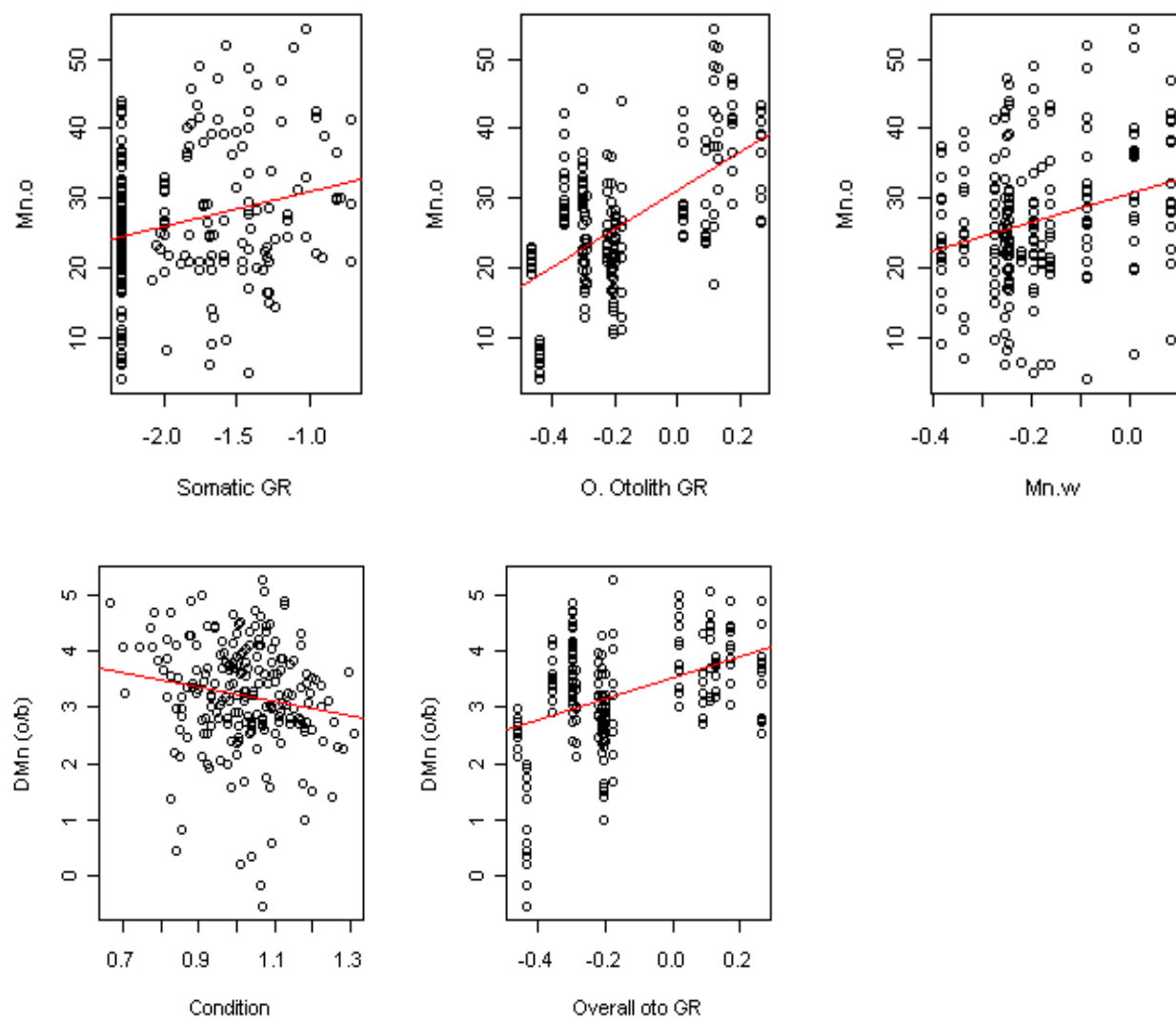


Figure 4.20 Relationships between somatic growth rate (GR,  $(x+0.1)\ln$  transformed, in cm/day), overall otolith growth rate (O.OtoGR,  $\ln$  transformed, in  $\mu\text{m}/\text{day}$ ),  $\text{Mn}_w$  ( $\log_{10}$  transformed, in ppb) and  $\text{Mn}_o$  (above), and between condition and overall otolith growth rate (O.OtoGR,  $\ln$  transformed, in  $\mu\text{m}/\text{day}$ ) and  $D_{\text{Mn}(O/B)}$  (below)

## Copper

$\text{Cu}_\text{O}$  models included a weakly negative effect of condition and  $\text{Cu}_\text{W}$  (or temperature), although the latter trend was most apparent in the females (Figure 4.21). The relationship between  $\text{Cu}_\text{W}$  and  $\text{Cu}_\text{O}$  values in the females was driven almost entirely by the elevated otolith concentrations exhibited during the spawning season, when temperature and ambient concentrations were at their lowest.  $D_{\text{Cu(O/B)}}$  values were driven primarily by a negative relationship with temperature, although as above, this was primarily exhibited in the females and driven by concentrations exhibited specifically during the spawning season. There was also a strong negative correlation between  $D_{\text{Cu(O/B)}}$  values and condition and protein.

## Zinc

$\text{Zn}_\text{O}$  values were largely explained by a significant positive effect of temperature or  $\text{Zn}_\text{W}$  in the females and non-linear negative relationships in the males (Figure 4.22). Overall,  $\text{Zn}_\text{O}$  values were higher in the males and lower in spawning fish. Zn was the only element whose concentrations in the otolith were significantly correlated with GSI, with  $\text{Zn}_\text{O}$  values negatively related to GSI in spawning females but no relationship exhibited by non spawning fish. Overall model fits were relatively low, but slightly more was explained by the fixed effects in the female only model (28% vs. 23%) and a relatively low proportion of the variance explained by the random effect (9-15%). Similar to the  $\text{Zn}_\text{O}$  model, there was a significant interaction between temperature and sex in the  $D_{\text{Zn(O/B)}}$  model, indicating elevated incorporation rates at low temperatures in the males, however the model fit was poor, with only 6% explained by the fixed effects. This contrasted with the female only model, where a significant negative effect of protein and a weak positive effect of condition on  $D_{\text{Zn(O/B)}}$  resulted in a reasonable model with 31% of the variation explained by the fixed effects.

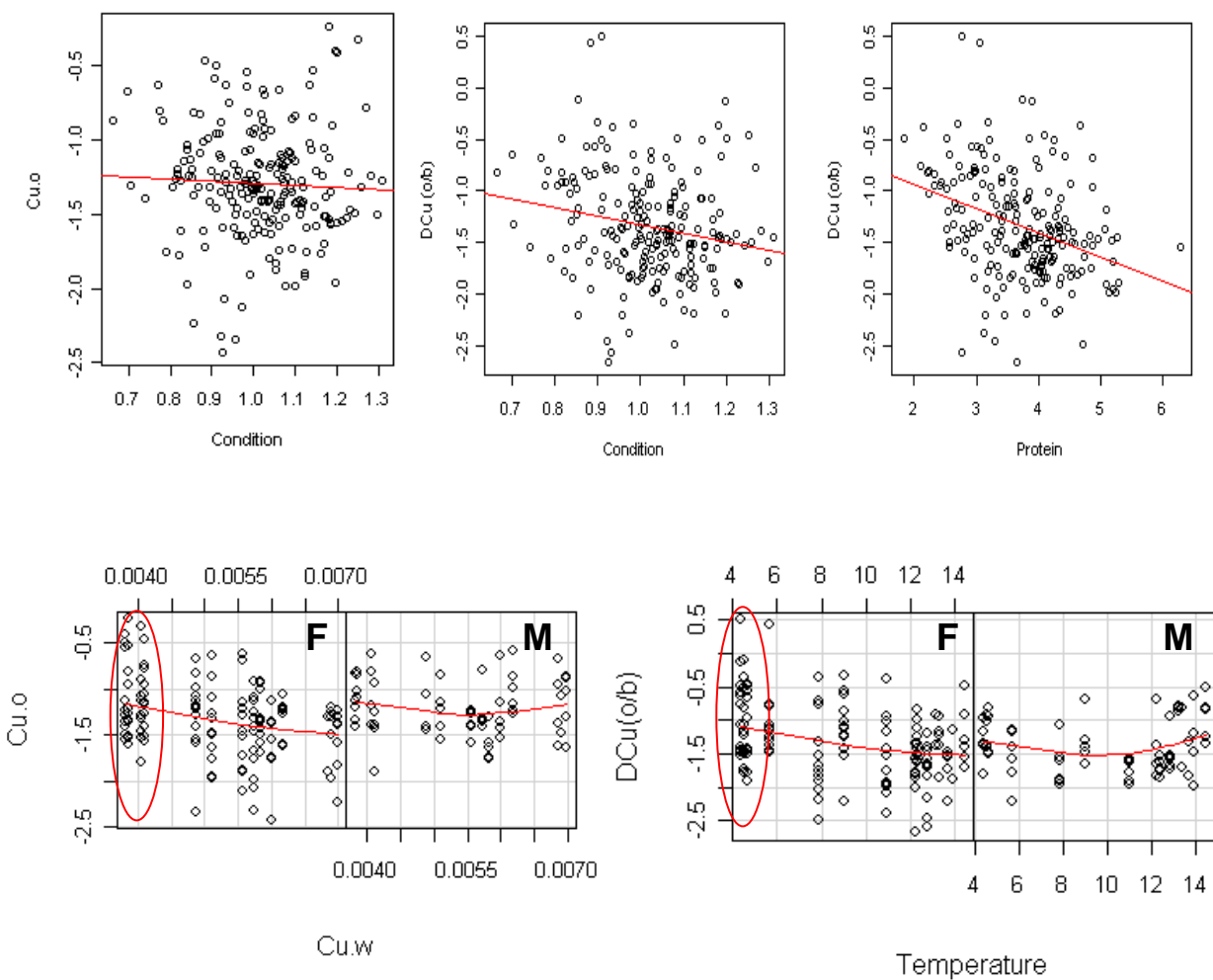


Figure 4.21 Relationships between condition, protein concentrations (g/dL), Cu<sub>W</sub> (ppm), temperature (°C) and Cu<sub>O</sub> (Ln transformed Cu/Ca ratios in  $\mu\text{mol/mol}$ ) and D<sub>Cu(O/B)</sub> values. Coplots in the lower row indicate the relationships between ambient concentrations and Cu<sub>O</sub>, and temperature and D<sub>Cu(O/B)</sub> values in females (F) and males (M) separately. The relationship in the females was largely driven by the enriched Cu<sub>O</sub> values exhibited at the start of the spawning season (red circle)

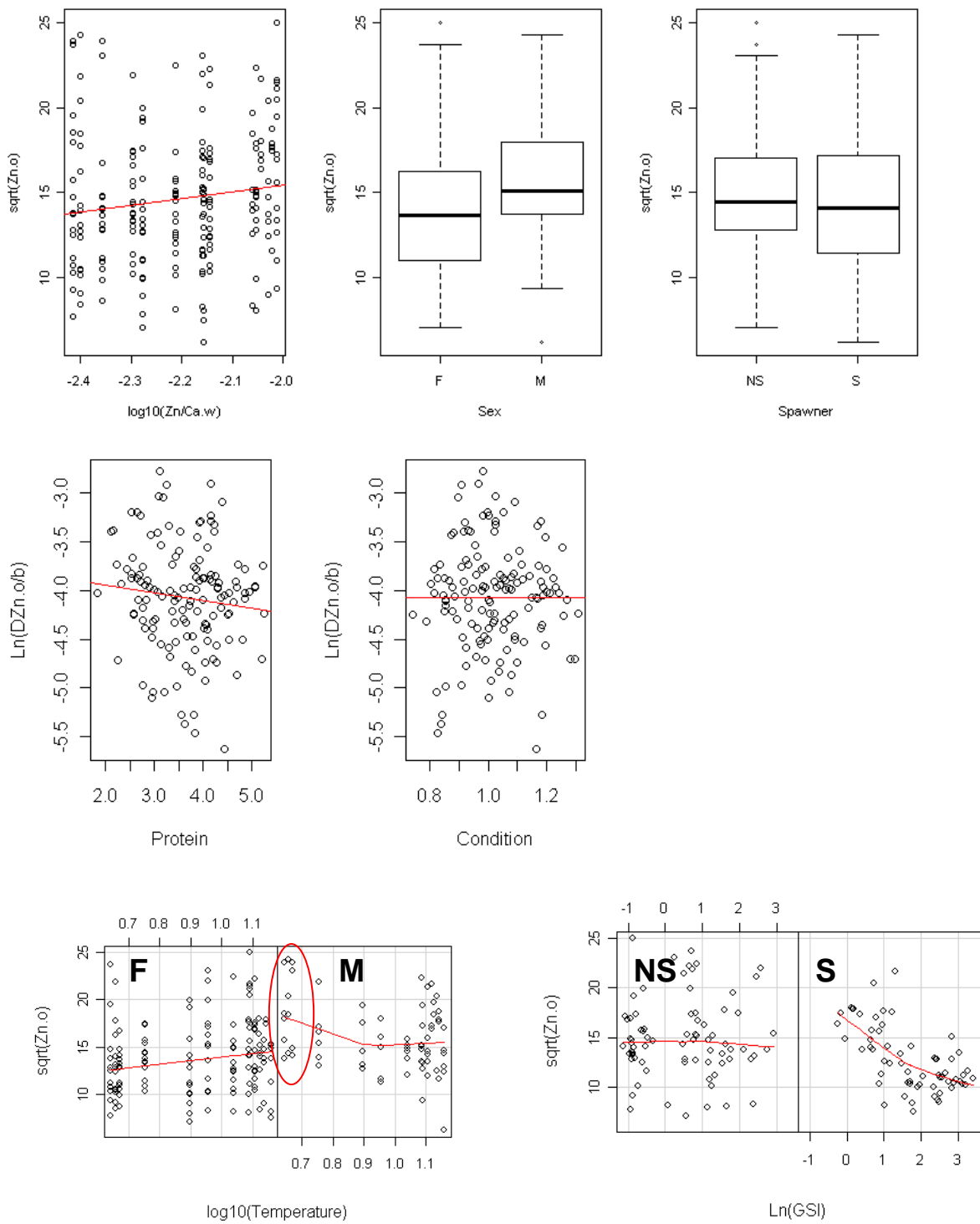


Figure 4.22 Main trends in  $Zn_O$  and  $D_{Zn(O/B)}$ . Note that the temperature\*sex interaction was also significant in the full  $D_{Zn(O/B)}$  model, but the effect was similar to  $Zn_O$  so is not displayed. Also note that the negative relationship between temperature (or  $Zn_W$ ) in the males was driven largely by enriched otolith concentrations exhibited at the start of the spawning period when temperatures were at their lowest (red circle). In the coplot on the right, the relationship between GSI and  $Zn_O$  values in the females differed significant between spawning (S) and non-spawning (NS) fish. The boxplot whiskers extend 1.5 times the inter-quartile range from the 25<sup>th</sup> and 75<sup>th</sup> quartiles (lower and upper ranges of the box, respectively), while the bold line indicates the median

## 4.4 Discussion

While the experimental design used in the current study does not allow for formal hypothesis testing, if the null hypothesis was that “otoliths incorporate elements in proportion to ambient concentrations” then the results presented herein would allow us to reject it with confidence. If otoliths had been faithfully recording water chemistry, then correlations between water and otolith element concentrations and (or) El/Ca ratios would have been consistently positive and the otolith:water distribution coefficients would not have varied over time or among groups of fish. This is further corroborated by the simple observation that for most of the elements examined (Li, K, Sr, Ba, Cu and Zn) the highest otolith concentrations were found between January and March, when salinity and ambient concentrations were at their lowest. In the blood, concentrations of Li, Rb, Mg and Zn exhibited positive, albeit weak, correlations with ambient concentrations, but most elements exhibited no correlations, negative correlations or contradictory results between the males, IS females and EC females (e.g. Cu<sub>B</sub> and Pb<sub>B</sub>). This, along with the limited number of elements to bear positive relationships between blood and otolith and water and otolith, indicates significant partitioning of elements at all major interfaces. Given the impressive osmoregulatory abilities of marine fish (Evans, 1993), it is not particularly surprising that the movement of ions from water to blood is tightly regulated and ambient fluctuations dampened in the blood. Moreover, the endolymph exhibits depletion of all major ions apart from K (Kalish, 1991), but similar levels of most trace elements (Melancon *et al.*, 2009), implying that fractionation between endolymph and otolith is also important. An observation of clear importance was the existence of significant differences in otolith element concentrations between the sexes and between fish from different populations and/or maturity status, that came about whilst coexisting under identical conditions. These observations have potentially serious implications for studies using otolith microchemistry as a natural tag in marine systems, although intrinsic, inter-population differences in elemental processing could theoretically increase its value as a stock discriminator (e.g. Clarke *et al.*, 2011).

Before discussing patterns in individual elements, it is important to again mention the limitations of the current study. Discussed more fully in Chapter 3, it is clear that a mensurative experiment such as this is innately complex. In lieu of controlled, multi-level experiments it is not possible to isolate specific controlling factors with confidence. Similarly, the observed differences in otolith chemistry among groups of fish, under these particular conditions, might be minor compared with differences among wild populations. However, as discussed in Chapter 1, the sea is relatively stable and homogeneous compared with most aquatic systems (Turekian, 1968). Given the coastal water used in the current study, salinities varied more in the current experiment than they do in most open ocean settings. Finally, the different sources of the female fish was not ideal, comprising two groups differing on many levels. The IS females were almost entirely mature, while the

EC females were generally young, large and immature. Thus, it was not possible to fully explain significant 'origin effects'.

Given the variety of trends and patterns observed in this chapter, elements will be discussed in four pairs:  $\text{Li}_\text{O}$  and  $\text{K}_\text{O}$ ,  $\text{Mg}_\text{O}$  and  $\text{Mn}_\text{O}$ ,  $\text{Sr}_\text{O}$  and  $\text{Ba}_\text{O}$ ,  $\text{Cu}_\text{O}$  and  $\text{Zn}_\text{O}$  due to broadly similar patterns in otolith concentrations.

#### 4.4.1 $\text{Li}_\text{O}$ and $\text{K}_\text{O}$

The high correlation between  $\text{Li}_\text{O}$  and  $\text{K}_\text{O}$  values (PCC = 0.83) implied similar modes of incorporation, and for both, concentrations were largely explained by otolith opacity, suggesting a common biomineralisation effect. Other studies have also observed significant enrichment of K and (or) Na in opaque regions (Fuiman and Hoff, 1995; Tomás *et al.*, 2006), however, the factors governing differences otolith opacity are not well understood. While translucent zones are 'traditionally' described as 'winter zones' in Northern hemisphere temperate species, the timing of growth zone deposition can vary significantly among subpopulations (Van Neer *et al.*, 2004; Høie *et al.*, 2009), species (Beckman and Wilson, 1995) and life history stages, with decoupling of temperature and growth zone transition increasingly common in mature fish (Høie and Folkvord, 2006). It has been suggested that opacity is driven by protein concentrations in the organic matrix (OM) (Hüssy *et al.*, 2004), however in one study found no difference in soluble protein concentrations between vateritic and aragonitic otoliths (Tomás *et al.*, 2004), implying that soluble proteins are not the main driver of otolith opacity. It is also widely stated that opaque zones are deposited during warm, high productivity periods, however, this too appears to be erroneous, particularly in mature fish (Høie and Folkvord, 2006). It could be that differences in crystal properties or concentrations of OM components such as insoluble proteins, lipids, sugars and(or) proteoglycans vary as a function of opacity, resulting in preferential inclusion of monovalent ions in these regions.

Concentrations of  $\text{Li}_\text{O}$  and  $\text{K}_\text{O}$  were higher in the males than the females, although this difference was clearly driven by the divergence among the IS fish, particularly during the first half of the experiment. Given the similar otolith concentrations exhibited by the males and EC females, the 'sex effect' is most likely to be explained by differences in otolith opacity. While the opacity 'scoring system' used in this study was crude, there were clear trends that were consistent with the differences in  $\text{Li}_\text{O}$  values observed among the three 'groups' of fish. However there also appeared to be significant additional 'environmental effects', with concentrations of both otolith elements increasing in all fish while temperature and salinity were decreasing. Both elements were negatively correlated with ambient concentrations (or temperature) and  $D_{\text{Li(O/B)}}$  was

negatively correlated with temperature. The only empirical study to examine the effects of ambient concentrations on  $\text{Li}_\text{O}$ , using larvae of two galaxiid species and salinities of 2 to 34, observed a strong positive relationship between  $\text{Li}_\text{O}$  and salinity, with the linearity of the slope indicating an effect of absolute  $\text{Li}_\text{W}$  concentrations rather than  $\text{Li}/\text{Ca}_\text{W}$  ratios (Hicks *et al.*, 2010). However, in the same study a strong negative linear relationship was observed between  $\text{Rb}_\text{O}$  and salinity, implying different modes of incorporation and(or) uptake mechanisms among the different monovalent ions. Here, we observed a near perfect correlation between  $\text{Rb}_\text{B}$  and  $\text{K}_\text{B}$  values ( $\text{PCC} = 0.96$ ), a weak correlation between  $\text{K}_\text{B}$  and  $\text{Li}_\text{B}$  ( $\text{PCC} = 0.13$ ), and a high correlation between  $\text{K}_\text{O}$  and  $\text{Li}_\text{O}$  ( $\text{PCC} = 0.82$ ). This suggests that the most important interface controlling the ultimate incorporation of these monovalent ions into the otolith is blood-endolymph or endolymph-otolith. Based on the observed effects of otolith opacity it is perhaps more likely to be the latter. There may still be ‘environmental influence’ however. The most parsimonious explanation for the apparent contradiction of the  $\text{Li}_\text{O}$  vs  $\text{Li}_\text{W}$  relationship reported by Hicks *et al.* (2010) is that the ‘environmental effect’ observed in the current experiment was driven by temperature rather than ambient concentrations. Indeed, temperature sensitivity is well documented in foraminifera (Marriott *et al.*, 2004) and temperature was a significant explanatory variable in the  $D_{\text{Li}(\text{O/B})}$  model.

Finally, there is also the possibility that the lower  $\text{Li}_\text{O}$  and  $\text{K}_\text{O}$  concentrations in the IS females was related to ovary maturation.  $\text{K}_\text{O}$  values were depleted in the GnRH treated and spawning fish, although the effects were not significant. Fuiman and Hoff (1995) observed annual cycles in  $\text{K}_\text{O}$  and  $\text{Na}_\text{O}$  that became apparent following onset of sexual maturity, were depleted during the spawning season, and appeared asynchronous with ambient temperatures, leading to speculation of a link between  $\text{K}_\text{O}$  and  $\text{Na}_\text{O}$  and reproductive activity. If, as suggested in the previous chapter, there is a requirement for plasma  $\text{K}^+$  to be rerouted to the ovaries during the early stages of ovary maturation, then the depleted  $\text{K}_\text{O}$  levels in the IS females might corroborate this. However, neither GSI, treatment or spawning were included in the final models, suggesting that any such effect might be an indirect effect of spawning on otolith growth rates or biomineralisation, or that any direct effects were temporally lagged.

#### 4.4.2 $\text{Mn}_\text{O}$ and $\text{Mg}_\text{O}$

$\text{Mn}_\text{O}$  and  $\text{Mg}_\text{O}$  values exhibited similar trends over time ( $\text{PCC} = 0.66$ ), and unlike all of the other elements examined, were not enriched during the winter spawning season. Both elements were positively correlated with otolith growth rate, both in terms of their absolute concentrations and otolith:blood distribution coefficients. Also,  $\text{Mn}_\text{O}$  was partly explained by somatic growth rate and  $\text{Mg}_\text{O}$  positively related to condition, although the effect was not significant.  $\text{Mg}_\text{O}$  and  $D_{\text{Mn}(\text{O/B})}$  values were also positively correlated with

temperature. There is evidence of significant positive temperature and growth rate effects on  $Mg_O$  in juvenile Chinook salmon (*Oncorhynchus tshawytscha*) (Miller, 2011), however other experiments have identified no or negative effects (Martin and Thorrold, 2005; Martin and Wuenschel, 2006; DiMaria *et al.*, 2010).

Teasing apart the effects of temperature and growth rate is one of the most challenging aspects of otolith microchemistry, however, based on the model outputs and conflicting evidence from the literature, temperature-mediated changes in growth rate appear to be the most likely drivers of the similar patterns in otolith  $Mg_O$  and  $Mn_O$  observed.

$Mg_O$  was also negatively correlated with salinity, predominantly due to the increase in  $Mg_O$  from January onwards which was observed in all groups of fish and concurrent with decreasing salinity. In the literature, relationships between  $Mg_O$  and ambient concentrations are generally non significant (Miller, 2011; Woodcock *et al.*, 2011) and occasionally, like here, sometimes even negative (Wells *et al.*, 2003). Mn was the only element to exhibit a significant (and consistent) positive correlation between water and otolith concentrations and the effect was highly similar using  $Mn_W$  concentrations or  $Mn/Ca_W$  ratios. For most elements such a result might as well be interpreted as a positive temperature effect, however,  $Mn_W$  was only weakly correlated with temperature ( $PCC = 0.12$ ) and the use of temperature in place of  $Mn_W$  reduced the  $r^2$  value of the fixed effects by more than half. The only study to report a significant temperature effect on  $Mn_O$  incorporation (that we are aware of) observed a negative relationship (Miller, 2009), further strengthening the argument for the observed trend to be an effect of ambient concentrations over temperature. It should be noted, however, that  $Mn_W$  measurements in the current study were close to detection limits and there was considerable noise in the data that were smoothed when extracting monthly values (Chapter 3). Also, while positive relationships between ambient and otolith Mn concentrations have been observed in the field (Forrester, 2005; Dorval *et al.*, 2007), no single laboratory study has observed a positive relationship (reviewed in Miller, 2009). The cause of this discrepancy remains elusive, however it might be that the method by which  $Mn_w$  was manipulated in the laboratory does not emulate true  $Mn^{2+}$  availability in natural seawater or that the positive effects in wild fish and the current study were caused by varying dietary concentrations. Indeed, a study examining stable isotope ( $^{65}Zn$  and  $^{54}Mn$ ) uptake and accumulation in plaice concluded that water plays a minor role compared to dietary sources (Pentreath, 1973; 1976). Here, the lugworm diet was sourced locally and would have likely varied according to ambient water and sediment chemistry.

#### 4.4.3 $\text{Sr}_\text{O}$ and $\text{Ba}_\text{O}$

$\text{Sr}_\text{O}$  and  $\text{Ba}_\text{O}$  exhibited similar sinusoidal trends over the experimental period ( $\text{PCC} = 0.72$ ), with minimum concentrations during the summer and maximum concentrations over the winter spawning period.  $\text{Sr}_\text{O}$  was strongly negatively correlated with  $\text{Sr}_\text{W}$  values, however this is unlikely to be a true effect given the number of studies that have identified significant positive relationships between ambient and otolith Sr concentrations (e.g. Elsdon and Gillanders, 2003b; Zimmerman, 2005; Miller, 2011). In the current experiment, the seasonal salinity fluctuation was accompanied by near constant  $\text{Sr}/\text{Ca}_\text{W}$  ratios, implying that the effects observed in  $\text{Sr}_\text{O}$  were likely driven entirely by correlated trends in physiology and(or) temperature.

$\text{Sr}/\text{Ca}_\text{O}$  thermometry has received considerable attention in the literature given systematic negative temperature effects on Sr incorporation into abiotic aragonite (Kinsman and Holland, 1969). However, as discussed in Chapter 1, the relationship between temperature and  $\text{Sr}/\text{Ca}_\text{O}$  ratios is far from clear, with evidence for positive (Martin and Wuenschel, 2006) and negative (DiMaria *et al.*, 2010) temperature effects, as well as interactions with salinity (Elsdon and Gillanders, 2002) and physiology (Kalish, 1991). Such discrepancies imply that in the current study, often, the strong negative correlations observed between otolith and seawater concentrations were likely reflecting an effect of ‘spawning season’, with water concentrations less noisy than most physiological data and at their minimum during peak spawning between December and March. Both condition and growth rates were reduced during the spawning period and likely to be the true ‘seasonal effect’ highlighted by this pattern.

Based on the simple observation that  $\text{Sr}/\text{Ca}_\text{O}$  cycles tend to be smaller in juveniles despite exposure to larger temperature variations (Fuiman and Hoff, 1995; Brown and Severin, 2009), the cause of the cycles is likely to be dominated by temperature-related physiological changes or other seasonal factors. The most important physiological variable influencing  $\text{Sr}_\text{O}$  in the current study was  $\text{Sr}/\text{Ca}_\text{B}$ , while in the blood models,  $\text{Sr}_\text{B}$  was explained by growth rate, protein and GSI effects. Thus, a significant proportion of the variance in  $\text{Sr}_\text{O}$  concentrations is explained by blood chemistry. Negative growth rate effects on  $\text{Sr}_\text{O}$  values have been reported for a number of marine species (Sadovy and Severin, 1994) while gonad maturation appears to cause additional effects in  $\text{Sr}_\text{O}$  with concentrations enriched in the mature IS females during February and March. GSI was positively correlated with  $\text{Sr}_\text{O}$  but was not significant, and any effects of GSI were likely explained by the  $\text{Sr}/\text{Ca}_\text{B}$  term in the  $\text{Sr}_\text{O}$  model. The significant ‘condition\*treatment’ interaction likely explained some of the additional variation caused by gonad development, with treated fish investing more into reproduction and exhibiting strong positive relationships between condition and  $\text{Sr}_\text{O}$ . Effects of gonad maturation on  $\text{Sr}/\text{Ca}_\text{O}$  were also observed in sea-caged salmon (Clarke and Friedland, 2004) and wild bearded rock cod

(Kalish, 1991) and it is hypothesised that both gonad maturation and changes in growth rate can alter the blood protein composition and modify ion availability to the endolymph and otolith (Kalish, 1991). It should be noted, however, that despite large fluctuations in absolute  $Sr_B$  relating to gonad maturation, the effect was 'dampened' in  $Sr/Ca_B$  ratios and the otoliths, implying that transfer of  $Sr^{2+}$  ions from blood to endolymph and(or) endolymph to otolith occurs as a function of  $Ca^{2+}$  concentrations.

The high correlation between  $Ba_O$  and  $Sr_O$ , despite such different blood concentrations implies a high degree of error in  $Ba_B$  measurements and(or) significant filtering between blood-endolymph and(or) endolymph-otolith. As for  $Sr_O$  values, the apparent negative relationship with  $Ba_W$  and/or temperature are more likely to be an artefact resulting from multicollinearity within the dataset. The similarities in  $Ba_O$  and  $Sr_O$  patterns over time most likely result from a negative effect of growth rates and(or) condition. Given elevated  $Sr_O$  and  $Ca_O$  in the translucent bands of hake (Tomás *et al.*, 2006), a biomineralisation effect could provide additional explanation for the sinusoidal variation in  $Ba_O$  and  $Sr_O$  concentrations. However, in the current dataset, there were no significant effects of 'opacity' on  $Sr_O$  and  $Ba_O$  concentrations or otolith:blood distribution coefficients. However, without a more sophisticated measure of otolith opacity, such as image luminescence (Tomás *et al.*, 2006), such an effect cannot be ruled out.

#### 4.4.4 $Cu_O$ and $Zn_O$

$Cu_O$  and  $Zn_O$  were the least correlated of the four pairs of elements presented in the current chapter (PCC = 0.40). Both elements exhibited enrichment in the males during the spawning season, however, similar to patterns in the blood,  $Zn_O$  was relatively depleted in both sets of females during this period.

The strongest correlation for  $Cu_O$  was a negative relationship between  $Cu_W$  (or temperature) in the females, driven by the elevated otolith concentrations exhibited during the spawning season, when temperatures and ambient concentrations were at their lowest. There also was a strong negative relationship between  $D_{Cu(O/B)}$  and temperature, condition and protein. These patterns indicate greater uptake of  $Cu^{2+}$  from the blood when blood protein levels are low, possibly resulting from a greater proportion of free 'available' ions, (Fletcher and Fletcher, 1980).

With all fish pooled,  $Zn_O$  values were positively correlated with ambient concentrations (or temperature), although the significant interaction between  $Zn_W$  and sex occurred due to a positive effect in the females but a negative effect in the males. Similar to the trends observed in the females for  $Cu_O$  above, the negative effect

here was driven primarily by the elevated concentrations exhibited during the height of the spawning season. Importantly, there was significant depletion of  $Zn_O$  in the females compared with the males, in spawning fish as well as a clear negative relationship between  $Zn_O$  and GSI in the spawning females. These findings corroborate the results observed in the blood, with  $Zn_B$  levels depleted in the mature IS females and exhibiting significant negative correlations with GSI. The results are likely due to binding of blood  $Zn^{2+}$  to vitellogenin, which transports it to the ovaries, thereby removing it from the blood (Fletcher *et al.*, 1975; Fletcher and King, 1978; Fletcher and Fletcher, 1978; 1980). Corroboration among trends in the blood and otolith imply good potential for  $Zn_O$  to be a useful as 'spawning signal' within the otoliths of female plaice. Such a chemical signal would be of great value in fisheries management as they could potentially identify age-at-maturity and skipped spawning years (Engelhard and Heino, 2005; Jørgensen *et al.*, 2006), both of which could significantly improve current estimates of spawning stock biomass. For female plaice, the decision to skip spawning is generally taken 'early', by individuals exhibiting low condition at the onset of vitellogenesis (Horwood *et al.*, 1989; Kennedy *et al.*, 2008). In such individuals,  $Zn_O$  should not be depleted over the spawning period and provide a true measure of skipped spawning behaviour. However, if the decision to skip spawning occurred later in the season via mass atresia (Kennedy *et al.*, 2008), vitellogenesis and  $Zn_O$  would have already taken place and the marker would presumably miss such events.

The elevated concentrations of  $Cu_O$  and  $Zn_O$  values in many of the groups of fish during the spawning season, when ambient concentrations were at their minimum, could potentially be explained by a change in the source of metal ions to the fish. It is widely believed that the soft metal ions such as  $Zn^{2+}$  (and presumably therefore also  $Cu^{2+}$ ) are primarily sourced from the diet (Pentreath, 1973; 1976), however, during the spawning season plaice stop feeding, even in the presence of food (Rijnsdorp, 1989). During starvation, the percentage of water in fish flesh increases as it replaces constituents such as proteins and lipids (Dawson and Grimm, 1980). During this period, Zn concentrations in the ovaries continue to rise and thus it is thought that the major source of  $Zn^{2+}$  might switch to waterborne  $Zn^{2+}$  (Fletcher and King, 1978). Given that the lack of feeding during this period also results in significantly reduced blood protein levels, the increase in waterborne ions may result in increased relative availability to the otolith and the elevated uptake observed during this period. If such an effect could explain the elevation in  $Zn_O$  in the males during spawning, then it may also help to explain the trends observed in  $Cu_O$  concentrations.

# Chapter 5

---

## *Can otolith chemistry describe movements of marine, adult fish? Insights from DST-tagged wild fish*

### 5.1 Introduction

Theoretical and empirical studies strongly suggest that physiological processes can significantly affect element uptake and incorporation into the otolith (Chapters 1,3,4). A key objective for investigations wishing to use otolith chemistry to provide a natural marker of location is to demonstrate that variations in otolith chemistry caused by intrinsic effects are smaller than those reflecting changes in ambient environmental conditions. If they are not, the implications are serious. Based on the data presented in the previous chapters, physiological influences on blood and otolith microchemistry in plaice are significant, complex and difficult to predict, giving a rather bleak outlook for the use of otolith microchemistry as tag for tracking individual movements. However, while every effort was made to maintain natural conditions and minimise manipulation of the experimental fish, it remains a possibility that their behaviour and physiology differed from their wild equivalents. Similarly, free-ranging plaice are likely to encounter larger environmental gradients than those experienced by the experimental population. In order to gain a fuller picture of the relative importance of intrinsic and extrinsic influences on otolith microchemistry in plaice, a sample of wild

individuals with “known” movements and environmental histories based on data storage tag (DST) records were studied. A previous study of otolith chemistry in DST tagged female plaice revealed cycles in otolith Sr/Ca ratios (Hunter and Darnaude, 2004), similar to those observed in Chapter 4 and in the literature (Brown and Severin, 2009). In the results from Hunter & Darnaude (2004), otolith Sr/Ca cycles increased in amplitude following onset of maturity, with Sr/Ca levels peaking during the spawning season, and their amplitude correlating with migration distance (Figure 5.1). These data imply that environmental conditions and/or migratory behaviour may significantly influence concentrations in wild plaice populations. This would corroborate the experimental results presented in Chapter 4 and the theoretical model suggested by Tomás *et al* (2006), in which otolith Sr/Ca ratios represent an interplay between ontogeny, water composition and environmentally mediated physiological effects.

Plaice is a highly migratory species, whose movements have been extensively studied (Metcalfe *et al.* 2006). Over the course of the twentieth century, mark-recapture experiments have seen the return of over 50,000 individuals (Bolle *et al.*, 2005). Plaice, in fact, were the first ever fish to be deployed with DSTs (Metcalfe *et al.*, 2011), with 1019 DST-tagged plaice released in the North Sea (NS) since December 1993. The culmination of this body of work (partly reviewed by Metcalfe *et al.*, 2006), reveals the NS plaice stock to comprise a spatially structured population with ontogenetic shifts in their distribution and well-defined seasonal migrations between adult spawning and feeding grounds (Hunter *et al.*, 2004). Plaice are able to draw on the fast flowing tidal stream currents in the southern NS to reduce the costs of migration using a means of environmental transport (“selective tidal stream transport”, STST, see Metcalfe *et al.* 2006). Consequently, individual plaice often migrate distances in excess of 300km to distantly located spawning grounds (Hunter *et al.* 2004b). For those plaice located in more northerly areas of the NS, where tidal current flow is slower and cannot provide environmental transport, plaice swim directly to spawning areas (Hunter *et al.*, 2003b; Hunter *et al.*, 2009), usually over shorter distances. From spring onwards, adult plaice aggregate on three major feeding grounds (Figure 5.2), then from late September onwards the fish migrate south and mix on four main spawning grounds in the southern NS and eastern English Channel (Harding *et al.*, 1978; Hunter *et al.*, 2004). The spawning grounds are located upstream of suitable coastal nursery grounds, a phenomenon common to many demersal fish species (Harding *et al.*, 1978), and juveniles recruit into the adult stock at about 2-3 years old (Rijnsdorp, 1989; Metcalfe *et al.*, 2006).

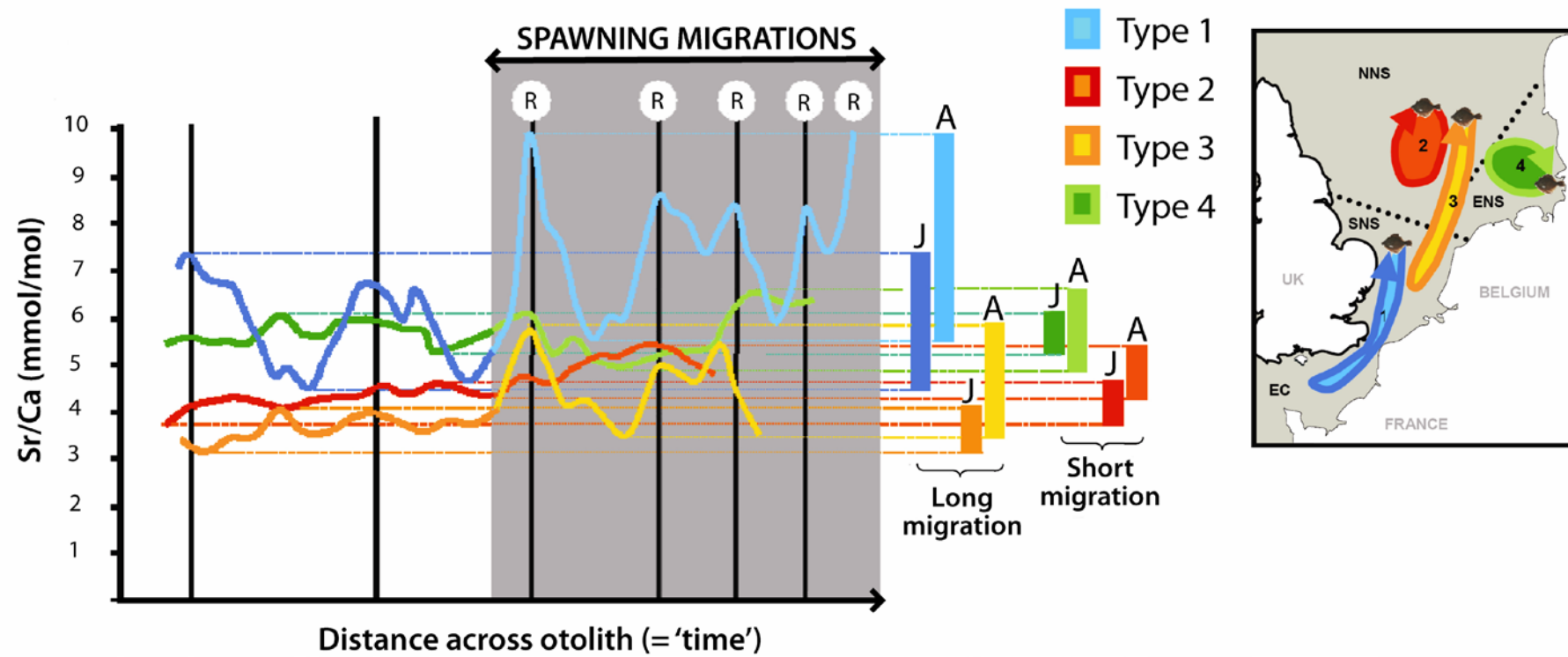


Figure 5.1 Variation in Sr/Ca ratios in female plaice otoliths exhibiting four migration types (shown on the right hand side), before (white) and after (grey shading) onset of sexual maturity. R = reproduction; J = juvenile; A = adult (Hunter & Darnaude, 2004). Vertical bars indicate opaque zones

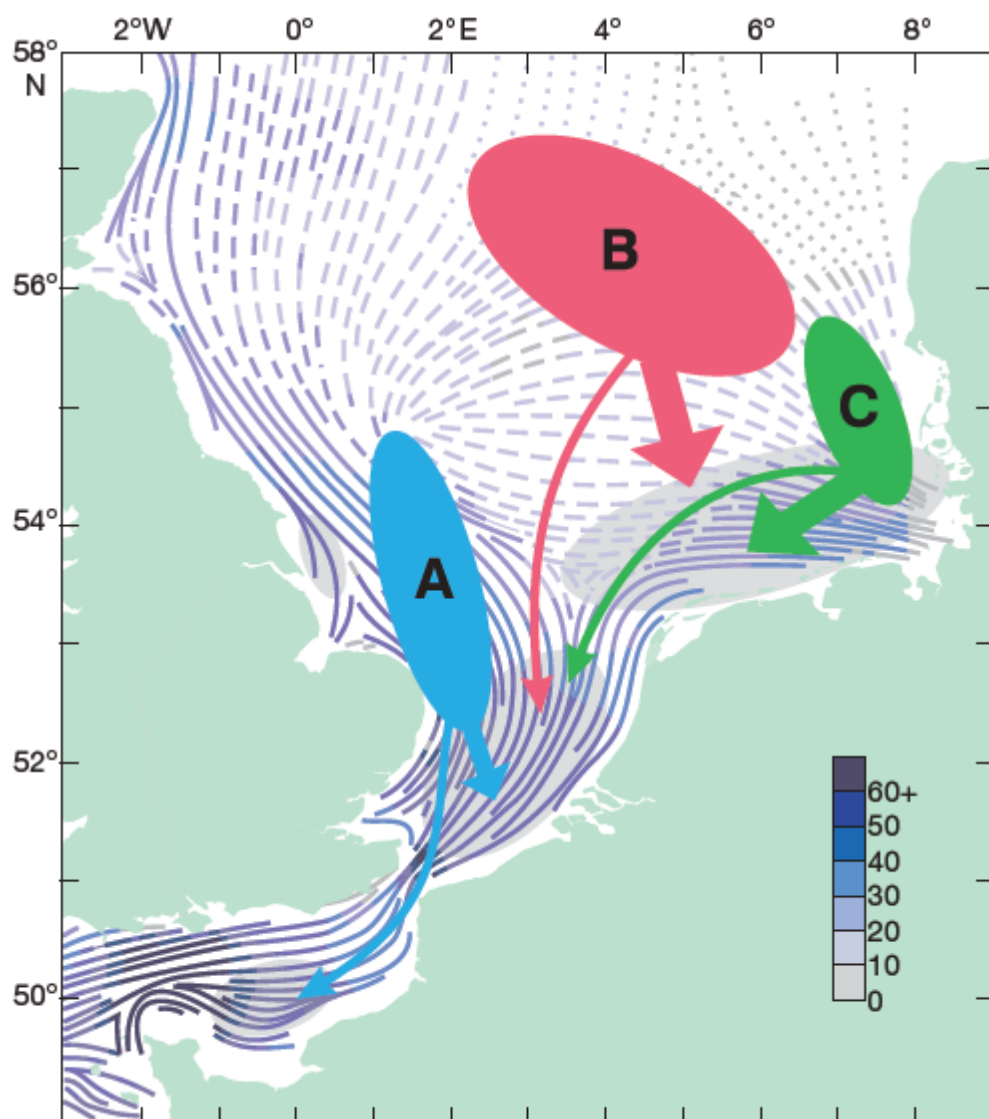


Figure 5.2 Plaice population sub-units (A) western, (B) northern, and (C) eastern summer feeding aggregations. Arrows indicate direction of spawning migrations. Spawning grounds (grey shading) are shown in relation to tidal currents. Lines: direction of tidal flow (broken lines = weaker tidal currents). Line colours: average tidal current velocities across the study area (scale units =  $\text{cm s}^{-1}$ ). From Hunter *et al.* (2009)

The extensive literature on their population dynamics (Metcalfe *et al.*, 2006) and physiological behaviour (Rijnsdorp, 1989) make plaice an ideal model in which to investigate the factors regulating otolith chemistry in a exclusively marine fish. Physicochemical heterogeneity across the NS (Statham *et al.*, 1993; Tappin *et al.*, 1995) also provides support for the application of otolith microchemistry as a natural tag within this marine system. In the current chapter we focus on behaviours of the four elements (Li, Mn, Sr and Ba) that are readily detected in otoliths and that we feel are most likely to be under significant environmental control and thus hold the greatest potential for successful application as a geographic marker in the North Sea plaice. The elements that appeared to be under the greatest physiological control (Cu and Zn) were not examined in the current chapter, as they were deemed less likely to vary with environmental conditions and we had only limited knowledge about the physiological states of the subject animals. The potential for environmental sensitivity of the four otolith elements examined in the current chapter is reviewed below, summarising the main patterns presented in the previous chapters as well as the trends observed in the literature.

Note that throughout the document, otolith elemental concentrations will be denoted ' $El_O$ ' and water concentrations, ' $El_W$ '.

### **Lithium**

The only study to date to have systematically manipulated ambient concentrations and measured both  $Li_W$  and  $Li_O$  observed a strong positive relationship between the two (Hicks *et al.*, 2010). Another study observed a positive effect of salinity but a negative effect of  $Li/Ca_W$  on  $Li_O$  (Milton and Cheshire, 2001b). The experimental results presented in Chapter 4 suggested that  $Li_O$  values were primarily influenced by negative relationships with ambient  $Li_W$  and/or temperature, as well as a positive relationship between  $Li_O$  values and otolith opacity. It was thus hoped that Li concentrations in otoliths of wild, DST-tagged plaice might help to unravel these discrepancies, and also to elucidate whether the significant sex effect (M>F) in the experimental plaice  $Li_O$  was a phenomenon common among wild populations.

### **Manganese**

The experimental results presented in Chapter 4 suggested a positive effect of growth rate and condition on Mn incorporation into the otolith, as well as a positive influence of ambient concentrations. Dissolved Mn also exhibits large spatial and temporal variability among the regions under study (Burton *et al.*, 1993). While there is no empirical evidence for a positive effect of  $Mn_W$  on  $Mn_O$  there have been positive correlations in field studies (e.g. Forrester, 2005) and it is a commonly utilized element in stock discrimination studies (e.g.

Longmore *et al.*, 2010). It was thus hypothesised that Mn<sub>O</sub> might vary among North Sea plaice population subunits.

### **Strontium**

Based on the experimental data presented in Chapter 4, Sr<sub>O</sub> appeared to be primarily under physiological control (blood proteins, growth rate and condition), however it was not possible to rule out a direct, negative temperature effect on Sr<sub>O</sub>. A number of studies have observed a positive effect of ambient Sr concentrations and thus salinity on Sr<sub>O</sub> (e.g. Zimmerman, 2005), while correlations between migration distance and Sr<sub>O</sub> variability (Hunter and Darnaude, 2004) also suggest that Sr<sub>O</sub> might be useful for elucidating movements patterns of North Sea plaice.

### **Barium**

Controls on Ba<sub>O</sub> values in the experimental plaice (Chapter 4) were somewhat inconclusive, partly due to relatively low levels of variation in the ambient water and analytical difficulties, but temperature, water chemistry, and growth rates were highlighted as potential influencing factors. In the literature, however, relationships between Ba<sub>W</sub> and Ba<sub>O</sub> are common (e.g. Elsdon and Gillanders, 2003b) and thus it was hypothesized that Ba<sub>O</sub> concentrations might vary significantly among regions characterised by different salinities.

Time-resolved otolith trace elemental concentrations were measured in plaice with ‘known movements’ based on DST records from the western (WNS), central (CNS) and eastern North Sea (ENS) subunits. For each element, spatial and temporal trends are examined and linear mixed effects models used to explore whether concentrations are best explained by extrinsic (population subunit, migratory behaviour, temperature, salinity) or intrinsic (sex, age, size, growth rate, condition) factors. Finally, the potential for each element to serve as a natural geolocator in North Sea plaice is discussed.

## 5.2 Methods

### 5.2.1 Analytical methods

Otoliths were prepared and analysed using the methods described in Chapter 4, but in brief, spot analyses were carried out in transects perpendicular to growth bands across the DST-tagged period for  $\delta^{18}\text{O}$  ( $\sim 20\mu\text{m}$  resolution, SIMS). Note that in the current document, such measures of 'spot resolution' indicate centre-to-centre measurements), Sr, Ba, Mg, K and Li ( $10\mu\text{m}$  resolution, SIMS), Sr, Ba, Mn, Zn, Cu ( $\sim 20\mu\text{m}$  resolution by offsetting transect lines of  $35\mu\text{m}$  spots, HR-LA-ICPMS). Predicted vs. measured  $\delta^{18}\text{O}$  profiles were 'wiggle matched' in AnalySeries 2.0 (Paillard *et al.*, 1996) to assign a timeline to each section (profiles presented in Appendix 1.3). Predicted  $\delta^{18}\text{O}$  values were calculated using DST-recorded temperatures, salinity values predicted by the General Estuarine Transport Model (GETM) and a temperature-dependent fractionation equation derived from Atlantic cod (Hoie *et al.*, 2004). There was generally greater subjectivity in timeline assignment compared with previous chapters, given a lack of an artificial start check on the otolith, two individuals with substantial lags between the end of the DST record and their recapture, and generally older subjects and thus narrower otolith growth increments. However, some of the otoliths exhibited a slight check at the start of the DST period and correlation coefficients between predicted and measured  $\delta^{18}\text{O}$  values were still generally  $>0.8$ . The lower spatial resolution achievable for LA-ICPMS analyses ( $35\mu\text{m}$  spot size) was particularly limiting, particularly for elements close to detection limits (e.g. Cu and Zn) and for transverse sections of older fish. For studies aiming to obtain detailed intra-annual information, it is clearly advantageous to use frontal sections and younger subjects where possible. While there were some concerns regarding calibration of SIMS measured-Ba (Chapter 4), the greater spatial resolution meant that SIMS-measured Ba and Sr concentrations were used for mixed model analyses, however, the same correlations were observed between LA-ICPMS measurements and predictor variables, indicating similar trends among analysis types.

As mentioned above, ambient temperatures and salinities for the estimated daily locations of DST-tagged plaice were predicted using the General Estuarine Transport Model (GETM) for the North Sea (Stips *et al.*, 2004). The model domain extends from a boundary in the western English Channel ( $-5^\circ\text{E}$ ) into the North Sea with an eastern boundary in the Baltic ( $16^\circ\text{E}$ ) and then northwards as far as the Shetland Isles ( $60^\circ\text{N}$ ) at a resolution of  $\sim 6\text{nm}$  and with 25 terrain-following vertical levels. Meteorological forcing in the model was derived from the European Center for Medium-range Weather Forecasting ERA datasets. Tidal boundaries were calculated from Topex-Poseidon satellite altimetry, and temperature and salinity boundary conditions were taken from the climatologic predictions of the POLCOMS S12 model (<http://cobs.pol.ac.uk/modl>).

## 5.2.2 Description of study animals

The DST experiments were carried out in two main ‘phases’: in 1997-1998 when mature females were targeted and in 2004-2005, when DSTs had been further miniaturised allowing males and smaller, younger females to be tagged as well. The experiment methods and results have been described in full (Hunter *et al.*, 2003a; Hunter *et al.*, 2003b; Hunter *et al.*, 2004a; Hunter *et al.*, 2004b; Hunter *et al.*, 2009), but in brief, geolocations were estimated by matching DST-recorded pressure (depth) records with a tidal database when an individual spent a full tidal cycle on the seabed. Temperature records, hidden Markov models and ‘behavioural switching’ between high and low activity states were used to refine geolocation estimates and provide a ‘most probable track’ for each fish (Pedersen *et al.*, 2008).

Eleven North Sea plaice (7 females, 4 males) are featured in the current chapter. Details of the fish, their migration pathways and their temperature histories are provided in Table 5.1 and Figures 5.3-5.5. The youngest animal (A12431), a female from the CNS, was two years old on release and carried out undirected movements for the following 15 months. It was only at the latter end of the spawning season (2 months before recapture) that there was any sign of directed movement, when she began migrating south east. Given her age and migratory behaviour it was assumed that she was immature for most if not all of her time at liberty. The directed movement towards the end of the experiment (just turned 5 years old) might have represented a ‘dummy run’ following onset of maturation, a fairly common phenomenon among maturing plaice in the year prior to their first full spawning migration (Metcalfe *et al.*, 2006).

Table 5.1 Details for the 11 fish (8F, 5M) presented in the current chapter, ordered by population subunit (Figure 5.2). Note that  $K$  = Fulton’s condition factor

Fish ID	Sex	Section type <sup>†</sup>	Release date	End of DST recording	N° DST days	Spawning migration ‘type’	End age (yrs)	Start TL (cm)	End TL (cm)	Growth rate (cm/mo)	End TW (g)	End $K$	Otolith growth rate ( $\mu\text{m}/\text{d}$ )
3.4-1000	F	At	18/02/98	06/04/99	411	>200km	9	52	52.3	0.02	1250	0.87	0.44
A12454	F	Af	20/10/04	22/10/05	367	>200km	5	31	32.1	0.09	335	1.01	0.83
A12382	M	Af	20/10/04	09/01/06	446	>200km	6	29	29.7	0.05	263	1.00	0.35
A12391	M	Af	22/10/05	14/08/06	296	>200km	5	29	28.8	-0.02	214	0.90	0.61
3.2-1120	F	At	28/10/97	17/07/98	262 <sup>†</sup>	<200km	7	40	41.2	0.08	748	1.07	0.53
3.2-1137	F	Af	12/11/97	03/06/98	202	<200km	5	40	41	0.15	717	1.04	0.99
3.2-1207	F	At	28/10/97	15/11/98	383	>200km	8	47	48.1	0.08	1227	1.10	
3.3-1127	F	At	05/12/97	26/12/98	386 <sup>†</sup>	<200km	13	40	40	0.00	592	0.93	
A12431	F	Af	19/10/04	02/05/06	560	Undirected	4	27	29.9	0.15			0.71
A12388	M	Af	19/10/04	31/1/06	469	<200km	7	32	33.1	0.07	278	0.77	0.21
A12522	M	Af	19/10/04	30/1/06	468	<200km	5	30	30.6	0.04	213	0.74	0.49

<sup>†</sup>A = left (‘Asymmetric’) otolith, t = transverse section and f = frontal section; <sup>†</sup>180-187 day lag between end of DST recording and recapture

### WNS FISH (BLUE SUBUNIT)

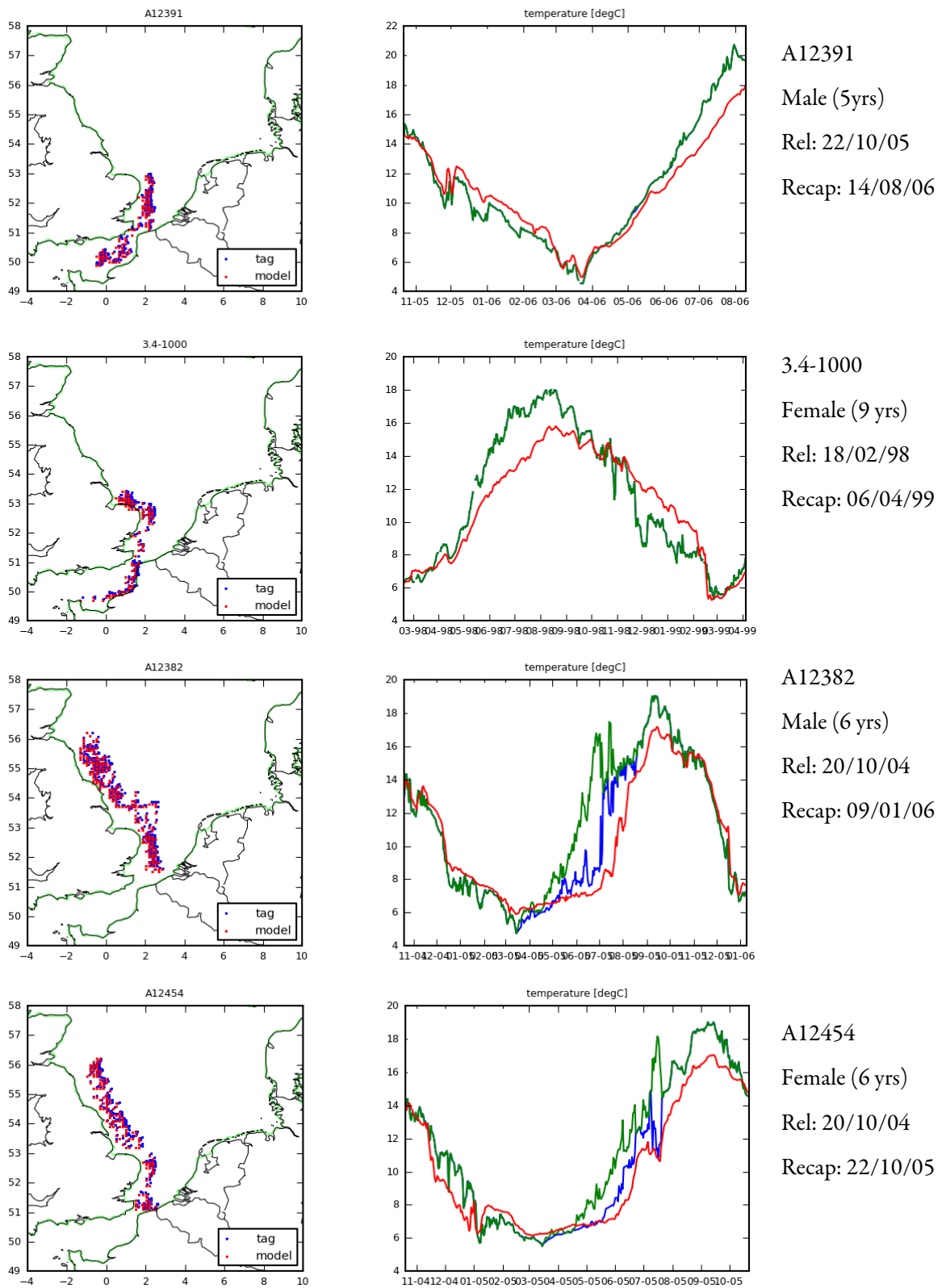


Figure 5.3 Migration pathways (blue spots indicating 'best daily fits' based on DST tag records; red spots indicating closest daily positions constrained by model grid cells), details and temperature histories (red = DST measured; blue = seabed, green = sea surface) of four WNS (blue subunit) plaice tagged by DST. Note different release years.

## CNS FISH (RED SUBUNIT)

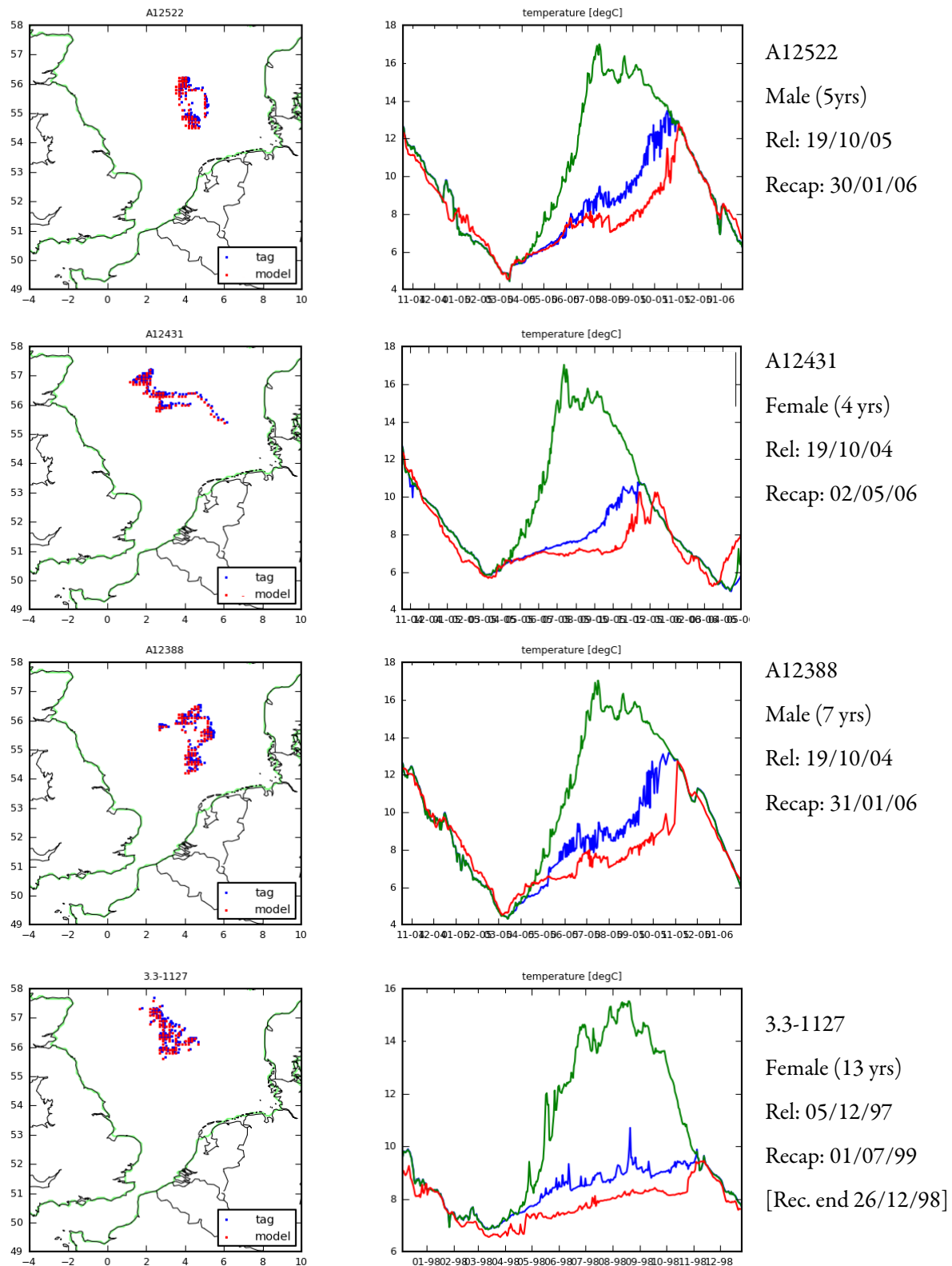


Figure 5.4 Migration pathways (blue spots indicating 'best daily fits' based on DST tag records; red spots indicating closest daily positions constrained by model grid cells), details and temperature histories (red = DST measured; blue = seabed, green = sea surface) of four CNS (red subunit) plaice tagged by DST. Note different release years.

## ENS FISH (GREEN SUBUNIT)

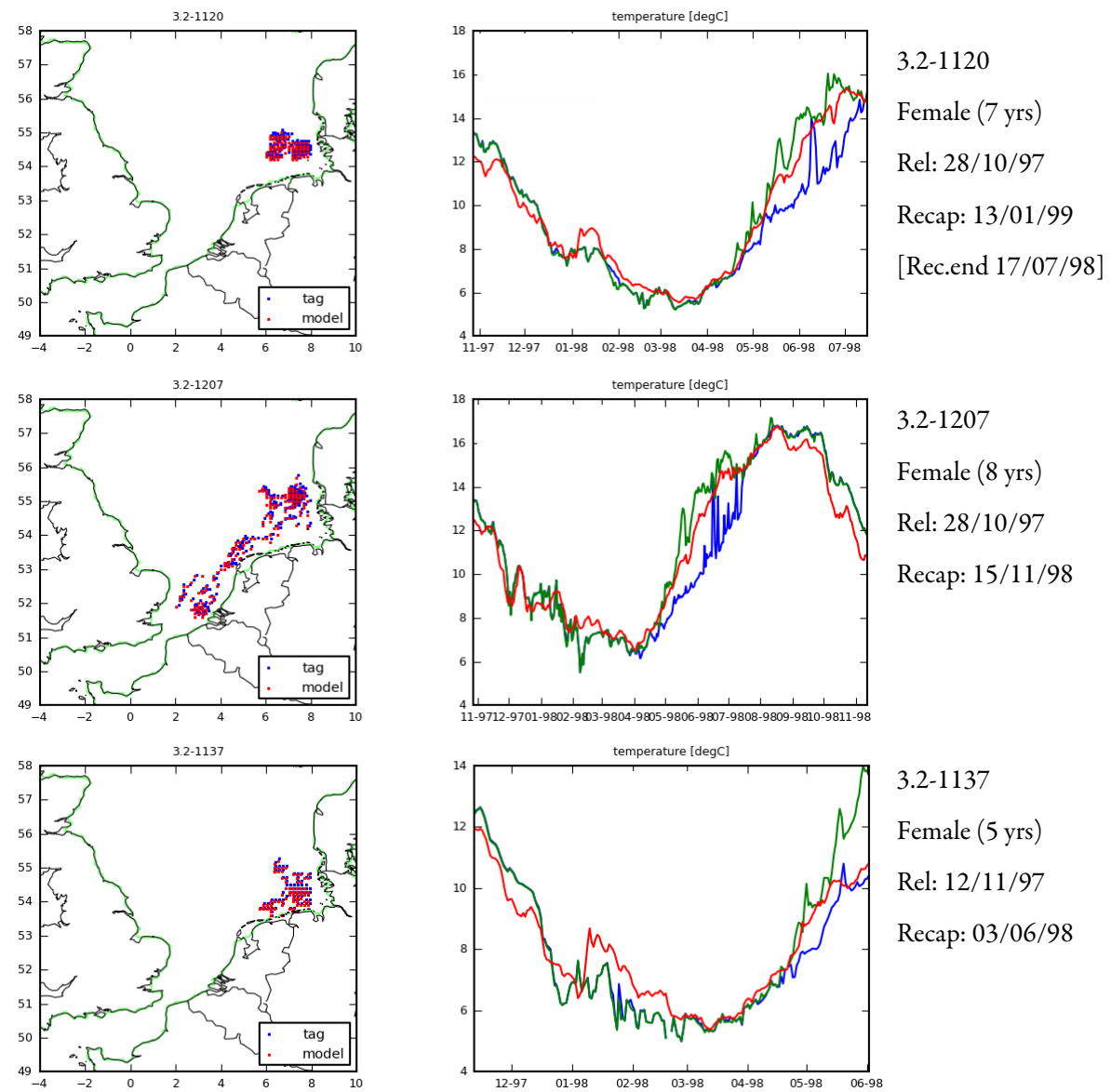


Figure 5.5 Migration pathways (blue spots indicating 'best daily fits' based on DST tag records; red spots indicating closest daily positions constrained by model grid cells), details and temperature histories (red = DST measured; blue = seabed, green = sea surface) of three ENS (green subunit) plaice tagged by DST.

### 5.2.3 Data analysis

Linear mixed model analyses (lmer, lme4 package) were carried out in R to see which combination of terms explained most variation in  $\text{Sr}_\text{O}$ ,  $\text{Mn}_\text{O}$ ,  $\text{Li}_\text{O}$  and  $\text{Ba}_\text{O}$ . Methods for the model selection process are outlined fully in Chapter 3, but in brief, a ‘global model’ was built using the set of terms listed in Equation 1, standardized and entered into a multi-model inference package (‘dredge’, MuMIn package). Dredge tries every combination of terms to find the most ‘parsimonious’ model based on Akaike information criterion (AIC). AIC measures ‘model fit’ whilst penalising for the number of terms. The final model was selected based on (i) its AIC value, (ii) the homogeneity and normality of the model residuals and (iii) the model fit, based on the Nagelkerke pseudo  $r^2$  value of the model and the fixed effects. Because of fewer data points, it was not possible to include every possible first order interaction in the global model, so only those defined in equation 1 were included, and any deemed potentially important based on observed patterns.

‘Global model’	(1)
$\text{El}_\text{O} \sim \underline{\text{Sex}} + \underline{\text{Opacity}} + \underline{\text{Subunit}} + \underline{\text{Season}}^\dagger + \underline{\text{Subunit}^*\text{Season}}^{\ddagger} + \text{Month} + \text{Temp}^*\text{Salinity} + \text{Lat} + \text{Long} + \text{Lat.range}^*\text{Long.range} + \text{Somatic GR} + \text{Otolith GR} + \text{Condition} + \text{TW} + \text{end TL} + \text{Age} + (1 \text{ID}))$	

Underlined terms were entered into the model as categorical ‘factors’; others all defined as continuous variables. Where interactions are indicated with an asterisk, terms were also entered separately.

<sup>†</sup> Season defined as spawning (‘Sp’: December-March) or non-spawning (‘NS’: April-November). The exception was the immature CNS female (A12431), which was assigned NS for all time periods

<sup>‡</sup> Subunit\*Season was included as a separate term, where A12431 was assigned CNS\_NS for all time periods and Dec-March for 3.2-1207 was assigned ‘WNS\_Sp’ due to its migration to WNS spawning grounds.

Most model terms were introduced in previous chapters or Table 5.1, but some additional details are provided below. DST-recorded temperatures for the dates assigned to each analysis spot were used, along with a GETM-estimated seabed salinity value for the given geolocation and date. ‘Start TL’ was rounded to the nearest centimetre, which may have introduced error to the somatic growth rates and condition. It was assumed that fish cannot shrink over time, so negative growth rates were modified to zero (A12391). Final age was estimated by counting translucent growth rings and any questionable otoliths were discussed with an ageing expert at CEFAS. ‘Migration distance’ was included in the model in three forms: (i) latitude (‘Lat’) range, (ii) longitude (‘Long’) range, (iii) Lat range x Long range, based on the assumption that the larger the geographic ‘area’, the greater the likelihood for encountering larger environmental gradients. However, such measures are purely geographical and may not represent ‘effort’, with active swimming and feeding behaviour, particularly in the central and north NS potentially more energy expensive than long migrations utilising STST (De Veen, 1978; Hunter *et al.*, 2009).

## 5.3 Results

### 5.3.1 Environmental and physiological trends

As indicated by the individual and averaged temperature profiles (Figures 5.3-5.6), WNS and ENS plaice remain in thermally-mixed water throughout the year and experience a full annual temperature cycle, with winter minima of approximately 6 °C and summer maxima up to ~18 °C (Hunter *et al.* 2004). By contrast, CNS plaice are located in cold, thermally stratified water to the north of the North Sea thermal front (Pingree and Griffiths, 1978). CNS plaice therefore rarely experience temperatures above 8 °C until mature individuals commence their pre-spawning migration and move (horizontally) through the thermocline during the autumn, or when the thermocline starts to break down shortly thereafter (Hunter *et al.*, 2003b). The average monthly temperatures experienced by the 11 fish were very similar, despite sometimes >7 years between tagging periods (Figure 5.6). GETM-estimated salinities ranged from 30.1 to 35.1, however WNS and CNS fish generally experienced fluctuations <1 psu. The ENS plaice experienced the lowest overall salinities and the largest variation within and between months due to freshwater inputs from continental Europe (Tappin *et al.*, 1995) (Figure 5.7).

Sexual dimorphism is well documented in plaice, with females growing faster and larger than similarly aged males (Bromley, 2000). In the current study, females were found to be older (Figure 5.8) and faster growing than the males on average, although these differences were not significant. Otolith and somatic growth rates were positively correlated (PCC = 0.69) and females also exhibited faster otolith growth rates on average, although the difference was not significant. The tagged females were, however, significantly larger (TW:  $F_{1,8} = 9.49, p = 0.015$ , TL:  $F_{1,10} = 5.98, p = 0.037$ ) and in significantly better condition ( $F_{1,8} = 5.43, p = 0.048$ ) than their male equivalents.

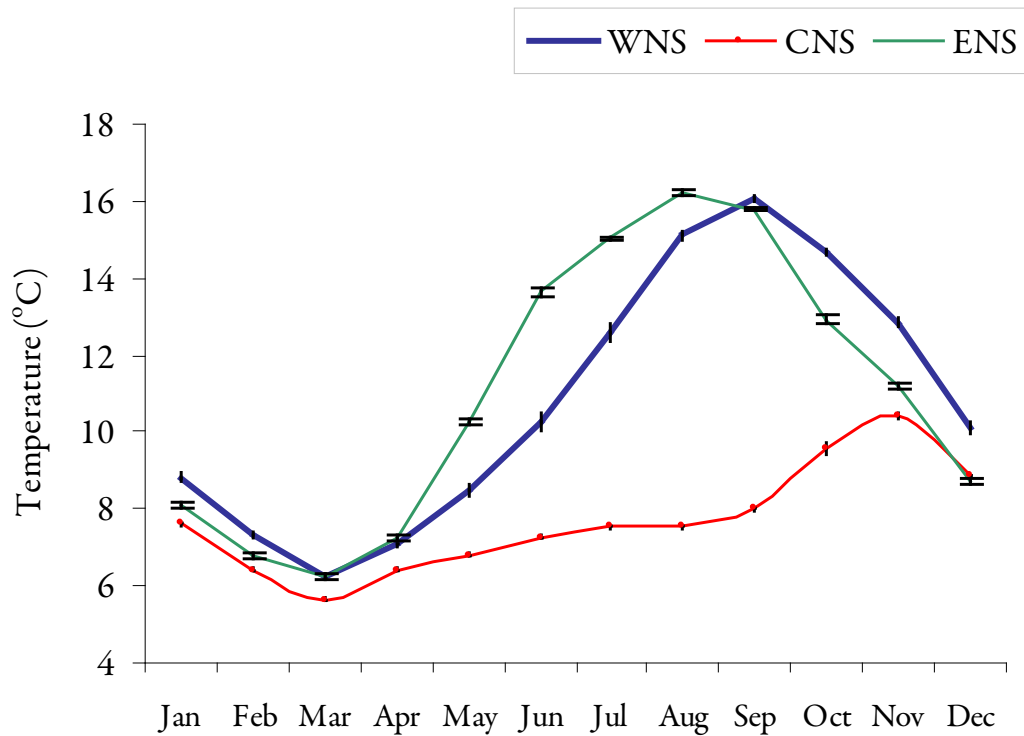


Figure 5.6 Average ( $\pm$ SEM) monthly DST recorded temperature for the eleven featured plaice, separated by west (WNS, blue), central (CNS, red) and east (ENS, green) North Sea population subunits.

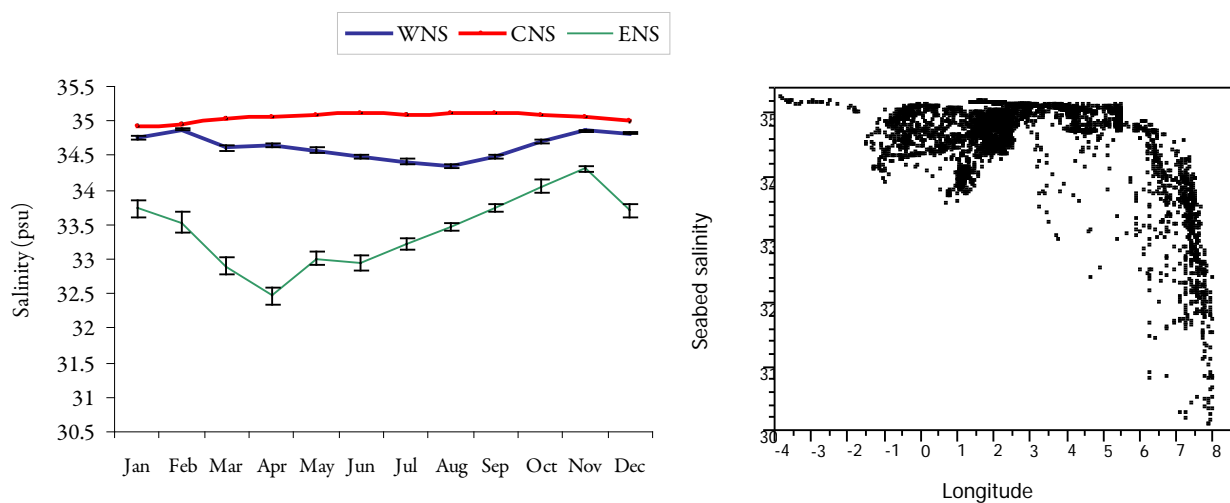


Figure 5.7 (A) Average ( $\pm$ SEM) monthly GETM-estimated salinity for the eleven featured plaice, separated by west (WNS, blue), central (CNS, red) and east (ENS, green) North Sea population subunits.  
 (B) Longitudinal variation in daily salinity estimates for the eleven featured fish ( $n = 4945$ )

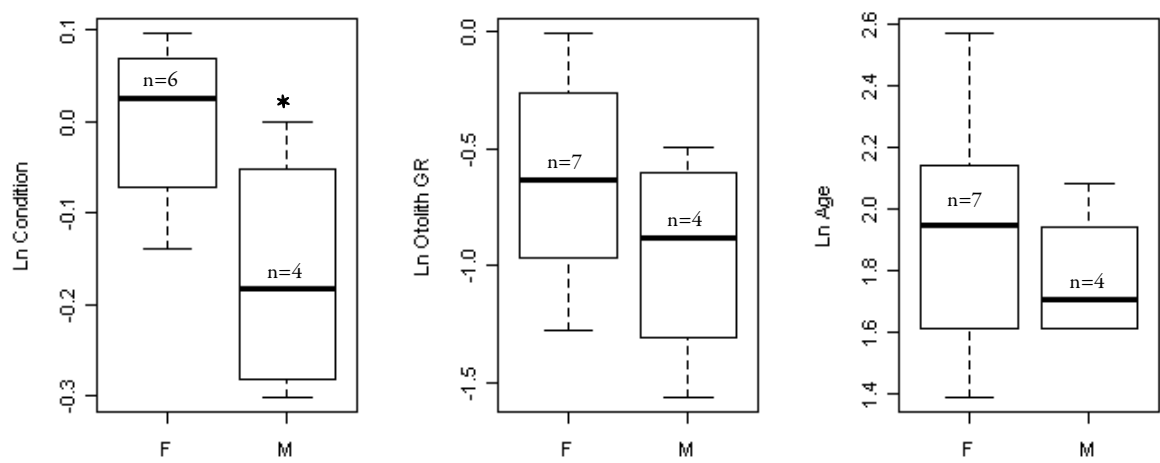


Figure 5.8 Boxplots showing the differences in end condition, otolith growth rate (GR) and age between the tagged males (M) and females (F) featured in the current study (all continuous variables Ln-transformed). Only condition was significantly different ( $p<0.05$ ), however the females also exhibited significantly higher TL and TW (not displayed). The boxplot whiskers extend 1.5 times the inter-quartile range from the 25<sup>th</sup> and 75<sup>th</sup> quartiles (lower and upper ranges of the box, respectively), while the bold line indicates the median

## 5.3.2 Otolith elemental concentrations vs. environmental and physiological variables in wild plaice

### 5.3.2.1 Lithium

Similar to the patterns exhibited by the experimental plaice, average  $\text{Li}_\text{O}$  was highest in April and lowest between June and October (Figure 5.9). There was no overall difference in  $\text{Li}_\text{O}$  values among population subunits, but concentrations were generally lowest in WNS (blue) fish. The highest  $\text{Li}_\text{O}$  values were exhibited by the ENS females, particularly during non spawning periods (Figure 5.9). Similar to the experimental results, negative effects of water concentrations (here, salinity) and temperature were highly significant, as were positive effects of otolith opacity (Figure 5.10). Salinity effects were highly influenced by the sporadic drops in salinity in the ENS. ‘Season’ was also significant and season\*subunit almost significant, with  $\text{Li}_\text{O}$  values generally lower during spawning periods, but particularly in the ENS and CNS (Figure 5.9). The negative relationship between  $\text{Li}_\text{O}$  and latitudinal range was also almost significant (Figure 5.10).

#### Was there any evidence of a sex effect in $\text{Li}_\text{O}$ ?

Unlike the experimental results,  $\text{Li}_\text{O}$  was on average, higher in the females than the males, however the effect was not significant (Table 5.2). Given the potentially confounding effects of comparing among unbalanced sex ratios, different years and areas,  $\text{Li}_\text{O}$  were also plotted for the most similarly aged CNS and WNS male and female pairs. There were no clear differences between the males and females, although concentrations were consistently lower in the WNS fish than the CNS fish (Figure 5.11).

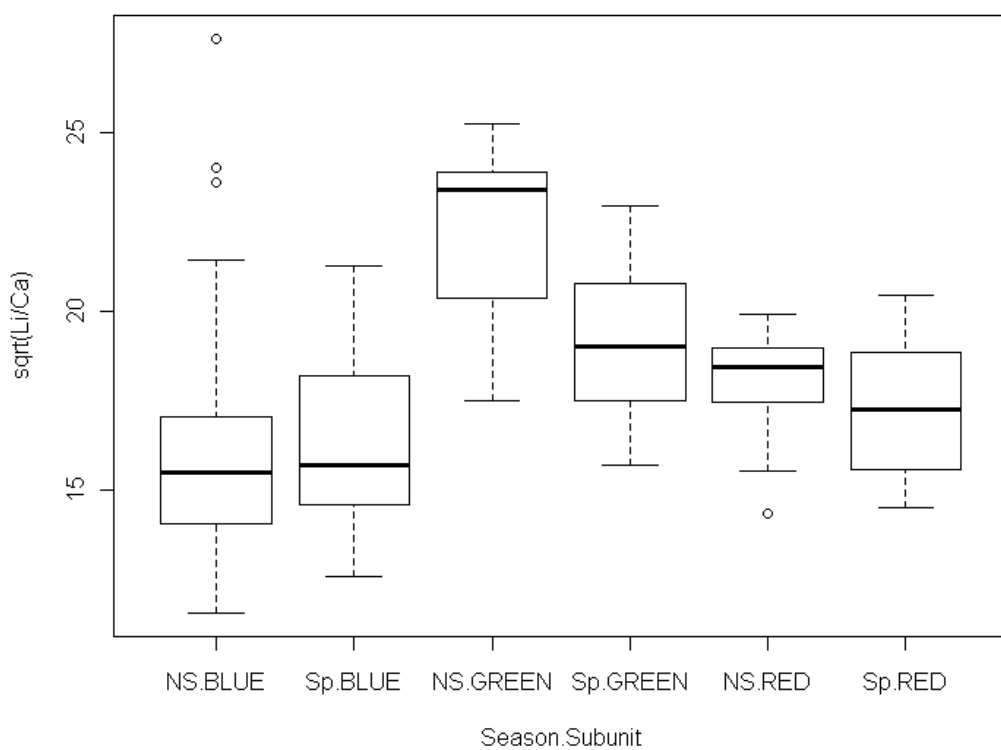
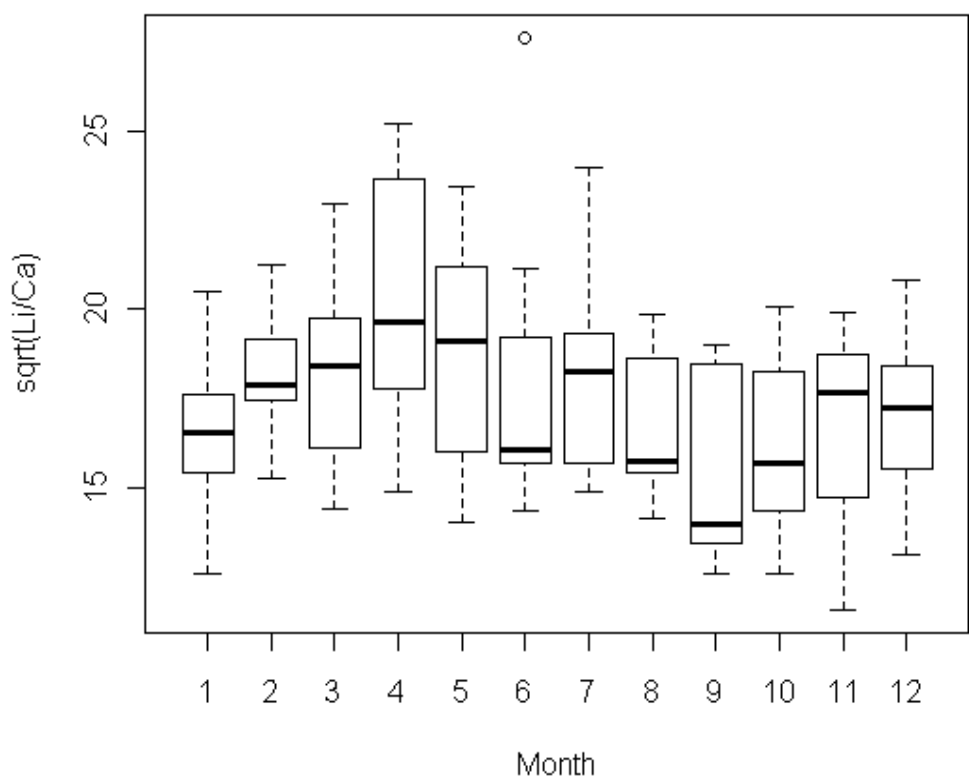


Figure 5.9 Boxplots to show averaged trends in  $\text{Li}_\text{O}$  (SQRT-transformed  $\text{Li/Ca}$  ratios in mmol/mol) over time and among North Sea population subunits (blue = WNS, green = ENS, red = CNS) by season (spawning = 'Sp', Dec-Mar; non-spawning = 'NS', Apr-Nov). The boxplot whiskers extend 1.5 times the inter-quartile range from the 25<sup>th</sup> and 75<sup>th</sup> quartiles (lower and upper ranges of the box, respectively), while the bold line indicates the median

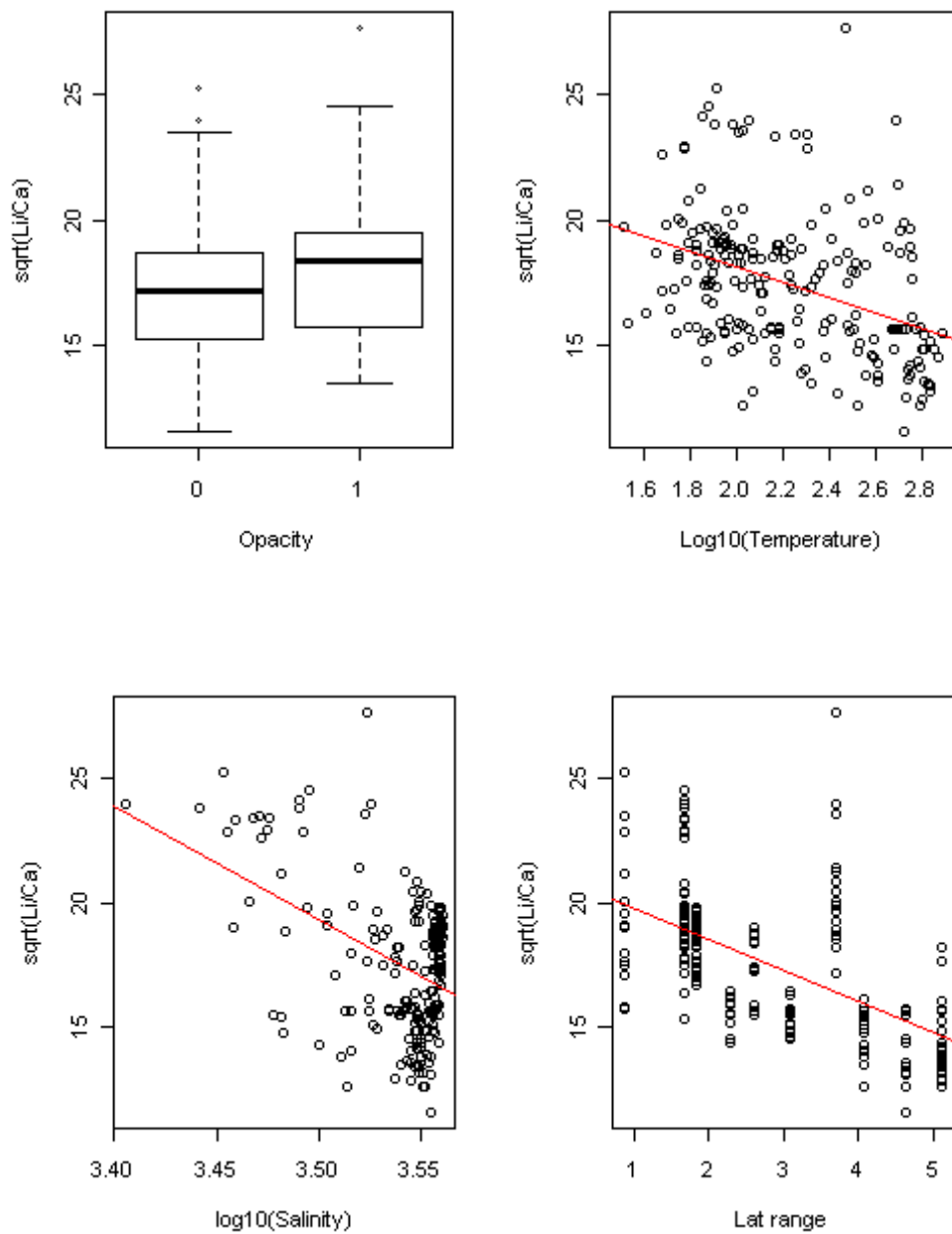


Figure 5.10 Trends in  $\text{Li}_\text{O}$  (SQRT-transformed Li/Ca ratios in mmol/mol) in wild plaice tagged by DST. The relationship between  $\text{Li}_\text{O}$  and latitudinal range was almost significant, while all other displayed terms were highly significant. The boxplot whiskers extend 1.5 times the inter-quartile range from the 25<sup>th</sup> and 75<sup>th</sup> quartiles (lower and upper ranges of the box, respectively), while the bold line indicates the median

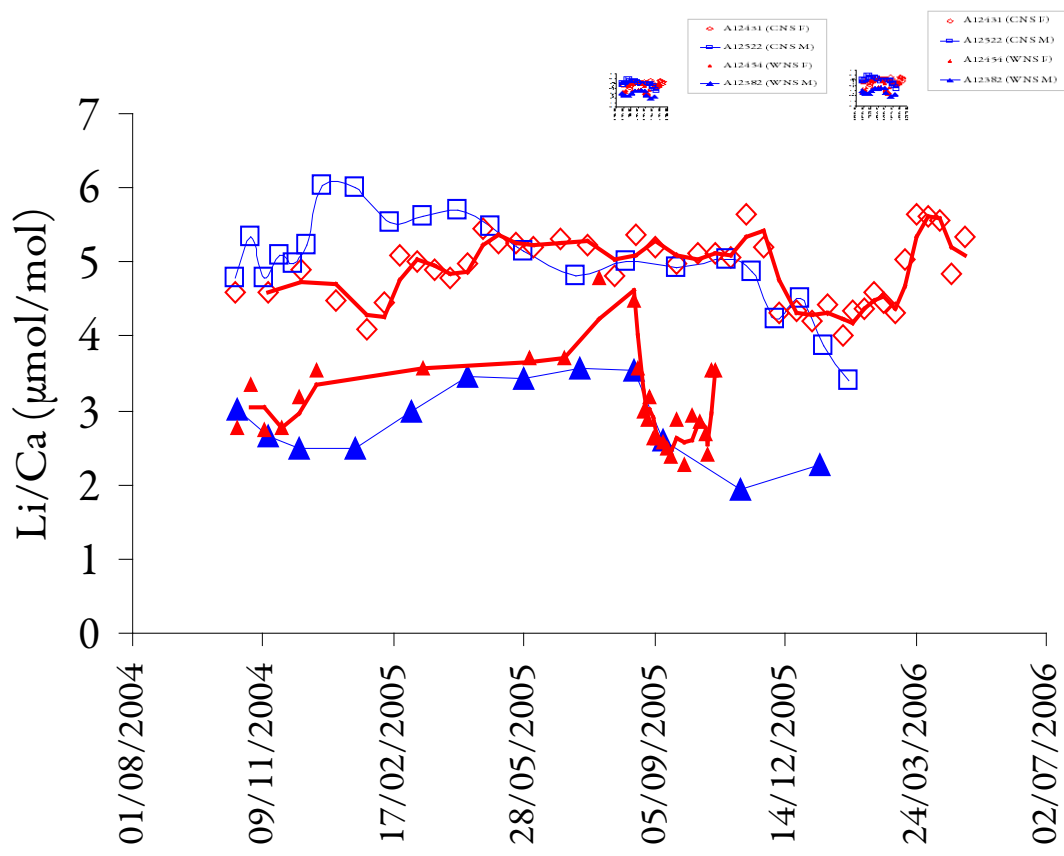


Figure 5.11  $\text{Li}_\text{O}$  concentrations over time for the two pairs of male (blue) and female (red) fish from the WNS (closed symbols) and CNS (open symbols) during the tagged period only. Dates were inferred from patterns in  $\delta^{18}\text{O}$  and growth bands

### 5.3.2.2 Manganese

$Mn_O$  varied in a broadly sinusoidal manner over time, exhibiting the highest average concentrations in September and the lowest in March (Figure 5.12). The most parsimonious model for explaining variation in  $Mn_O$  included temperature and somatic GR (Table 5.2). Within this model, somatic GR was not significant, but its inclusion improved residual structure and model fit, so it was retained. The positive correlation between  $Mn_O$  and condition was slightly less noisy than with somatic GR (Figure 5.13), but its inclusion resulted in a slightly lower model fit, presumably due to missing data. The model explained just over half of the variation in  $Mn_O$ , although 22% was explained by the random effect, suggesting significant among-fish variability. There was also a negative relationship between  $Mn_O$  and age, although it was not significant. There was no difference in  $Mn_O$  among the three North Sea regions, among the sexes, nor any clear correlation with salinity.

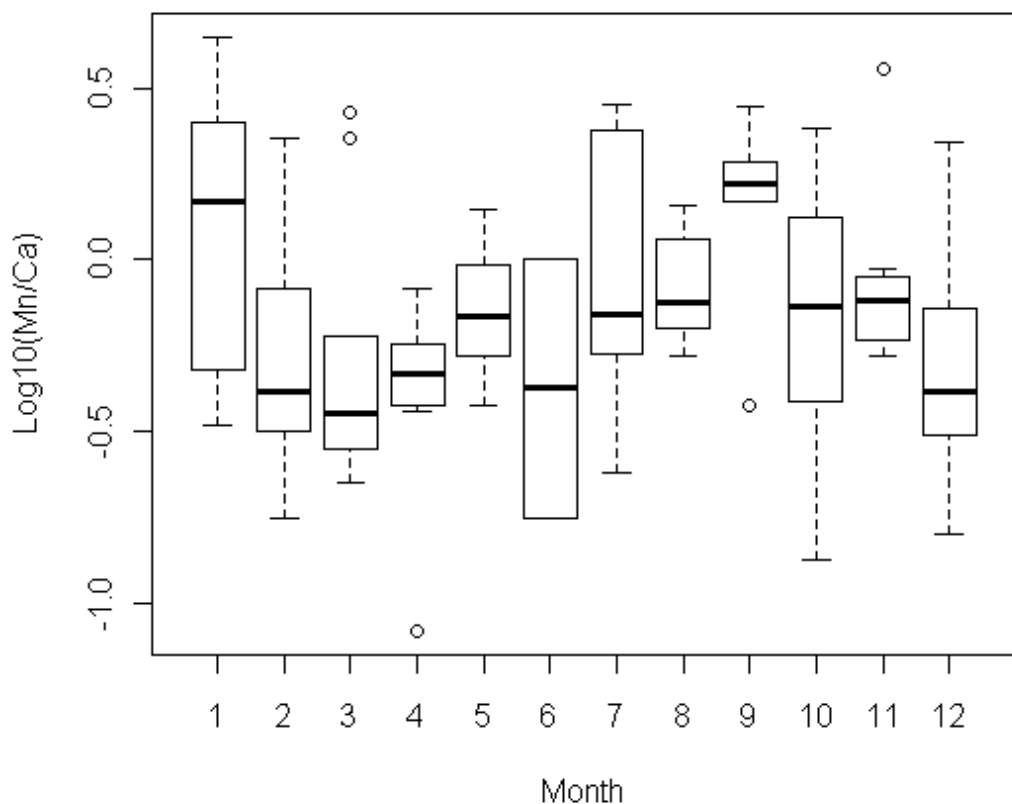


Figure 5.12 Boxplots to show trends in  $Mn_O$  (Ln-transformed Mn/Ca ratios in mmol/mol) over time in DST tagged plaice. The boxplot whiskers extend 1.5 times the inter-quartile range from the 25<sup>th</sup> and 75<sup>th</sup> quartiles (lower and upper ranges of the box, respectively), while the bold line indicates the median

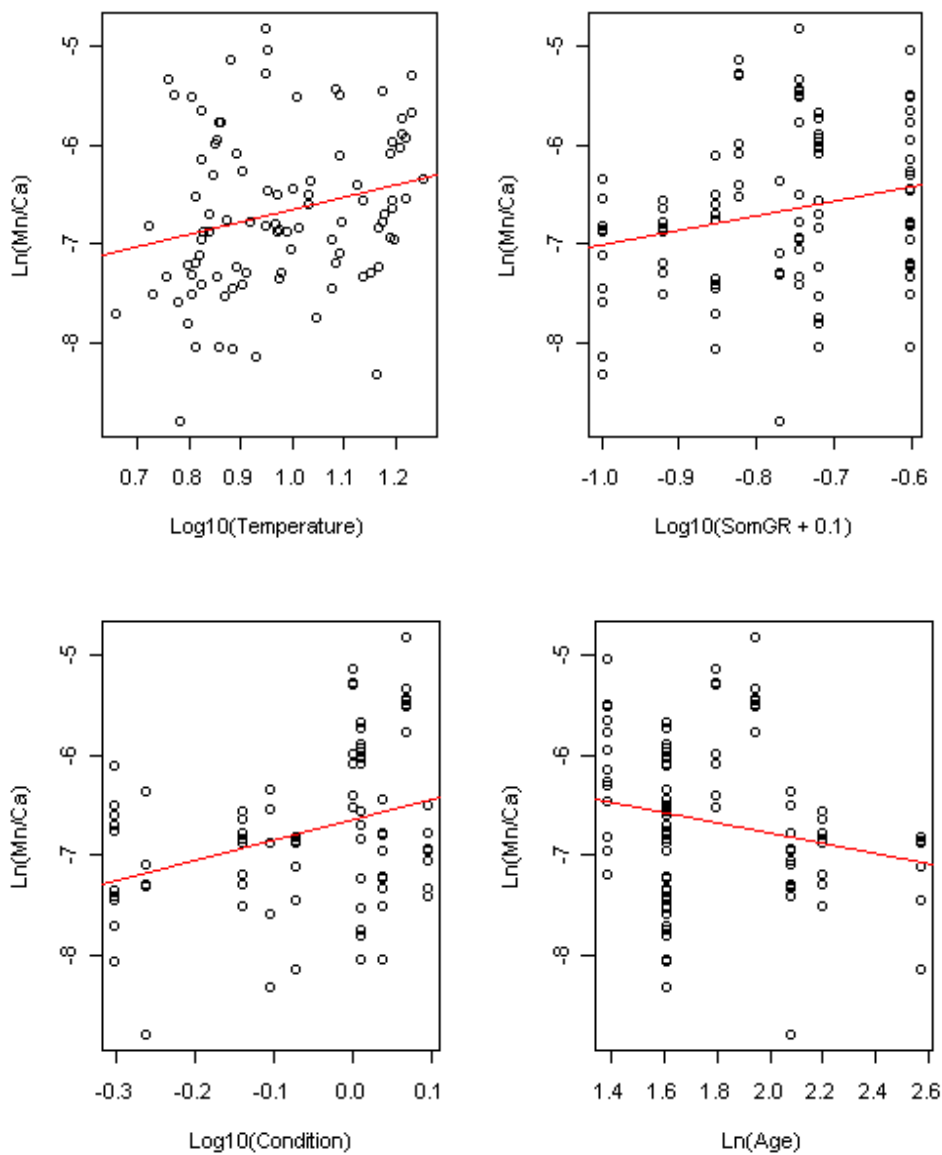


Figure 5.13 Trends in  $\text{Mn}_\text{O}$  in wild plaice tagged with DST. The relationship between  $\text{Mn}_\text{O}$  and temperature was the only one deemed significant, but adding somatic growth rate (SomGR,  $\text{Log}_{10}(x+0.1)$  transformed) improved model fit and residual structure.

### 5.3.2.3 Strontium

Over time,  $\text{Sr}_\text{O}$  varied in a broadly sinusoidal manner, similar to the patterns exhibited by the experimental fish, although within-month variation was high (Figure 5.14). The lowest concentrations were observed in September, but there was no clear maximum that was common across all fish. There was a significant effect of sex (Table 5.2), with males exhibiting higher  $\text{Sr}_\text{O}$  concentrations than females, but there was no difference among population subunits, nor consistent differences when separated by sex (Figure 5.14).

The most parsimonious model for explaining  $\text{Sr}_\text{O}$  values in DST fish included age, temperature and sex. While the positive relationship between age and  $\text{Sr}_\text{O}$  was stronger than the negative relationship between  $\text{Sr}_\text{O}$  and otolith growth rate (GR), the model fit was similar using either term and improved by using both, even though otolith GR was deemed not significant (Table 5.2). Similar to the experimental results, there were negative correlations between  $\text{Sr}_\text{O}$  and temperature, condition, otolith and somatic GR (Figure 5.15). Unlike the experimental results, there was a clear sex effect, with  $\text{Sr}_\text{O}$  higher in the males. The effect of temperature was less clear, particularly when fish were separated by sex (Figure 5.15). There was also a weakly positive relationship between  $\text{Sr}_\text{O}$  and salinity, although it was not significant and was heavily influenced by the limited number of data points in the ENS when salinity dropped below 32 (Figure 5.7 and Figure 5.15).

Given potentially confounding effects of comparing among years, section types and ages,  $\text{Sr}_\text{O}$  was also examined in the five younger WNS and CNS fish released in October 2004, for which frontal sections were available. As indicated by Figure 5.16, the females exhibited similar  $\text{Sr}_\text{O}$  levels despite remaining geographically separate and exhibiting different migratory behaviours.  $\text{Sr}_\text{O}$  in the males was consistently higher, although concentrations in the two CNS males differed substantially, with  $\text{Sr}_\text{O}$  in the older male (A12522) almost double that of A12388, despite both inhabiting the same area and carrying out almost identical migrations. The only overlap between the sexes was in the final two analyses for A12454, which coincided with material deposited in October during her southward migration to spawning grounds.

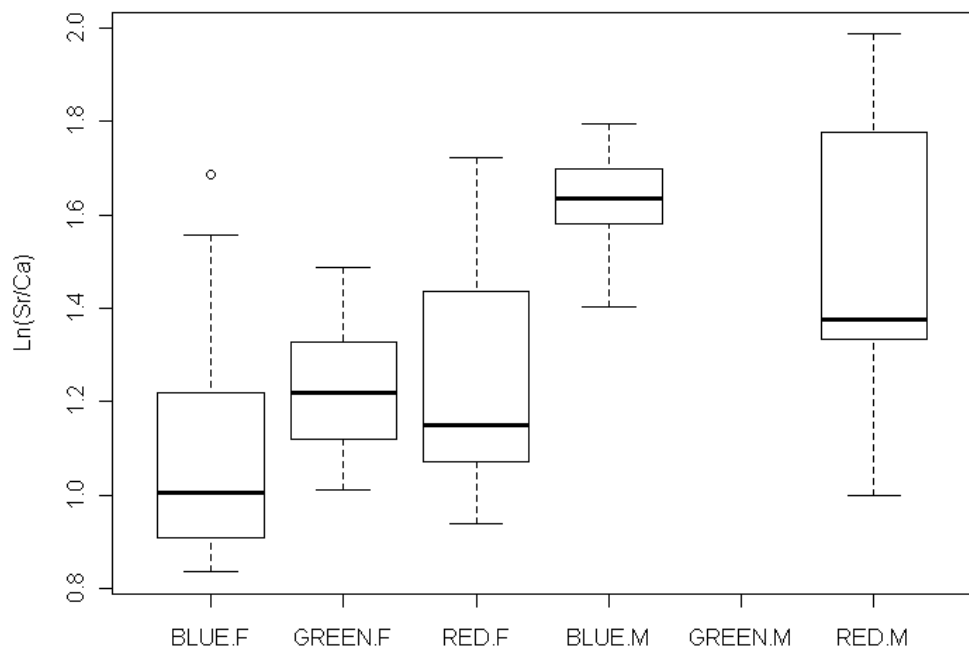
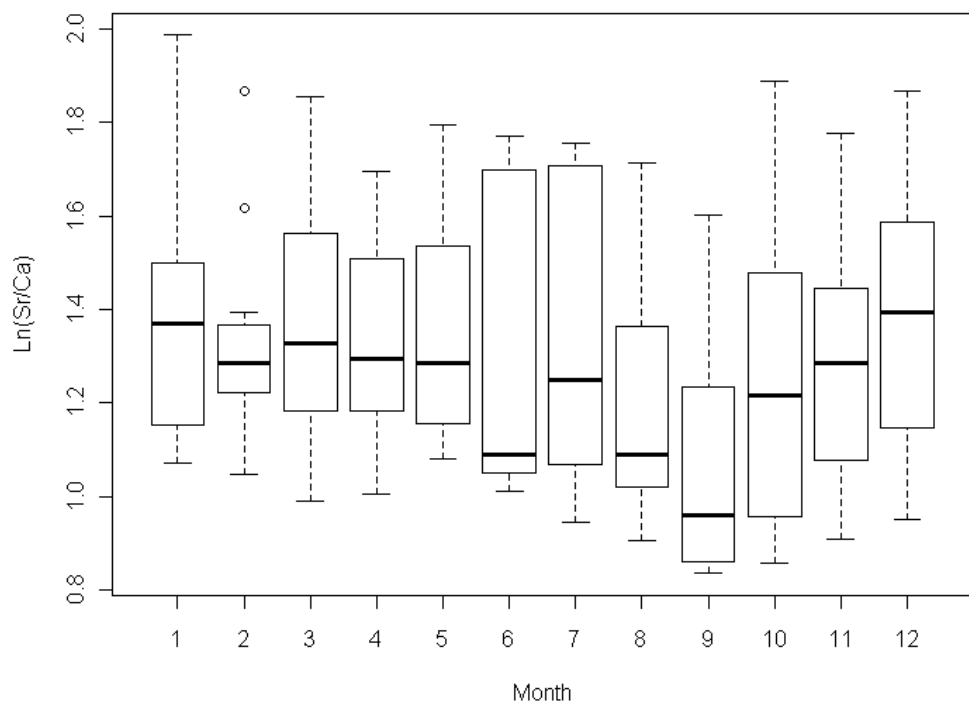


Figure 5.14 Boxplots to show trends in  $\text{Sr}_\text{O}$  ( $\text{Ln}$ -transformed  $\text{Sr/Ca}$  ratios in  $\text{mmol/mol}$ ) over time and among North Sea population subunits (separated by sex) in DST tagged plaice. The boxplot whiskers extend 1.5 times the inter-quartile range from the 25<sup>th</sup> and 75<sup>th</sup> quartiles (lower and upper ranges of the box, respectively), while the bold line indicates the median

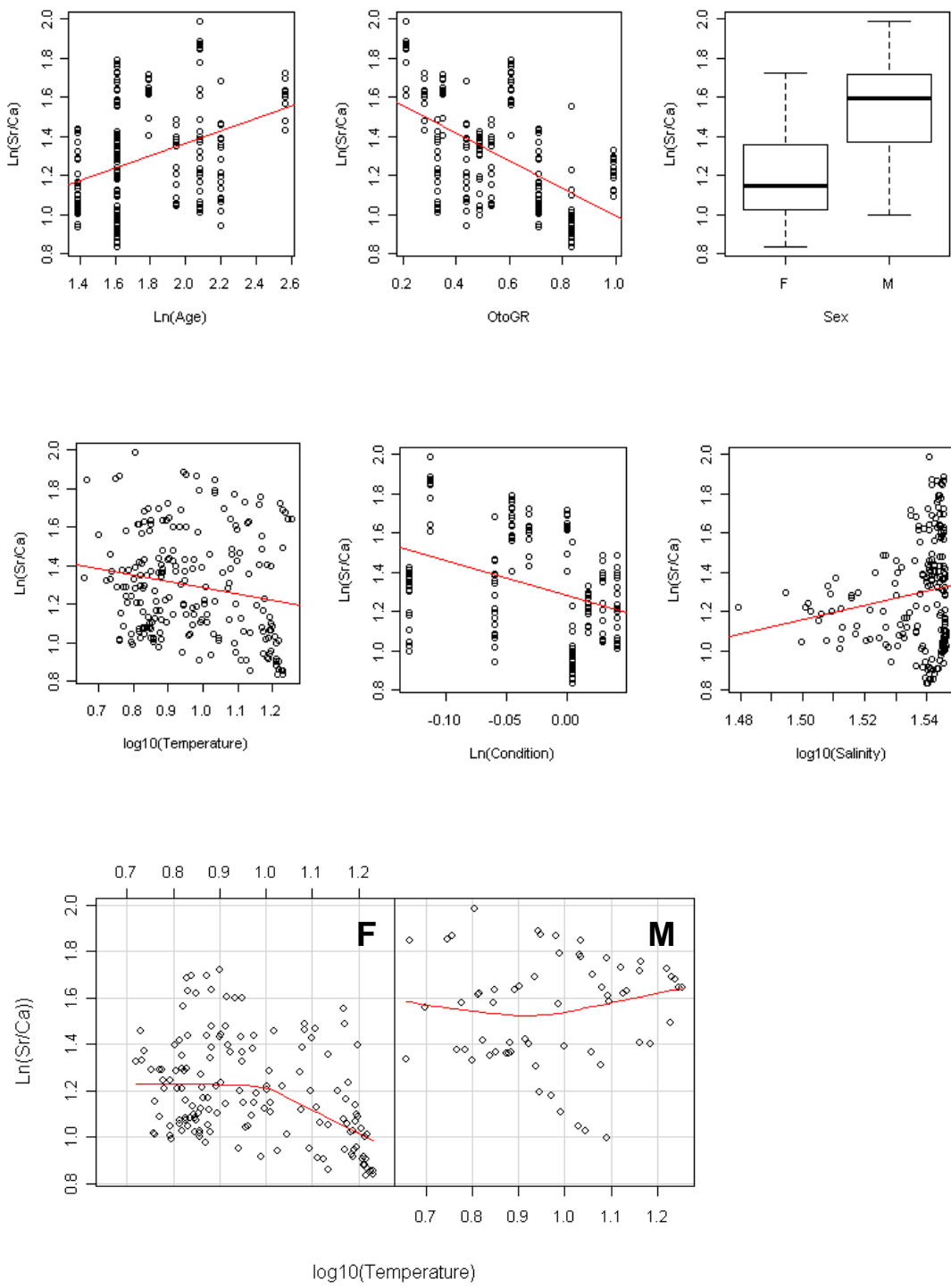
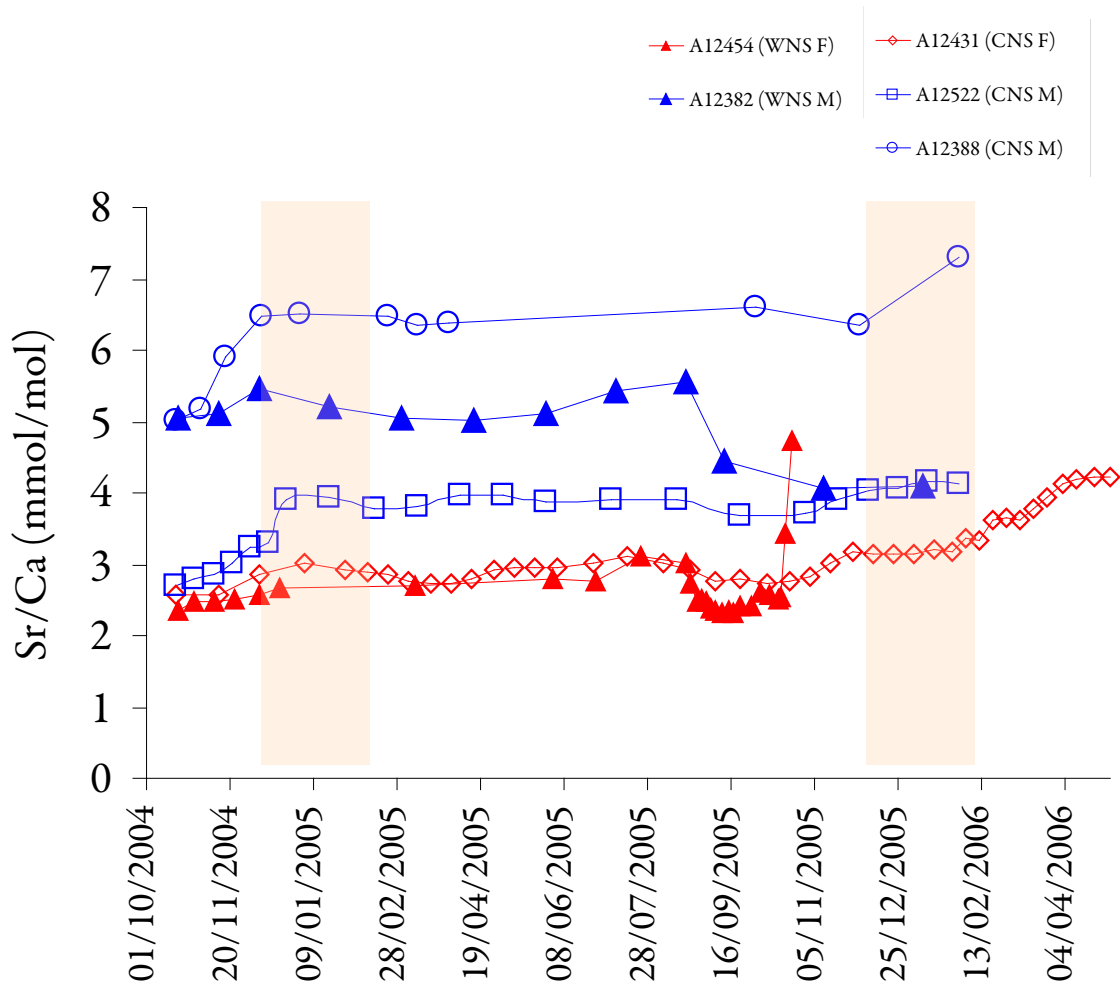


Figure 5.15 Trends in  $\text{Sr}_\text{O}$  (Ln-transformed Sr/Ca ratios in mmol/mol) concentrations in wild plaice tagged with DST. Age (Ln transformed, in years), otolith growth rate (OtoGR, in  $\mu\text{m}/\text{day}$ ), sex and temperature ( $\log_{10}$  transformed, in  $^\circ\text{C}$ ) were included in the final mixed effects model. The boxplot whiskers extend 1.5 times the inter-quartile range from the 25<sup>th</sup> and 75<sup>th</sup> quartiles (lower and upper ranges of the box, respectively), while the bold line indicates the median



Based on the experimental data (Chapter 4) and previous studies (e.g. Kalish, 1991; Clarke and Friedland, 2004), there is evidence to suggest that reproductive investment can result in enrichment of  $\text{Sr}_\text{O}$ , particularly in female fish. There was no direct measure of GSI in the DST plaice, so it was not possible to examine such effects directly, however, the mature females did exhibit higher average  $\text{Sr}_\text{O}$  during the months corresponding to the spawning season, while males exhibited no clear difference (Figure 5.17). Also, if temperature was excluded from the model, 'season' was highly significant.

Unlike previous observations (Hunter and Darnaude, 2004), there were no clear relationships between within-fish variation in  $\text{Sr}_\text{O}$  and migration distance (latitudinal or longitudinal range) or area (latitudinal range\* longitudinal range) (Figure 5.18).

Table 5.2 Results from mixed effects model analyses for the four selected otolith elements in the DST fish, with Nagelkerke pseudo  $r^2$  values displayed for the full model, the fixed effects 'FE' and the random effect (RE)

El <sub>O</sub>	Term	Effect	Chi Sq	df	P	Pseudo $r^2$		Comments
						Full	FE (RE)	
$\text{Sr}_\text{O}$	Sex	M>F	10.521	1	0.0012	**	0.82	0.34
	Temperature	-ve	15.84	1	<0.0001	***	(0.48)	when age included, but improved fit by >5%
	Age	+ve	4.3	1	0.0380	*		
	OtoGR	n.s. (-ve)	n.s.	1	>0.05			
$\text{Mn}_\text{O}$	Temperature	+ve	26.765	1	<0.0001	***	0.54	0.32
	SomGR	n.s. (+ve)	n.s.	1	>0.05		(0.22)	SomGR n.s., but improved fit by ~5%
	Season	NS>Sp	6.355	1	0.0117	*	0.87	0.58
$\text{Li}_\text{O}$	Opacity	+ve	21.231	1	<0.0001	***	(0.28)	Excl. Sal, FE $r^2$ = 0.42; excl. season FE = 0.34
	Temperature	-ve	11.359	1	0.0008	***		
	Salinity	-ve	63.552	1	<0.0001	***		
	Subunit	C>E>WNS	26.084	2	<0.0001		0.99	0.86
$\text{Ba}_\text{O}$	Season	Sp>NS	5.762	1	0.016		(0.12)	Lat. range almost as good a fit in place of subunit
	OtoGR	-ve	21.868	1	<0.0001			

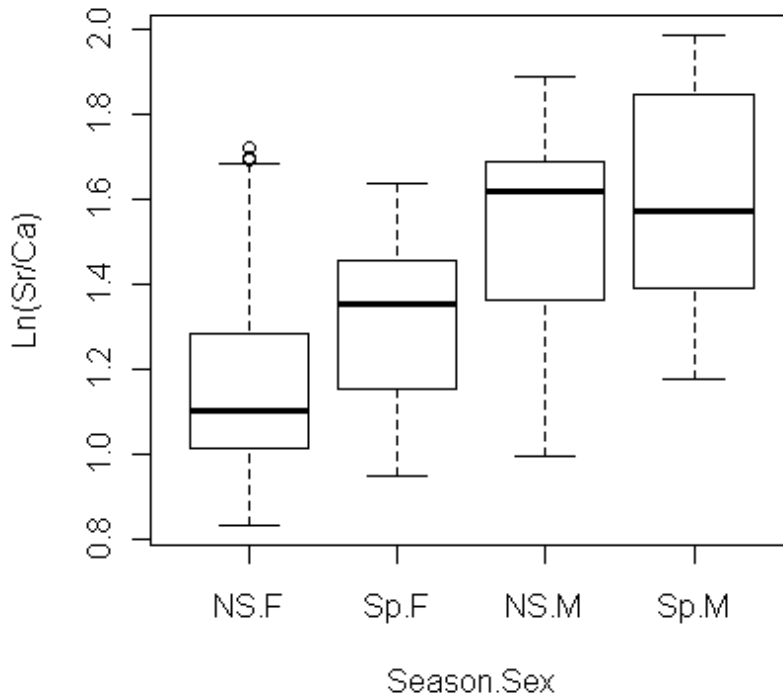


Figure 5.17 Boxplot showing  $\text{Sr}_\text{O}$  (Ln-transformed Sr/Ca ratios in mmol/mol) in females (F) and males (M) during spawning ('Sp', Dec-Mar) and non-spawning (NS, Apr-Nov) seasons. The boxplot whiskers extend 1.5 times the inter-quartile range from the 25<sup>th</sup> and 75<sup>th</sup> quartiles (lower and upper ranges of the box, respectively), while the bold line indicates the median. Note that fish A12431 was assumed immature and assigned 'NS' throughout.

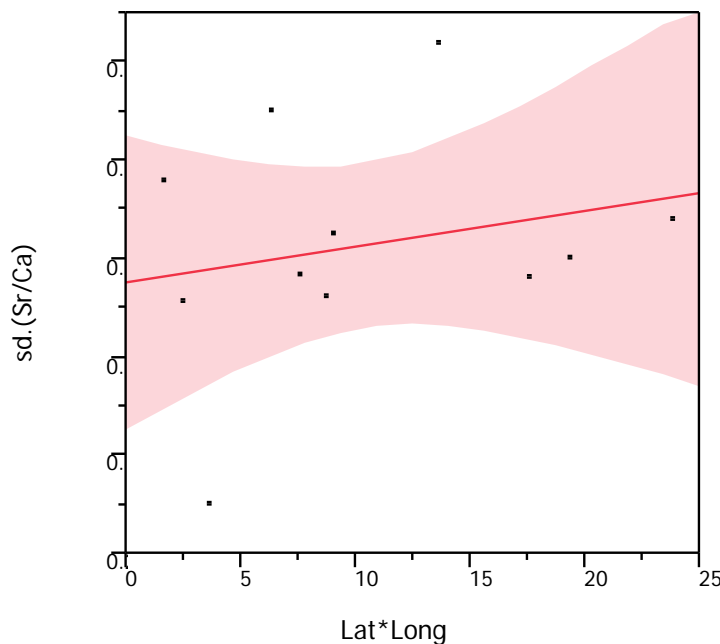


Figure 5.18 Relationship ( $\pm 95\%$  CI) between within-fish  $\text{Sr/Ca}_\text{O}$  variance (standard deviation) during time at liberty vs. 'migration area' (latitudinal range x longitudinal range) for 11 plaice tagged by DST. Similarly weak relationships were produced using any of the 'distance proxies'.

### 5.3.2.4 Barium

Similar to  $\text{Sr}_{\text{O}}$  and  $\text{Ba}_{\text{O}}$  patterns in the experimental plaice,  $\text{Ba}_{\text{O}}$  was lowest in September and highest during winter, although concentrations appeared to increase earlier in the tagged fish than in the experimental population. There were highly significant differences in  $\text{Ba}_{\text{O}}$  among subunits and seasons (Table 5.2). Concentrations were consistently highest in the CNS and lowest in the WNS, and elevated during the spawning season, although the seasonal effect was less apparent in the WNS fish (Figure 5.19).  $\text{Ba}_{\text{O}}$ , like  $\text{Sr}_{\text{O}}$ , was higher in the males than the females, although the difference was not significant.

#### What was driving the differences in $\text{Ba}_{\text{O}}$ among subunits?

There was a strong latitudinal gradient in  $\text{Ba}_{\text{O}}$  concentrations (Figure 5.21) although the model fit was better using 'latitudinal range' than 'latitude'. The two most parsimonious models differed only by their inclusion of 'subunit' or 'latitudinal range', and both exhibited high  $r^2$  values ( $>0.9$ ), although the fit was marginally better with the former. One of the clearest latitudinal gradients was a negative correlation with temperature, and 'latitudinal range' was also positively correlated with temperature, indicating that the fish exhibiting the longest north-south migrations (WNS fish) experienced the highest overall temperatures during their time at liberty. However, a negative temperature effect alone cannot explain the geographic variations in  $\text{Ba}_{\text{O}}$ , with the coplot in Figure 5.21 indicating weak (if any) relationship between  $\text{Ba}_{\text{O}}$  and temperature within subunits, and elevated  $\text{Ba}_{\text{O}}$  in the CNS fish at any given temperature.

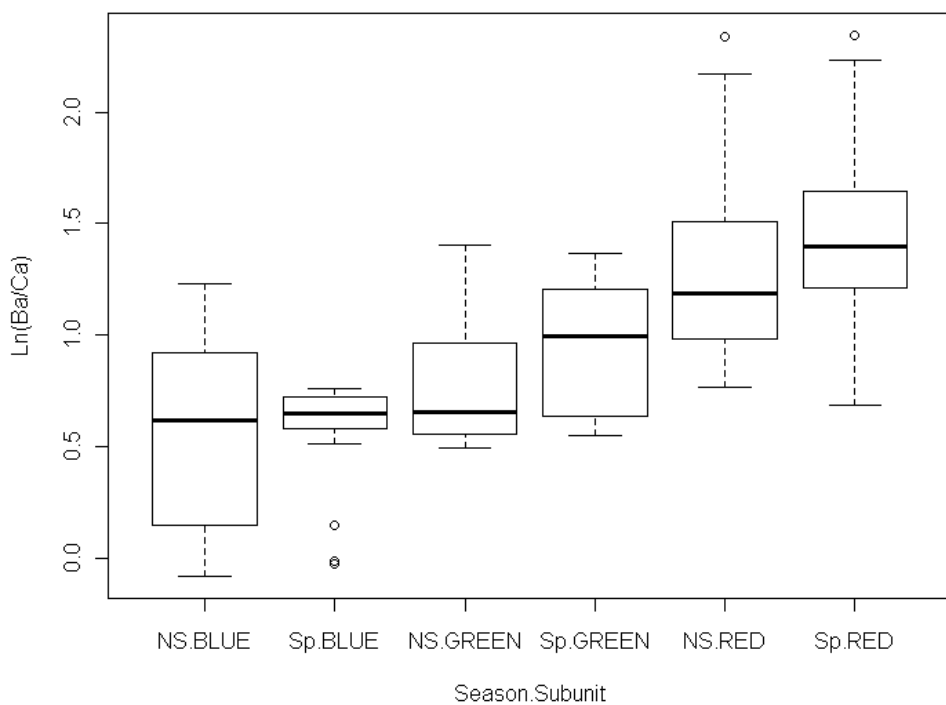
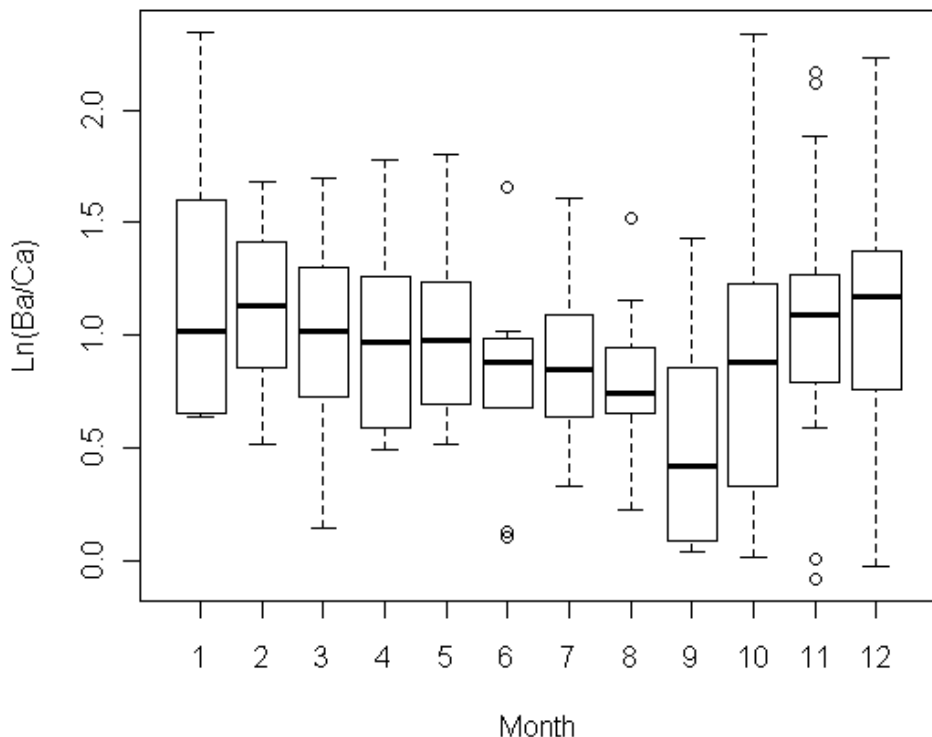


Figure 5.19 Boxplots to show trends in  $\text{Ba}_\text{O}$  ( $\text{Ln}$  transformed concentrations in ppm) over time and among North Sea subunits by season (spawning 'Sp', Dec-Mar and non-spawning, NS, Apr-Nov) in DST tagged plaice. The boxplot whiskers extend 1.5 times the inter-quartile range from the 25<sup>th</sup> and 75<sup>th</sup> quartiles (lower and upper ranges of the box, respectively), while the bold line indicates the median

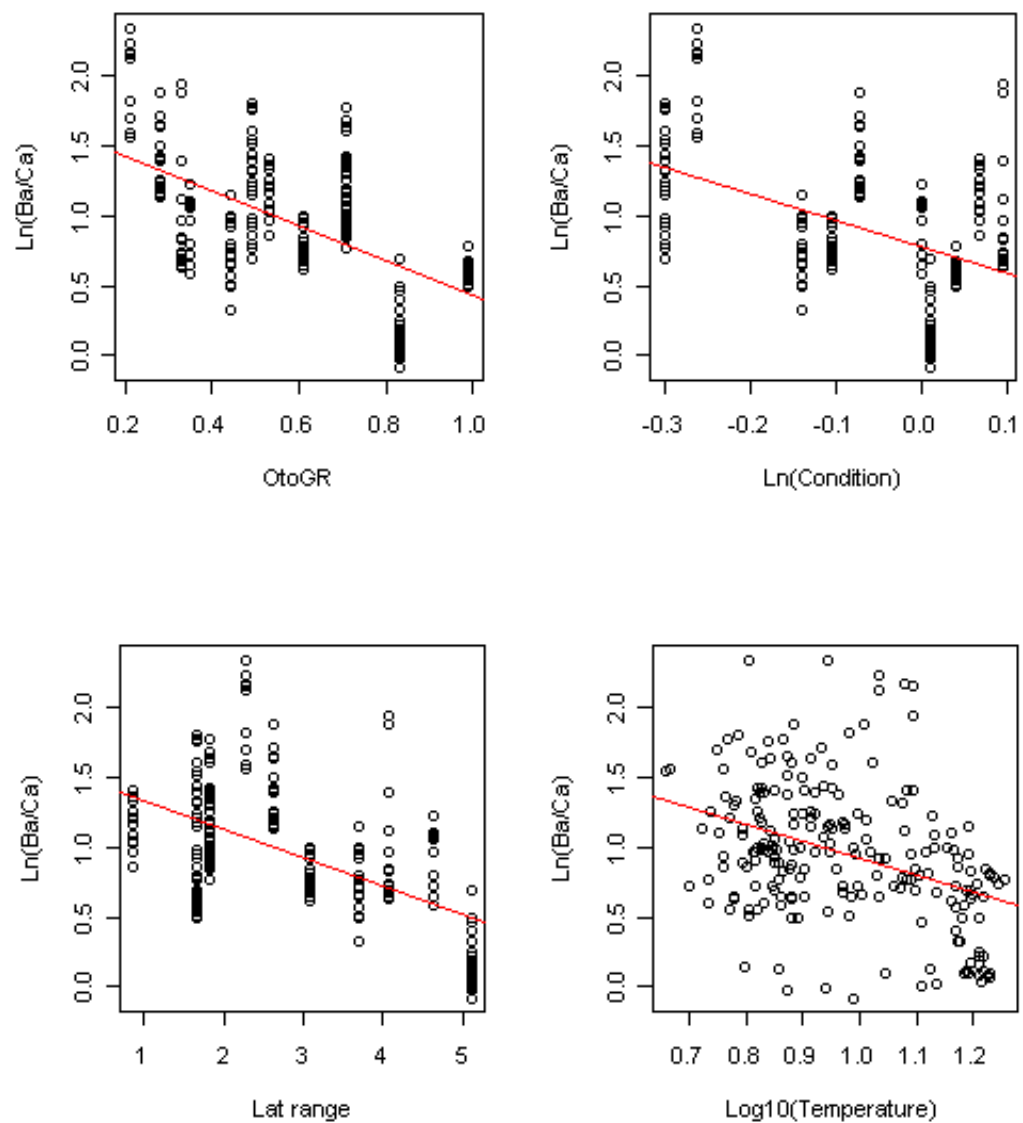


Figure 5.20 Trends in  $\text{Ba}_\text{O}$  ( $\ln$  transformed concentrations in ppm) in wild plaice tagged by DST. The relationship between  $\text{Ba}_\text{O}$  and otolith growth rate (OtoGR, in  $\mu\text{m/day}$ ) was the only significant term included in the final model, but the relationships between  $\text{Ba}_\text{O}$  and condition and latitudinal range were almost significant and displayed for discussion purposes.

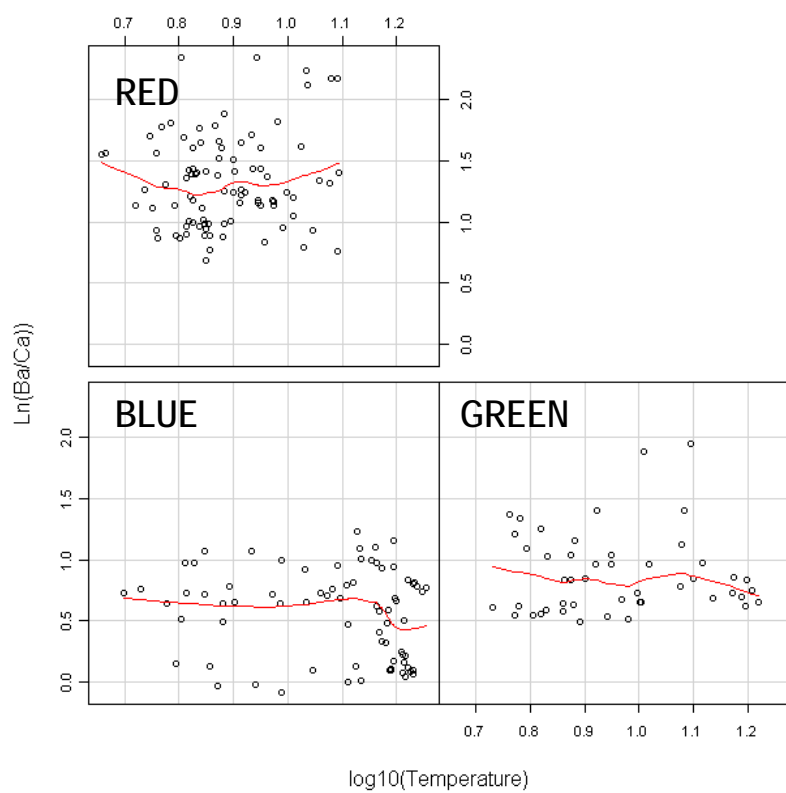
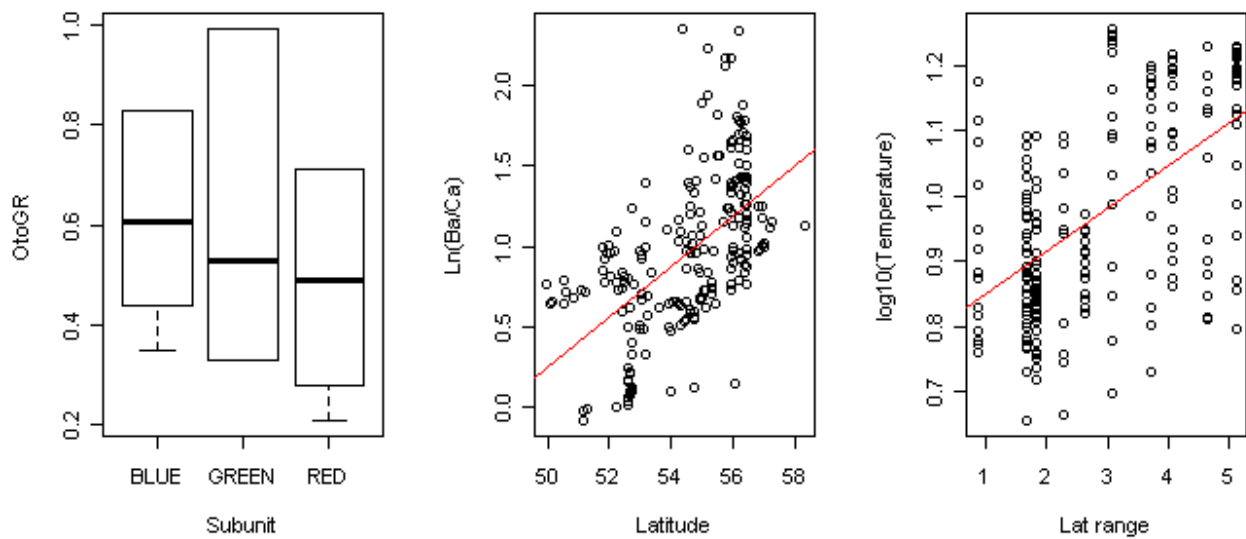


Figure 5.21 Exploring differences in  $\text{Ba}_\text{O}$  ( $\text{Ln}$ -transformed concentrations in ppm) among population subunits in the North Sea (blue = WNS, green = ENS, red = CNS). The boxplot whiskers extend 1.5 times the inter-quartile range from the 25<sup>th</sup> and 75<sup>th</sup> quartiles (lower and upper ranges of the box, respectively), while the bold line indicates the median

### 5.3.3 Temporal trends in otolith elemental concentrations within fish

To examine temporal patterns and inter-relationships between elements, multi-elemental profiles are displayed for eight tagged plaice in Figure 5.22 and Figure 5.23. Note that all profiles apart from 3.4-1000 were obtained from frontal sections. Individual data points within each plot were obtained from the same spot analysis, and thus directly comparable, however, the displayed temperature profiles and dates were inferred, so potentially include some error. What is immediately striking in the SIMS analyses is how much more correlated  $\text{Li}_\text{O}$ ,  $\text{Ba}_\text{O}$  and  $\text{Sr}_\text{O}$  are in the WNS fish and how much higher  $\text{Ba}_\text{O}$  concentrations are in the CNS fish, particularly in the older male (A12388, 8 yrs), with maximum concentrations  $>10\mu\text{mol/mol}$ . Cycles at c. yearly periodicity were observed in  $\text{Ba}_\text{O}$  in all of the CNS fish, but only in the final, tagged year for the younger CNS male (A12522, 5 yrs). There was no clear cycling of  $\text{Ba}_\text{O}$  in the young ENS female (3.2-1137, 5 yrs), however, due to fast growth rates,  $<2$  years worth of material is displayed. In all fish apart from 3.4-1000, there was a general increase in  $\text{Sr}/\text{Ca}$  ratios over time, corroborating the significant age effect in the mixed model analyses. The increase was incremental, punctuated by increases, usually during winter, and declining concentrations through spring and summer. The cycling of  $\text{Sr}/\text{Ca}$  was most apparent in the transverse section of the mature (9yrs) WNS female 3.4-1000, which carried out a long migration into the east English Channel to spawn, and the WNS male (A12382) which carried out a repeat migration from the Scottish borders to the same southern spawning ground. Note that otolith growth during time at liberty was slow for A12382, and  $\text{Sr}/\text{Ca}$  ratios remained relatively high and constant for its 446 days at liberty, while  $\text{Li}/\text{Ca}$  and  $\text{Ba}/\text{Ca}$  ratios exhibited two clear cycles in these two final years of growth.

During the tagged period, concentrations of  $\text{Li}_\text{O}$  were highest in the ENS female (3.2-1137, note use of  $2^\circ$  axis), and in 3.4-1000 (although this spike may be contamination or artefact). In both cases and across most of the profiles, the highest Li concentrations were located in opaque regions of the otolith, and appeared to result in markedly different concentrations in the younger vs. older CNS fish.  $\text{Li}_\text{O}$  generally varied inversely with temperature, but the elevated concentrations in the ENS fish, when water temperature was not particularly low, suggest that additional influences such as salinity and/or opacity might have also been playing a role, as suggested by the mixed model analyses.

The LA-ICPMS results show a relatively consistent negative relationship between  $\text{Sr}_\text{O}$  and  $\text{Mn}_\text{O}$ , particularly apparent in the younger fish and WNS fish.  $\text{Mn}_\text{O}$  was highest in the opaque zones the year prior to tagging in the ENS female (3.2-1137) and young WNS male (A12382 – for both note use of  $2^\circ$  axis), as well as during time of maximum water temperatures in the immature CNS female (A12431) in November.  $\text{Mn}_\text{O}$  and  $\text{Sr}_\text{O}$  appeared to exhibit positive and negative correlations with water temperature, respectively.

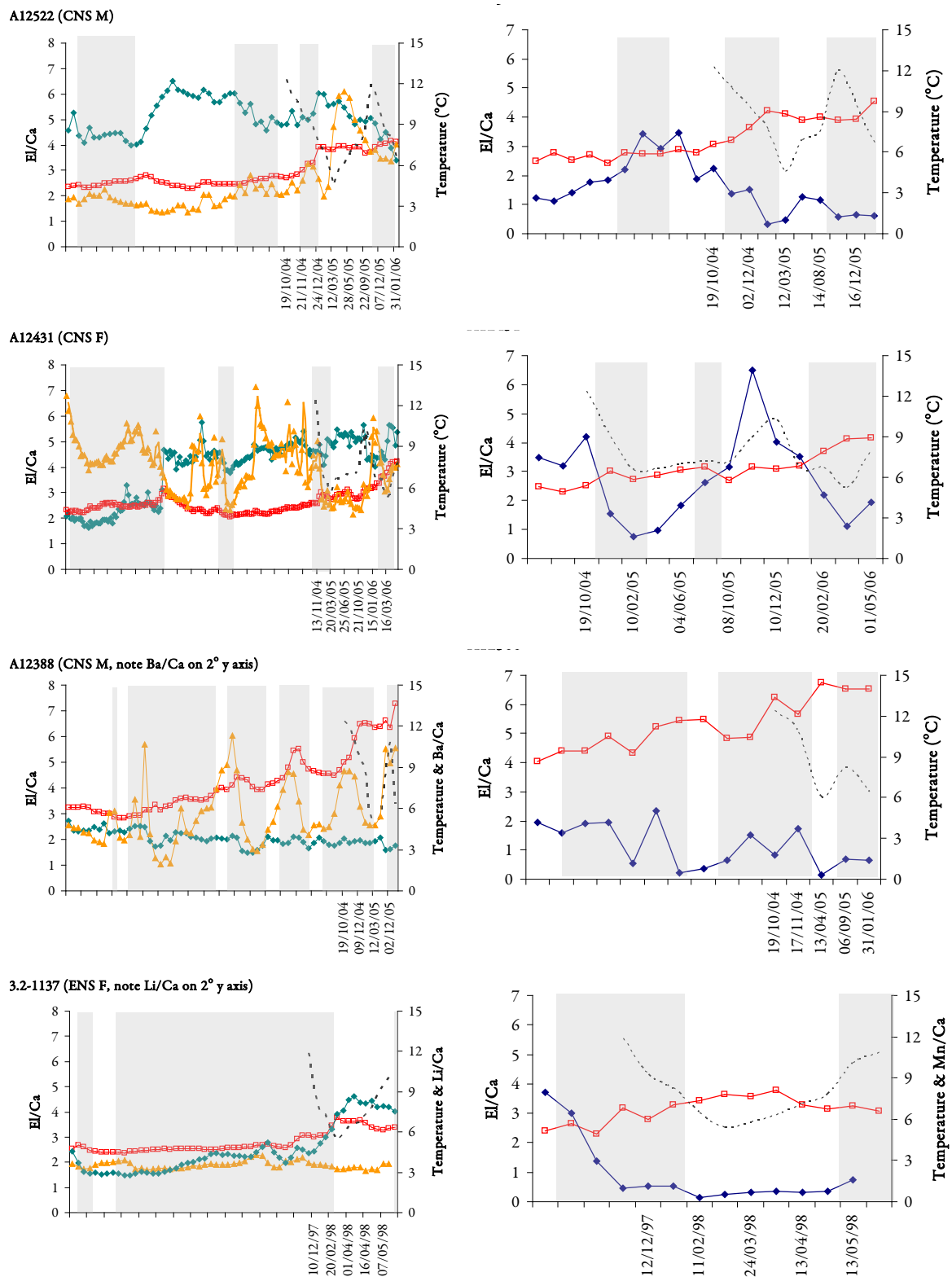
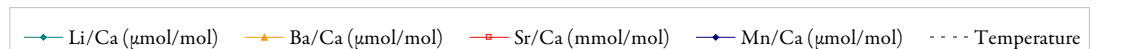


Figure 5.22 Trace element profiles for 4 DST tagged plaice. Plots on the left represent SIMS measurements (Sr = red, Li = green, Ba = orange); plots on the right, HR-LA-ICPMS measurements (Sr = red, Mn = blue). DST recorded temperature (dashed line), fish identity, sex and subunit are displayed. Unless otherwise stated, El/Ca ratios are scaled to the 1° y-axis (Sr in mmol/mol; Ba, Mn, Li in  $\mu\text{mol/mol}$ ). Background colour indicates opaque (white) and translucent (grey) otolith zones. The x-axis is not scaled, representing sequential analyses to the otolith margin, but dates inferred by growth bands and  $\delta^{18}\text{O}$  patterns are displayed.

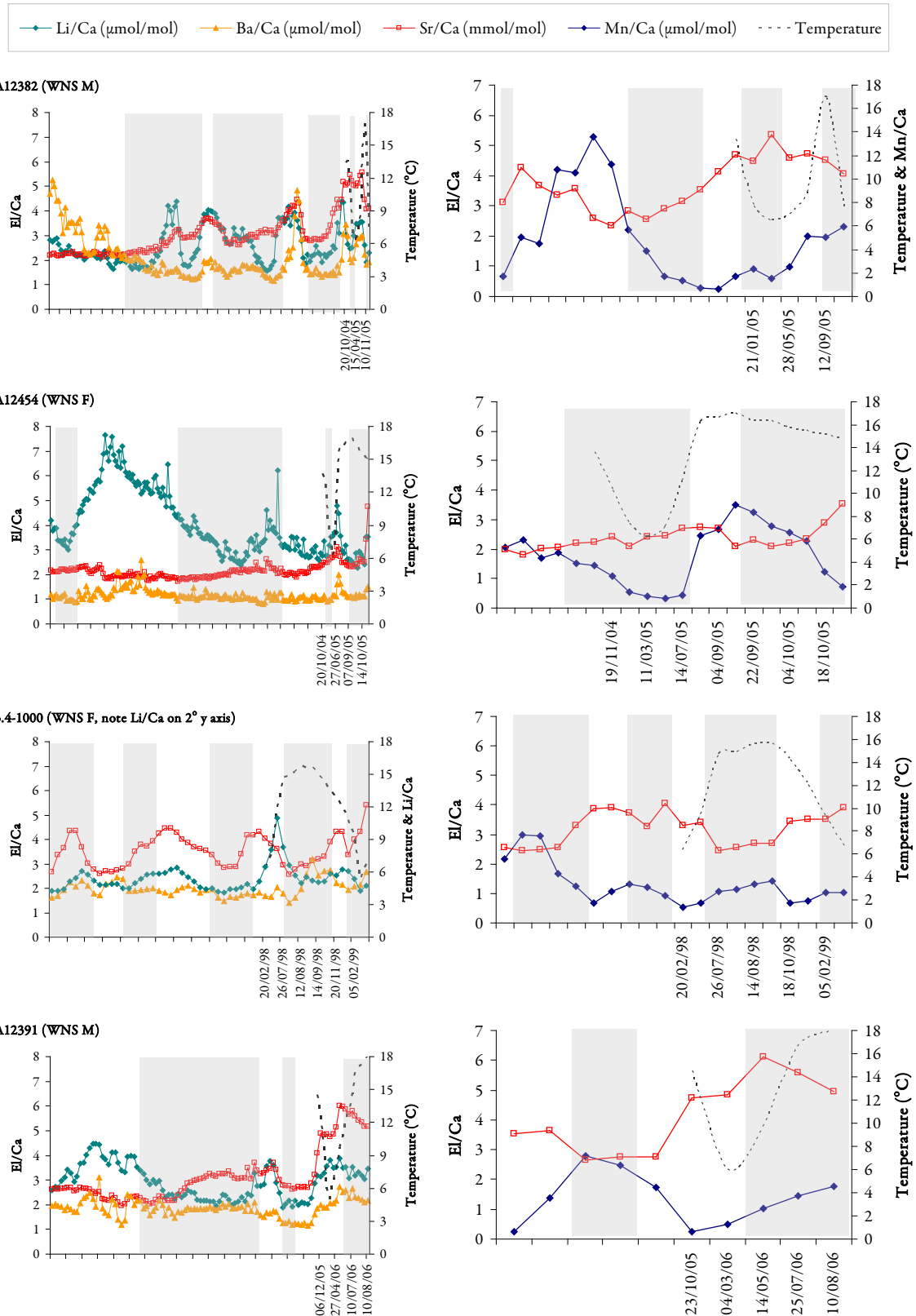


Figure 5.23 Trace element profiles for 4 DST tagged plaice. Plots on the left represent SIMS measurements ( $\text{Sr} = \text{red}$ ,  $\text{Li} = \text{green}$ ,  $\text{Ba} = \text{orange}$ ); plots on the right, HR-LA-ICPMS measurements ( $\text{Sr} = \text{red}$ ,  $\text{Mn} = \text{blue}$ ). DST recorded temperature (dashed line), fish identity, sex and subunit are displayed. Unless otherwise stated,  $\text{El/Ca}$  ratios are scaled to the  $1^\circ$  y-axis ( $\text{Sr in mmol/mol}$ ;  $\text{Ba, Mn, Li in } \mu\text{mol/mol}$ ). Background colour indicates opaque (white) and translucent (grey) otolith zones. The x-axis is not scaled, representing sequential analyses to the otolith margin, but dates inferred by growth bands and  $\delta^{18}\text{O}$  patterns are displayed.

### 5.3.4 Otolith oxygen stable isotopic composition

During DST periods, otolith  $\delta^{18}\text{O}$  values ranged between  $-0.71\text{\textperthousand}$  (ENS female, 3.2-1120) and  $3.20\text{\textperthousand}$  (CNS female, 3.3-1127). Average otolith  $\delta^{18}\text{O}$  values differed significantly among feeding aggregations ( $F_{2,8} = 39.28$ ,  $p < 0.001$ ), with CNS fish exhibiting higher otolith  $\delta^{18}\text{O}$  values than either other subunit ( $p < 0.05$ , Tukey's test), but there was no difference between  $\delta^{18}\text{O}$  values among the WNS and ENS feeding aggregations nor between any spawning aggregations.

### 5.3.5 Evidence for repeat migrations?

Multi-year  $\delta^{18}\text{O}$  profiles for two of the younger tagged plaice (A12522, CNS male and A12454, WNS female) were examined alongside  $\text{Ba}_{\text{O}}$  and  $\text{Li}_{\text{O}}$  respectively to see whether the markers gave any indication of repeat migration behaviour and whether patterns corroborated each other (Figure 5.25). For A12522, the Ba cycles commonly observed in the CNS fish were much lower in the previous year and non-existent between ages 2 and 3. Similarly, the summer  $\delta^{18}\text{O}$  minima were slightly lower in the previous year and much lower for ages 1-3, implying that the fish had inhabited different areas prior to tagging and the patterns observed were likely to have coincided with its first full spawning migration. A12454 exhibited near identical otolith  $\delta^{18}\text{O}$  and Li/Ca profiles the year prior to tagging implying that it had experienced near identical conditions the previous year, and the DST period had recorded its second year of migration.

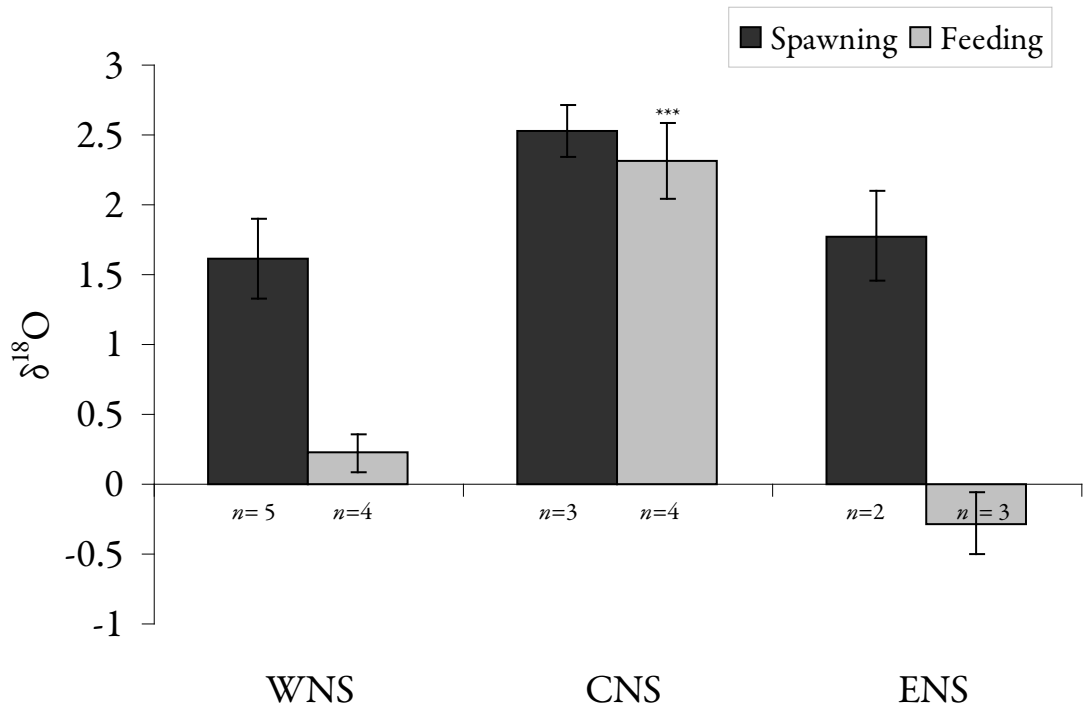


Figure 5.24 Average ( $\pm$ SEM) otolith  $\delta^{18}\text{O}$  for plaice from blue (WNS), red (CNS) and green (ENS) subunits. Averages were based on within fish average  $\delta^{18}\text{O}$  when DST records indicated active feeding or spawning. Note that ENS individual 3.2-1207 spawned in the southern North Sea so was grouped within the WNS spawning group. Significant differences among subunit otolith  $\delta^{18}\text{O}$  values ( $p < 0.05$ , Tukey's *post hoc* test) are indicated by asterisks.

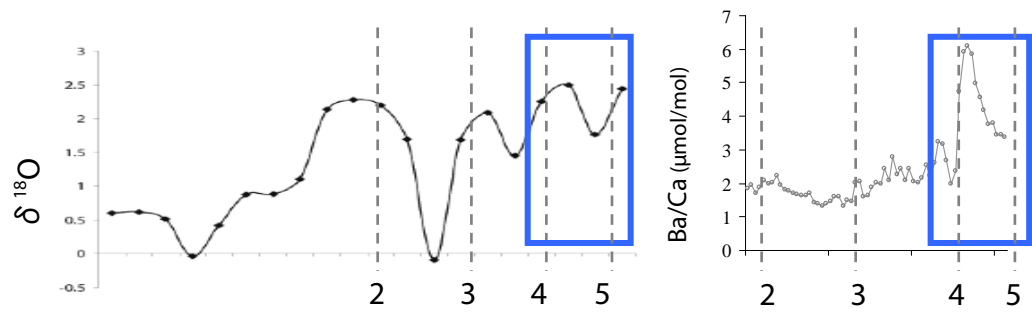
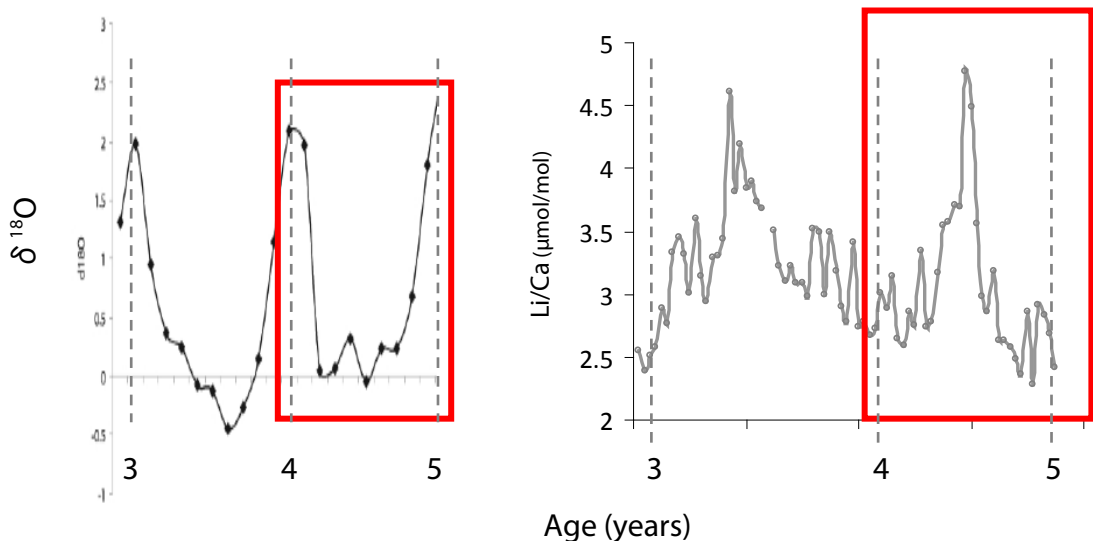
**A****B**

Figure 5.25 (A) Otolith  $\delta^{18}\text{O}$  and Ba<sub>O</sub> profiles for the final 4 years of A12522 (CNS male) and (B)  $\delta^{18}\text{O}$  and Li<sub>O</sub> profiles for the final 2 years of A12454 (WNS female). DST periods are indicated by blue (male) and red (female) boxes and ages by vertical dashed lines

## 5.4 Discussion

This represents the first study to couple otolith trace elemental profiles for wild marine fish with known migration pathways. The results generally corroborate the patterns reported in the experimental population, suggesting that potentially confounding effects associated with the sampling regime were minor compared with the intrinsic and environmental effects observed. Variations in otolith element concentrations associated with DST periods were generally well explained by the mixed effects models presented in this chapter ( $r^2 = 0.54 - 0.99$ ), with each model based on only 2-4 terms. Of the four elements examined, only Ba exhibited significant differences in otolith concentrations among population subunits, indicating clear potential to act as a geographic marker in North Sea plaice.  $\text{Sr}_\text{O}$ ,  $\text{Mn}_\text{O}$  and  $\text{Li}_\text{O}$  models all included a significant temperature effect, although, as will be discussed, we argue that the effect is likely indirect for  $\text{Sr}_\text{O}$  and possibly  $\text{Mn}_\text{O}$ . A direct temperature effect on  $\text{Li}_\text{O}$  concentrations would provide an exciting new possible geothermometer, however, biomineralisation effects require better explanation before the results can be taken with confidence. Interpretations of the trends and their implications are discussed on an element-by-element basis below.

### 5.4.1 Lithium

The variables that explained the most variation in  $\text{Li}_\text{O}$  values were opacity, temperature, season and salinity. As observed in the experimental plaice, there was a significant, negative relationship between  $\text{Li}_\text{O}$  and salinity. However in the wild fish, the relationship was driven heavily by the elevated  $\text{Li}_\text{O}$  concentrations in the ENS fish and with the intermittent drops in salinity in this region. Low salinities in the south east North Sea are well documented, driven largely by freshwater inputs from the Rhine (OSPAR, 2000), however, the salinity data were highly skewed and GETM model performance is known to be poorer in coastal regions (Stips *et al.*, 2004), reducing some confidence in this trend. The only experiment to have systematically tested relationships between salinity and  $\text{Li}_\text{O}$  reported a strong positive relationship, although in the same study, a strong negative relationship was observed between  $\text{Rb}_\text{O}$  and salinity (Hicks *et al.*, 2010). Moreover, in the experimental plaice, the negative relationship between  $\text{Li}_\text{O}$  and  $\text{Li}_\text{W}$  occurred despite a weakly positive relationship between  $\text{Li}_\text{W}$  and  $\text{Li}_\text{B}$  concentrations (Chapter 3 and 4). Clearly, the mechanisms governing uptake and incorporation of monovalent ions into the otolith are complex. Whether such salinity effects prove reliable or not, the negative effect of temperature appeared consistent and additive to any opacity and salinity effects. Li/Ca ratios in foraminifera also exhibit inverse relationships with temperature, although interspecific differences in temperature sensitivity

imply potential for physiological (or biomineralisation) effects (Marriott *et al.*, 2004). These would need to be investigated fully before any thermal effects in  $\text{Li}_\text{O}$  values could be considered reliable. However, many applications could be imagined if  $\text{Li}_\text{O}$  values can be shown to exhibit temperature sensitivity particularly combined with the natural chronometry in otoliths. Most studies thus far have focused on the two elements that have most commonly exhibited temperature effects in coral geochemistry:  $\text{Sr}_\text{O}$  (e.g. Radtke *et al.*, 1990; Townsend *et al.*, 1992; Martin *et al.*, 2004) and  $\text{Mg}_\text{O}$  (e.g. Martin and Thorrold, 2005; Martin and Wuenschel, 2006; Miller, 2011). However, contradictory results among studies, species and life history stages are rife (Chapter 1), strongly implying that any apparent temperature sensitivity in  $\text{Mg}_\text{O}$  and particularly  $\text{Sr}_\text{O}$  values is indirect. The relationship between otolith oxygen stable isotopic composition, temperature and salinity is well established (e.g. Hoie *et al.*, 2004), and the congruent patterns exhibited in  $\delta^{18}\text{O}$  and  $\text{Li}_\text{O}$  in the final two years of life for A12454 suggest that this WNS female experienced near identical temperature and salinity regimes during her 'year at liberty' and year prior. These data offer support for the potential use of  $\text{Li}_\text{O}$  to act as an 'environmental marker' as well as providing valuable information about repeat-migration behaviour, with artificial tags rarely providing multi-year information.

The effect of otolith biomineralisation on  $\text{Li}_\text{O}$  would clearly need further investigation. While our measure of opacity was subjective and relatively crude, there was consistent enrichment of Li in opaque zones, both in wild and experimental populations. These observations corroborate other studies that have reported significant elevation of Na and K concentrations in opaque zones (Hoff and Fuiman, 1995; Tomás *et al.*, 2006). The mechanisms governing enrichment of monovalent ions in opaque regions remains elusive; however, it may be related to differences in crystal properties or organic components such as proteins, lipids and sugars (Tomás *et al.*, 2006). A possible additional effect of *post-mortem* contamination cannot be ruled out, however, in the study of Milton & Chenery (1998) a significant effect was observed for Na but not Li. Importantly, in the current study, the effect of opacity on  $\text{Li}_\text{O}$  appeared additive to any environmental effects, rather than interactive. However, it would have the potential to confound absolute temperature interpretations. For example, the two CNS males (A12522 and A12388) exhibited almost identical temperature histories, but absolute concentrations of  $\text{Li}_\text{O}$  were almost three times higher in the younger male and annual fluctuations in  $\text{Li}_\text{O}$  were very small in the older individual (A12388). While these observations are largely anecdotal, otoliths from the younger fish consistently exhibited wider opaque regions of higher reflectivity than the older fish (including A12388). Often in the older individuals, yearly bands were indicated only by fine 'striations'; in such cases, opacity was

often scored zero (translucent) for sequential analyses across multiple years. Here, quantification of opacity using a continuous measure, such as luminescence (Tomás *et al.*, 2006), would be of a clear advantage, and may help to separate biomineralisation and environmental effects.

The significant ‘sex effect’ observed in the experimental plaice was not apparent in the tagged fish. As discussed in Chapter 4, the ‘sex effect’ was most likely attributed to differences in otolith opacity among the mature females and males in the experimental population. Thus if opacity can be controlled for (e.g. by only comparing among similarly aged fish) there does not appear to be a systematic difference between males and females.

### 5.4.2 Manganese

The  $Mn_O$  model for wild fish included a significant positive temperature effect and a non-significant effect of somatic growth rate on  $Mn_O$  concentrations. These patterns corroborate the trends reported in the previous chapter; however, in the experimental fish, variations in  $Mn_O$  concentrations were primarily explained by otolith and somatic growth rates, and temperature was more important for explaining variations in  $D_{Mn(O/B)}$  values (although growth rate and condition were still highly significant). It should be noted that in the current chapter, the growth rate data were of relatively low quality, with initial values rounded to the nearest centimetre and no information about changes within their time at liberty. Separating temperature and growth rate effects in otolith microchemistry is clearly a significant and ongoing challenge. Past studies have observed negative temperature effects on  $Mn_O$  (Miller, 2009) as well as a positive relationship between temperature and  $D_{Mn/Ca(O/W)}$  at lower salinities, but no relationship with  $D_{Mn/Ca(O/W)}$  at higher salinities, and no relationship with absolute  $Mn_O$  concentrations (Martin and Thorrold, 2005). Such conflicting results, as well as the observations in the experimental fish, suggest that the most parsimonious effect is one of a positive, temperature-mediated growth rate effect, although further validation is required. Potentially further complicating its application as an environmental marker is the fact that  $Mn_O$  is one of the most ontogenetically regulated elements, exhibiting elevated concentrations in the core (Brophy *et al.*, 2004; Ruttenberg *et al.*, 2005) and younger otolith regions (Miller, 2009). Such effects may help to explain the negative (albeit non significant) relationship between  $Mn_O$  and age observed in the wild fish during their time at liberty. While the models built in the current chapter only included data associated with the DST period, examination of individual chemical profiles (Figures 5.22 and 5.23) indicated  $Mn_O$  values an order of

magnitude higher in the otolith opaque zones the year prior to tagging in A12382 and 3.2-1137, and suggested a general decline over time in one of the older females (3.4-1000).

Regarding the usefulness of  $Mn_O$  as a geographic marker in marine systems, concentrations did not differ among the subunits examined and did not exhibit any relationship with salinity. Without direct knowledge of  $Mn_W$  concentrations for the relevant areas and time periods, it is not possible to conclude much from this, past the obvious suggestion that  $Mn_O$  might not be so useful a marker for discriminating among these particular North Sea plaice subpopulations. However, significant differences in  $Mn_W$  among the three regions were highly likely (Burton *et al.*, 1993). This, along with the fact that no empirical studies have observed a positive relationship between  $Mn_O$  and  $Mn_W$  (Miller, 2009), suggest that the positive correlation between  $Mn_W$  and  $Mn_O$  values in the experimental fish may not have been the main effect.

### 5.4.3 Strontium

$Sr_O$  values followed a similar overall pattern to those exhibited by the experimental plaice, with the lowest annual concentrations coinciding with the period of warmest water temperatures. Also, similar to the experimental results, the wild fish exhibited a negative relationship between  $Sr_O$  values and growth rate, although here, the positive relationship with age was more significant. In the DST tagged plaice there was also a significant negative effect of temperature, although when separated by sex, the effect was weak and inconclusive (Figure 5.10). There was no indication of consistent differences in  $Sr_O$  values among subunits, nor any relationship between migration distance and  $Sr_O$  variation, contradicting previous observations in mature female North Sea plaice (Hunter and Darnaude, 2004) and appearing to indicate little worth as a natural tag in this system.

While there may be some minor direct effects of temperature on otolith Sr incorporation, based on the various pieces of evidence outlined below, it appears that any such 'temperature effects' are primarily governed by temperature-mediated changes in physiology in marine fish. First, conflicting results are rife, undermining any observed relationship between temperature and  $Sr_O$  and  $D_{Sr}$  values. While negative temperature effects on  $Sr_O$  have been observed in larvae of some temperate species (e.g. DiMaria *et al.*, 2010), the majority of studies report positive or non-significant effects (e.g. Martin *et al.*, 2004). The negative relationship observed in the current study thus directly contradicts the most parsimonious relationship currently in the literature. Second, as observed for plaice (e.g. Figure 5.23, fish 3.4-1000 and Hunter and Darnaude, 2004), sea-caged salmon (Clarke and Friedland, 2004) and a number of other marine species

(Kalish, 1989),  $\text{Sr}_\text{O}$  values generally increase around age at maturity then exhibit fluctuations sometimes greater than reported for diadromous species (Brown and Severin, 2009). Such patterns cannot be explained by ambient Sr concentrations in the sea, with only minor fluctuations in salinity and almost no variation in  $\text{Sr}/\text{Ca}_\text{W}$  values (Zimmerman, 2005). However, neither can they be explained by a direct temperature effect, for temperature fluctuations in coastal nursery grounds tend to be far greater than in the open sea (Fuiman and Hoff, 1995). Third, in the current study, the differences in  $\text{Sr}_\text{O}$  among tagged males and females were far greater than among individuals with contrasting (and known) temperature histories (Figure 5.11).

The effects of physiology on  $\text{Sr}_\text{O}$  values are clearly important in marine fish, although it is unclear whether the main drivers of the intra-annual variations are growth rate, condition and/or reproductive investment. The results presented in Chapters 3 and 4 indicated a strong positive relationship between  $\text{Sr}_\text{B}$  and blood protein concentrations, condition, growth rates and GSI, and a strong relationship between  $\text{Sr}/\text{Ca}_\text{B}$  and  $\text{Sr}/\text{Ca}_\text{O}$ . Multiple studies have observed (or inferred) a positive relationship between reproductive investment and  $\text{Sr}_\text{O}$  (Kalish, 1991; Hoff and Fuiman, 1995; Clarke and Friedland, 2004). While no GSI measures were available for the tagged plaice,  $\text{Sr}_\text{O}$  was generally elevated during the spawning season in the females, but not in the males, however the effect was not significant. Reproductive investment in female plaice is approximately twice that of males, and increases with age (Bromley, 2000). Despite this, there was only very slight enrichment in  $\text{Sr}_\text{O}$  values in the mature experimental females compared with the males and immature fish. Previous studies have ascertained that the main driver of otolith  $\text{Sr}_\text{O}$  in marine fish is growth rate (Sadovy and Severin, 1992; 1994). Based on the results presented in the current study and in the literature, this would appear to be the most parsimonious explanatory variable for the various trends observed, however, it is likely that almost any physiological behaviour that significantly modifies blood protein (and thus Ca) composition, will likely result in changes in  $\text{Sr}/\text{Ca}_\text{O}$ . If, based on these various arguments, growth rate is the main driver for the seasonal and inter-annual fluctuations in  $\text{Sr}_\text{O}$  values, then the negative relationships between  $\text{Sr}_\text{O}$  and  $\text{Mn}_\text{O}$  values, exhibited by all profiles in Figures 5.22 and 5.23, would appear to support the hypothesis that  $\text{Mn}_\text{O}$  concentrations are also primarily governed by growth rate, rather than a direct effect of temperature.

#### 5.4.4 Barium

Ba was the only element to vary systematically with population subunit and was thus considered the strongest candidate for use as a natural tag within this system. The geographic differences were consistent despite seasonal variations that were broadly similar to those of  $\text{Sr}_\text{O}$  and exhibited by the experimental plaice.

Indeed, the  $\text{Ba}_\text{O}$  model explained almost all the variation in otolith concentrations based on subunit, season and otolith growth rate. While 'season' was significant, reflecting consistent elevation of  $\text{Ba}_\text{O}$  values during the winter spawning period, the term did not appear to be a 'proxy' for temperature, as temperature was only weakly correlated with  $\text{Ba}_\text{O}$ , and when separated by subunit, the correlation was undetectable. Here, the seasonal effect in  $\text{Ba}_\text{O}$  was most likely driven by the strong negative relationship observed between otolith growth rate and(or) condition. Otolith growth rate and condition were both highly negatively correlated with  $\text{Ba}_\text{O}$ , but missing values in the latter term resulted in a slightly poorer model fit. However, there is no particularly convincing argument to favour one over the other. The higher concentrations in the CNS fish were consistent across all temperatures, although similar to the patterns in  $\text{Sr}_\text{O}$  values, concentrations in the older, slower growing male (A12388) were almost double those exhibited by the two younger CNS fish, exhibiting  $\text{Ba}/\text{Ca}_\text{O}$  ratios as high as  $11.3 \mu\text{mol/mol}$ . Migration pathways for A12522 and A12388 were very similar, suggesting that the enrichment of Ba in the older male related to his slower growth rate, rather than exposure to higher ambient concentrations. However, the potential for large seasonal fluctuations in  $\text{Ba}_\text{O}$  values to be related, at least in part, to fluctuations in environmental conditions cannot be ruled out.

Consistent positive relationships have been observed between  $\text{Ba}/\text{Ca}_\text{W}$  and  $\text{Ba}/\text{Ca}_\text{O}$  in the laboratory (e.g. Elsdon and Gillanders, 2003b), and Ba in seawater follows a nutrient-type distribution (Steele *et al.*, 2009), linked to primary productivity (Dehairs *et al.*, 1997). One of the most unique features of the CNS is the persistence of the thermocline, resulting in CNS plaice being exposed to cold, thermally stratified water for the majority of the year (Pingree and Griffiths, 1978). Breakdown of (or migration through) the thermocline in the CNS occurs in autumn (Hunter *et al.*, 2003b). If this event resulted in sudden flux of nutrient rich waters to the lower depths, this could provide a possible explanation for the elevated, but fluctuating,  $\text{Ba}_\text{O}$  concentrations in CNS plaice.

Weak positive correlations between  $\text{Sr}_\text{O}$  and  $\text{Ba}_\text{O}$  were observed in the current study ( $r^2$  for pairwise correlation of all data points = 0.15) and have also been observed in Patagonian toothfish (*Dissostichus eleginoides*) another fully marine species (Ashford *et al.*, 2005). In estuarine systems  $\text{Sr}/\text{Ca}_\text{W}$  and  $\text{Ba}/\text{Ca}_\text{W}$  ratios are commonly negatively correlated due to the efficient removal of Ba from seawater, and stability of Sr (Ashford *et al.*, 2005). This effect has proved valuable for using otolith chemistry to track movements of estuarine dependent and diadromous species (Elsdon and Gillanders, 2005b). However for plaice, a fully marine species, the positive relationship between  $\text{Sr}_\text{O}$  and  $\text{Ba}_\text{O}$  values indicates that influences of growth rate and/or condition on the incorporation of both elements outweigh small variations in ambient water concentrations. In the WNS fish the peaks in  $\text{Ba}_\text{O}$  values appeared highly correlated with  $\text{Li}_\text{O}$  as well as  $\text{Sr}_\text{O}$  values (Figure 5.23), however there was no overall relationship between  $\text{Li}_\text{O}$  and  $\text{Ba}_\text{O}$  ( $r^2 < 0.01$ ) and the

increases in  $\text{Li}_{\text{O}}$  values generally occurred slightly earlier than the increases in  $\text{Ba}_{\text{O}}$  and  $\text{Sr}_{\text{O}}$  values, further implying temperature and temperature-mediated growth rate effects, respectively. The 'lag' effect is subtle however, so the final four years of the  $\text{Li}_{\text{O}}$  and  $\text{Ba}_{\text{O}}$  profiles for A12382 (WNS male) are displayed in Figure 5.26. Such lags may well have been lost through signal attenuation if a larger spot size had been used. Lags between temperature and Sr/Ca changes have formed the basis of many arguments for an indirect temperature effect on otolith Sr/Ca ratios (e.g. Clarke and Friedland, 2004), but it has been suggested that such lags could be artefact of signal attenuation due to ablation depth (C. Jones, pers. comm.). Here, the effect was observed in SIMS analyses, whose ablations penetrate  $< 5\mu\text{m}$  (Fairchild *et al.*, 2001), and where ablation depth is unlikely to have explained the observed lag. Similarly, the use of a static spot size despite known intra-annual variations in otolith growth rate could also add to such 'lag effects', particularly during periods of slowed growth, such as in the winter spawning months. If this were a significant problem however, one would expect to observe depressed  $\delta^{18}\text{O}$  values during the winter months as a result of signal attenuation and a larger spot size ( $\sim 20\mu\text{m}$ ). Generally, however, absolute  $\delta^{18}\text{O}$  values reflected those predicted by temperature and salinity, implying that the 'lags' observed within the higher resolution trace metal analyses ( $\sim 8\mu\text{m}$ ) were not caused by sampling artefact.

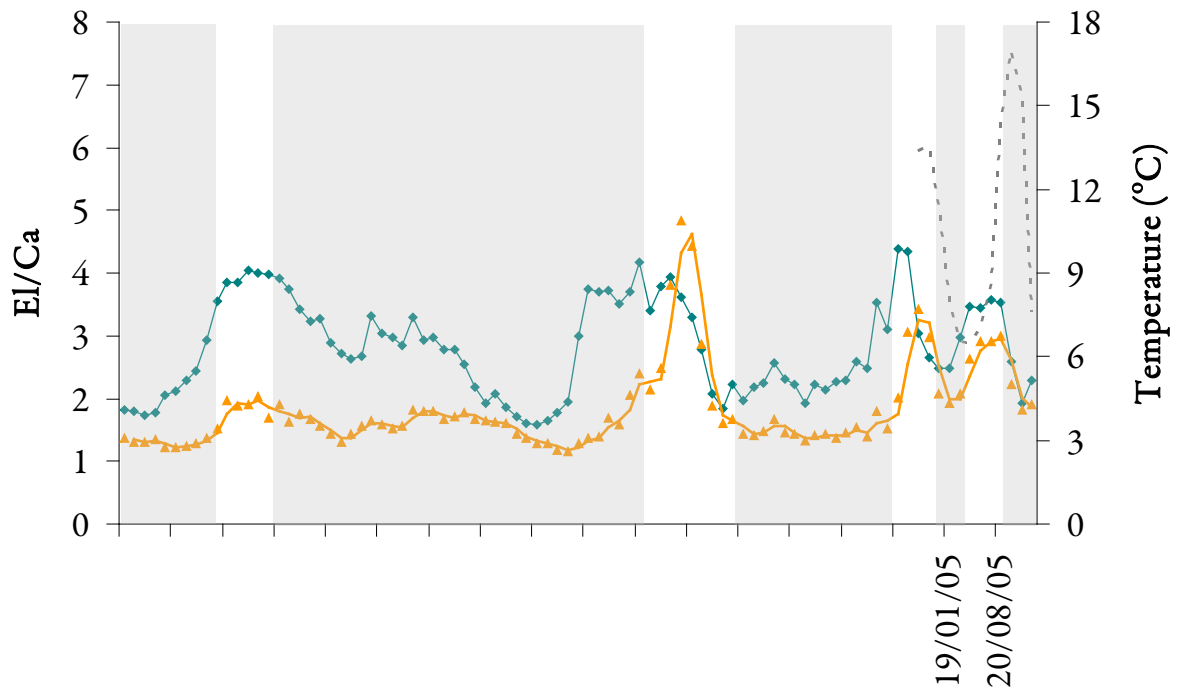


Figure 5.26 Temporal variations in  $\text{Li}_\text{O}$  (green) and  $\text{Ba}_\text{O}$  (orange) concentrations in  $\mu\text{mol/mol/Ca}$  for WNS male A12382. The plot is identical to that displayed in Figure 5.23, but enlarged to highlight the final four years of life. The DST temperature profile is also displayed (dashed line) along with the dates during the DST period inferred by  $\delta^{18}\text{O}$  profiles. Note the slight mismatch between  $\text{Li}_\text{O}$  and  $\text{Ba}_\text{O}$  peaks, presumed here to be related direct vs. indirect effects of temperature, respectively

### 5.4.5 Implications and applications

By coupling otolith microchemistry with 'known migrations', it was possible to examine physiological and environmental effects on otolith microchemistry in a natural marine setting. To our knowledge, *in situ* validation studies of this nature have not been carried out before. The value of such an approach is clear; even when attempting to mimic natural conditions in the laboratory, the removal of the subject from their natural habitat can have severe, unforeseen consequences, with factors such as stress having the potential to significantly alter otolith element concentrations (Kalish, 1992). This may explain, in part, some of the contradictions observed among studies in the literature (reviewed in Chapter 1). Given broad similarities in the responses of tank-maintained and free-ranging plaice in the current study, it suggests that here at least, any 'captivity effects' were minimal compared to the observed main effects, and provides additional confidence to the results presented in previous chapters.

Whilst using a very different approach, the tagging study has clear similarities with the mensurative experiment presented in Chapters 2-4. Both approaches produced datasets that were innately complex and uncontrolled. While such datasets have some clear disadvantages, with interpretations often relying on correlations among collinear variables, the major advantage is the capture of natural physiological and migratory behaviours. Given collinearity among many of the variables, the results of the models and interpretations must be treated with caution, however, wherever possible, results were examined in the context of complementary empirical studies. Clearly, element incorporation into the otolith is a complex process and without a combination of empirical, theoretical and field-based approaches it is impossible to obtain a full and robust picture of the controls on, and applications of, otolith microchemistry.

Of the four elements examined in the current study, Ba and possibly Li, appeared to hold greatest promise for inferring habitat use in North Sea plaice. The marine environment exhibits inherently lower variations in elemental concentrations than other aquatic systems (Turekian, 1968). From an otolith microchemistry perspective, this means that the importance of physiological effects is greater, as they hold greater potential to confound the smaller environmentally induced variations. This is most clear for  $\text{Sr}_\text{O}$  and  $\text{Ba}_\text{O}$ , where variations in otolith concentrations are strongly driven by both ambient concentrations and physiology. However, while ambient concentrations in  $\text{Ba}/\text{Ca}_\text{W}$  can and do vary in the marine environment,  $\text{Sr}/\text{Ca}_\text{W}$  remains near constant across the entire possible range of salinities. While in the current study, the use of otolith  $\delta^{18}\text{O}$  measurements were primarily used as a tool to assign timelines to individual otolith sections, the potential for this marker as a stock discriminator is significant (Thorrold *et al.*, 1997). However, its use as a natural tag to assign individual fish to locations in the open ocean is often precluded by limited data on the

distribution of ambient  $\delta^{18}\text{O}$ , temperature and salinity. Another potentially limiting factor associated with using otolith  $\delta^{18}\text{O}$  measurements to infer movement patterns is obtaining high enough resolution with a micromill to obtain intra-annual samples while avoiding signal attenuation (Høie and Folkvord, 2006). This is particularly an issue in older fish, where otolith increments are narrower. Here, the use of SIMS offers a clear advantage, providing high resolution, high-precision analyses across the time periods of interest (Hanson *et al.*, 2010). Indeed, even with only 11 data points per season, it was possible to significantly separate CNS from WNS and ENS feeding aggregations. Used in combination with  $\text{Ba}_{\text{O}}$  and  $\text{Li}_{\text{O}}$ ,  $\delta^{18}\text{O}$  values appeared to indicate differences in habitat use during pre-DST periods. While the aim of the current study was to better understand controls on element incorporation into the otolith, these preliminary data imply that multi-marker approaches such as this, combining both natural and artificial tags, provide a powerful approach for tracking individual movements in the open ocean.



# Chapter 6

---

## *Conclusions*

The aim of this project was to determine whether otolith trace element chemistry can be used to track migrations in fully marine fish. This question was addressed through:

1. a semi-controlled experiment where fish were maintained in a monitored environment and the relationship between water, blood and otolith chemistry assessed with reference to environmental and physiological variables.
2. Analysis of variations in otolith trace element chemistry in wild fish tagged with data storage tags (DST)

The work here represents the first repeated-measures for both blood and otolith element concentrations in individual mature and immature marine fish. A novel method of calibrating time within annual increments in otoliths using SIMS oxygen isotope analysis was developed and used in both experimental and wild fish. The study is also the first (to our knowledge) to have coupled archival tag records (i.e. 'known' migrations) with otolith trace element concentrations in free-ranging marine fish. Given considerable discussion of results within each chapter, here, the main findings and interpretations are summarised, along with a brief synopsis of the study limitations and possible future directions.

The thesis was divided broadly into three sections:

1. a review of the current literature examining how otolith elemental concentrations might be used to track individual movements of marine fish
2. a mensurative experiment examining the main intrinsic and extrinsic variables governing element concentrations in the blood and otoliths of plaice, a fully marine flatfish. This section includes method developments carried out to measure trace element concentrations in fish blood plasma and a new method using otolith  $\delta^{18}\text{O}$  values to assign a timeline to individual otolith sections.
3. a study coupling otolith elemental concentrations with geographic, environmental and physiological variables in DST tagged plaice in order to examine the effects on, and possible applications of, otolith elements as natural tags in wild North Sea plaice.

Overall, we observed significant physiological influences on blood and (or) otolith composition in every one of the 12 elements considered. These data have clear implications for studies attempting to use otolith microchemistry as a natural tag as they may obscure valuable information present in the otolith. Without acknowledging or attempting to control for them, such intrinsic effects could confound interpretations of otolith microchemistry, with potentially serious management consequences. One of the more reassuring observations was that the sometimes large differences in plasma elemental concentrations between males, females, immature and mature fish were usually far smaller in the otolith, and where present, could almost always be attributed to specific (often linked) physiological parameters, such as condition, sex, protein content and growth rate. If such variables can be accounted for in the sampling design or their effects much smaller than among-region differences, then it should be possible to obtain robust geospatial information from otolith elemental concentrations. It is critical to remember that the ability to resolve spatial questions depends on the relative magnitude of spatial variations in water chemistry and physiological effects on element incorporation into the otolith. Controlling for some of the physiological sources of variation can only improve the potential for recovering spatial information from otolith chemistry.

For studies attempting to use otolith microchemistry as an environmental recorder, it would appear that, at least in the marine environment, there are considerable limits on the choice of elements that might record ambient concentrations or temperature. Elemental fractionation from water to blood indicated considerable 'dampening' of most environmental variations, but generation of new patterns relating to enrichment of the

blood for physiological events such as spawning. The general lack of congruence between blood and otolith element concentrations, however, implied either that total blood concentrations may be a poor proxy for available concentrations, and(or) that significant further elemental fractionation occurs from blood to endolymph, endolymph to otolith. Most likely a combination of factors is involved, but the inferences that can be made about these final steps are limited without (lethal) endolymph sampling. Further validation experiments are clearly required, but the limits imposed on interpretation by necessarily co-linear variables reduce the potential for finding definitive causal relationships between environmental and physiological variables and otolith element partitioning. If it is possible to recreate natural condition whilst keeping water chemistry constant over time, it would help to tease apart the environmental effects. Also, given clear ontogenetic and physiological effects in elemental processing, it is important to include both juveniles and adults in such experiments.

## 6.1 Otolith element concentrations as natural tags

Trends in blood and(or) otolith concentrations of the ‘softer’ elements (Cu, Zn, Se, Pb) as well as the quasiconservative elements Ca and Sr indicated major physiological processing relating to blood protein concentrations, condition and ovary maturation. These appear to limit the usefulness of these elements as natural tags, although in most cases the observed patterns did not refute a potential effect of water concentrations. In fact, the suite of elements mentioned above all exhibited some modification relating to spawning, particularly in the female plaice, for which reproductive investment is greater. This opens up the exciting potential for otolith chemistry to reveal physiological behaviour in marine fish, particularly in elements, such as Sr, which are unlikely to vary considerably within the open ocean, and for which ‘temperature’ effects are often contradictory. A chemical ‘spawning marker’ might allow determination of age-at-maturity and skipped spawning behaviour. Such information would be valuable in marine fisheries management, as it would improve estimates of spawning stock biomass and could allow current and historical trends in spawning behaviours to be linked with anthropogenic pressures such as fishing and pollution, and climatic events such as El Niño. The main factor currently limiting the potential for such a chemical marker, aside from limited validation, is that of all the potential markers mentioned, the effect of spawning on the element most readily measured (Sr) is subtle, and interpretations could easily be confounded by unrelated reductions in growth rate or condition.

Based on the results presented here and previous studies, Sr incorporation into the otoliths of fully marine fish appears to be driven almost entirely by condition and/or growth rate effects, which may themselves be

influenced by age, spawning, migration stress and temperature. It appears that any physiological function that results in elevation of blood protein and  $\text{Ca}^{2+}$  levels are accompanied by increases  $\text{Sr}/\text{Ca}_\text{O}$  ratios. Thus an 'otolith spawning' marker would ideally include a suite of the above mentioned elements. Then, unfortunately, the limiting factor is technology. While ICPMS systems are constantly evolving, in the current study, a HR-ICPMS with a spot size of 35  $\mu\text{m}$  was required to obtain reliable Zn and Cu measurements, and even then, 8.5% of Zn measurements were <LOD and it was not possible to determine Se or Pb concentrations. Clearly, if attempting to identify skipped spawning years in adult otoliths, where increment width is often well under 30  $\mu\text{m}$ , this would be a significantly limiting factor. However, if the aim were to identify onset of maturity, the wider growth increments in juvenile portions of otoliths would likely allow intra-annual sampling of even larger spot sizes.

In both the wild and experimental plaice, a significant negative effect of temperature and (or) salinity was observed on otolith Li/Ca. Based on evidence in the literature, the temperature effect is the more likely and importantly, the effect appeared to be direct, rather than via a temperature-mediated physiological response, such as growth rate. A robust temperature response in an otolith element would be of great use for inferring past thermal conditions, however, validation work is clearly required, as is a better understanding of biominerallisation effects on Li incorporation.

The only otolith element to exhibit clear geographic differences among the three subpopulations examined was  $\text{Ba}_\text{O}$ , which was significantly elevated in CNS plaice. The effect was consistent, even with significant effects of season and otolith growth rate, supporting its value as a natural tag in a fully marine fish.

Finally, whilst the primary focus of the current study was to examine influences on the incorporation of elements into the otolith, the patterns observed in SIMS-measured  $\delta^{18}\text{O}$  values were consistent with those predicted by temperature and salinity and provided clear and robust differences among North Sea feeding aggregations. Future studies attempting to examine multi-year migrations in plaice would be well advised to focus on these three otolith chemical markers in particular ( $\text{Li}_\text{O}$ ,  $\text{Ba}_\text{O}$  and  $\delta^{18}\text{O}$ ).

## 6.2 Limitations of the current study

- Both studies presented herein were largely uncontrolled and incorporated the full complexity of the natural marine system. For this reason they could not be used to formally test hypotheses, but complement empirical studies whilst providing increased control than most field based studies.

Multicollinearity in the data was clearly a major disadvantage, as it made it difficult to tease apart the main effects. Because of this, it is likely that terms that appear significant in models could be spurious, hiding stronger underlying drivers, such as growth rate.

- While the results of the study are of great importance for plaice, there are a large numbers of studies reporting significant species- and regional-specific effects in otolith microchemistry leading to the potential that the results from this body of work may not apply to other species or systems.
- The variations in water chemistry exhibited in this experiment were realistic but perhaps too small to have produced any detectable relationship with otolith concentrations. Ideally, one would carry out a similar experiment while controlling and manipulating water chemistry, however the logistics and cost of such an experiment would be prohibitive, given the need for at least 12 month experiments to ensure sufficient new otolith growth in the narrower adult increments and capture the full spawning cycle. Related to this, the selection of the experimental fish in the current study, based on greater otolith increment width, allow intra-annual analyses across the experimental period, but was not random and also may have 'dampened' effects of otolith growth rate in the subject animals.

### 6.3 Future directions

- A possible future study could include testing the effect of controlling for major physiological parameters, such as sex, age and size, during sampling on the ability to separate fish stocks using otolith microchemistry.
- Expanding the study to examine growth rate effects on otoliths and other biominerals and to see whether such effects have a phylogenetic, crystal habit and/or geographical basis. This would help to understand the causal effects (e.g. kinetic vs. protein) and has wider implications for other geochemical proxies.
- To expand on the DST study, it would be exciting to take advantage of the extensive otolith archives in CEFAS and IMARES to build a large spatio-temporal map of otolith edge 'capture' site multi-elemental signatures, then use this to assign each analysis across the DST transect to a physical location using Random Forest. These predicted tracks could be compared with 'known' pathways obtained from DST records and would enable statistical 'testing' of the use of otolith profiles to infer individual migrations of a fully marine fish.
- Finally the potential for otolith Li/Ca ratios to infer temperature histories requires controlled validation studies and improved understanding of the relationship between otolith Li/Ca and otolith opacity so as to avoid any potentially confounding biomineralisation effects.



# References

Abramoff, M. D., Magelhaes, P. J. & Ram, S. J. (2004). Image Processing with ImageJ. *Biophotonics International* **11**, 36-42.

Andreasen, P. (1985). Free and total calcium concentrations in the blood of rainbow trout, *Salmo Gairdneri*, during "stress" conditions. *Journal of Experimental Biology* **118**, 111-120.

Arai, T., Otake, T. & Tsukamoto, K. (2000). Timing of metamorphosis and larval segregation of the Atlantic eels *Anguilla rostrata* and *A. anguilla*, as revealed by otolith microstructure and microchemistry. *Marine Biology* **137**, 39-45.

Arnegard, M. E., Markert, J. A., Danley, P. D., Stauffer, J. R., Ambali, A. J. & Kocher, T. D. (1999). Population structure and colour variation of the cichlid fishes *Labeotropheus fuelleborni* Ahl along a recently formed archipelago of rocky habitat patches in southern Lake Malawi. *Proceedings of the Royal Society of London. Series B: Biological Sciences* **266**, 119-130.

Arslan, Z. & Paulson, A. J. (2003). Solid phase extraction for analysis of biogenic carbonates by electrothermal vaporization inductively coupled plasma mass spectrometry (ETV-ICP-MS): an investigation of rare earth element signatures in otolith microchemistry. *Analytica Chimica Acta* **476**, 1-13.

Ashford, J., Arkhipkin, A. I. & Jones, C. (2007). Otolith chemistry reflects frontal systems in the Antarctic Circumpolar Current. *Marine Ecology Progress Series* **351**, 249-260.

Ashford, J., Jones, C., Hofmann, E., Everson, I., Moreno, C., Duhamel, G. & Williams, R. (2005). Can otolith elemental signatures record the capture site of Patagonian toothfish (*Dissostichus eleginoides*), a fully marine fish in the Southern Ocean? *Canadian Journal of Fisheries and Aquatic Sciences* **62**, 2832-2840.

Ashford, J., La Mesa, M., Fach, B. A., Jones, C. & Everson, I. (2010). Testing early life connectivity using otolith chemistry and particle-tracking simulations. *Canadian Journal of Fisheries and Aquatic Sciences* **67**, 1303-1315.

Ashford, J. R., Arkhipkin, A. I. & Jones, C. M. (2006). Can the chemistry of otolith nuclei determine population structure of Patagonian toothfish *Dissostichus eleginoides*? *Journal of Fish Biology* **69**, 708-721.

Ashford, J. R., Jones, C. M., Hofmann, E. E., Everson, I., Moreno, C. A., Duhamel, G. & Williams, R. (2008). Otolith chemistry indicates population structuring by the Antarctic Circumpolar Current. *Canadian Journal of Fisheries and Aquatic Sciences* **65**, 135-146.

Audet, C. I., Besner, M., Munro, J. & Dutil, J.-D. (1993). Seasonal and diel variations of various blood parameters in Atlantic cod (*Gadus morhua*) and American plaice (*Hippoglossoides platessoides*). *Canadian Journal of Zoology* **71**, 611-618.

Babaluk, J. A., Halden, N. M., Reist, J. D., Kristofferson, A. H., Campbell, J. L. & Teesdale, W. J. (1997). Evidence for Non-Anadromous Behaviour of Arctic Charr (*Salvelinus alpinus*) from Lake Hazen, Ellesmere Island, Northwest Territories, Canada, Based on Scanning Proton Microprobe Analysis of Otolith Strontium Distribution. *Arctic* **50**, 224-233.

Barany, E., Bergdahl, I. A., Bratteby, L., Lundhd, T., Samuelson, G., Schutz, A., Skerfving, S. & Oskarsson, A. (2002). Trace element levels in whole blood and serum from Swedish adolescents. *The Science of the Total Environment* **286**, 129-141.

Bates, D. (2006). [R] lmer, p-values and all that.

Bath, G. E., Thorrold, S. R., Jones, C. M., Campana, S. E., McLaren, J. W. & Lam, J. W. H. (2000). Strontium and barium uptake in aragonitic otoliths of marine fish. *Geochimica et Cosmochimica Acta* **64**, 1705-1714.

Beckman, D. W. & Wilson, C. A. (1995). Seasonal timing of opaque zone formation in fish otoliths. In *Recent Developments in Fish Otolith Research* (Secor, D., Campana, S. E. & Dean, J. M., eds.), pp. 27-43: Univ of South Carolina Pr.

Bedwal, R. S. & Bahuguna, A. (1994). Zinc, copper and selenium in reproduction. *Cellular and Molecular Life Sciences* **50**, 626-640.

Beer, N. A., Wing, S. R. & Swearer, S. E. (2011). Otolith elemental evidence for spatial structuring in a temperate reef fish population. *Marine Ecology Progress Series* **442**, 217-227.

Begg, G. & Waldman, J. (1999). An holistic approach to fish stock identification. *Fisheries Research* **43**, 34-44.

Ben-Tzvi, O., Abelson, A., Gaines, S. D., Sheehy, M. S., Paradis, G. L. & Kiflawi, M. (2007). The inclusion of sub-detection limit LA-ICPMS data, in the analysis of otolith microchemistry, by use of a palindrome sequence analysis (PaSA). *Limnology and Oceanography: Methods* **5**, 97-105.

Bergenius, M. A. J., Mapstone, B. D., Begg, G. A. & Murchie, C. D. (2005). The use of otolith chemistry to determine stock structure of three epinepheline serranid coral reef fishes on the Great Barrier Reef, Australia. *Fisheries Research* **72**, 253-270.

Block, B. A., Jonsen, I. D., Jorgensen, S. J., Winship, A. J., Shaffer, S. A., Bograd, S. J., Hazen, E. L., Foley, D. G., Breed, G. A., Harrison, A. L., Ganong, J. E., Swithenbank, A., Castleton, M., Dewar, H., Mate, B. R., Shillinger, G. L., Schaefer, K. M., Benson, S. R., Weise, M. J., Henry, R. W. & Costa, D. P. (2011). Tracking apex marine predator movements in a dynamic ocean. *Nature* **475**, 86-90.

Bocca, B., Alimonti, A., Petrucci, F., Violante, N., Sancesario, G., Forte, G. & Senofonte, O. (2004). Quantification of trace elements by sector field inductively coupled plasma mass spectrometry in urine, serum, blood and cerebrospinal fluid of patients with Parkinson's disease. *Spectrochimica Acta Part B: Atomic Spectroscopy* **59**, 559-566.

Bolle, L., Hunter, E., Rijnsdorp, A., Pastoors, M., Metcalfe, J. & Reynolds, J. (2005). Do tagging experiments tell the truth? Using electronic tags to evaluate conventional tagging data. *ICES Journal of Marine Science* **62**, 236-246.

Botsford, L., Brumbaugh, D., Grimes, C., Kellner, J., Largier, J., O'Farrell, M., Ralston, S., Soulanille, E. & Wespestad, V. (2009). Connectivity, sustainability, and yield: bridging the gap between conventional fisheries management and marine protected areas. *Reviews in Fish Biology and Fisheries* **19**, 69-95.

Bourne, P. K. (1986). Changes in haematological parameters associated with capture and captivity of the marine teleost, *Pleuronectes platessa* L. *Comparative Biochemistry and Physiology Part A: Physiology* **85**, 435-443.

Bradbury, I. R., Campana, S. E. & Bentzen, P. (2008). Estimating contemporary early life-history dispersal in an estuarine fish: integrating molecular and otolith elemental approaches. *Molecular Ecology* **17**, 1438-1450.

Bromley, P. J. (2000). Growth, sexual maturation and spawning in central North Sea plaice (*Pleuronectes platessa* L.), and the generation of maturity ogives from commercial catch data. *Journal of Sea Research* **44**, 27-43.

Brophy, D., Jeffries, T. E. & Danilowicz, B. S. (2004). Elevated manganese concentrations at the cores of clupeid otoliths: possible environmental, physiological, or structural origins. *Marine Biology* **144**, 779-786.

Brown, R. J. & Severin, K. P. (2009). Otolith chemistry analyses indicate that water Sr:Ca is the primary factor influencing otolith Sr:Ca for freshwater and diadromous fish but not for marine fish. *Canadian Journal of Fisheries and Aquatic Sciences* **66**, 1790-1808.

Bruland, K. W. & Lohan, M. C. (2003). 6.02 - Controls of Trace Metals in Seawater. In *Treatise on geochemistry, Vol. 6. The oceans and marine geochemistry* (Holland, H. D. & Turekian, K. K., eds.), pp. 23-47: Elsevier.

Burton, J. D., Althaus, M., Millward, G. E., Morris, A. W., Statham, P. J., Tappin, A. D., Turner, A., Balls, P. & Stebbing, A. R. D. (1993). Processes Influencing the Fate of Trace Metals in the North Sea [and Discussion]. *Philosophical Transactions: Physical Sciences and Engineering* **343**, 557-568.

Campana, S. E. (1999). Chemistry and composition of fish otoliths: pathways, mechanisms and applications. *Marine Ecology Progress Series* **188**, 263-297.

Campana, S. E. (2005). Otolith elemental composition as a natural marker of fish stocks. In *Stock identification methods: applications in fishery science* (Cadrin, S. X., Friedland, K. D. & Waldman, J. R., eds.), pp. 227-245: Elsevier.

Campana, S. E. & Casselman, J. M. (1993). Stock discrimination using otolith shape analysis. *Canadian Journal of Fisheries and Aquatic Sciences* **50**, 1062-1083.

Campana, S. E., Chouinard, G. A., Hanson, J. M., Frechet, A. & Brattey, J. (2000). Otolith elemental fingerprints as biological tracers of fish stocks. *Fisheries Research* **46**, 343-357.

Campana, S. E. & Gagne, J. (1995). Cod stock discrimination using ICPMS elemental assays of otoliths. In *Recent developments in fish otolith research* (Secor, D., Dean, J. & Campana, S. E., eds.). Columbia: University of South Carolina Press.

Campana, S. E. & Neilson, J. D. (1985). Microstructure of fish otoliths. *Canadian Journal of Fisheries and Aquatic Sciences* **42**, 1014-1032.

Campana, S. E. & Thorrold, S. R. (2001). Otoliths, increments, and elements: keys to a comprehensive understanding of fish populations? *Canadian Journal of Fisheries and Aquatic Sciences* **58**, 30-38.

Campana, S. E., Thorrold, S. R., Jones, C. M., Günther, D., Tubrett, M., Longerich, H., Jackson, S., Halden, N., Kalish, J., Piccoli, P., Pontual, H. d., Troadec, H., Panfili, J., Secor, D., Severin, K., Sie, S., Thresher, R., Teesdale, W. & Campbell, J. (1997). Comparison of accuracy, precision, and sensitivity in elemental assays of fish otoliths using the electron microprobe, proton-induced X-ray emission, and laser ablation inductively coupled plasma mass spectrometry. *Canadian Journal of Fisheries and Aquatic Sciences* **54**, 2068-2079.

Carbines, G. & McKenzie, J. (2004). Movement patterns and stock mixing of blue cod in Dusky Sound in 2002. In *New Zealand Fisheries Assessment Report 2004*, p. 28. Wellington: Ministry of Fisheries.

Casado-Martinez, M. C., Smith, B. D., DelValls, T. A. & Rainbow, P. S. (2009). Pathways of trace metal uptake in the lugworm *Arenicola marina*. *Aquatic Toxicology* **92**, 9-17.

Chen, Z. & Jones, C. M. (2006). Simultaneous determination of 33 major, minor, and trace elements in juvenile and larval fish otoliths by high resolution double focusing sector field inductively coupled plasma mass spectrometry. In *Winter Conference on Plasma Spectrochemistry*. Tucson, Arizona.

Chittaro, P. M., Fryer, B. J. & Sale, P. F. (2004). Discrimination of French grunts (*Haemulon flavolineatum*, Desmarest, 1823) from mangrove and coral reef habitats using otolith microchemistry. *Journal of Experimental Marine Biology and Ecology* **308**, 169-183.

Clark, T. D., Donaldson, M. R., Drenner, S. M., Hinch, S. G., Patterson, D. A., Hills, J., Ives, V., Carter, J. J., Cooke, S. J. & Farrell, A. P. (2011). The efficacy of field techniques for obtaining and storing blood samples from fishes. *Journal of Fish Biology* **79**, 1322-1333.

Clarke, L. M. & Friedland, K. D. (2004). Influence of growth and temperature on strontium deposition in the otoliths of Atlantic salmon. *Journal of Fish Biology* **65**, 744-759.

Clarke, L. M., Munch, S. B., Thorrold, S. R. & Conover, D. O. (2010). High connectivity among locally adapted populations of a marine fish (*Menidia menidia*). *Ecology* **91**, 3526-3537.

Clarke, L. M., Thorrold, S. R. & Conover, D. O. (2011). Population differences in otolith chemistry have a genetic basis in *Menidia menidia*. *Canadian Journal of Fisheries and Aquatic Sciences* **68**, 105-114.

Cleveland, W. S., Grosse, E. & Shyu, W. M. (1992). Local regression models. In *Statistical Models in S* (Chambers, J. M. & Hastie, T. J., eds.): Wadsworth & Brooks/Cole.

Cobb, J. L. S., Fox, N. C. & Santer, R. M. (1973). A specific ringer solution for the plaice (*Pleuronectes platessa* L.). *Journal of Fish Biology* **5**, 587-591.

Cook, B. D., Bunn, S. E. & Hughes, J. M. (2007). Molecular genetic and stable isotope signatures reveal complementary patterns of population connectivity in the regionally vulnerable southern pygmy perch (*Nannoperca australis*). *Biological Conservation* **138**, 60-72.

Coplen, T. B. (1996). New guidelines for reporting stable hydrogen, carbon, and oxygen isotope-ratio data. *Geochimica et Cosmochimica Acta* **60**, 3359-3360.

Crawley, M. J. (2007). *The R Book*: John Wiley & Sons Ltd.

Daglish, R. W., Nowak, B. F. & Lewis, T. W. (2004). Copper/Metal Ratios in the Gills of Rainbow Trout (*Oncorhynchus mykiss*) Provide Evidence of Copper Exposure Under Conditions of Mixed-Metal Exposure. *Archives of Environmental Contamination and Toxicology* **47**, 110-116.

Davies, C. A., Brophy, D., Jeffries, T. & Gosling, E. (2011). Trace elements in the otoliths and dorsal spines of albacore tuna (*Thunnus alalunga*, Bonnaterre, 1788): An assessment of the effectiveness of cleaning procedures at removing postmortem contamination. *Journal of Experimental Marine Biology and Ecology* **396**, 162-170.

Dawson, A. S. & Grimm, A. S. (1980). Quantitative seasonal changes in the protein, lipid and energy content of the carcass, ovaries and liver of adult female plaice, *Pleuronectes platessa* L. *Journal of Fish Biology* **16**, 493-504.

de Pontual, H., Lagardère, F., Amara, R., Bohn, M. & Ogor, A. (2003). Influence of ontogenetic and environmental changes in the otolith microchemistry of juvenile sole (*Solea solea*). *Journal of Sea Research* **50**, 199-211.

De Veen, J. F. (1978). On selective tidal transport in the migration of North Sea Plaice (*pleuronectes platessa*) and other flatfish species. *Netherlands Journal of Sea Research* **12**, 115-147.

de Vries, M. C., Gillanders, B. M. & Elsdon, T. S. (2005). Facilitation of barium uptake into fish otoliths: Influence of strontium concentration and salinity. *Geochimica et Cosmochimica Acta* **69**, 4061-4072.

Dehairs, F., Shopova, D., Ober, S., Veth, C. & Goeyens, L. (1997). Particulate barium stocks and oxygen consumption in the Southern Ocean mesopelagic water column during spring and early summer: relationship with export production. *Deep Sea Research Part II: Topical Studies in Oceanography* **44**, 497-516.

Dickson, K. A. (1995). Unique adaptations of the metabolic biochemistry of tunas and billfishes for life in the pelagic environment. *Environmental Biology of Fishes* **42**, 65-97.

DiMaria, R., Miller, J. & Hurst, T. (2010). Temperature and growth effects on otolith elemental chemistry of larval Pacific cod, *Gadus macrocephalus*. *Environmental Biology of Fishes* **89**, 453-462.

Dorval, E., Jones, C. M., Hannigan, R. & Montfrans, J. (2007). Relating otolith chemistry to surface water chemistry in a coastal plain estuary. *Canadian Journal of Fisheries and Aquatic Sciences* **64**, 411-424.

Edmonds, J., Caputi, N. & Morita, M. (1991). Stock discrimination by trace-element analysis of otoliths of orange roughy (*Hoplostethus atlanticus*), a deep-water marine teleost. *Marine and Freshwater Research* **42**, 383-389.

Edmonds, J. S., Caputi, N., Moran, M., Fletcher, W. & Morita, M. (1995). Population discrimination by variation in concentrations of minor and trace elements in sagittae of two Western Australian teleosts. In *Recent developments in fish otolith research* (Secor, D., Dean, J. & Campana, S. E., eds.). Columbia: University of South Carolina Press.

Edmonds, J. S., Moran, M. J., Caputi, N. & Morita, M. (1989). Trace element analysis of fish sagittae as an aid to stock identifications: pink snapper (*Chrysophrys auratus*) in Western Australian waters. *Canadian Journal of Fisheries and Aquatic Sciences* **46**, 50-54.

Elsdon, T. & Gillanders, B. (2005a). Consistency of patterns between laboratory experiments and field collected fish in otolith chemistry: an example and applications for salinity reconstructions. *Marine and Freshwater Research* **56**, 609-617.

Elsdon, T. S. & Gillanders, B. (2002). Interactive effects of temperature and salinity on otolith chemistry: challenges for determining environmental histories of fish. *Canadian Journal of Fisheries and Aquatic Sciences* **59**, 1796-1808.

Elsdon, T. S. & Gillanders, B. M. (2003a). Reconstructing migratory patterns of fish based on environmental influences on otolith chemistry. *Reviews in Fish Biology and Fisheries* **13**, 217-235.

Elsdon, T. S. & Gillanders, B. M. (2003b). Relationship between water and otolith elemental concentrations in juvenile black bream *Acanthopagrus butcheri*. *Marine Ecology Progress Series* **260**, 263-272.

Elsdon, T. S. & Gillanders, B. M. (2004). Fish otolith chemistry influenced by exposure to multiple environmental variables. *Journal of Experimental Marine Biology and Ecology* **313**, 269-284.

Elsdon, T. S. & Gillanders, B. M. (2005b). Alternative life-history patterns of estuarine fish: barium in otoliths elucidates freshwater residency. *Canadian Journal of Fisheries and Aquatic Sciences* **62**, 1143-1152.

Elsdon, T. S. & Gillanders, B. M. (2006). Temporal variability in strontium, calcium, barium, and manganese in estuaries: Implications for reconstructing environmental histories of fish from chemicals in calcified structures. *Estuarine, Coastal and Shelf Science* **66**, 147-156.

Elsdon, T. S., Wells, B. K. C., S.E., Gillanders, B. M., Jones, C. M., Limburg, K. E., Secor, D. H., Thorrold, S. R. & Walther, B. D. (2008). Otolith chemistry to describe movements and life-history parameters of fishes: hypotheses, assumptions, limitations, and inferences. *Oceanography and Marine Biology: An Annual Review* **46**, 297-330.

Engelhard, G. H. & Heino, M. (2005). Scale analysis suggests frequent skipping of the second reproductive season in Atlantic herring. *Biology Letters* **1**, 172-175.

Evans, D. H. (1993). *The Physiology of Fishes*. Boca Raton, Florida: CRC Press, Inc.

Everaarts, J. M. (1986). The uptake and distribution of copper in the lugworm, *Arenicola marina* (annelida, polychaeta). *Netherlands Journal of Sea Research* **20**, 253-267.

Fairchild, I. J., Baker, A., Borsato, A., Frisia, S., Hinton, R. W., McDermott, F. & Tooth, A. F. (2001). Annual to sub-annual resolution of multiple trace-element trends in speleothems. *Journal of the Geological Society* **158**, 831-841.

Fairclough, D. V., Edmonds, J. S., Lenanton, R. C. J., Jackson, G., Keay, I. S., Crisafulli, B. M. & Newman, S. J. (2011). Rapid and cost-effective assessment of connectivity among assemblages of *Choerodon rubescens* (Labridae), using laser ablation ICP-MS of sagittal otoliths. *Journal of Experimental Marine Biology and Ecology* **403**, 46-53.

Farrell, J. & Campana, S. E. (1996). Regulation of calcium and strontium deposition on the otoliths of juvenile tilapia, *Oreochromis niloticus*. *Comparative Biochemistry and Physiology Part A: Physiology* **115**, 103-109.

Ferguson, G. J., Ward, T. M. & Gillanders, B. M. (2011). Otolith shape and elemental composition: Complementary tools for stock discrimination of mulloway (*Argyrosomus japonicus*) in southern Australia. *Fisheries Research* **110**, 75-83.

Fletcher, G. L. (1975). The effects of capture, "stress," and storage of whole blood on the red blood cells, plasma proteins, glucose, and electrolytes of the winter flounder (*Pseudopleuronectes americanus*). *Canadian Journal of Fisheries and Aquatic Sciences* **53**, 197-206.

Fletcher, G. L. & King, M. J. (1978). Seasonal dynamics of  $\text{Cu}^{2+}$ ,  $\text{Zn}^{2+}$ ,  $\text{Ca}^{2+}$ , and  $\text{Mg}^{2+}$  in gonads and liver of winter flounder (*Pseudopleuronectes americanus*): evidence for summer storage of  $\text{Zn}^{2+}$  for winter gonad development in females. *Canadian Journal of Zoology* **56**, 284-290.

Fletcher, G. L., Watts, E. G. & King, M. J. (1975). Copper, zinc, and total protein levels in the plasma of sockeye salmon (*Oncorhynchus nerka*) during their spawning migration. *Journal of the Fisheries Research Board of Canada* **32**, 78-82.

Fletcher, P. E. & Fletcher, G. L. (1978). The binding of zinc to the plasma of winter flounder (*Pseudopleuronectes americanus*): affinity and specificity. *Canadian Journal of Zoology* **56**, 114-120.

Fletcher, P. E. & Fletcher, G. L. (1980). Zinc- and copper-binding proteins in the plasma of winter flounder (*Pseudopleuronectes americanus*). *Canadian Journal of Zoology* **58**, 609-613.

Folmar, L. C., Moody, T., Bonomelli, S. & Gibson, J. (1992). Annual cycle of blood chemistry parameters in striped mullet (*Mugil cephalus* L.) and pinfish (*Lagodon rhomboides* L.) from the Gulf of Mexico. *Journal of Fish Biology* **41**, 999-1011.

Forrester, G. (2005). A field experiment testing for correspondence between trace elements in otoliths and the environment and for evidence of adaptation to prior habitats. *Estuaries and Coasts* **28**, 974-981.

Fowler, A., Campana, S. E., Jones, C. M. & Thorrold, S. R. (1995). Experimental assessment of the effect of temperature and salinity on elemental composition of otoliths using laser ablation ICPMS. *Canadian Journal of Fisheries and Aquatic Sciences* **52**, 1431-1441.

Fowler, A. J., Gillanders, B. M. & Hall, K. C. (2005). Relationship between elemental concentration and age from otoliths of adult snapper (*Pagrus auratus*, Sparidae): implications for movement and stock structure. *Marine and Freshwater Research* **56**, 661-676.

Friedland, K. D., Reddin, D. G., Shimizu, N., Haas, R. E. & Youngson, A. F. (1998). Strontium:calcium ratios in Atlantic salmon (*Salmo salar*) otoliths and observations on growth and maturation. *Canadian Journal of Fisheries and Aquatic Sciences* **55**, 1158-1168.

Fromentin, J.-M., Ernande, B., Fablet, R. & de Pontual, H. (2009). Importance and future of individual markers for the ecosystem approach to fisheries. *Aquatic Living Resources* **22**, 395-408.

Fuiman, L. A. & Hoff, G. R. (1995). Natural variation in elemental composition of sagittae from red drum. *Journal of Fish Biology* **47**, 940-955.

Gaetani, G. A. & Cohen, A. L. (2006). Element partitioning during precipitation of aragonite from seawater: A framework for understanding paleoproxies. *Geochimica et Cosmochimica Acta* **70**, 4617-4634.

Gauldie, R. W., Thacker, C. E., West, I. F. & Wang, L. (1998). Movement of water in fish otoliths. *Comparative Biochemistry and Physiology Part A: Physiology* **120**, 551-556.

Geffen, A., Pearce, N. & Perkins, W. (1998). Metal concentrations in fish otoliths in relation to body composition after laboratory exposure to mercury and lead. *Marine Ecology Progress Series* **165**, 235-245.

Gillanders, B. (2002). Temporal and spatial variability in elemental composition of otoliths: implications for determining stock identity and connectivity of populations. *Canadian Journal of Fisheries and Aquatic Sciences* **59**, 669-679.

Gillanders, B. M. (2005). Otolith chemistry to determine movements of diadromous and freshwater fish. *Aquatic Living Resources* **18**, 291-300.

Goulle, J.-P., Mahieu, L., Castermant, J., Neveu, N., Bonneau, L., Laine, G., Bouige, D. & Lacroix, C. (2005). Metal and metalloid multi-elementary ICP-MS validation in whole blood, plasma, urine and hair Reference values. *Forensic Science International* **153**, 39-44.

Hamer, P. A. & Jenkins, G. P. (2007). Comparison of spatial variation in otolith chemistry of two fish species and relationships with water chemistry and otolith growth. *Journal of Fish Biology* **71**, 1035-1055.

Hamilton, S. L. & Warner, R. R. (2009). Otolith barium profiles verify the timing of settlement in a coral reef fish. *Marine Ecology Progress Series* **385**, 237-244.

Hansen, N., Folsom, T. R. & Weitz Jr, W. E. (1978). Determination of alkali metals in blood from North Pacific albacore. *Comparative Biochemistry and Physiology Part A: Physiology* **60**, 491-495.

Hanson, N. N., Wurster, C. M., Eimf & Todd, C. D. (2010). Comparison of secondary ion mass spectrometry and micromilling/continuous flow isotope ratio mass spectrometry techniques used to

acquire intra-otolith  $\delta^{18}\text{O}$  values of wild Atlantic salmon (*Salmo salar*). *Rapid Communications in Mass Spectrometry* **24**, 2491-2498.

Hanson, P. J. & Zdanowicz, V. S. (1999). Elemental composition of otoliths from Atlantic croaker along an estuarine pollution gradient. *Journal of Fish Biology* **54**, 656-668.

Hanssen, R. G., Lafeber, F. P., Flik, G. & Wendelaar Bonga, S. E. (1989). Ionic and total calcium levels in the blood of the European eel (*Anguilla anguilla*): effects of stannectomy and hypocalcin replacement therapy. *Journal of Experimental Biology* **141**, 177-186.

Harvey, B. R. (1978). Spark source mass spectrometric procedure employing stable isotopes to study the uptake of copper by fish from seawater and food. *Analytical Chemistry* **50**, 1866-1870.

Harwood, A. J. P., Dennis, P. F., Marca, A. D., Pilling, G. M. & Millner, R. S. (2008). The oxygen isotope composition of water masses within the North Sea. *Estuarine, Coastal and Shelf Science* **78**, 353-359.

Henderson, P. (1984). *Inorganic Geochemistry*. Oxford: Pergamon Press.

Hicks, A. S., Closs, G. P. & Swearer, S. E. (2010). Otolith microchemistry of two amphidromous galaxiids across an experimental salinity gradient: A multi-element approach for tracking diadromous migrations. *Journal of Experimental Marine Biology and Ecology* **394**, 86-97.

Hixon, M., Pacala, S. & Sandin, S. (2002). Population regulation: historical context and contemporary challenges of open vs. closed systems. *Ecology* **83**, 1490-1508.

Hoarau, G., Piquet, A. M.-T., Van der Veer, H. W., Rijnsdorp, A. D., Stam, W. T. & Olsen, J. L. (2004). Population structure of plaice (*Pleuronectes platessa* L.) in northern Europe: a comparison of resolving power between microsatellites and mitochondrial DNA data. *Journal of Sea Research* **51**, 183-190.

Hoff, G. R. & Fuiman, L. A. (1995). Environmentally induced variation in elemental composition of red drum (*Sciaenops ocellatus*) otoliths. *Bulletin of Marine Science* **56**, 578-591.

Høie, H. & Folkvord, A. (2006). Estimating the timing of growth rings in Atlantic cod otoliths using stable oxygen isotopes. *Journal of Fish Biology* **68**, 826-837.

Hoie, H., Millner, R. S., McCully, S., Nedreaas, K. H., Pilling, G. M. & Skadal, J. (2009). Latitudinal differences in the timing of otolith growth: A comparison between the Barents Sea and southern North Sea. *Fisheries Research* **96**, 319-322.

Hoie, H., Otterlei, E. & Folkvord, A. (2004). Temperature-dependent fractionation of stable oxygen isotopes in otoliths of juvenile cod (*Gadus morhua* L.). *ICES Journal of Marine Science: Journal du Conseil* **61**, 243-251.

Horwood, J. W., Walker, M. G. & Withthames, P. (1989). The effect of feeding levels on the fecundity of plaice (*Pleuronectes platessa*). *Journal of the Marine Biological Association of the United Kingdom* **69**, 81-92.

Hrubec, T. C. & Smith, S. A. (1999). Differences between Plasma and Serum Samples for the Evaluation of Blood Chemistry Values in Rainbow Trout, Channel Catfish, Hybrid Tilapias, and Hybrid Striped Bass. In *Journal of Aquatic Animal Health*, pp. 116-122: Taylor & Francis.

Hunter, E., Aldridge, J., Metcalfe, J. & Arnold, G. (2003a). Geolocation of free-ranging fish on the European continental shelf as determined from environmental variables. I. Tidal location method. *Marine Biology* **142**, 601-609.

Hunter, E., Aldridge, J., Metcalfe, J. & Arnold, G. (2004a). Geolocation of free-ranging fish on the European continental shelf as determined from environmental variables II. Reconstruction of plaice ground tracks. *Marine Biology* **144**, 787-798.

Hunter, E., Cotton, R., Metcalfe, J. & Reynolds, J. (2009). Large-scale variation in seasonal swimming patterns of plaice in the North Sea. *Marine Ecology Progress Series* **392**, 167-178.

Hunter, E. & Darnaude, A. M. (2004). Determination of plaice lifetime movements in the North Sea by linking natural and electronic data records. In *ICES Annual Science Conference ASC 2004/ theme session K:05*, p. 11. Vigo, Spain: International Council for the Exploration of the Sea.

Hunter, E., Metcalfe, J., Arnold, G. & Reynolds, J. (2004b). Impacts of migratory behaviour on population structure in North Sea plaice. *Journal of Animal Ecology* **73**, 377-385.

Hunter, E., Metcalfe, J. & Reynolds, J. (2003b). Migration route and spawning site fidelity by North Sea plaice. *Proceedings of the Royal Society of London. Series B, Biological Sciences* **270**, 2097-2103.

Hunter, K. A. & Boyd, P. (1999). Biogeochemistry of trace metals in the ocean. *Marine and Freshwater Research* **50**, 739-753.

Hurlbert, S. H. (1984). Pseudoreplication and the Design of Ecological Field Experiments. *Ecological Monographs* **54**, 187-211.

Hüssy, K., Mosegaard, H. & Jessen, F. (2004). Effect of age and temperature on amino acid composition and the content of different protein types of juvenile Atlantic cod (*Gadus morhua*) otoliths. *Canadian Journal of Fisheries and Aquatic Sciences* **61**, 1012-1020.

Jochum, K. P., Weis, U., Stoll, B., Kuzmin, D., Yang, Q., Raczek, I., Jacob, D. E., Stracke, A., Birbaum, K., Frick, D. A., Günther, D. & Enzweiler, J. (2011). Determination of Reference Values for NIST SRM 610-617 Glasses Following ISO Guidelines. *Geostandards and Geoanalytical Research* **35**, 397-429.

Jones, C. M. & Chen, Z. (2003). New techniques for sampling larval and juvenile fish otoliths for trace-element analysis with laser-ablation sector-field inductively-coupled plasma mass spectrometry (SF-ICP-MS). In *The Big Fish Bang. Proceedings of the 26th Annual Larval Fish Conference* (Browman, H. I. & Skiftesvik, A. B., eds.), pp. 431-443. Bergen: The Institute of Marine Research, Postboks.

Jørgensen, C., Ernande, B., Fiksen, Øyvind & Dieckmann, U. (2006). The logic of skipped spawning in fish. *Canadian Journal of Fisheries and Aquatic Sciences* **63**, 200-211.

Kacem, A., Gustafsson, S. & Meunier, F. J. (2000). Demineralization of the vertebral skeleton in Atlantic salmon *Salmo salar* L. during spawning migration. *Comparative Biochemistry and Physiology - Part A: Molecular & Integrative Physiology* **125**, 479-484.

Kai, N., Ueda, T. & Takeda, Y. (1992). The state of oxidation and its distribution of selenium in the blood of tuna and marlins. *Nippon Suisan Gakkaishi* **58**, 1883-1886.

Kaim, W. & Schwederski, B. (1994). *Bioinorganic chemistry: inorganic elements in the chemistry of life*. Chichester: John Wiley & Sons Ltd.

Kalish, J. (1990). Use of otolith microchemistry to distinguish the progeny of sympatric anadromous and non-anadromous salmonids. *Fishery Bulletin* **88**, 657-666.

Kalish, J. (1991). Determinants of otolith chemistry: seasonal variation in the composition of blood plasma, endolymph and otoliths of bearded rock cod *Pseudophycis barbatus*. *Marine Ecology Progress Series* **74**, 137-159.

Kalish, J. (1992). Formation of a stress-induced chemical check in fish otoliths. *Journal of Experimental Marine Biology and Ecology* **162**, 265-277.

Kalish, J. M. (1989). Otolith microchemistry: validation of the effects of physiology, age and environment on otolith composition. *Journal of Experimental Marine Biology and Ecology* **132**, 151-178.

Kaplan, I. C., Levin, P. S., Burden, M. & Fulton, E. A. (2010). Fishing catch shares in the face of global change: a framework for integrating cumulative impacts and single species management. *Canadian Journal of Fisheries and Aquatic Sciences* **67**, 1968-1982.

Kennedy, Witthames, Nash & Fox (2008). Is fecundity in plaice (*Pleuronectes platessa* L.) down-regulated in response to reduced food intake during autumn? *Journal of Fish Biology* **72**, 78-92.

Kinsman, D. J. J. & Holland, H. D. (1969). The co-precipitation of cations with  $\text{CaCO}_3$ -IV. The co-precipitation of  $\text{Sr}^{2+}$  with aragonite between 16° and 96°C. *Geochimica et Cosmochimica Acta* **33**, 1-17.

Kraus, R. T. & Secor, D. H. (2004). Incorporation of strontium into otoliths of an estuarine fish. *Journal of Experimental Marine Biology and Ecology* **302**, 85-106.

Kremling, K. (1999). Determination of trace metals. In *Methods of seawater analysis* (Grasshoff, K., Kremling, K. & Ehrhardt, M., eds.). Weinheim: Wiley-VCH.

Lawton, R. J., Wing, S. R. & Lewis, A. M. (2010). Evidence for discrete subpopulations of sea perch (*Helicolenus percooides*) across four fjords in Fiordland, New Zealand. *New Zealand Journal of Marine and Freshwater Research* **44**, 309-322.

Longmore, C., Fogarty, K., Neat, F., Brophy, D., Trueman, C., Milton, A. & Mariani, S. (2010). A comparison of otolith microchemistry and otolith shape analysis for the study of spatial variation in a deep-sea teleost, *Coryphaenoides rupestris*. *Environmental Biology of Fishes* **89**, 591-605.

Maddock, D. M. & Burton, M. P. M. (1998). Gross and histological observations of ovarian development and related condition changes in American plaice. *Journal of Fish Biology* **53**, 928-944.

Marriott, C. S., Henderson, G. M., Crompton, R., Staubwasser, M. & Shaw, S. (2004). Effect of mineralogy, salinity, and temperature on Li/Ca and Li isotope composition of calcium carbonate. *Chemical Geology* **212**, 5-15.

Martin, G. B. & Thorrold, S. R. (2005). Temperature and salinity effects on magnesium, manganese, and barium incorporation in otoliths of larval and early juvenile spot *Leiostomus xanthurus*. *Marine Ecology Progress Series* **293**, 223-232.

Martin, G. B., Thorrold, S. R. & Jones, C. M. (2004). Temperature and salinity effects on strontium incorporation in otoliths of larval spot (*Leiostomus xanthurus*). *Canadian Journal of Fisheries and Aquatic Sciences* **61**, 34-42.

Martin, G. B. & Wuenschel, M. J. (2006). Effect of temperature and salinity on otolith element incorporation in juvenile gray snapper *Lutjanus griseus*. *Marine Ecology Progress Series* **324**, 229-239.

Martinez, C. B. R., Nagae, M. Y., Zaia, C. T. B. V. & Zaia, D. A. M. (2004). Acute morphological and physiological effects of lead in the neotropical fish *Prochilodus lineatus*. *Brazilian Journal of Biology* **64**, 797-807.

Melancon, S., Fryer, B. J. & Markham, J. L. (2009). Chemical analysis of endolymph and the growing otolith: Fractionation of metals in freshwater fish species. *Environmental Toxicology and Chemistry* **28**, 1279-1287.

Mercier, L., Darnaude, A. M., Bruguier, O., Vasconcelos, R. P., Cabral, H. N., Costa, M. J., Lara, M., Jones, D. L. & Mouillot, D. (2011). Selecting statistical models and variable combinations for optimal classification using otolith microchemistry. *Ecological Applications* **21**, 1352-1364.

Mercier, L., Mouillot, D., Bruguier, O., Vigliola, L. & Darnaude, A. M. (2012). Multi-element otolith fingerprints unravel sea-lagoon lifetime migrations of the gilthead sea bream (*Sparus aurata* L.) *Marine Ecology Progress Series* **444**, 175-194.

Merck (2011). Common Medical Tests. In *Merck Manuals* (Kaplan, J. L. & Porter, R. S., eds.). Whitehouse Station, N.J., U.S.A.: Merck Sharp & Dohme Corp.

Metcalfe, J. & Arnold, G. (1997). Tracking fish with electronic tags. *Nature* **387**, 665-666.

Metcalfe, J., Hunter, E. & Buckley, A. (2006). The migratory behaviour of North Sea plaice: Currents, clocks and clues. *Marine and Freshwater Behaviour and Physiology* **39**, 25-36.

Miller, J., Banks, M., Gomez-Uchida, D. & Shanks, A. (2005). A comparison of population structure in black rockfish (*Sebastodes melanops*) as determined with otolith microchemistry and microsatellite DNA. *Canadian Journal of Fisheries and Aquatic Sciences* **62**, 2189-2198.

Miller, J. A. (2009). The effects of temperature and water concentration on the otolith incorporation of barium and manganese in black rockfish *Sebastodes melanops*. *Journal of Fish Biology* **75**, 39-60.

Miller, J. A. (2011). Effects of water temperature and barium concentration on otolith composition along a salinity gradient: Implications for migratory reconstructions. *Journal of Experimental Marine Biology and Ecology* **405**, 42-52.

Miller, M. B., Clough, A. M., Batson, J. N. & Vachet, R. W. (2006). Transition metal binding to cod otolith proteins. *Journal of Experimental Marine Biology and Ecology* **329**, 135-143.

Milton, D. A. & Chinery, S. R. (1998). The effect of otolith storage methods on the concentrations of elements detected by laser-ablation ICPMS. *Journal of Fish Biology [J. Fish Biol.]* **53**, 785-794.

Milton, D. A. & Chenery, S. R. (2001a). Can otolith chemistry detect the population structure of the shad *hilsa Tenualosa ilisha*? Comparison with the results of genetic and morphological studies. *Marine Ecology Progress Series* **222**, 239-251.

Milton, D. A. & Chenery, S. R. (2001b). Sources and uptake of trace metals in otoliths of juvenile barramundi (*Lates calcarifer*). *Journal of Experimental Marine Biology and Ecology* **264**, 47-65.

Milton, D. A. & Chenery, S. R. (2005). Movement patterns of barramundi *Lates calcarifer*, inferred from  $^{87}\text{Sr}/^{86}\text{Sr}$  and Sr/Ca ratios in otoliths, indicate non-participation in spawning. *Marine Ecology Progress Series* **301**, 279-291.

Milton, D. A., Tenakanai, C. D. & Chenery, S. R. (2000). Can the movements of barramundi in the Fly River Region, Papua New Guinea be traced in their otoliths? *Estuarine, Coastal and Shelf Science* **50**, 855-868.

Mugiya, Y. (1966). Calcification in fish and shellfish. Seasonal change in calcium and magnesium concentration of the otolith fluid in some fish with special reference to the zone formation of their otolith. *Bull. Jap. Soc. Scient. Fish.* **32**, 549-557.

OSPAR (2000). Quality Status Report 2000, Region II - Greater North Sea. (2000, O. C., ed.), p. 136 + xiii pp. London.

Paillard, D., Labeyrie, L. & Yiou, P. (1996). Macintosh program performs time-series analysis. p. 379: EOS, Transactions, American Geophysical Union.

Panfili, J., Darnaude, A., Lin, Y. C., Chevalley, M., Iizuka, Y., Tzeng, W. N. & Crivelli, A. J. (In press). European eel movements during continental life in the Rhône river delta (South of France): high level of sedentarity revealed by otolith microchemistry. *Aquatic biology*.

Payan, P., Borelli, G., Priouzeau, F., De Pontual, H., Boeuf, G. & Mayer-Gostan, N. (2002). Otolith growth in trout *Oncorhynchus mykiss*: supply of  $\text{Ca}^{2+}$  and  $\text{Sr}^{2+}$  to the saccular endolymph. *Journal of Experimental Biology* **205**, 2687-2695.

Payan, P., De Pontual, H., Boeuf, G. & Mayer-Gostan, N. (2004a). Endolymph chemistry and otolith growth in fish. *Comptes Rendus Palevol* **3**, 535-547.

Payan, P., De Pontual, H., Boeuf, G. & Mayer-Gostan, N. (2004b). Effects of stress on plasma homeostasis, endolymph chemistry, and check formation during otolith growth in rainbow trout (*Oncorhynchus mykiss*). *Canadian Journal of Fisheries and Aquatic Sciences* **61**, 1247-1255.

Pearson, R. G. (1963). Hard and soft acids and bases. *Journal of the American Chemical Society* **85**, 3533-3539.

Pedersen, M. W., Righton, D., Thygesen, U. H., Andersen, K. H. & Madsen, H. (2008). Geolocation of North Sea cod (*Gadus morhua*) using hidden Markov models and behavioural switching. *Canadian Journal of Fisheries and Aquatic Sciences* **65**, 2367-2377.

Pentreath, R. J. (1973). The accumulation and retention of  $^{65}\text{Zn}$  and  $^{54}\text{Mn}$  by the plaice, *Pleuronectes platessa* L. *Journal of Experimental Marine Biology and Ecology* **12**, 1-18.

Pentreath, R. J. (1976). Some further studies on the accumulation and retention of  $^{65}\text{Zn}$  and  $^{54}\text{Mn}$  by the plaice, *Pleuronectes platessa* L. *Journal of Experimental Marine Biology and Ecology* **21**, 179-189.

Popper, A. N. & Fay, R. R. (2011). Rethinking sound detection by fishes. *Hearing Research* **273**, 25-36.

Proctor, C. H. & Thresher, R. E. (1998). Effects of specimen handling and otolith preparation on concentration of elements in fish otoliths. *Marine Biology* **131**, 681-694.

Proctor, C. H., Thresher, R. E., Gunn, J. S., Mills, D. J., Harrowfield, I. R. & Sie, S. H. (1995). Stock structure of the southern bluefin tuna *Thunnus maccoyii*: an investigation based on probe microanalysis of otolith composition. *Marine Biology* **122**, 511-526.

Pulliam, H. (1988). Sources, sinks, and population regulation. *The American Naturalist* **132**, 652-661.

Radtke, R., Townsend, D., Folsom, S. & Morrison, M. (1990). Strontium:calcium concentration ratios in otoliths of herring larvae as indicators of environmental histories. *Environmental Biology of Fishes* **27**, 51-61.

Radtke, R. L. (1989). Strontium-calcium concentration ratios in fish otoliths as environmental indicators. *Comparative Biochemistry and Physiology Part A: Physiology* **92**, 189-193.

Ranaldi, M. M. & Gagnon, M. M. (2008). Zinc incorporation in the otoliths of juvenile pink snapper (*Pagrus auratus* Forster): The influence of dietary versus waterborne sources. *Journal of Experimental Marine Biology and Ecology* **360**, 56-62.

Ranaldi, M. M. & Gagnon, M. M. (2009). Accumulation of cadmium in the otoliths and tissues of juvenile pink snapper (*Pagrus auratus* Forster) following dietary and waterborne exposure. *Comparative Biochemistry and Physiology Part C: Toxicology & Pharmacology* **150**, 421-427.

Reeder, R. J. & Rakovan, J. (1999). Surface structural controls on trace element incorporation during crystal growth. In *Growth, dissolution, and pattern formation in geosystems* (Jamtveit, B. & Meakin, P., eds.), pp. 143-162. Netherlands: Kluwer Academic Publishers.

Righton, D. A., Andersen, K. H., Neat, F., Thorsteinsson, V., Steingrund, P., Svedäng, H., Michalsen, K., Hinrichsen, H. H., Bendall, V., Neuenfeldt, S., Wright, P., Jonsson, P., Huse, G., van der Kooij, J., Mosegaard, H., Hüssy, K. & Metcalfe, J. (2010). Thermal niche of Atlantic cod *Gadus morhua*: limits, tolerance and optima. *Marine Ecology Progress Series* **420**, 1-13.

Rijnsdorp, A. D. (1989). Maturation of male and female North Sea plaice (*Pleuronectes platessa* L.). *Journal du Conseil International pour l'Exploration de la Mer* **46**, 35-51.

Rijnsdorp, A. D. (1990). The mechanism of energy allocation over reproduction and somatic growth in female North Sea plaice, *Pleuronectes platessa* L. *Netherlands Journal of Sea Research* **25**, 279-290.

Rijnsdorp, A. D. & Millner, R. S. (1996). Trends in population dynamics and exploitation of North Sea plaice (*Pleuronectes platessa* L.) since the late 1800s. *ICES Journal of Marine Science* **53**, 1170-1184.

Riveiro, I., Guisande, C., Iglesias, P., Basilone, G., Cuttitta, A., Giraldez, A., Patti, B., Mazzola, S., Bonanno, A., Vergara, A.-R. & Maneiro, I. (2011). Identification of subpopulations in pelagic marine fish species using amino acid composition. *Hydrobiologia* **670**, 189-199.

Rodgers, K. & Wing, S. (2008). Spatial structure and movement of blue cod (*Parapercis colias*) in Doubtful Sound, New Zealand, inferred from inferred from  $\delta^{13}\text{C}$  and  $\delta^{15}\text{N}$ . *Marine Ecology Progress Series* **359**, 239-248.

Rodushkin, I., Odman, F., Olofsson, R. & Axelsson, M. D. (2000). Determination of 60 elements in whole blood by sector field inductively coupled plasma mass spectrometry. *Journal of Analytical Atomic Spectrometry* **15**, 937-944.

Rooker, J., Kraus, R. & Secor, D. (2004). Dispersive behaviors of black drum and red drum: Is otolith Sr:Ca a reliable indicator of salinity history? *Estuaries and Coasts* **27**, 334-341.

Ruttenberg, B. I., Hamilton, S. L., Hickford, M. J., Paradis, G. L., Sheehy, M. S., Standish, J. D., Ben-Tzvi, O. & Warner, R. R. (2005). Elevated levels of trace elements in cores of otoliths and their potential for use as natural tags. *Marine Ecology Progress Series* **297**, 273-281.

Sadovy, Y. & Severin, K. P. (1992). Trace-elements in biogenic aragonite - correlation of body growth-rate and strontium levels in the otoliths of the white grunt, *Haemulon-Plumieri* (Pisces, Haemulidae). *Bulletin of Marine Science* **50**, 237-257.

Sadovy, Y. & Severin, K. P. (1994). Elemental patterns in red hind (*Epinephelus-Guttatus*) otoliths from Bermuda and Puerto-Rico reflect growth-rate, not temperature. *Canadian Journal of Fisheries and Aquatic Sciences* **51**, 133-141.

Salini, J. P., Milton, D. A., Rahman, M. J. & Hussain, M. G. (2004). Allozyme and morphological variation throughout the geographic range of the tropical shad, hilsha *Tenualosa ilisha*. *Fisheries Research* **66**, 53-69.

Scott, A. P., Witthames, P. R., Vermeirissen, E. L. M. & Carolsfeld, J. (1999). Prolonged-release gonadotrophin-releasing hormone analogue implants enhance oocyte final maturation and ovulation, and increase plasma concentrations of sulphated C21 steroids in North Sea plaice. *Journal of Fish Biology* **55**, 316-328.

Scott, P., Witthames, P. R., Turner, R. J. & Canario, A. V. M. (1998). Plasma concentrations of ovarian steroids in relation to oocyte final maturation and ovulation in female plaice sampled at sea. *Journal of Fish Biology* **52**, 128-145.

Secor, D. H., Henderson-Arzapalo, A. & Piccoli, P. M. (1995). Can otolith microchemistry chart patterns of migration and habitat utilization in anadromous fishes? *Journal of Experimental Marine Biology and Ecology* **192**, 15-33.

Secor, D. H., Rooker, J. R., Zlokovitz, E. & Zdanowicz, V. S. (2001). Identification of riverine, estuarine, and coastal contingents of Hudson River striped bass based upon otolith elemental fingerprints. *Marine Ecology Progress Series* **211**, 245-253.

Sequeira, V., Gordo, L. S., Neves, A., Paiva, R. B., Cabral, H. N. & Marques, J. F. (2010). Macroparasites as biological tags for stock identification of the bluemouth, *Helicolenus dactylopterus* (Delaroche, 1809) in Portuguese waters. *Fisheries Research* **106**, 321-328.

Shearer, K. D. (1984). Changes in elemental composition of hatchery-reared rainbow trout, *Salmo gairdneri*, associated with growth and reproduction. *Canadian Journal of Fisheries and Aquatic Sciences* **41**, 1592-1600.

Silva, A. (2003). Morphometric variation among sardine (*Sardina pilchardus*) populations from the northeastern Atlantic and the western Mediterranean. *ICES Journal of Marine Science* **60**, 1352-1360.

Sims, D. W., Witt, M. J., Richardson, A. J., Southall, E. J. & Metcalfe, J. D. (2006). Encounter success of free-ranging marine predator movements across a dynamic prey landscape. *Proceedings of the Royal Society B: Biological Sciences* **273**, 1195-1201.

Sinclair, D. J. (2005). Correlated trace element "vital effects" in tropical corals: A new geochemical tool for probing biomineralization. *Geochimica et Cosmochimica Acta* **69**, 3265-3284.

Smith, H. W. (1930). The absorption and excretion of water and salts by marine teleosts. *American Journal of Physiology -- Legacy Content* **93**, 480-505.

Söllner, C., Burghammer, M., Busch-Nentwich, E., Berger, J., Schwarz, H., Riekel, C. & Nicolson, T. (2003). Control of crystal size and lattice formation by starmaker in otolith biomineralization. *Science* **302**, 282-286.

Steele, J. H., Turekian, K. K. & Thorpe, S. A. (2009). *Marine Chemistry & Geochemistry: A Derivative of the Encyclopedia of Ocean Sciences*: Academic Press.

Steer, M. A., Fowler, A. J. & Gillanders, B. M. (2009). Age-related movement patterns and population structuring in southern garfish, *Hyporhamphus melanochir*, inferred from otolith chemistry. *Fisheries Management and Ecology* **16**, 265-278.

Stips, A., Boldig, K., Pohlmann, T. & Burchard, H. (2004). Simulating the temporal and spatial dynamics of the North Sea using the new model GETM (general estuarine transport model). *Ocean Dynamics* **54**, 266-283.

Subramanian, K. S. (1996). Determination of metals in biofluids and tissues: sample preparation methods for atomic spectroscopic techniques. *Spectrochimica Acta Part B: Atomic Spectroscopy* **51**, 291-319.

Surge, D. & Walker, K. J. (2005). Oxygen isotope composition of modern and archaeological otoliths from the estuarine hardhead catfish (*Ariopsis felis*) and their potential to record low-latitude climate change. *Palaeogeography, Palaeoclimatology, Palaeoecology* **228**, 179-191.

Swan, S. C., Geffen, A. J., Gordon, J. D. M., Morales-Nin, B. & Shimmield, T. (2006). Effects of handling and storage methods on the concentrations of elements in deep-water fish otoliths. *Journal of Fish Biology* **68**, 891-904.

Swearer, S. E., Forrester, G. E., Steele, M. A., Brooks, A. J. & Lea, D. W. (2003). Spatio-temporal and interspecific variation in otolith trace-elemental fingerprints in a temperate estuarine fish assemblage. *Estuarine, Coastal and Shelf Science* **56**, 1111-1123.

Syndel Laboratories Ltd. (2009). Using Ovaplant to Induce Maturation in Cultured Fish. [www.syndel.com](http://www.syndel.com).

Tamura, T., Goldenberg, R. L., Johnston, K. E. & DuBard, M. (2000). Maternal plasma zinc concentrations and pregnancy outcome. *American Journal of Clinical Nutrition* **71**, 109-113.

Tanner, S. E., Vasconcelos, R. P., Cabral, H. N. & Thorrold, S. R. (2012). Testing an otolith geochemistry approach to determine population structure and movements of European hake in the northeast Atlantic Ocean and Mediterranean Sea. *Fisheries Research* <http://dx.doi.org/10.1016/j.fishres.2012.02.013>.

Tanner, S. E., Vasconcelos, R. P., Reis-Santos, P., Cabral, H. N. & Thorrold, S. R. (2011). Spatial and ontogenetic variability in the chemical composition of juvenile common sole (*Solea solea*) otoliths. *Estuarine, Coastal and Shelf Science* **91**, 150-157.

Tappin, A. D., Millward, G. E., Statham, P. J., Burton, J. D. & Morris, A. W. (1995). Trace metals in the central and southern North Sea. *Estuarine Coastal and Shelf Science* **41**, 275-323.

Thermo (2009a). Note 1: Rapid and accurate measurement of As and Cr in urine. *X Series ICP-MS Clinical Applications AN\_0601*.

Thermo (2009b). Note 5: Trace element quantification in blood and serum in a single analytical run. *X Series ICP-MS Clinical Applications AN\_E0649*.

Thompson, E. D., Mayer, G. D., Walsh, P. J. & Hogstrand, C. (2002). Sexual maturation and reproductive zinc physiology in the female squirrelfish. *Journal of Experimental Biology* **205**, 3367-3376.

Thorrold, S. R., Campana, S. E., Jones, C. M. & Swart, P. K. (1997). Factors determining [delta]13C and [delta]18O fractionation in aragonitic otoliths of marine fish. *Geochimica et Cosmochimica Acta* **61**, 2909-2919.

Thorrold, S. R., Latkoczy, C., Swart, P. K. & Jones, C. M. (2001). Natal homing in a marine fish metapopulation. *Science* **291**, 297-299.

Thorrold, S. R. & Shuttleworth, S. (2000). In situ analysis of trace elements and isotope ratios in fish otoliths using laser ablation sector field inductively coupled plasma mass spectrometry. *Canadian Journal of Fisheries and Aquatic Sciences* **57**, 1232-1242.

Thresher, R. (1999). Elemental composition of otoliths as a stock delineator in fishes. *Fisheries Research* **43**, 165-204.

Tohse, H. & Mugiyama, Y. (2001). Effects of enzyme and anion transport inhibitors on in vitro incorporation of inorganic carbon and calcium into endolymph and otoliths in salmon *Oncorhynchus masou*. *Comparative Biochemistry and Physiology - Part A: Molecular & Integrative Physiology* **128**, 177-184.

Tohse, H. & Mugiyama, Y. (2002). Diel variations in carbonate incorporation into otoliths in goldfish. *Journal of Fish Biology* **61**, 199-206.

Tomás, J., Geffen, A., Millner, R., Piñeiro, C. & Tserpes, G. (2006). Elemental composition of otolith growth marks in three geographically separated populations of European hake (*Merluccius merluccius*). *Marine Biology* **148**, 1399-1413.

Tomás, J., Geffen, A. J., Allen, I. S. & Berges, J. (2004). Analysis of the soluble matrix of vaterite otoliths of juvenile herring (*Clupea harengus*): do crystalline otoliths have less protein? *Comparative Biochemistry and Physiology - Part A: Molecular & Integrative Physiology* **139**, 301-308.

Townsend, D. W., Radtke, R. L., Corwin, S. & Libby, D. A. (1992). Strontium:calcium ratios in juvenile Atlantic herring *Clupea harengus* L. otoliths as a function of water temperature. *Journal of Experimental Marine Biology and Ecology* **160**, 131-140.

Treiman, A. H. & Essene, E. J. (1985). The Oka carbonatite complex, Quebec; geology and evidence for silicate-carbonate liquid immiscibility. *American Mineralogist* **70**, 1101-1113.

Turekian, K. (1968). *Oceans*: Prentice-Hall.

Tzeng, W., Chang, C., Wang, C., Shiao, J., Yoshiyuki, I., Yang, Y., You, C. & Lozys, L. (2007). Misidentification of the migratory history of anguillid eels by Sr/Ca ratios of vaterite otoliths. *Marine Ecology Progress Series* **348**, 285-295.

Uges, D. R. A. (1988). Plasma or serum in therapeutic drug monitoring and clinical toxicology. *Pharmacy World & Science* **10**, 185-188.

Underwood, E. J. (1977). *Trace elements in human and animal nutrition*. New York: Academic Press.

Urist, M. R. & Schjeide, A. O. (1961). The partition of calcium and protein in the blood of oviparous vertebrates during estrus. *The Journal of General Physiology* **44**, 743-756.

Valtonen, T. & Laitinen, M. (1988). Acid stress in respect to calcium and magnesium concentrations in the plasma of perch during maturation and spawning. *Environmental Biology of Fishes* **22**, 147-154.

Van Neer, W., Ervynck, A., Bolle, L. & Millner, R. S. (2004). Seasonality only works in certain parts of the year: the reconstruction of fishing seasons through otolith analysis. *International Journal of Osteoarchaeology* **14**, 457-474.

Vanhoe, H. & Dams, R. (1994). Use of Inductively Coupled Plasma Mass Spectrometry for the Determination of Ultra-trace Elements in Human Serum. *Journal of Analytical Atomic Spectrometry* **9**, 23-31.

Vermeirssen, E. L. M., Scott, A. P., Mylonas, C. C. & Zohar, Y. (1998). Gonadotrophin-Releasing Hormone Agonist Stimulates Milt Fluidity and Plasma Concentrations of 17,20[beta]-Dihydroxylated and 5[beta]-Reduced, 3[alpha]-Hydroxylated C21Steroids in Male Plaice (*Pleuronectes platessa*). *General and Comparative Endocrinology* **112**, 163-177.

Versieck, J. & Cornelis, R. (1980). Normal levels of trace elements in human blood plasma or serum. *Analytica Chimica Acta* **116**, 217-254.

Versieck, J. & Cornelis, R. (1989). *Trace elements in human plasma or serum*. Boca Raton, Florida, U.S.A.: CRC Press Inc.

Walther, B., Kingsford, M., O'Callaghan, M. & McCulloch, M. (2010). Interactive effects of ontogeny, food ration and temperature on elemental incorporation in otoliths of a coral reef fish. *Environmental Biology of Fishes* **89**, 441-451.

Walther, B. & Thorrold, S. R. (2006). Water, not food, contributes the majority of strontium and barium deposited in the otoliths of a marine fish. *Marine Ecology Progress Series* **311**, 125-130.

Walther, B. D. & Thorrold, S. R. (2009). Inter-annual variability in isotope and elemental ratios recorded in otoliths of an anadromous fish. *Journal of Geochemical Exploration* **102**, 181-186.

Walther, B. D. & Thorrold, S. R. (2010). Limited diversity in natal origins of immature anadromous fish during ocean residency. *Canadian Journal of Fisheries and Aquatic Sciences* **67**, 1699-1707.

Waring, C. P., Stagg, R. M. & Poxton, M. G. (1992). The effects of handling on flounder (*Platichthys flesus* L.) and Atlantic salmon (*Salmo salar* L.). *Journal of Fish Biology* **41**, 131-144.

Waring, C. P., Stagg, R. M. & Poxton, M. G. (1996). Physiological responses to handling in the turbot. *Journal of Fish Biology* **48**, 161-173.

Watanabe, T., Kiron, V. & Satoh, S. (1997). Trace minerals in fish nutrition. *Aquaculture* **151**, 185-207.

Watts, P. C., Nash, R. D. M. & Kemp, S. J. (2004). Genetic structure of juvenile plaice *Pleuronectes platessa* on nursery grounds within the Irish Sea. *Journal of Sea Research* **51**, 191-197.

Wedemeyer, G. & Yasutake, W. (1977). Clinical methods for the assessment of the effects of environmental stress on fish health. In *Tech. Pap. USFWS*.

Weiner, S. (2008). Biomineralization: A structural perspective. *Journal of Structural Biology* **163**, 229-234.

Wells, B. K., Rieman, B. E., Clayton, J. L., Horan, D. L. & Jones, C. M. (2003). Relationships between Water, Otolith, and Scale Chemistries of Westslope Cutthroat Trout from the Coeur d'Alene River, Idaho: The Potential Application of Hard-Part Chemistry to Describe Movements in Freshwater. *Transactions of the American Fisheries Society* **132**, 409-424.

Williams, D. R. (1971). *The Metals Of Life*. London: Van Nostrand Reinhold Company.

Wolf, K. E. N. (1959). Plasmoptysis and Gelation of Erythrocytes in Coagulation of Blood of Freshwater Bony Fishes. *Blood* **14**, 1339-1344.

Woodcock, S. H., Gillanders, B. M., Munro, A. R., McGovern, F., Crook, D. A. & Sanger, A. C. (2011). Using enriched stable isotopes of barium and magnesium to batch mark otoliths of larval golden perch (*Macquaria ambigua*, Richardson). *Ecology of Freshwater Fish* **20**, 157-165.

Woodhead, P. M. J. (1968). Seasonal changes in the calcium content of the blood of arctic cod. *Journal of the Marine Biological Association of the United Kingdom* **48**, 81-91.

Yoshinaga, J., Nakama, A., Morita, M. & Edmonds, J. S. (2000). Fish otolith reference material for quality assurance of chemical analyses. *Marine Chemistry* **69**, 91-97.

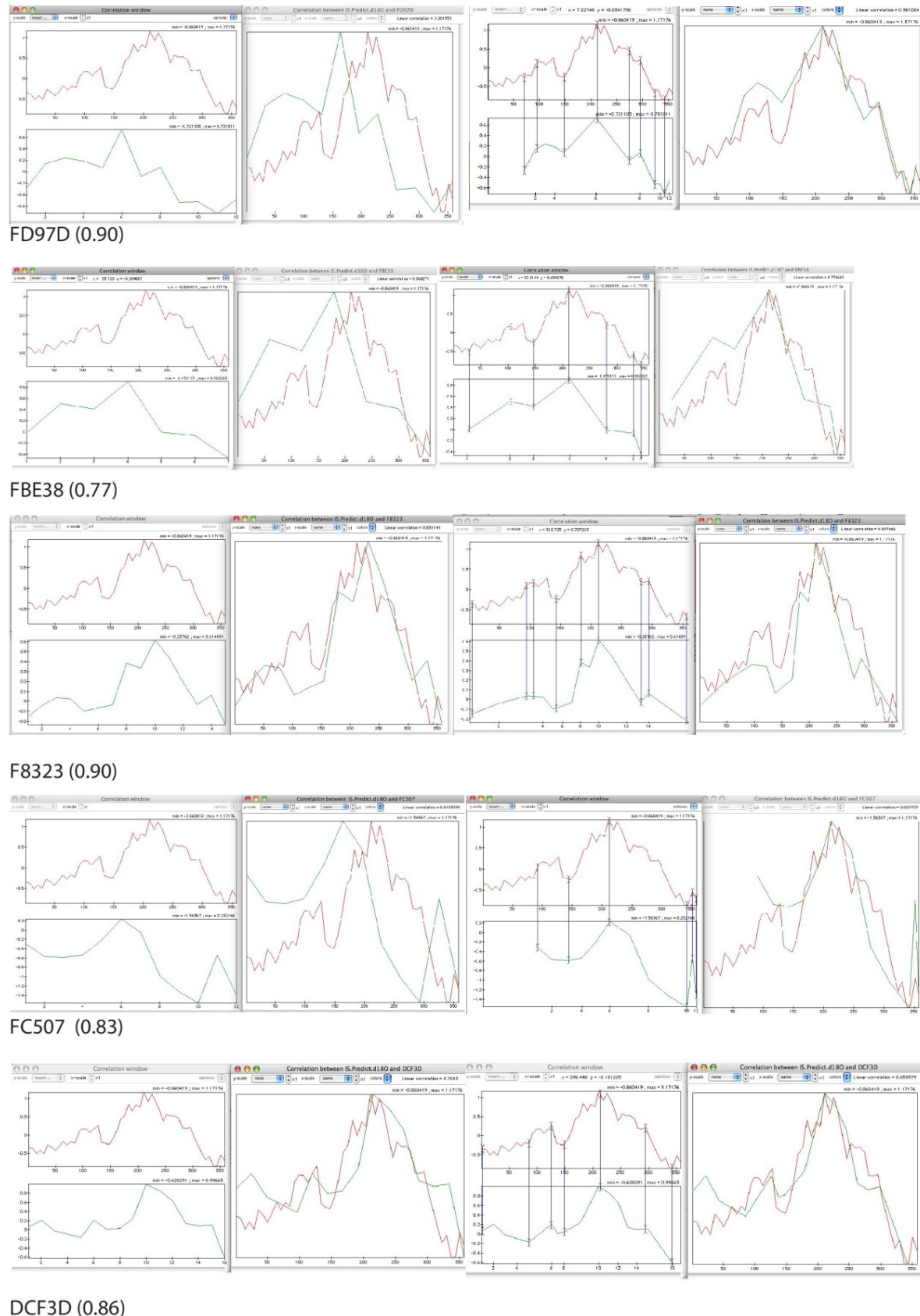
Zimmerman, C. (2005). Relationship of otolith strontium-to-calcium ratios and salinity: experimental validation for juvenile salmonids. *Canadian Journal of Fisheries and Aquatic Sciences* **62**, 88-97.

Zohar, Y. & Mylonas, C. C. (2001). Endocrine manipulations of spawning in cultured fish: from hormones to genes. *Aquaculture* **197**, 99-136.

Zuur, A. F., Ieno, E. N., Walker, N. J., Saveliev, A. A. & Smith, G. M. (2009). Mixed effects models and extensions in ecology with R. Springer.

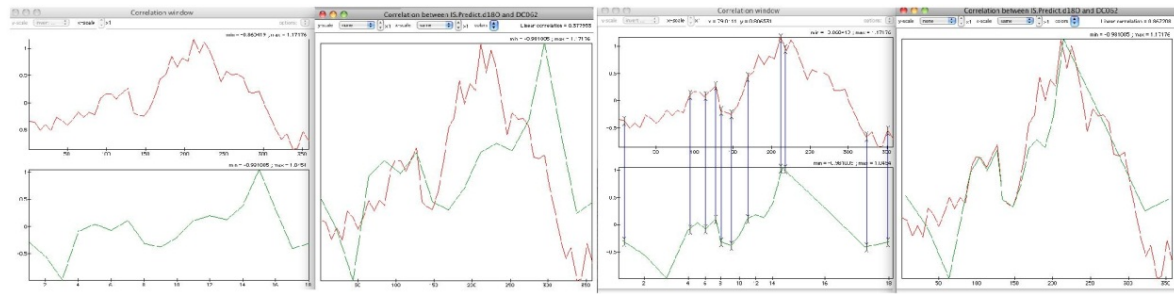
**Appendix 1.1** 'Wiggle matched'  $\delta^{18}\text{O}$  profiles in Analyseries 2.0 for experimental plaice maintained in natural but monitored conditions for 7-12 months. Predicted (red) and measured (green) profiles are displayed; plots on the left show raw data, plots on the right show wiggle matched profiles. The blue vertical lines indicate 'anchor points' picked out by eye. The fish ID and the correlation coefficient for predicted vs. measured profiles (in parentheses) are displayed below each plot

### Irish Sea males

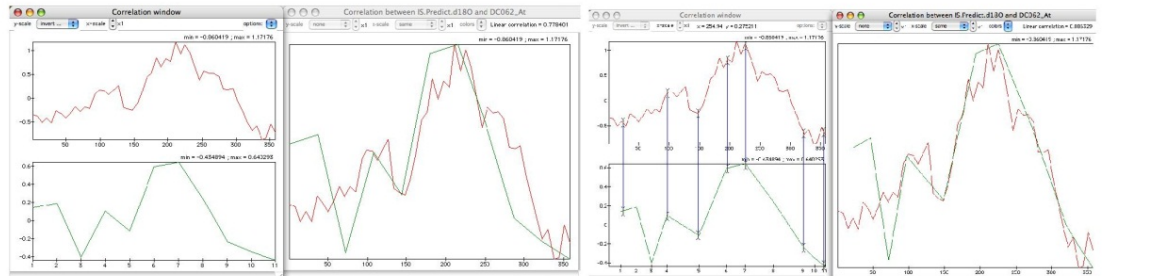


## Appendix 1.1 continued

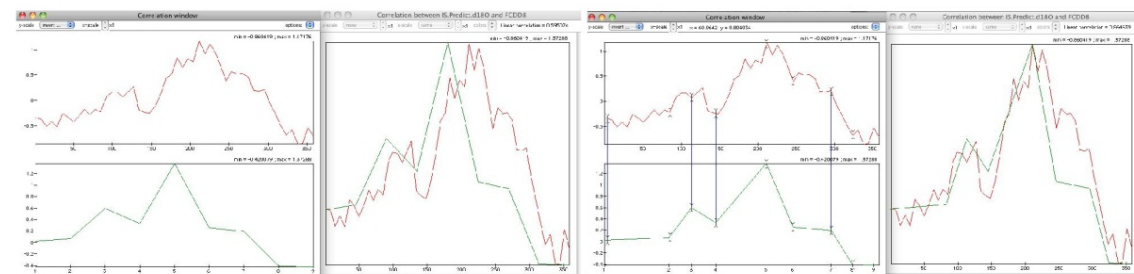
### Irish Sea females



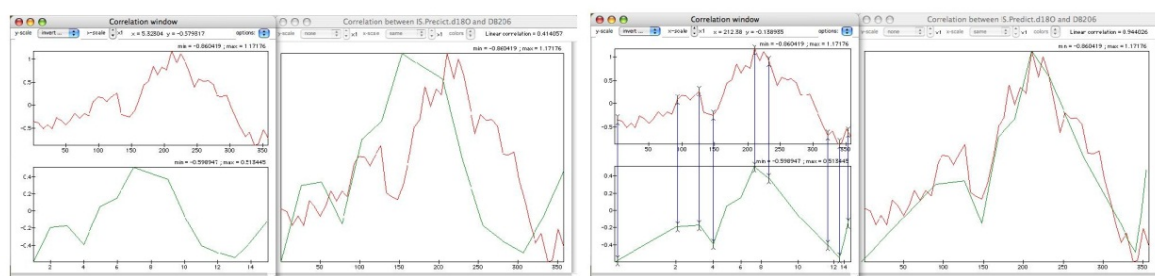
DC062 (0.87)



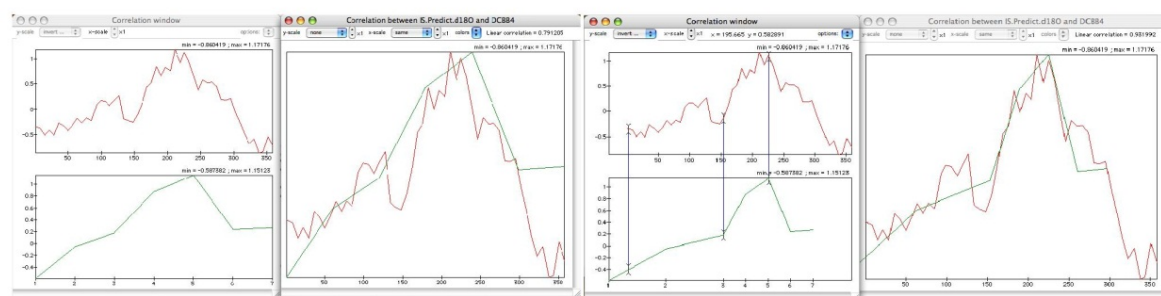
DC062\_transverse (0.89)



FCDD8 (0.86)



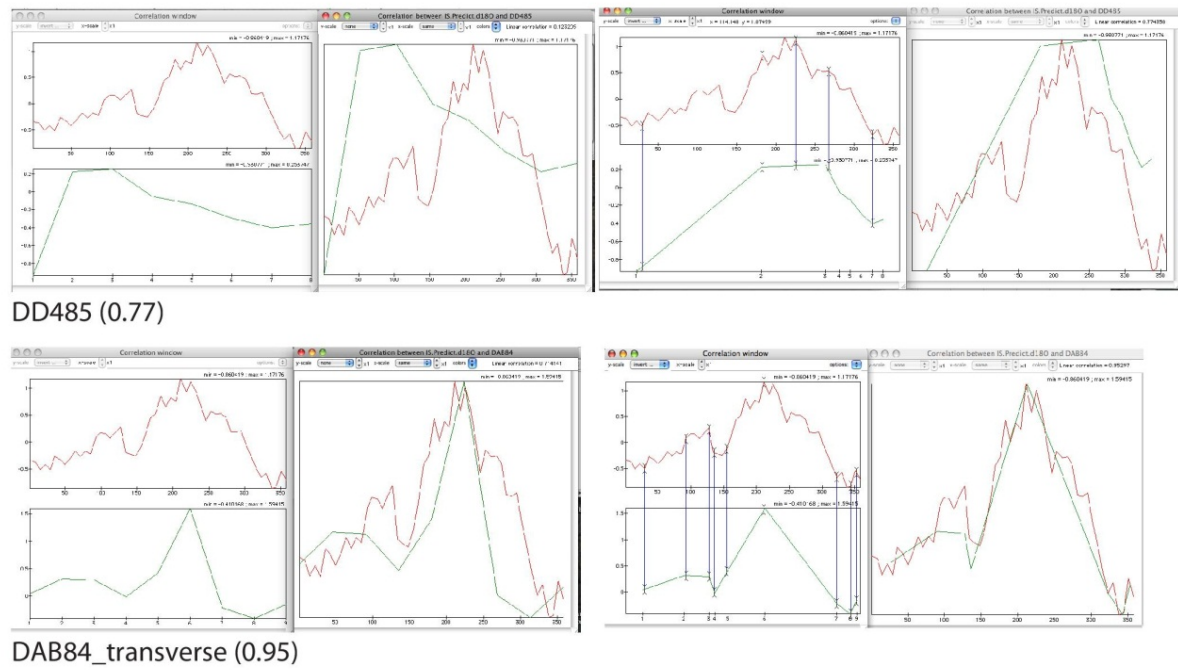
DB206 (0.94)



DCBB4 (0.93)

## Appendix 1.1 continued

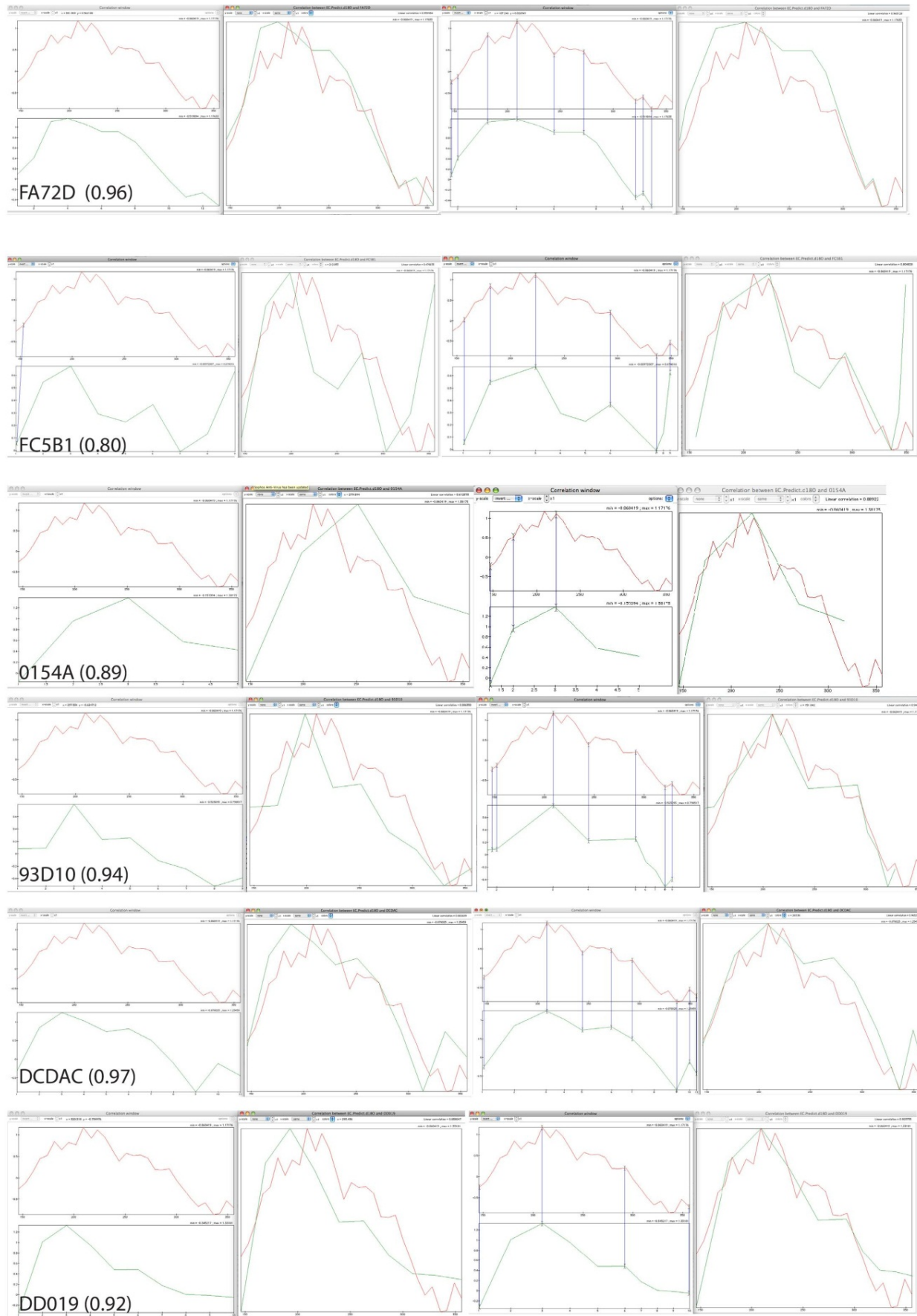
### Irish Sea females (continued)



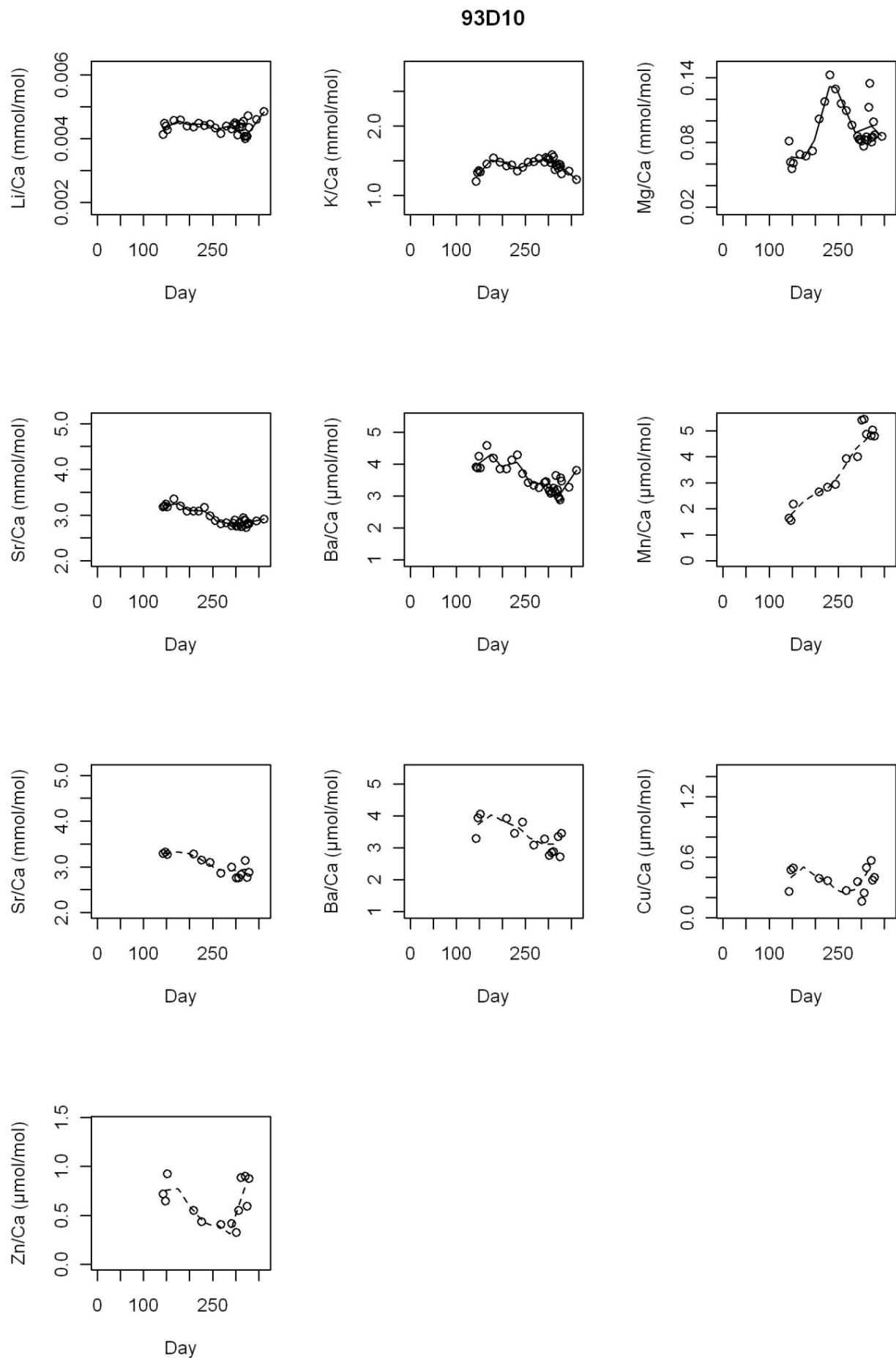
### DAB84\_transverse (0.95)

## Appendix 1.1 continued

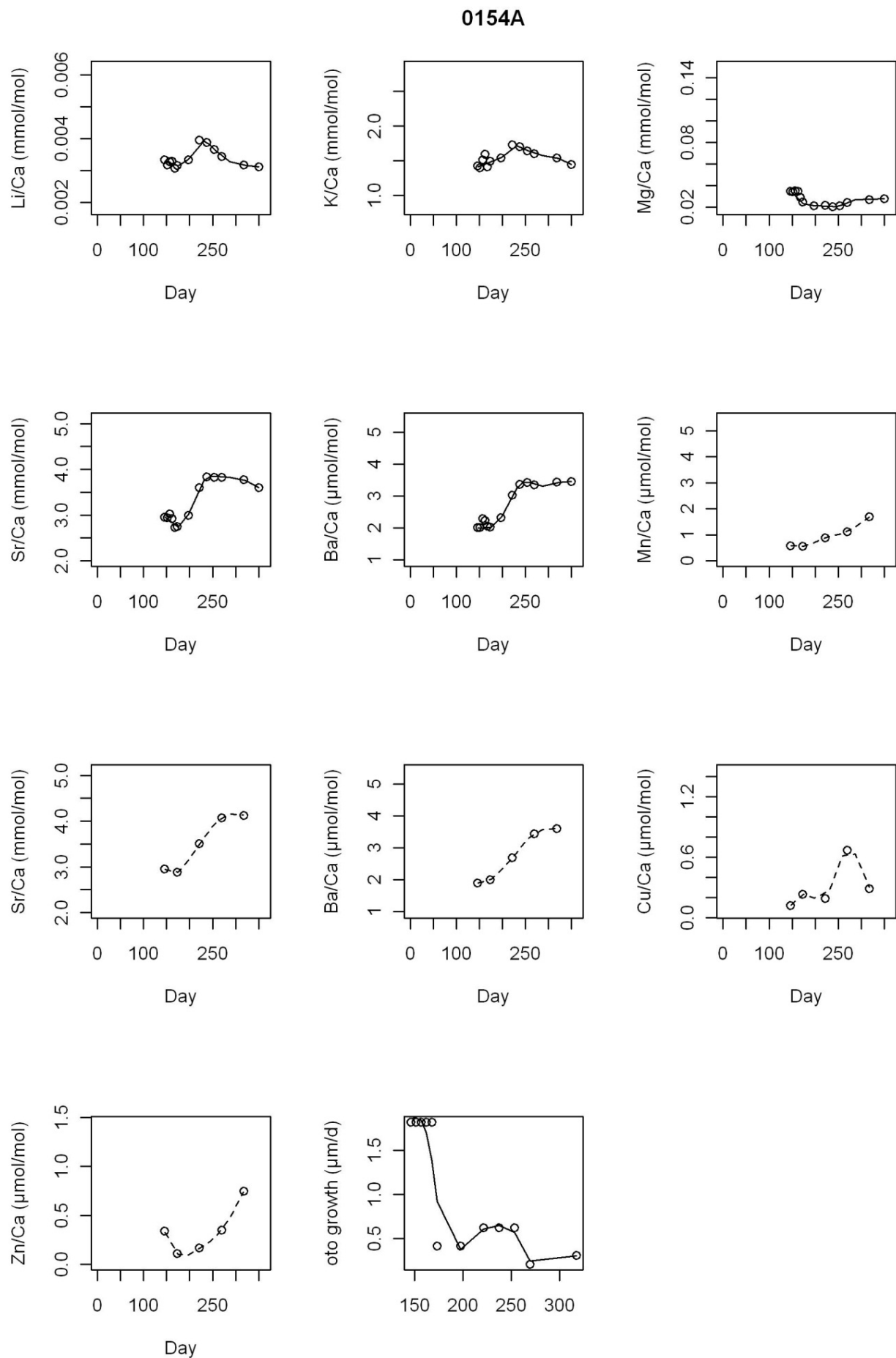
### English Channel females



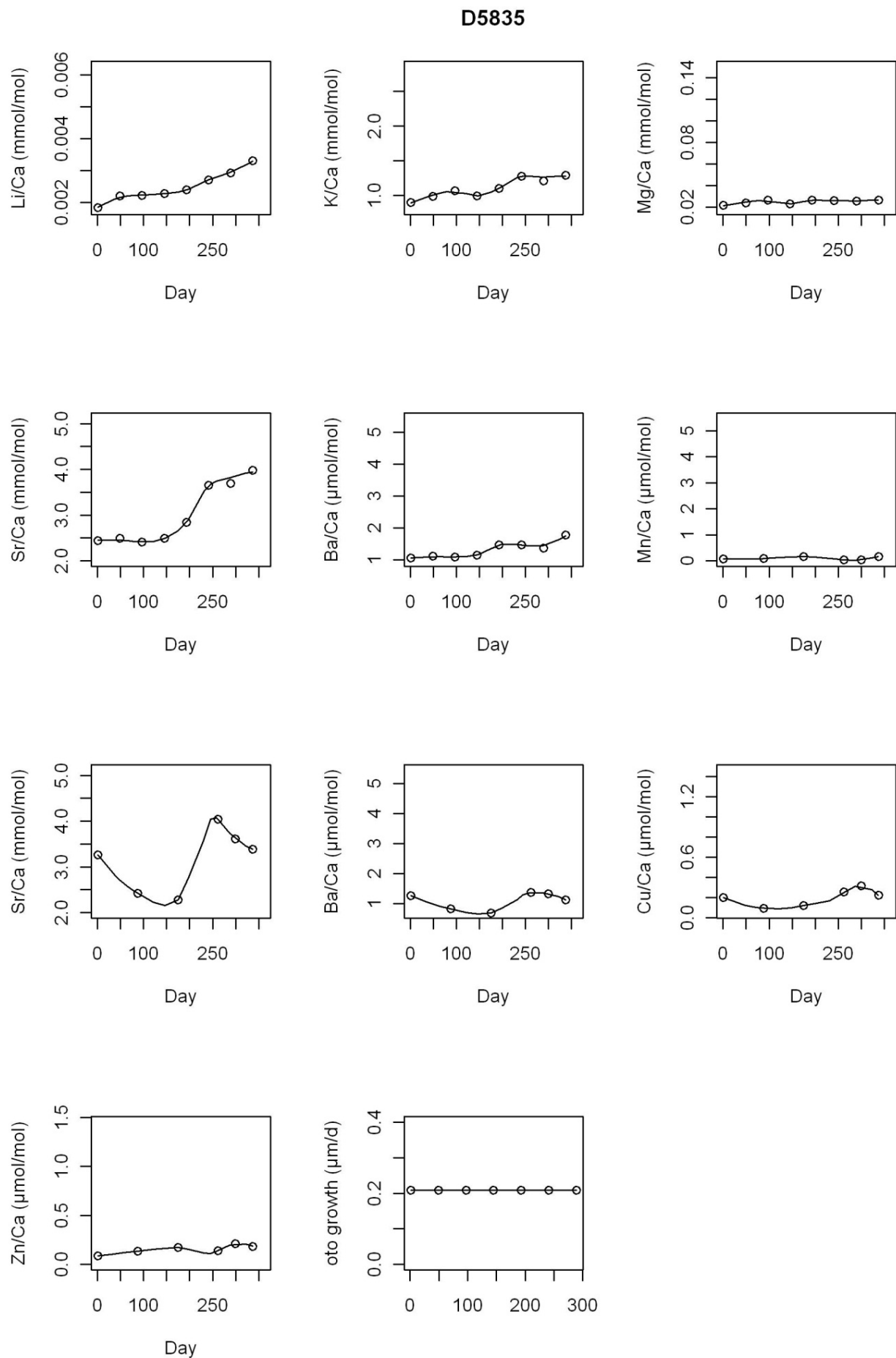
**Appendix 1.2** Smoothed and time ‘corrected’ trace elemental data for experimental plaice maintained in natural but monitored conditions for 7-12 months. SIMS measured concentrations indicated by solid line, LA-HR-ICPMS analyses by dashed lines



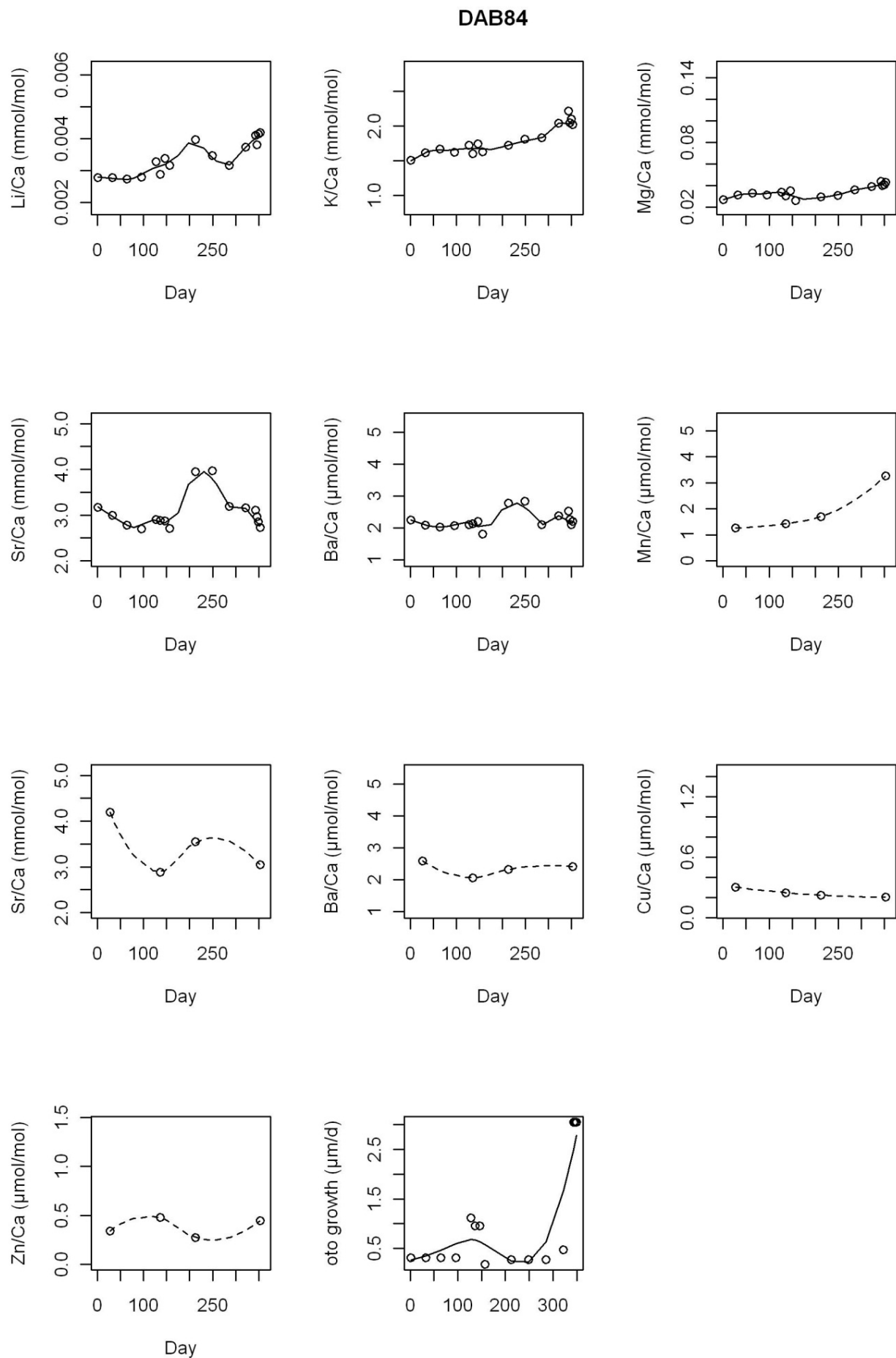
Appendix 1.2 continued



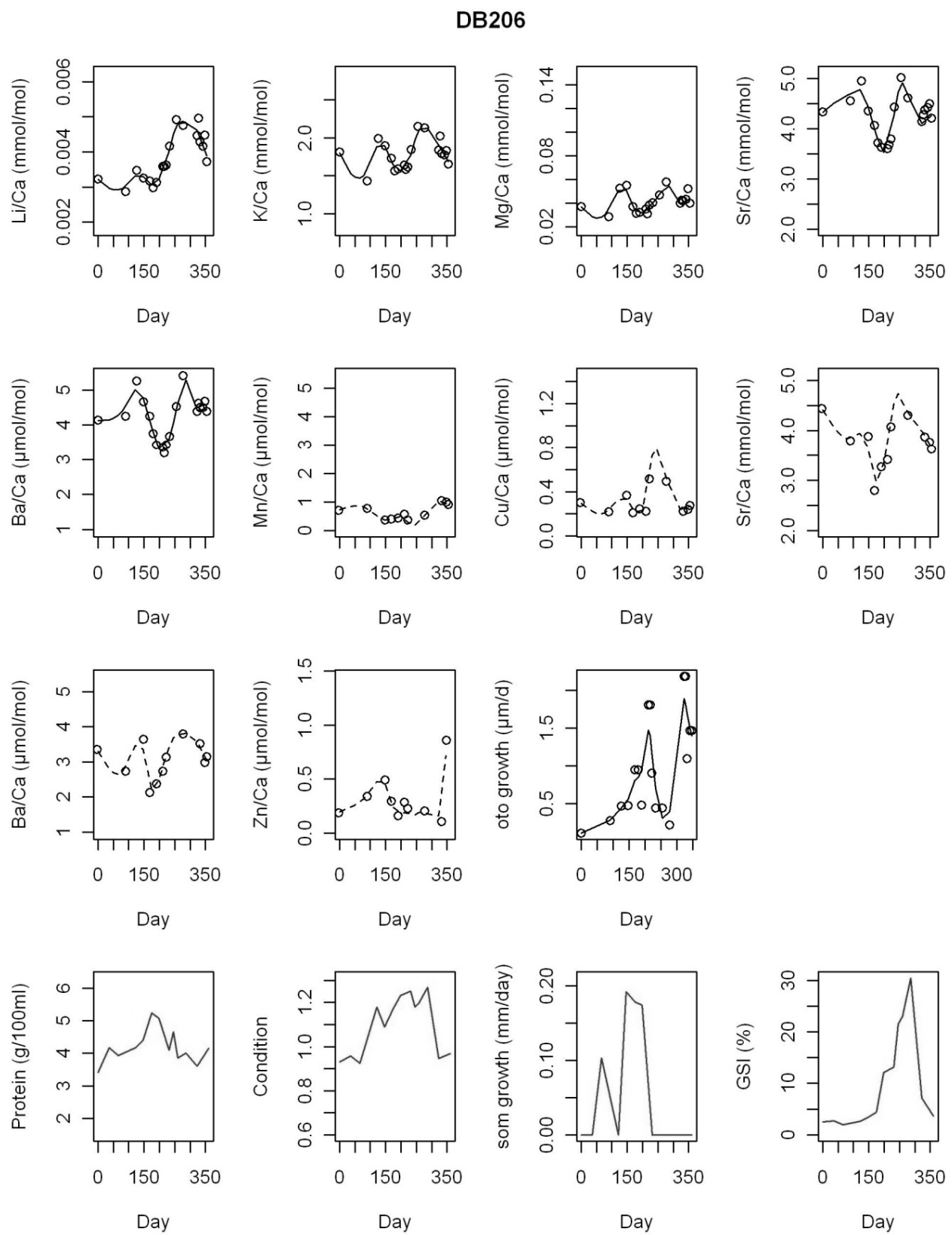
Appendix 1.2 continued



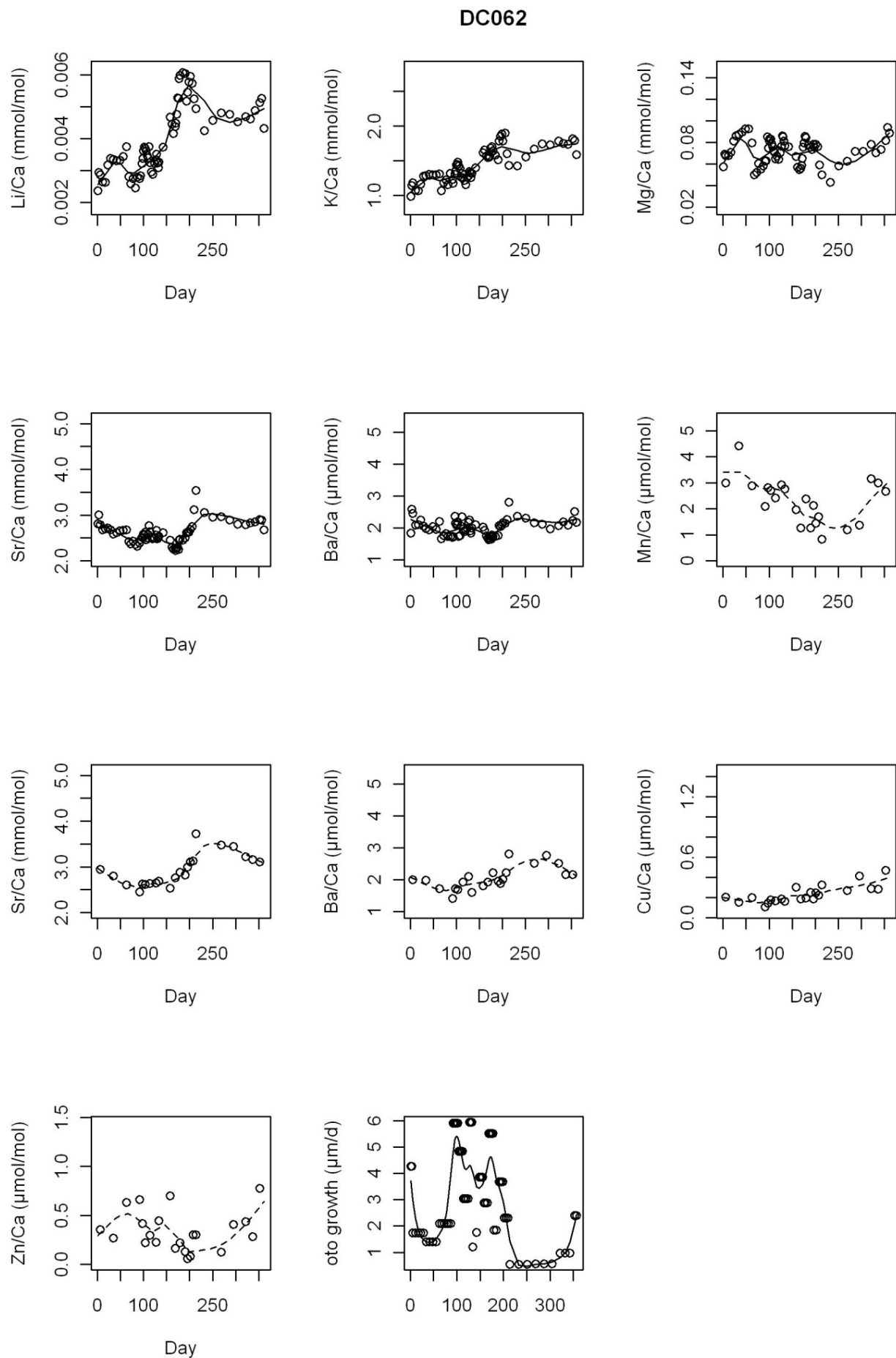
## Appendix 1.2 continued



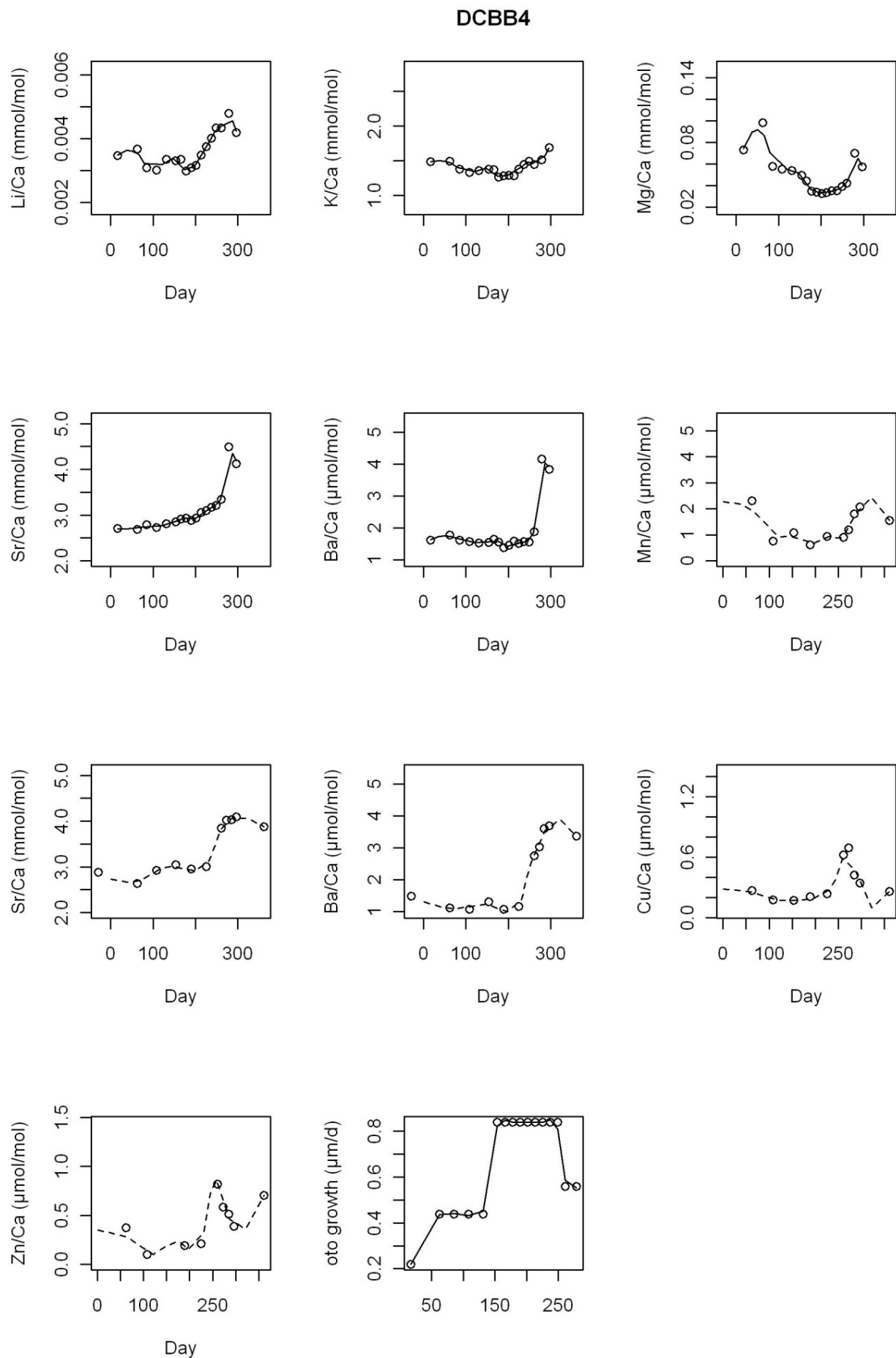
## Appendix 1.2 continued



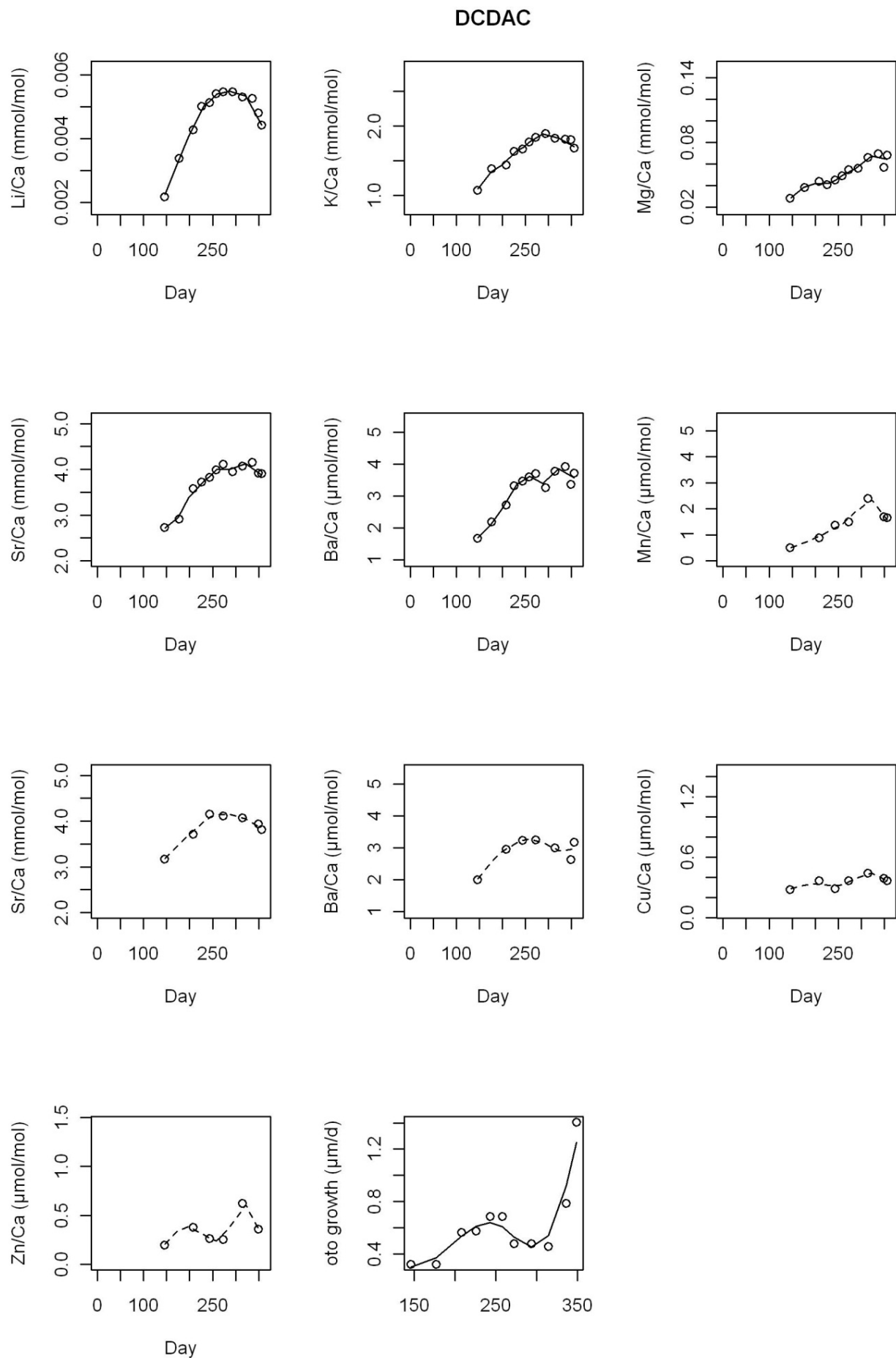
Appendix 1.2 continued



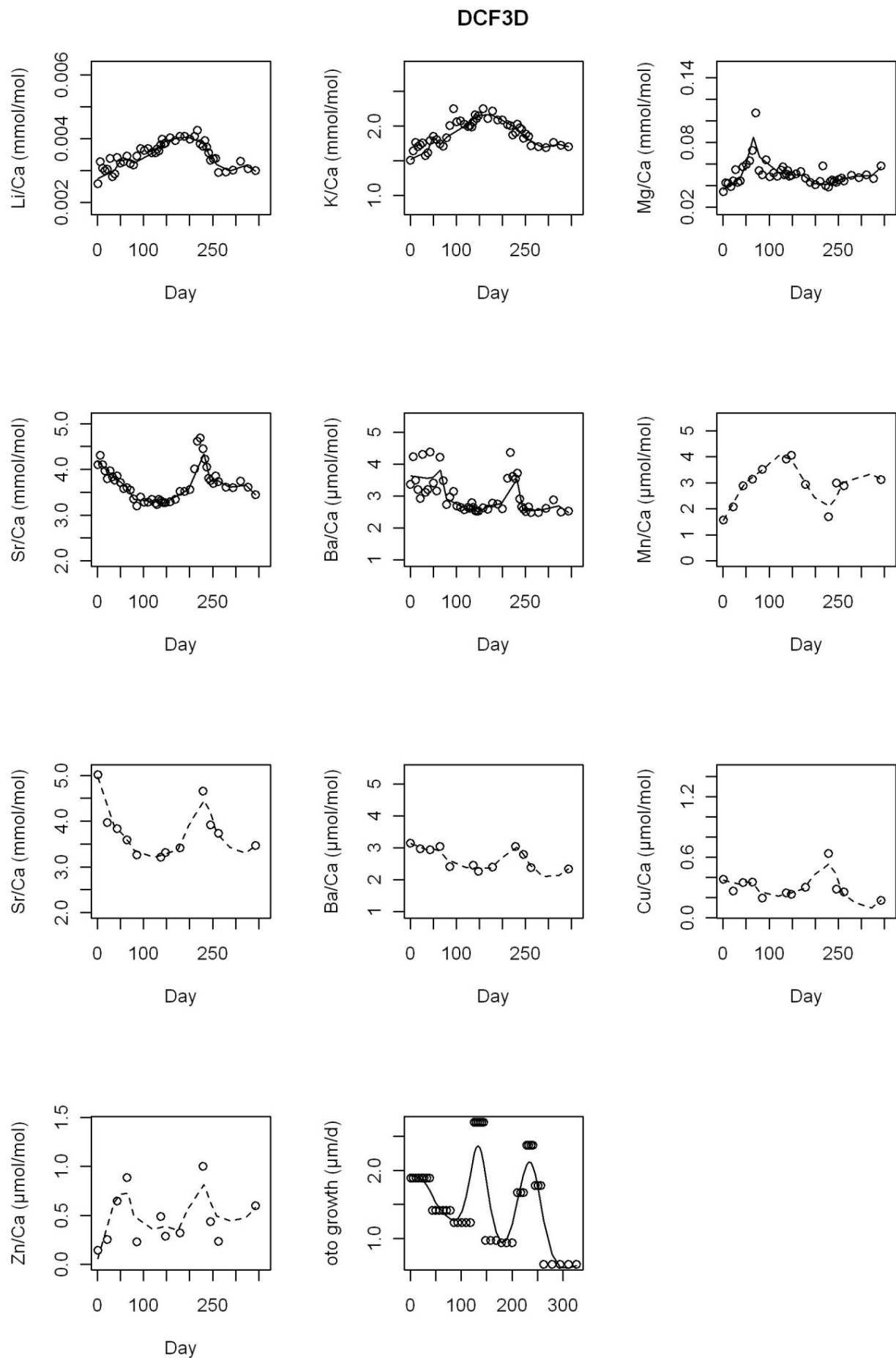
Appendix 1.2 continued



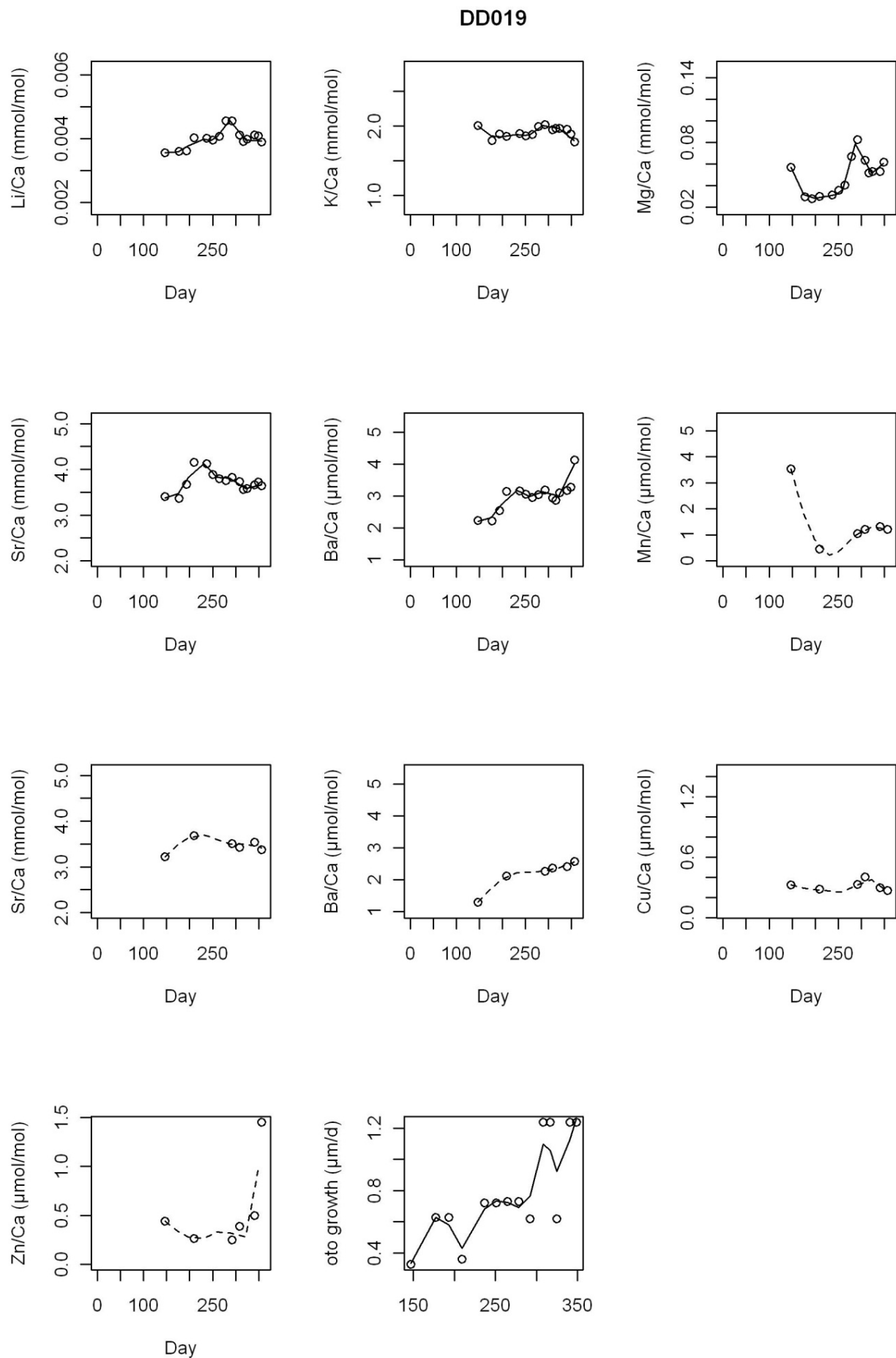
Appendix 1.2 continued



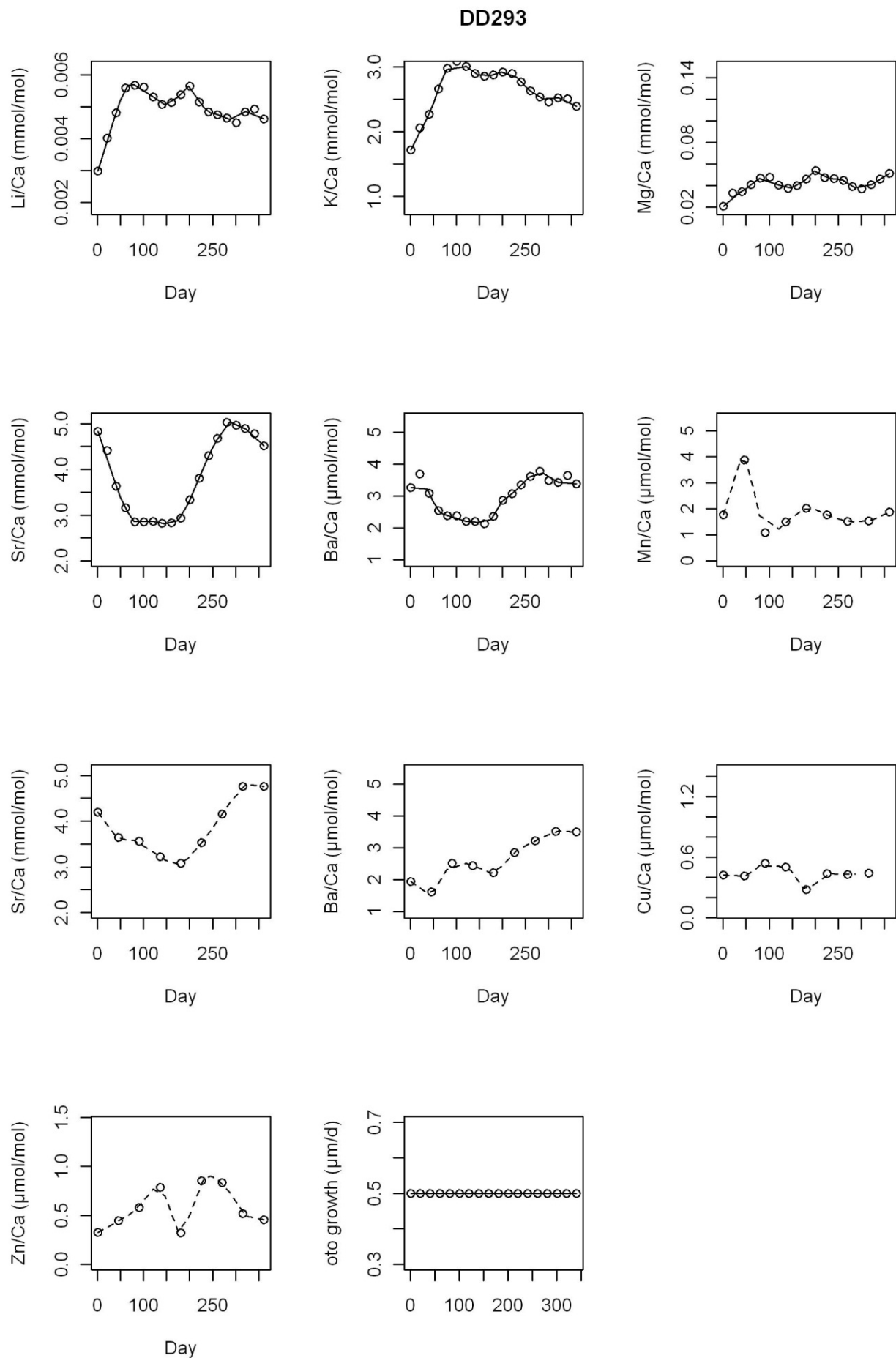
Appendix 1.2 continued



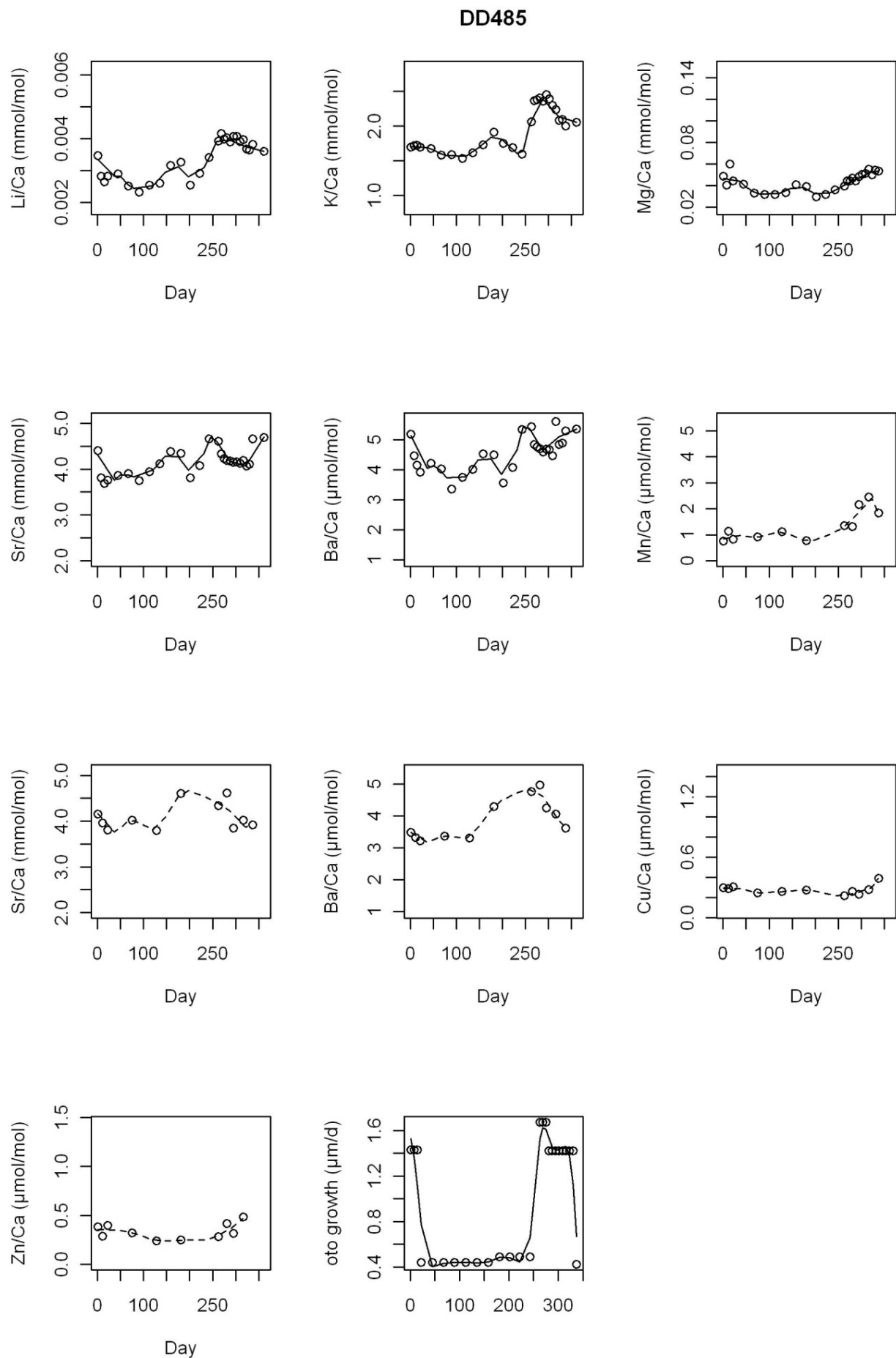
Appendix 1.2 continued



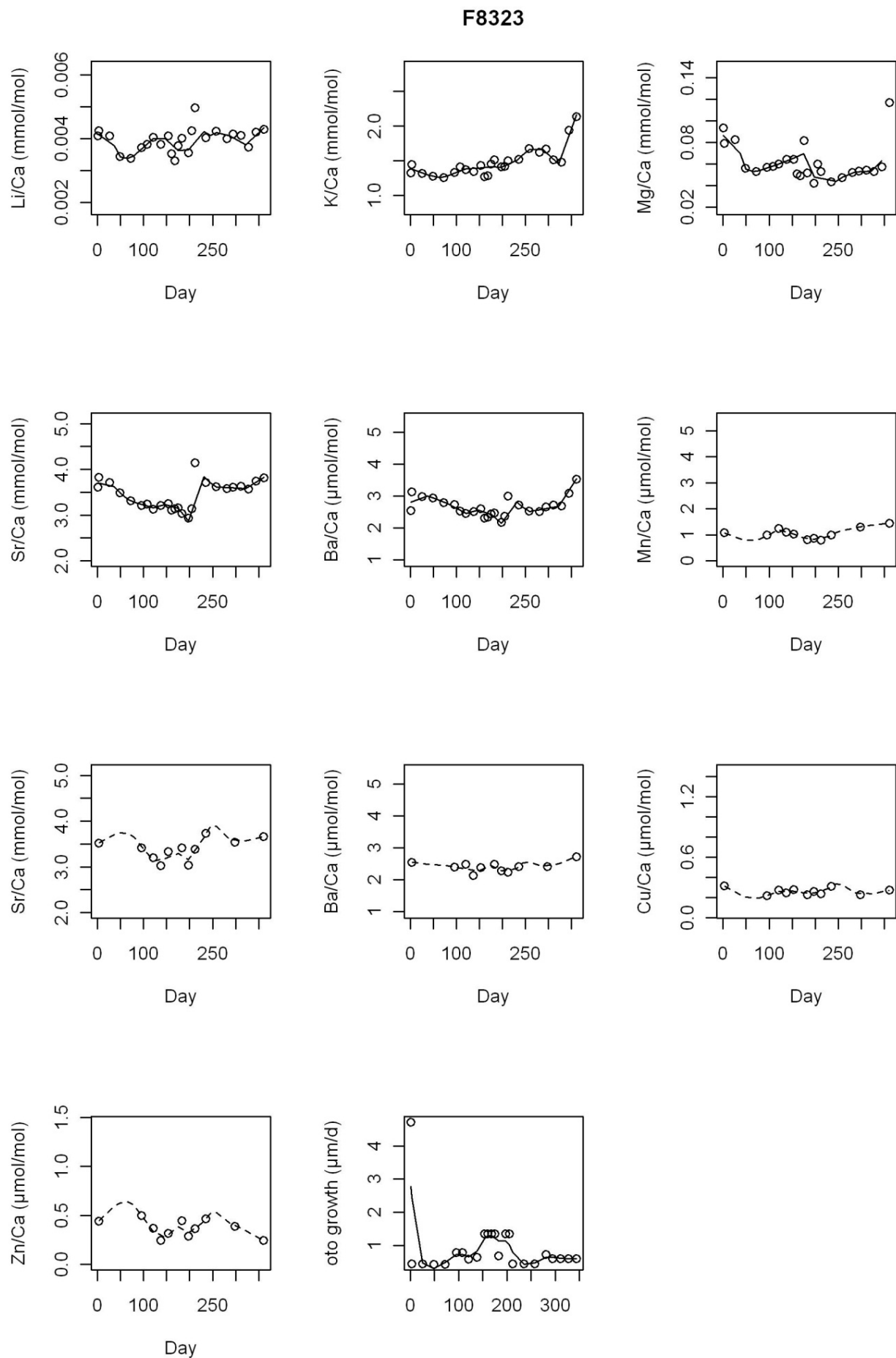
Appendix 1.2 continued



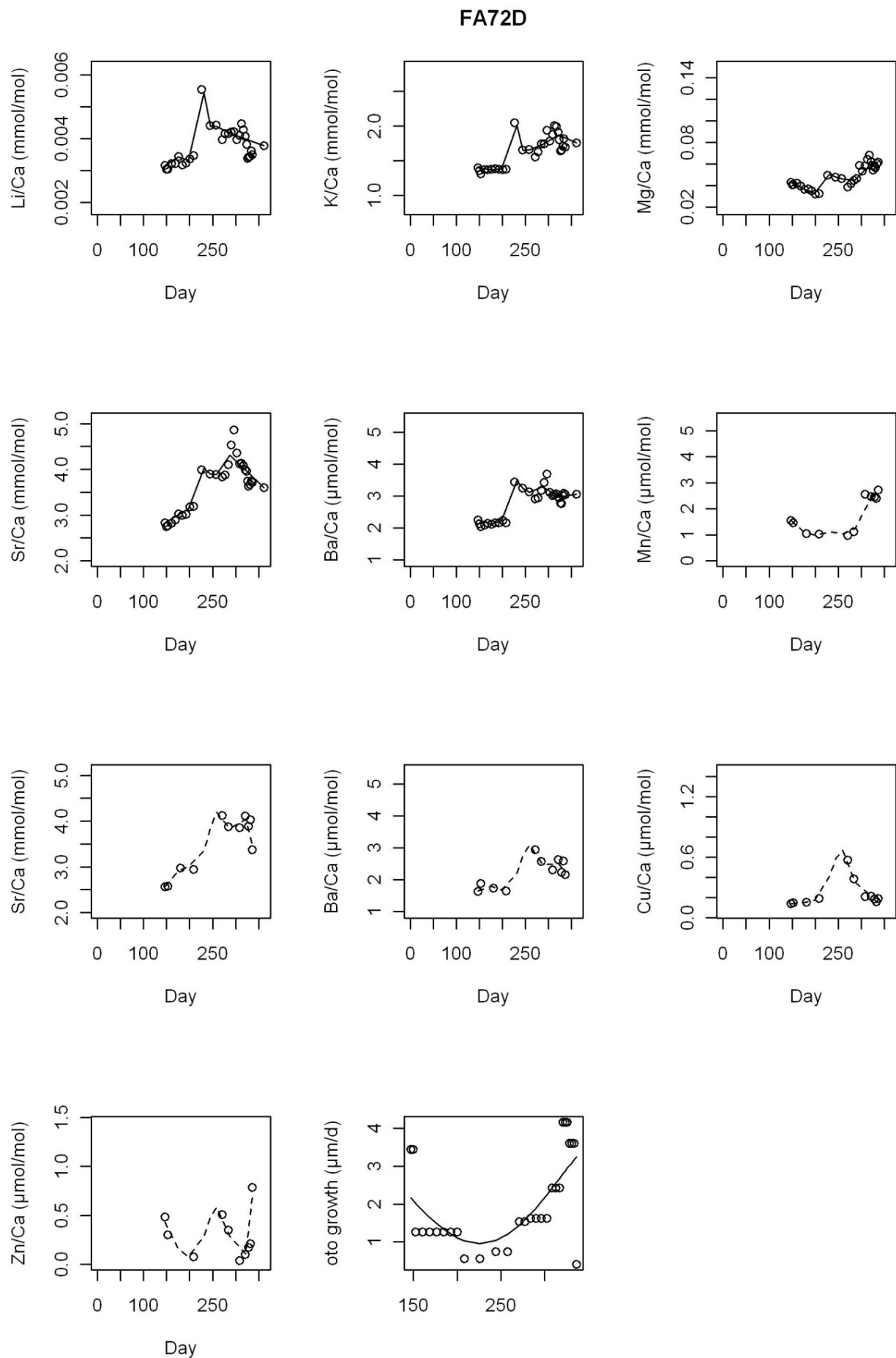
Appendix 1.2 continued



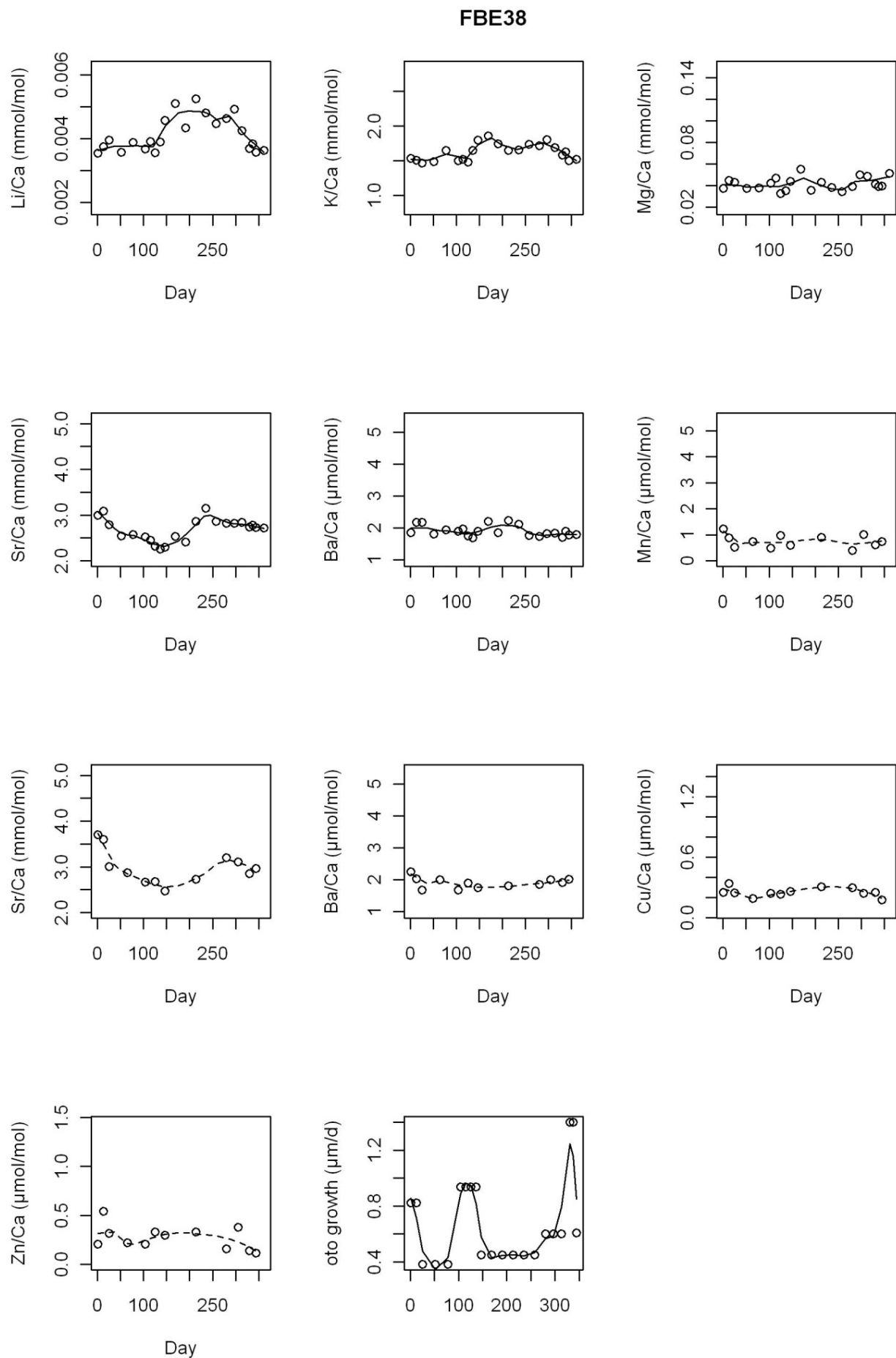
Appendix 1.2 continued



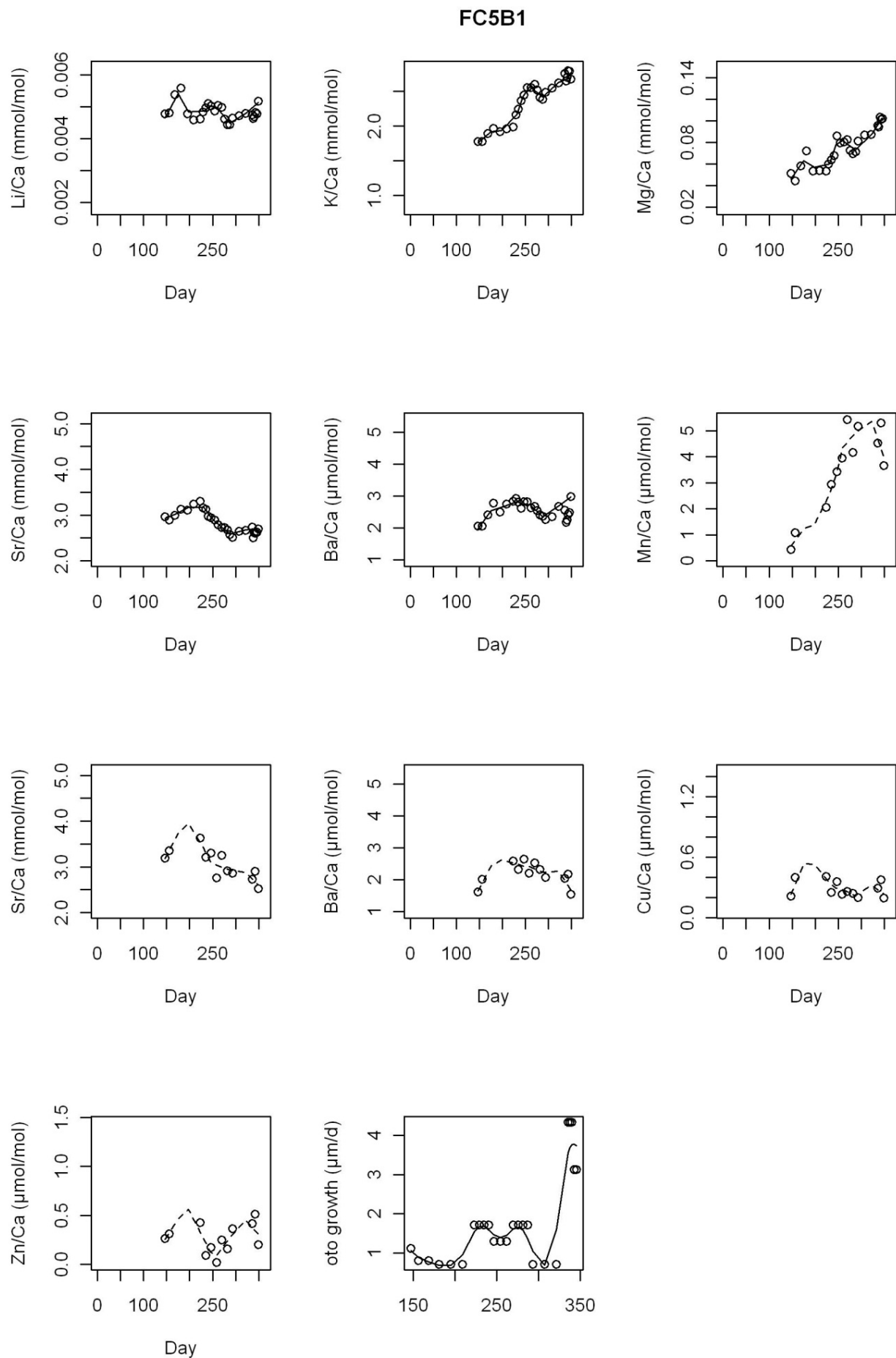
Appendix 1.2 continued



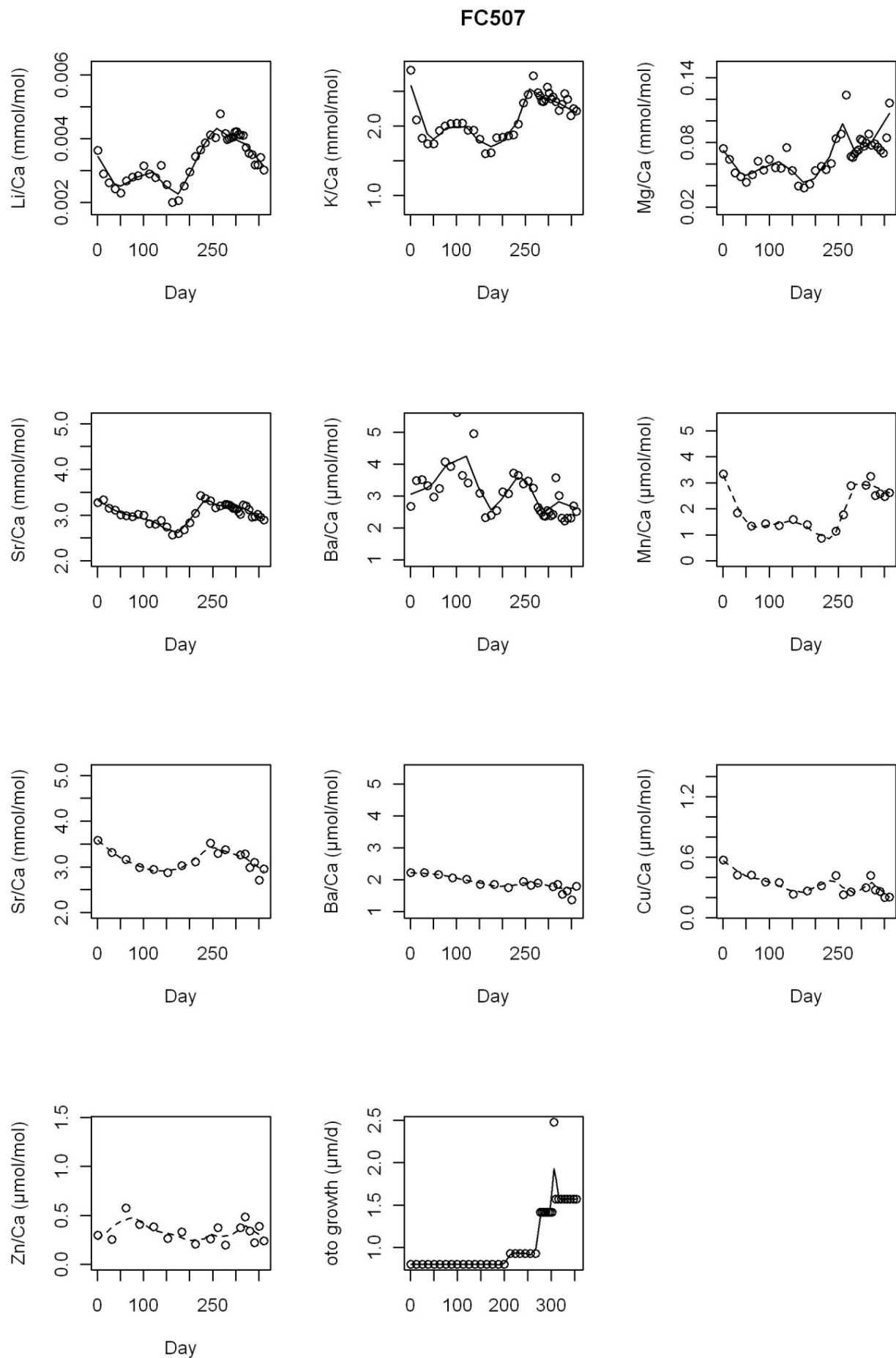
Appendix 1.2 continued



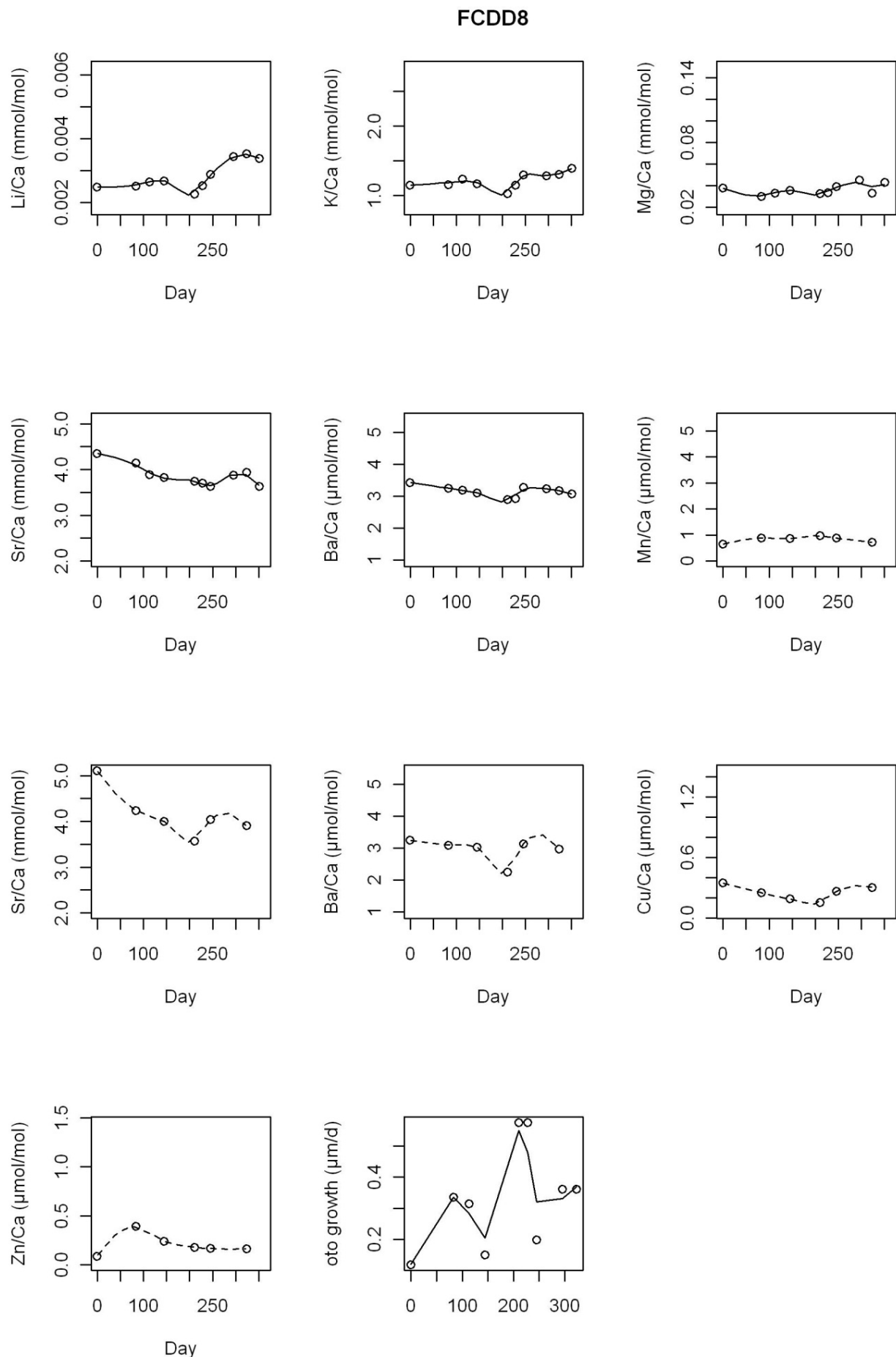
Appendix 1.2 continued



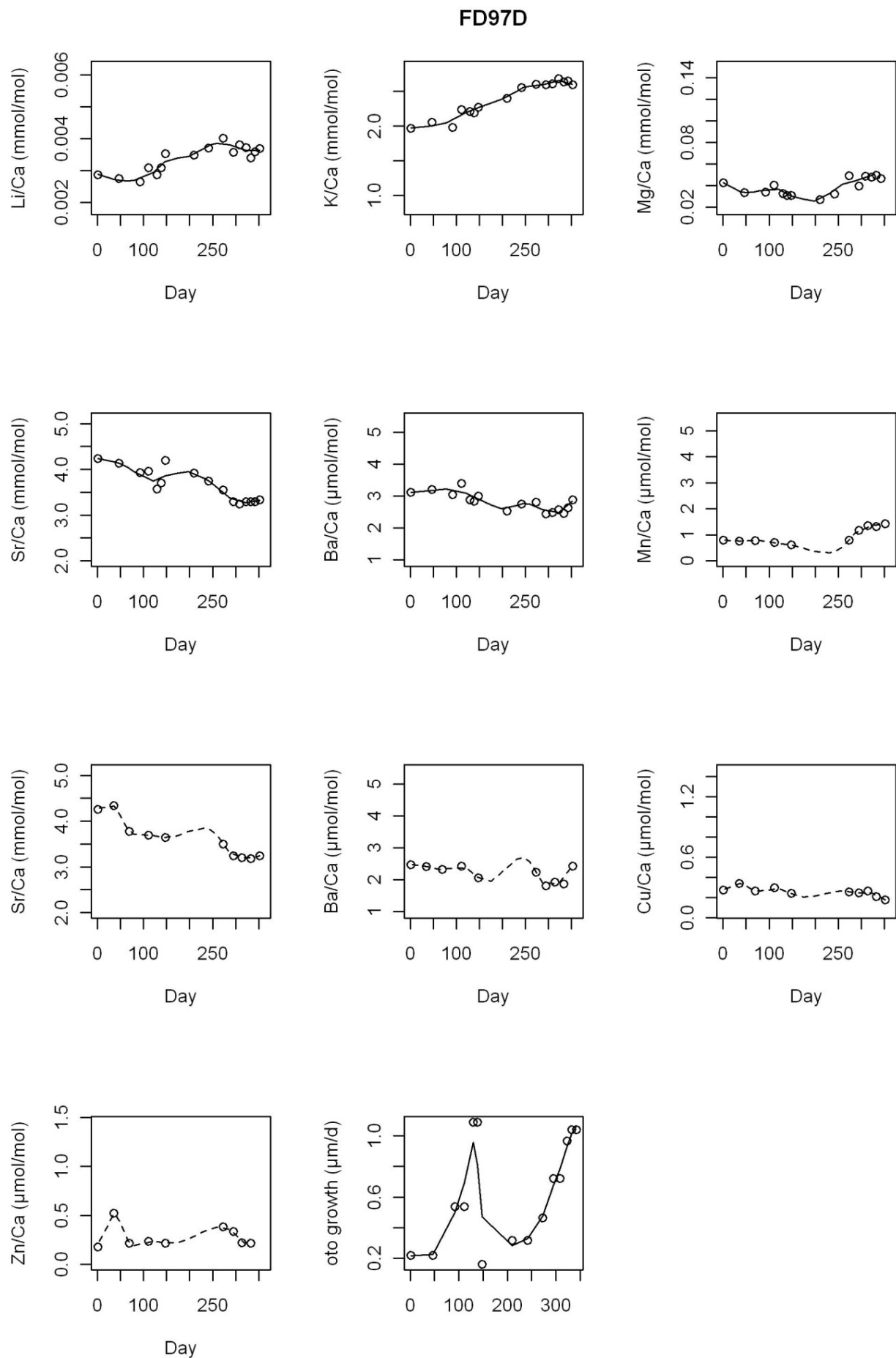
Appendix 1.2 continued



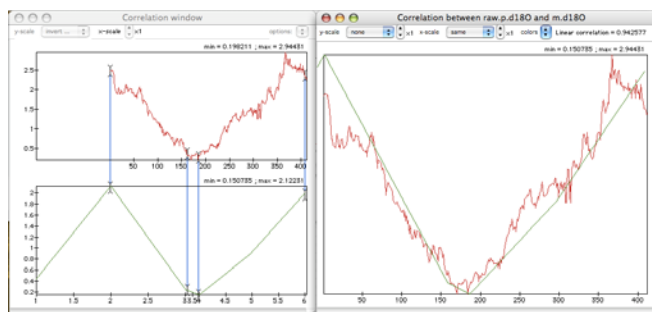
Appendix 1.2 continued



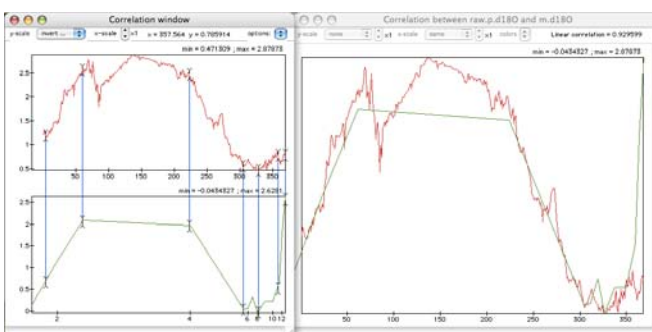
Appendix 1.2 continued



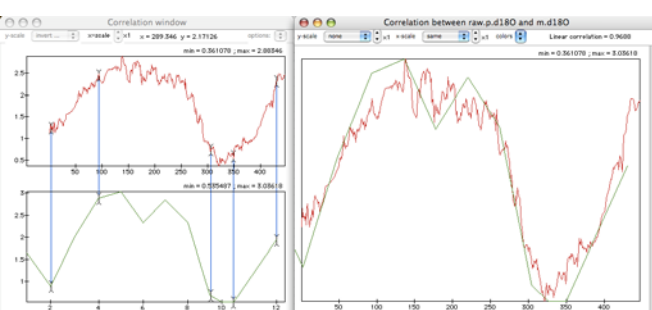
**Appendix 1.3** 'Wiggle matched'  $\delta^{18}\text{O}$  profiles in Analyseries 2.0 for DST tagged at liberty for 202-560 days. Predicted (red) and measured (green) profiles are displayed; blue vertical lines indicate 'anchor points' picked out by eye. The fish ID is indicated next to each plot, along with its North Sea region, sex and the correlation coefficient for predicted vs. measured profiles (in parentheses). Predicted  $\delta^{18}\text{O}$  values were calculated using DST-recorded temperatures and GETM-estimated salinity values



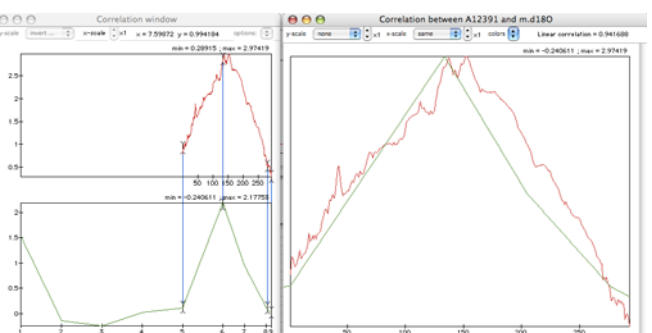
3.4-1000 (WNS F, 0.94)



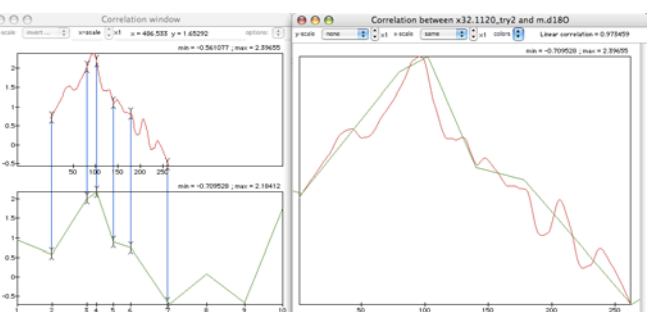
A12454 (WNS F, 0.93)



A12382 (WNS M, 0.97)

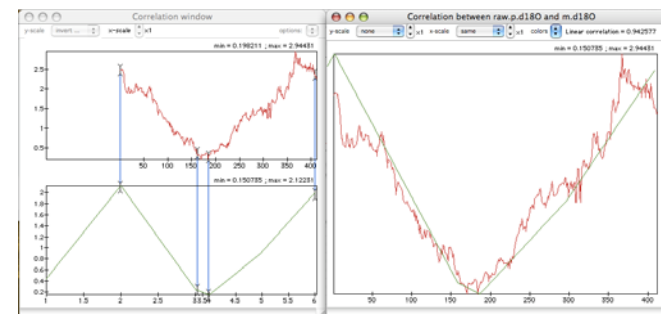


A12391 (WNS M, 0.94)

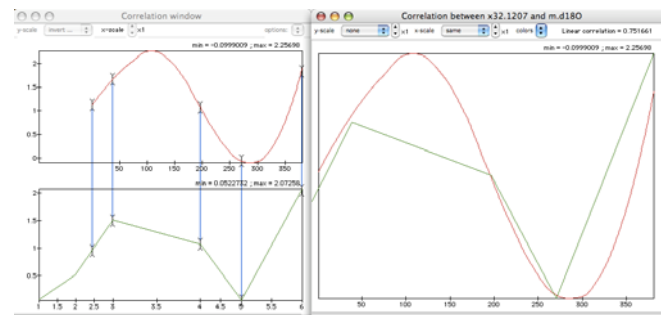


3.2-1120 (ENS F, 0.97)

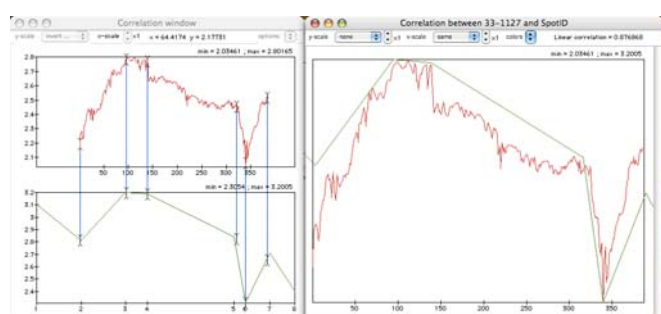
### Appendix 1.3 continued



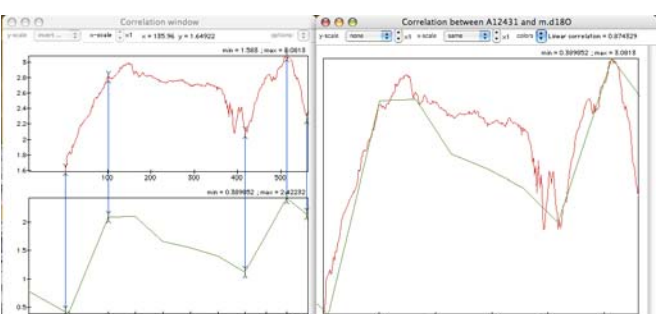
3.2-1137 (ENS F, 0.88)



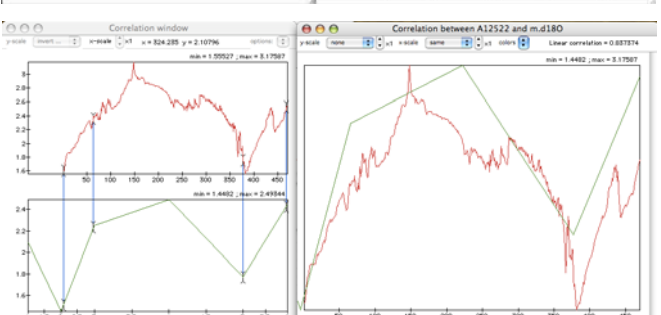
3.2-1207 (ENS F, 0.75)



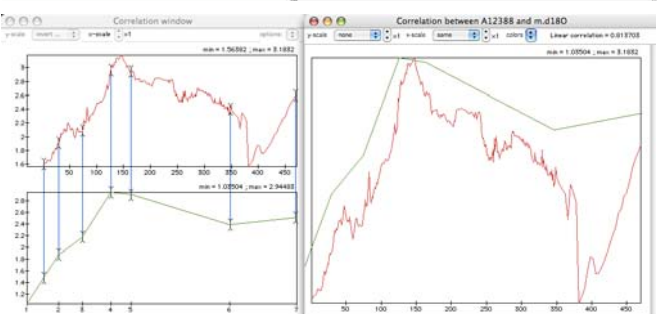
3.3-1127 (CNS F, 0.88)



A12431 (CNS F, 0.87)



A12522 (CNS M, 0.84)



A12388 (CNS M, 0.81)